

International Agreement Report

Post-Test-Analysis and Nodalization Studies of OECD LOFT Experiment LP-02-6 With RELAP5/MOD2 CY36-02

Prepared by
D. Lübbesmeyer

Paul Scherrer Institute (PSI)
Würenlingen and Villigen
5232 Villigen PSI
Switzerland

Office of Nuclear Regulatory Research
U.S. Nuclear Regulatory Commission
Washington, DC 20555

August 1992

Prepared as part of
The Agreement on Research Participation and Technical Exchange
under the International Thermal-Hydraulic Code Assessment
and Application Program (ICAP)

Published by
U.S. Nuclear Regulatory Commission

NOTICE

This report was prepared under an international cooperative agreement for the exchange of technical information.* Neither the United States Government nor any agency thereof, or any of their employees, makes any warranty, expressed or implied, or assumes any legal liability or responsibility for any third party's use, or the results of such use, of any information, apparatus product or process disclosed in this report, or represents that its use by such third party would not infringe privately owned rights.

Available from

Superintendent of Documents
U.S. Government Printing Office
P.O. Box 37082
Washington, D.C. 20013-7082

and

National Technical Information Service
Springfield, VA 22161

NUREG/IA-0088
PSI-Bericht Nr. 92



International Agreement Report

Post-Test-Analysis and Nodalization Studies of OECD LOFT Experiment LP-02-6 With RELAP5/MOD2 CY36-02

Prepared by
D. Lübbesmeyer

Paul Scherrer Institute (PSI)
Würenlingen and Villigen
5232 Villigen PSI
Switzerland

Office of Nuclear Regulatory Research
U.S. Nuclear Regulatory Commission
Washington, DC 20555

August 1992

Prepared as part of
The Agreement on Research Participation and Technical Exchange
under the International Thermal-Hydraulic Code Assessment
and Application Program (ICAP)

Published by
U.S. Nuclear Regulatory Commission

NOTICE

This report is based on work performed under the sponsorship of the Swiss Federal Office of Energy. The information in this report has been provided to the USNRC under the terms of the International Code Assessment and Application Program (ICAP) between the United States and Switzerland (Research Participation and Technical Exchange between the United States Nuclear Regulatory Commission and the Swiss Federal Office of Energy in the field of reactor safety research and development, May 1985). Switzerland has consented to the publication of this report as a USNRC document in order to allow the widest possible circulation among the reactor safety community. Neither the United States Government nor Switzerland or any agency thereof, or any of their employees, makes any warranty, expressed or implied, or assumes any legal liability of responsibility for any third party's use, or the results of such use, or any information, apparatus, product or process disclosed in this report, or represents that its use by such third party would not infringe privately owned rights.

Abstract

Experiment LP-02-6 was conducted on October 3, 1983. It was the first large-break loss-of-coolant accident (LOCA) simulation and the fourth experiment at all conducted in the Loss-Of-Fluid-Test (LOFT) facility at the Idaho National Engineering Laboratory under the auspices of the OECD. This experiment, which was designed to meet requirements outlined by the USNRC as specified in the OECD LOFT Project Agreement, simulated a double-ended off-set shear of a commercial pressurized water reactor (PWR) main coolant inlet pipe coincident with loss of off-site power. Experiment LP-02-6 addressed the response of a PWR to conditions closely resembling a USNRC "Design Basis Accident" in that prepressurized fuel rods were installed and minimum US emergency coolant injections were used.

This report presents the results and analysis of nine post-test calculations of the experiment LP-02-6 by using the RELAP5/Mod2 cy36-02 computer code with different nodalizations; these calculations have been performed within the International Code Assessment Program (ICAP). Starting with a "standard nodalization" as more or less used by the code developers at EG&G, we have reduced the number of volumes and junctions (especially in the pressurizer, the steam generator secondary side and the intact loop) as well as the number of radial zones in the fuel rods, for different nodalization studies.

Generally, the code has calculated most of the thermohydraulic parameters of the LOFT-experiment within an accuracy of approximately $\pm 20\%$. For the cladding temperatures, these deviations are sometimes higher, but the code has never underpredicted the peak cladding temperatures significantly. Except for the cladding temperatures, only small discrepancies have been observed for the other main parameters of the results of runs using different nodalizations but reduced numbers of volumes and junctions usually have lead to a decreased running time for the problem.

The time behaviours of the cladding temperatures have been significantly affected by the chosen nodalizations. The most comparable results with the experimental data have been achieved by using a medium number of nodes.

With respect to high mass-flux, early bottom-up rewetting, one of the key-events of experiment LP-02-6 as well as of most of the other LOFT large break experiments, RELAP5/Mod2 was not able to predict this phenomenon except with a certain manipulation by initiating the reflood option.

Contents

1	Introduction	5
1.1	Short Description of the LOFT Experiment LP-02-6	5
1.2	The Aim of the Present Investigations	8
2	Nodalization Schemes Used to Analyse Experiment LP-02-6	10
2.1	Standard Nodalization	10
2.2	Stripped Nodalizations	14
3	Results	21
3.1	Experimental Results	22
3.2	Influence of the Nodalization on Computer Time and Mass Error	24
3.3	Discussion of the Code-Predictions of the Main Events	27
3.3.1	Calculation of Mass Flows in the Broken Leg	27
3.3.2	Minimum Collapsed Liquid Level	38
3.3.3	Emptying Points of Pressurizer and Accumulator	39
3.3.4	Peak Cladding Temperatures During the Blowdown Phase	39
3.3.5	Quench Front Positions During the Reflooding Phase	40
3.4	Time Behaviour of Significant Thermo-Hydraulic Parameters	41
3.4.1	Cladding Temperatures	41
3.4.2	Fuel Center Temperature	69
3.4.3	System Pressures	71
3.4.4	Fluid-Temperature in the Downcomer	71
3.4.5	Core Mass Flows	75
3.4.6	Core Average Liquid Fractions	78
3.4.7	Mass-Flow Out of the Broken Loop	82
3.4.8	Intact Loop Mass Flow and Pump Speed	85
3.4.9	ECC System	91
3.5	Investigation on the Prediction of Early Bottom-Up Rewetting	94
4	Conclusions	107
5	Appendices	110
5.1	References	110
5.2	Listing of RELAP5/Mod2 - Input Mk. 2-00C	112

List of Figures

1.1	LOFT components showing thermo-fluid instrumentation	6
2.1	Nodalization 2-00 of the LOFT system (most detailed version;	11
2.2	Detail of the nodalization of the LOFT core	13
2.3	nodalization 3-00 (3-005) of the LOFT-system	16
2.4	nodalization 3-02 of the LOFT system (most simplified version;	17
3.1	Measured cladding temperatures in center bundle 5	23
3.2	CPU-time to Real time ratio vs. time	26
3.3	Mass error as defined by RELAP5/Mod2 vs. time	28
3.4	Trip setpoints for experiment LP-02-6	29
3.5	Hot-channel cladding temperatures vs. time at axial level 02	42
3.6	Hot-channel cladding temperatures vs. time at axial level 11	44
3.7	Hot-channel cladding temperatures vs. time at axial level 21	45
3.8	Hot-channel cladding temperatures vs. time at axial level 24	46
3.9	Hot-channel cladding temperatures vs. time at axial level 27	47
3.10	Hot-channel cladding temperatures vs. time at axial level 31	48
3.11	Hot-channel cladding temperatures vs. time at axial level 39	49
3.12	Hot-channel cladd. temperatures vs. time at axial level 43.8	50
3.13	Hot-channel cladding temperatures vs. time at axial level 49	52
3.14	Hot-channel cladding temperatures vs. time at axial level 62	53
3.15	Average channel cladding temperatures vs. time at axial level 11	54
3.16	Averaged channel cladding temperatures vs. time at axial level 21	55
3.17	Averaged channel cladding temperatures vs. time at axial level 28	56
3.18	Averaged channel cladding temperatures vs. time at axial level 39	57
3.19	Axial cladding temperature distribution at time -1.2 s in hot channel	59
3.20	Axial cladding temperature distribution at time 5.3 s in hot channel	60
3.21	Axial cladding temperature distribution at time 40.5 s in hot channel	61
3.22	Calculated void fraction, flow regime and HTC (nodalization 2-00)	62
3.23	Calculated void fraction, flow regime and HTC (nodalization 3-005)	63
3.24	Calculated void fraction, flow regime and HTC (nodalization 3-02)	64
3.25	Calculated void fraction, flow regime and HTC (nodalization 2-00)	65
3.26	Calculated void fraction, flow regime and HTC (nodalization 3-005)	66
3.27	Calculated void fraction, flow regime and HTC (nodalization 3-02)	67

3.28	History of the fuel center temperature in the hot channel compared	70
3.29	System pressures in the cold leg vs. time compared with pressure	72
3.30	Pressures in the pressurizer vs. time compared with pressure	73
3.31	Downcomer fluid temperatures vs. time compared with	74
3.32	Mass fluxes into the hot channel of the core as calculated	76
3.33	Mass fluxes out of the hot channel of the core as calculated	77
3.34	Momentum fluxes into the hot channel of the core as calculated	79
3.35	Momentum fluxes out of the hot channel of the core as calculated	80
3.36	Core averaged liquid fractions vs. time	81
3.37	Calculated mass flows out of the broken cold leg vs. time	83
3.38	Calculated mass flows out of the broken hot leg vs. time	84
3.39	Calculated mass losses out of the double ended break vs. time	86
3.40	Calculated mass flows in the intact hot leg vs. time	88
3.41	Calculated mass flows in the intact cold leg vs. time	89
3.42	Calculated relative pump speed vs. time compared with	90
3.43	Calculated accumulator fluid levels vs. time compared with	92
3.44	Calculated accumulator pressure vs. time compared with	93
3.45	Calculated accumulator mass flows vs. time	95
3.46	Calculated LPIS discharges vs. time compared with the measurement	96
3.47	Comparison of cladding temperatures calculated by RELAP5/Mod2	98
3.47	Comparison of cladding temperatures calculated by RELAP5/Mod2	99
3.47	Comparison of cladding temperatures calculated by RELAP5/Mod2	101
3.47	Comparison of cladding temperatures calculated by RELAP5/Mod2	102
3.47	Comparison of cladding temperatures calculated by RELAP5/Mod2	103
3.48	Comparison of cladding temperatures calculated by RELAP5/Mod2	104
3.48	Comparison of cladding temperatures calculated by RELAP5/Mod2	105
3.49	Comparison of the fuel center temperatures calculated by RFLAP5/Mod2	106

List of Tables

1.1	Initial Conditions for LOFT-experiment LP-02-6	7
2.1	Numbers of volumes, junctions, heat-structures and fine-meshes as well	18
2.1	... cont.	20
3.1	RTM values in different intervals of the transient	25
3.2	Comparison of characteristic parameters inferred from experiment	30
3.2	... cont.	31
3.2	... cont.	32
3.2	... cont.	33
3.2	... cont.	34
3.2	... cont.	35
3.2	... cont.	36
3.2	... cont.	37

Chapter 1

Introduction

1.1 Short Description of the LOFT Experiment LP-02-6

The LOFT facility at Idaho National Engineering Laboratory was designed to simulate the major components and system responses of a commercial PWR during a LOCA for the determination of system transient characteristics and for the assessment of code predictive capabilities for design basis large- and small break LOCAs in pressurized water reactors. The experimental assembly includes five major subsystems which have been instrumented such that system variables can be measured and recorded during LOCA simulation. The subsystems include the reactor vessel, the intact and the broken loop, the blowdown suppression system and the ECC systems; the arrangement of these major components is shown in Fig. 1.1. The entire nuclear core consists of five square and four triangular fuel bundles with a total of 1300 fuel pins each of 1.67m long and an outside diameter of 10.72 mm. A complete system description is given in ref.[1] and a discussion of the LOFT scaling philosophy is provided in ref.[2].

Experiment LP-02-6 was conducted on October 3, 1983, in the Loss-Of-Fluid Test (LOFT) facility at the Idaho National Engineering Laboratory. It was the first large-

break loss-of-coolant accident (LOCA) simulation and the fourth experiment at all conducted in the LOFT facility under the auspices of the OECD. This experiment, which was designed to meet requirements outlined by the USNRC as specified in the OECD LOFT Project Agreement, simulated a double-ended off-set shear of a commercial pressurized water reactor (PWR) main coolant inlet pipe coincident with loss of off-site power. Experiment LP-02-6 addressed the response of a PWR to conditions closely resembling a USNRC "Design Basis Accident" in that prepressurized fuel rods were installed and minimum US emergency coolant injections were used.

The experiment was initiated from conditions representative of those in a commercial PWR; they have been listed in table 1.

The transient was initiated by opening the quick-opening blowdown valves in broken loop hot and cold legs. Pressure decreased rapidly due to the blowdown, with saturated conditions being reached in the upper plenum at 0.05 seconds.

The primary coolant pumps were tripped manually and allowed to coast down, simulating loss of off-site power coincident with the LOCA.

The core flow reversed immediately after the initiation of the transient and fuel rod

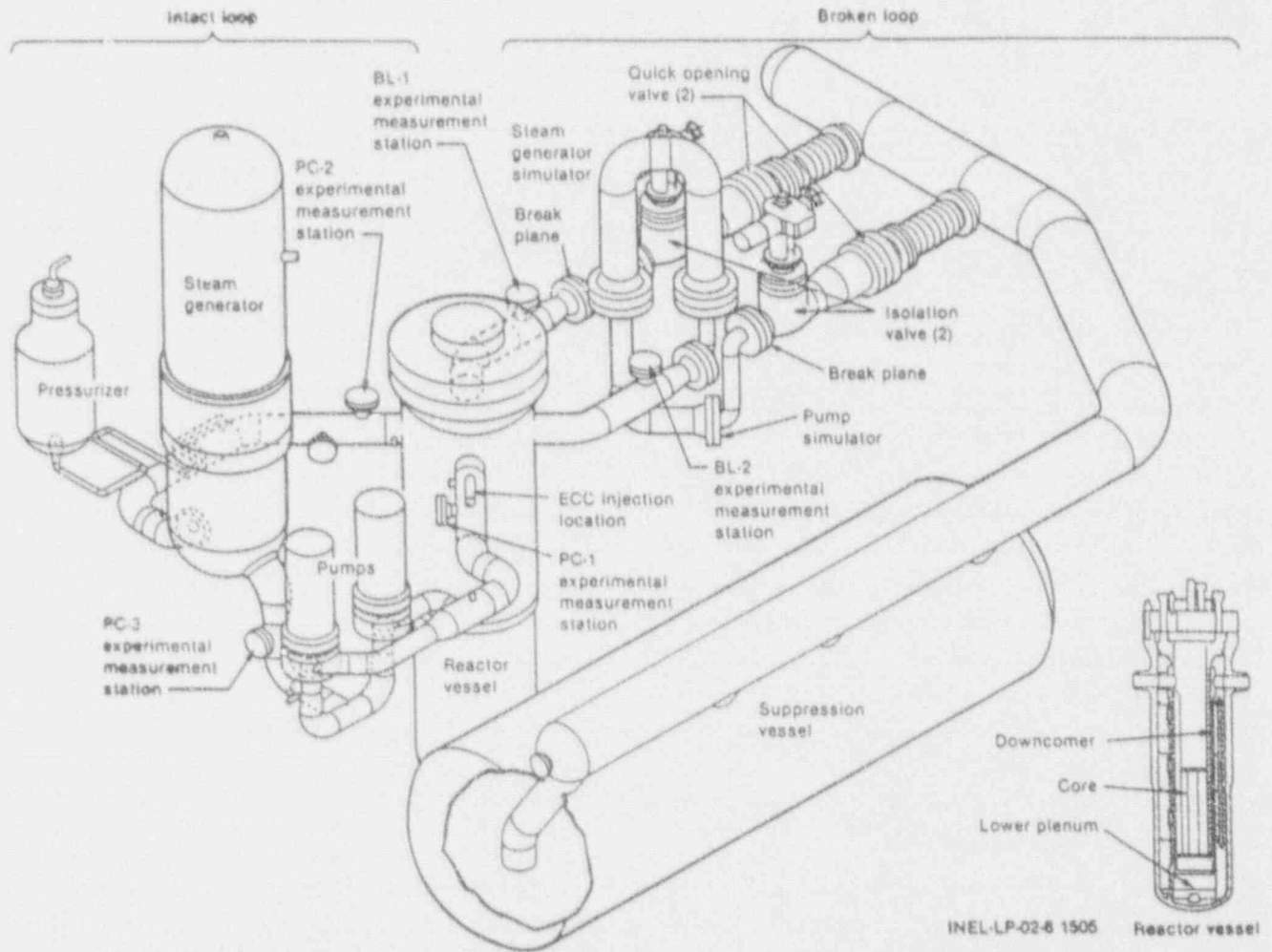


Figure 1.1: LOFT components showing thermo-fluid instrumentation

Initial Conditions for experiment LP-02-6		
parameter	unit	measured value
power	MW	46.0 ± 1.2
maximum linear heat	kW/m	48.8 ± 3.6
ΔT_{core}	K	33.1 ± 1.1
pressure _{hot leg}	MPa	15.09 ± 0.06
mass flow rate	kg/s	248.7 ± 2.6
fluid temperature _{cold leg,intact loop}	K	555.9 ± 1.1
fluid temperature _{cold leg,broken loop}	K	553.0 ± 6.0
fluid temperature _{cold leg,broken loop}	K	560.0 ± 6.0
pressurizer :		
liquid level	m	1.04 ± 0.04
pressure	MPa	15.3 ± 0.11
water temperature	K	615.6 ± 5.8
ECC system accumulator :		
liquid level	m	2.10 ± 0.0
standpipe position from bott.	m	1.44 ± 0.03
pressure	MPa	4.11 ± 0.06
liquid temperature	K	302.0 ± 6.1
ECC system HPIS :		
liquid temperature	K	305.0 ± 7.0
flow rate	l/s	1.04 ± 0.04
ECC system LPIS :		
liquid temperature	K	305.0 ± 7.0
flow rate	l/s	depending on pressure difference between LPIS and downcomer

Table 1.1: Initial Conditions for LOFT-experiment LP-02-6

cladding temperatures started to increase. This core-wide temperature increase continued until 4 seconds, when the flow in the broken cold leg saturated and choked with a concomitant decrease in mass flow to below the intact cold leg mass flow. During this period, cladding temperatures reached maximum values less than 1100 K; the maximum temperature has been measured on level 24 in the center bundle (24 inches from bottom, assembly 5) to 1040 K. The decrease in mass flow from the broken leg to below the intact cold leg mass flow reversed the reactor vessel mass loss and caused low quality fluid to flow into the core, causing a partial core bottom-up quench between 5.2 and 9.1 seconds, after which the core flow again reversed and the fuel rod cladding temperatures again increased; during this period maximum temperatures of less than 850 K have been reached. A partial core top-down quench occurred starting at 14.8 seconds which extended down to level 39, i.e. 39 inches from the bottom of the core. This quench has been assumed to be caused by liquid fallback from the upper plenum induced by gravity.

The fuel rod cladding again experienced departure from nucleate boiling. There were additional thermal cycles prior to the final core quench, which was complete at 56 seconds. For more details see ref. [3].

One of the major concerns with Experiment LP-02-6 was whether fuel rod damage would occur. Based on the indicated cladding temperatures, the pressure differential across the cladding and the evidence from isotope detection systems, no fuel rod ballooning or cladding rupture occurred.

A comparison of results of Experiment LP-02-6 with previous LOFT large break LOCA experiments L2-3 and L2-5 (the first with continuous pump operation, the second with pumps disconnected from their fly-

wheels) shows that the loss-of-offsite power-induced pump operation results in a core thermal response that closely matches that resulting from continued pump operation. That is, even though the pump is not powered during the early seconds of the blowdown, a typical pump coastdown results in sufficient pump head to cause a positive core flow and core quench during the early period of the blowdown.

1.2 The Aim of the Present Investigations

Codes like RELAP5/Mod2 and TRAC have been often used for the analysis of LOFT experiments and LOFT results have been extensively used to eliminate insufficiencies both in the codes themselves and the more plant-specific nodalization of the problem by comparing the predictions of the code with the real measurements. Therefore, one has to be aware of the fact that both the code and the LOFT-specific nodalization, normally used for pre- and post-test analyses, are somehow "LOFT-tuned" resulting in quite acceptable predicting capabilities.

To be sure of the code's predicting capability of abnormal situations in real power plants, two main conditions have to be fulfilled :

- the different models of the code have to be adequate for the problem
- the plant has to be nodalized adequately, such that main expected phenomena are simulated

For the verification and possibly also for the optimization of the different models of the code, comparisons of the results of "integral test" like LOFT may be not an appropriate

choice because possible deviations cannot be simply attributed to a specific model. Here, one should prefer the comparison with the results of "separate effect tests".

For the plant to be analysed an "adequate nodalization" is usually unknown and only some very rough criteria can be given to the code user. Consequently, the accuracy of a prediction may be strongly related to the "experience" of the user, a quite unsatisfactory conclusion.

To get a feeling, how the nodalization may influence the prediction of the code, Experiment LP-02-6 has been analysed with respect to the following questions :

- The general predicting capability of the code, i.e. how accurate the sequence of events of Experiment LP-02-6 is calculated by RELAP5/Mod2 cy36-02 in time and value, especially, if the code is able to predict the phenomena of bottom-up quenching during the blow-down phase of the experiment which has an important influence on the peak cladding temperature; in fact it limits the peak cladding temperature to a value of approximately 1000 K i.e. far away from the critical values.
- The influence of the nodalization (number of volumes, junctions and heat structures which describe the whole system) on the calculation, i.e. how the nodalization may influence the accuracy of the results obtained.

Therefore, in what follows, we shall analyse the LP-02-6 experiment by using the best estimate code RELAP5/Mod2 cy36-02 with different nodalizations of the LOFT system. Starting with a nodalization similar to the one used by the code developers at INEL (especially for the analysis of small break

LOCAs) we shall reduce the number of volumes, junctions and heat structures in the primary loop of the LOFT system to nearly half whereas the entire vessel stays nearly unchanged to meet the requirements of the given experimental axial positions in the core region, especially for the cladding temperature measurements. We shall further investigate on the influence of the coast down behaviour of the pumps by using both the rapid coast down as used e.g. in the LP-LB-1 experiment and by imposing the pump speed of experiment LP-02-6, as retrieved from the data tape.

Finally, we shall see, how the reduction of volumes and junctions will influence the computer time, needed to analyse the experiment, a question which is important from the financial point of view. On the other hand, in the framework of this contribution, no attempts will be made to improve models within the code.

Chapter 2

Nodalization Schemes Used to Analyse Experiment LP-02-6

The basis of all schemes of nodalization normally used for LOFT analyses are those developed at INEL for the RELAP5/Mod1 calculations of the small break Experiments LP-SB-1 to LP-SB-3. Similar schemes have been applied for the analyses of Experiment LP-SB-3 by Andreani and Grütter, ref. [4], as well as for all of the other LOFT post-test analyses initiated by the OECD- LOFT- Consortium and using RELAP5/Mod1 or -Mod2 codes.

This basic INEL LOFT nodalization scheme for the RELAP5/Mod1 as well as the -Mod2 code is divided in seven main parts which may be distinguished by their "capital component" numbers :

- (1...) Intact Loop
- (2...) Reactor Vessel
- (3...) Broken Loop
- (4...) Pressurizer
- (5...) Steam generator,
secondary side
- (6...) ECC system
- (7...) Containment
(suppression tank)

Similar to our LP-LB-1 calculations (ref. [7]), the ECC systems, the containment and the reactor vessel remained quite unchanged

for the different nodalizations discussed in due course, whereas the steam generator primary and secondary sides, the pressurizer as well as intact and broken loops have been undergone drastic reductions with respect to the initial number of volumes and junctions resulting in reduced computer time and simplification of the problem.

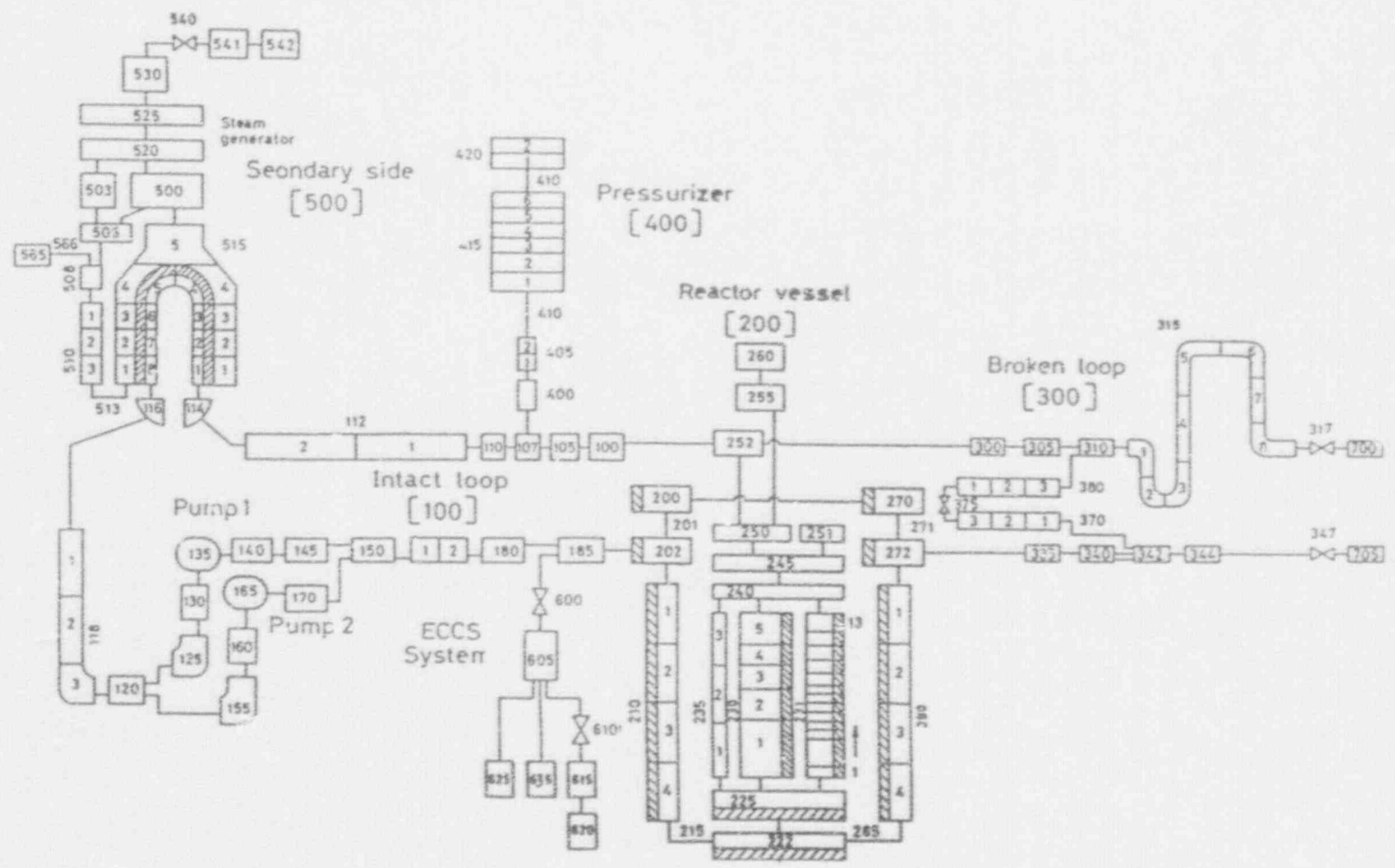
2.1 Standard Nodalization

Let us start with the "standard nodalization" (later on marked by 2-00...) which, compared to the above mentioned INEL-schemes, only has slightly modified to better meet the requirements of the large break experiment LP-02-6, especially in the core region (Fig. 2.1).

The REACTOR VESSEL consists of the reactor core, of the intact and broken loops downcomer sections (volumes 200 to 210 and 270 to 280 respectively), the lower plenum (220 to 225) and the upper plenum with the vessel dome (240 to 260).

The REACTOR CORE itself has been modeled by three parallel channels, the average channel (230) subdivided into 5 hydrodynamic volumes, the hot channel (231)

Figure 2.1: Nodalization 2-00 of the LOFT system (most detailed version; similar to EG&G nodalization)



subdivided into 13 volumes and the bypass channel (235) into three equally spaced volumes. In Fig. 2.2, a separate scheme illustrating the nodalization of the active core has been given. Here, the hydrodynamic volumes are not equally sized and they were dimensioned so that the "reference thermocouple location" (cladding temperature measurement indicated by arrows) are always located nearly in the axial center of the requested volume.

The hot channel represents the center part of the core (mainly fuel-assembly 5) and contains 219 pins, the remaining 1081 pins are assigned to the average channel. The axial linear heat flux distribution was chosen according to ref. [5].

The total mass-flow through the core is shared approximately 79% by the average channel, 16% by the hot channel and the remaining 5% by the bypass. Note that the mass-flow distribution in the core region is somehow arbitrary. The choice of these values is based on the relation of the pin numbers associated with each of the channels (arbitrary!) minus the bypass flow which is again an estimated parameter. No cross-flow has been assumed between the three channels, because preliminary runs using the crossflow option had shown that the amount of mass exchange in traverse direction remained negligible during the whole transient.

The fuel pins have been modeled by heat structures each radially meshed into 5 (average channel) and 10 nodes (hot channel) respectively. In the "average pin", one zone represents the cladding, one the gap and two the fuel. For the "hot channel", there are 3 cladding zones, one gap and 5 fuel zones. In case of reflooding, the code performs an axial finemeshing for better modelling the advancement of the quench front. The maximum number of allowable fine meshes has to

be preset. Because the preliminary investigations using different mesh numbers did not show significant differences between the results of runs using different preset numbers (see ref. [7]), for the sake of saving computer time, we normally have used a low number of fine meshes, namely 4 in the average channel and only 2 in the hot channel for the calculations presented in this report.

The INTACT LOOP consists of 20 volumes with 2 or 3 subvolumes. As in the actual LOFT system, the pumping system is divided into two pump lines with two individual pumps numbered 135 and 165 respectively. The ECC-injection is connected to the cold leg of the intact loop (volume 185). In addition to the usual ECC line valve (600), an supplementary control valve (610) has been inserted in the accumulator line to close this line when the accumulator is empty. This happens to be necessary in order to continue with the calculation. Probably due to the fact that the version RELAP5/Mod2 cy36-02 used for these calculations was not able to handle noncondensibles, the transient always was terminated by an execution error when the accumulator was just emptied and Nitrogen was released into the system.

The STEAM GENERATOR consists of 8 volumes on the primary and 5 volumes on the secondary side. A simplified feed, back-flow and steam separator modeling as well as a steam flow control valve and condenser unit complete the nodalization of the secondary side. The steam flow valve is controlled by a control logic which allows to keep the secondary side pressure constant. Heat is exchanged from the primary to the secondary side of the steam generator via the wall which is modeled by 8 heat structures each having 7 radial zones (8 nodes).

The PRESSURIZER is composed of the surge line (2 volumes) and the entire pressur-

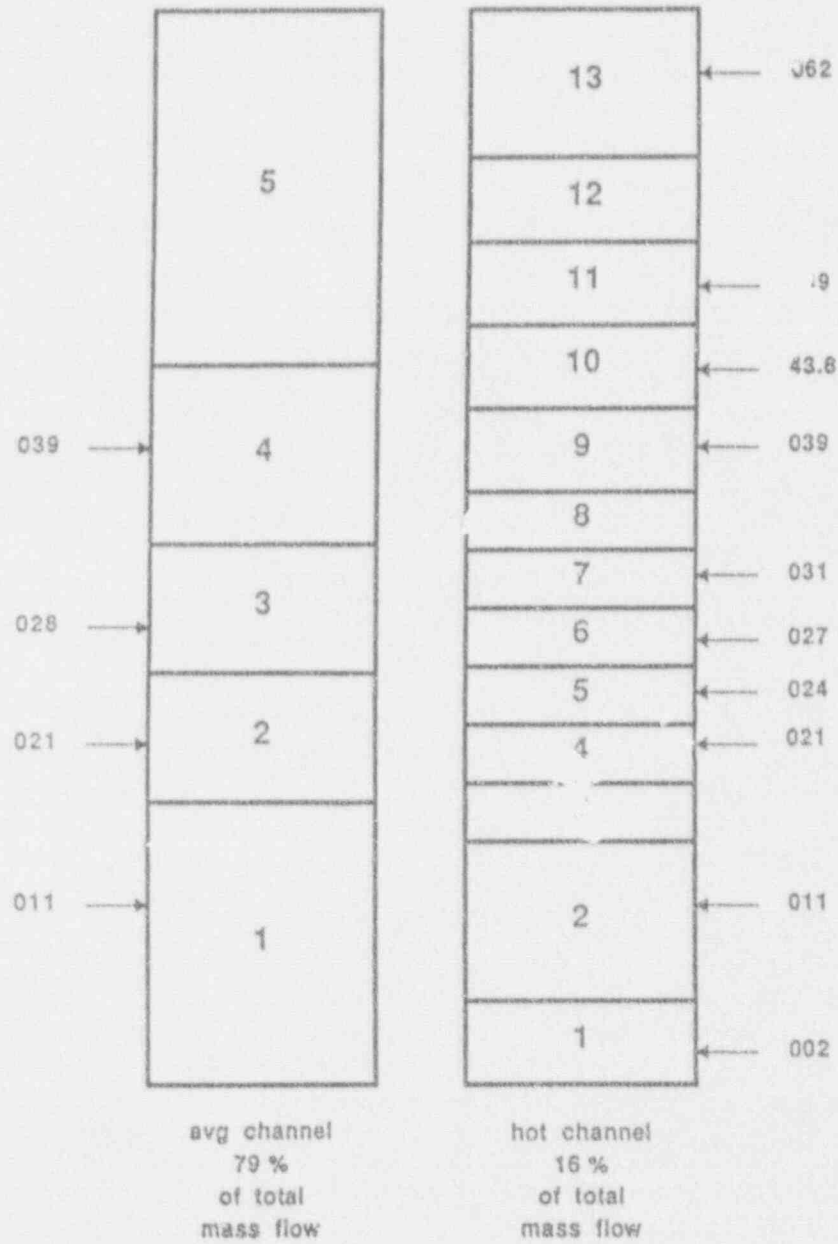


Figure 2.2: Detail of the nodalization of the LOFT core (average and hot channels)

izer. The latter is nodalised by a pipe component (6 subvolumes) which represents the main vessel, and another pipe (2 subvolumes) which describes the pressurizer dome.

The BROKEN LOOP consists of two individual lines. The hot line has been nodalised by 3 volumes (300 to 310) and one pipe component (315), representing the steam generator simulator. The cold line is consisting of 4 volumes (335-344). At the end of each lines, the two break-valves which have to be opened by a trigger signal are placed and connected with the suppression tank, modeled here by two time-dependent volumes (pressure is a function of time).

For preheating the broken loop, a bypass line exists between volumes 310 and 342. This bypass line has been nodalised by two pipe components. In our calculations, the connecting valve (375) remained always closed.

Not included in Fig. 2.1 are some additional control-valves and heat structures, especially for the pressurizer which are only necessary for steady-state runs to force the system to a stable stationary solution at the desired thermal conditions like circulation mass-flow, core-inlet and core-outlet fluid temperatures, liquid level in the pressurizer, etc.

Because of the rather fast transient of a large break LOCA (the total duration of the transient is about 100 seconds), heat capacity effects of the piping walls, vessel walls and other structures in thermal contact with the coolant, may not play an important role. Consequently, for the sake of saving computer time, in the normal versions of nodalization, heat structures were used only for modeling the heat generation in the reactor core and for the heat transfer from the primary to the secondary side of the steam generator. For some

runs, the influence of the heat capacity of the reactor vessel on the transient behaviour of the thermal-hydraulic parameters of interest has been investigated and therefore, some additional heat structures have been inserted in the downcomer and the lower plenum of the reactor vessel (heat-structures 200-210, 220, 222, 225 and 270-280); these runs are marked by an additional "C" to the nodalization number (e.g. 2-00C).

In contrary to LOF1-experiments L2-5 and LP-LB-1 where the main circulation pumps have been disconnected both from power as well as from their flywheels to enable rapid coastdown, in Experiment LP-02-6 the pumps have been switched off only but remained connected to their flywheels. This has led to a much slower coastdown of the pump-speed. To investigate the influence of the pump-speed (and consequently pump-head) on the accuracy of the calculations, in the Mk. 2-00 and 2-00C versions of nodalization we have allowed a rapid coastdown of the pumps similar to the L2-5 and LP-LB-1 experiments whereas for the 2-00PU and 2-00PU,C versions we have superimposed the time-dependent pump-speed curve as measured during the experiment; we have used the average value of the two individual pump speeds.

2.2 Stripped Nodalizations

To investigate the influence of reduced number of volumes and junctions on the accuracy of the analysis as well as on a probable saving of computer time, the number of junctions and volumes of the standard nodalization has been drastically reduced.

A scheme of the first stripped version, the nodalization 3-00, is shown in Fig. 2.3. The main changes have been made in the pressurizer, the intact- as well as in the broken loops and on the secondary side of the steam generator, whereas the reactor vessel and the ECC-system remained nearly unchanged.

With respect to nodalization 2-00, the REACTOR CORE remained nearly unchanged. The nodalization differs only in the maximum number of allowable fine meshes during reflooding; this number has been increased from two to eight in the hot and from four to 16 in the average channels.

The INTACT LOOP now mainly consists of three pipe sections (110, 120 and 150 with four, seven and six subvolumes respectively), only one pump component instead of two (but of course, with the same pump-head) and a steam generator primary side with six instead of the previous 8 subvolumes.

The BROKEN LOOP consists of only two pipe systems (310 and 330) with 11 and 4 subvolumes respectively. Since the bypass-valve (see component 375 in Fig.2.1) is always closed, in this stripped version of nodalization, the whole bypass-line has been omitted. Consequently, possible mass and heat capacity effects in this line are neglected.

The whole PRESSURIZER system (vessel and surge-line) has been reduced to one pipe component with four subvolumes only.

The SECONDARY SIDE of the steam generator and the attributed system has been undergone drastic reductions. In principle, the steam generator has been turned into a simple heat exchanger with single-phase flow on the secondary side. The flow is simply controlled by a time-dependent junction (566) and dumped into an outlet volume (542). To maintain correct primary side inlet and outlet conditions, the mass flow has been adjusted to quite higher values than for the real steam

generator conditions where the evaporation of the water is the main heat sink.

The wall between the primary and secondary side of the steam generator has been modeled by six heat structures each radially divided by three zones.

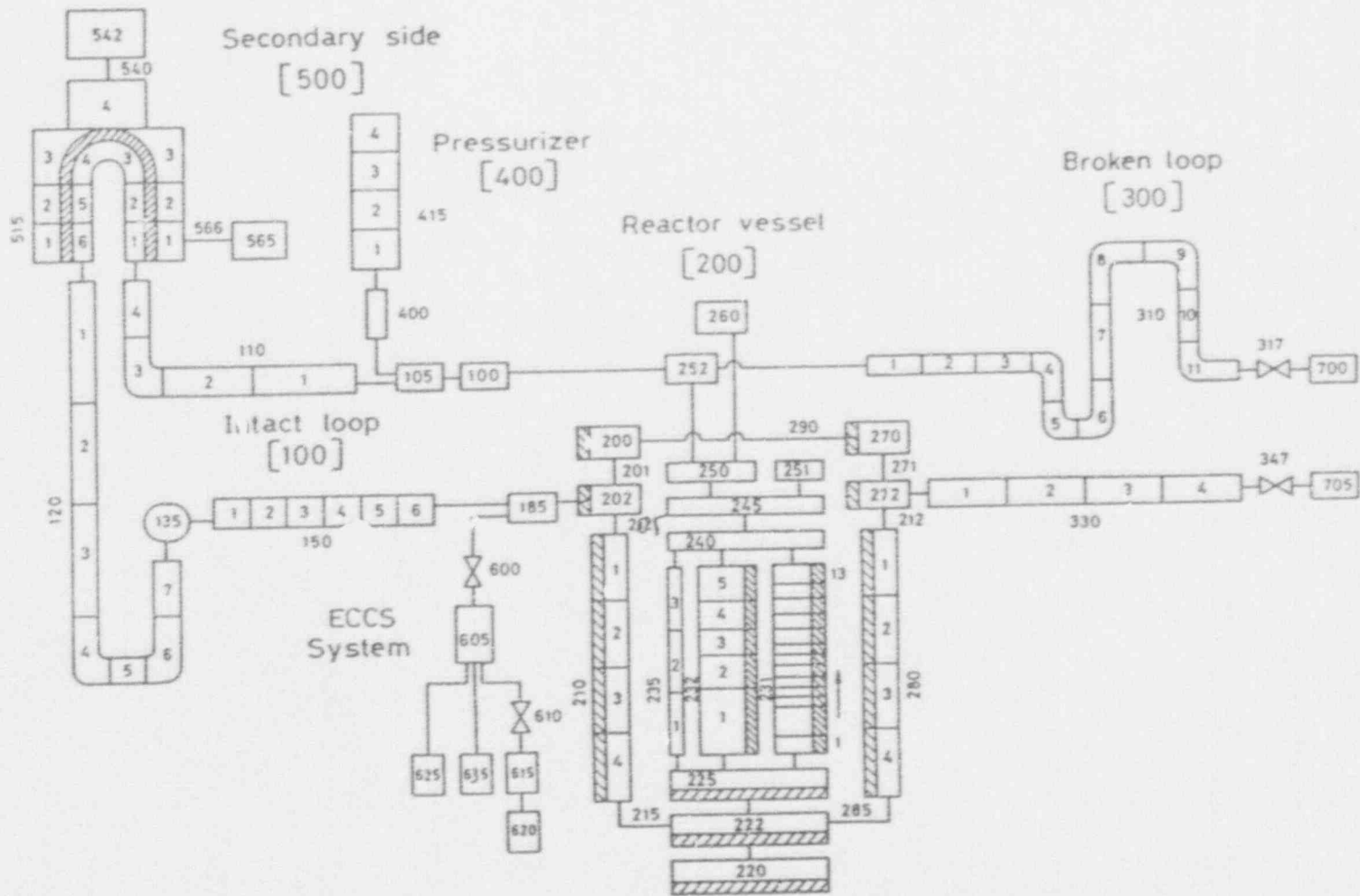
A derivative of nodalization 3-00 is the version 3-005 which differs from it in having a higher number of allowable fine-meshing during reflooding, namely an increase from 4 to 16 for the average and from 2 to 8 for the hot channel. The additional version 3-005T is identical to the version 3-005 except that the reflood option of the code is initiated externally; we shall come to this feature in due course.

The reduced nodalization 3-00 can be stripped even more by simply reducing the subvolumes of each of the pipe components; for the pipe 110 to two, for pipe 120 and 310 to three and for pipe 150 and 330 to only one subvolume each. The nodalization of the steam generator has been reduced to only two on both sides but the radial meshing of the related heat structures remained at three nodes (fig. 2.4).

The maximum number of fine meshes of the heat structures of the core during reflooding has been reduced again to two in the hot and to four in the average channels. This very much reduced nodalization is called 3-02.

Except version 3-005T, the stripped versions have been used with and without heat capacity contribution in the vessel component, as described above. For all stripped down versions of nodalization, the time dependent pump speed has been used.

Figure 2.3: nodalization 3-00 (3-005) of the LOFT-system
 (simplified nodalization; core remained unchanged)



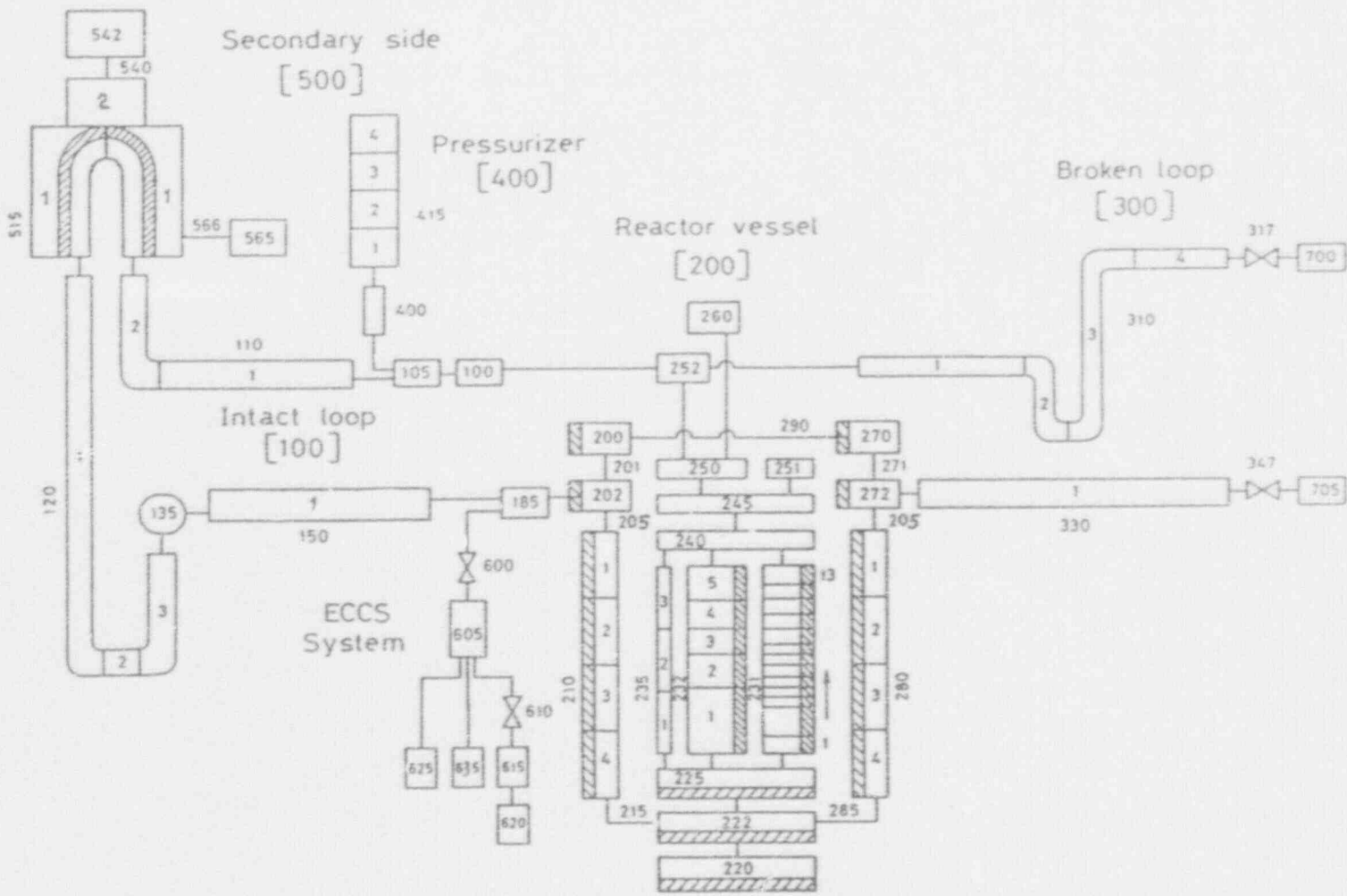


Figure 2.4: nodalization 3-02 of the LOPF system (most simplified version; core remained unchanged)

Table 2.1: Numbers of volumes, junctions, heat-structures and fine-meshes as well as the resulting Real-Time-Multiplier RTM

NAME	HYDRODYNAMICS				HEAT STRUCTURES				RTM0
	number of volum.	number of junct.	primary side mass to	primary side volume m ³	secondary side mass to	secondary side volume m ³	number struct./ meshp.	number finemesh avg/hot	
2-00 ¹	133	139	6.8	9.9	2.3	11.4	26/219	4/2	26.2
2-00C ²	133	139	6.8	9.9	2.3	11.4	41/296	4/2	27.6
2-00PU ³	133	139	6.8	9.9	2.3	11.4	26/219	4/2	25.0
2-00PUC ⁴	133	139	6.8	9.9	2.3	11.4	41/296	4/2	28.9
3-00 ⁵	101	103	6.6	9.6	1.6	1.9	24/173	4/2	(32.3) ⁶

$${}^0 RTM0 = [CPU(t_{end}) - CPU(t_{begin})] / [t_{end} - t_{begin}]$$

¹ Rapid pump coastdown similar to experiment LP-LB-1

² Rapid pump coastdown similar to experiment LP-LB-1

³ Pump-speed is controlled by table inferred from LP-02-5 experimental data

⁴ Pump-speed is controlled by table inferred from LP-02-6 experimental data

⁵ Reduced number of volumes in intact loop, broken loop and pressurizer

⁶ Abnormal termination of this calculation at 52.051 s of the transient just before accumulator has been nearly emptied. RTM0 only takes into account 52 seconds of the transient. (results of this calculation only partially have been used in this report)

Table 2.1: ... cont.

NAME	HYDRODYNAMICS				HEAT STRUCTURES		RTM0		
	number of volum.	number of junct.	primary side mass volume to m ³	secondary side mass volume to m ³	number struct./ meshp.	number finemesh avg/hot			
3-005 ⁷	101	103	6.6	9.6	1.6	1.9	24/173	16/8	21.1
3-005T ⁸	101	103	6.6	9.6	1.6	1.9	24/173	16/8	21.1
3-00C	101	103	6.6	9.6	1.6	1.9	39/248	4/2	21.8
3-02 ⁹	74	76	6.6	9.6	1.6	1.9	26/161	4/2	13.7
3-02C	74	76	6.6	9.6	1.6	1.9	35/236	4/2	(24.5) ¹⁰

⁷Same as 3-00 but number of fine meshes increased from 2 to 8 (hot) and 4 to 16 (avg.)

⁸Same as 3-005 but with reflooding option tripped by level dependent external trip (fluid level in channel less than 0.1 m)

⁹Same as 3-00 but with even more reduced number of volumes and junctions in the intact and broken loops as well as on the steam generator secondary side

¹⁰Abnormal termination after 42 seconds of the transient due to "water property error" (RTM0 only takes into account 42 s)

Finally, in table 2.1, characteristic parameters of the different nodalizations (e.g. number of volumes, junctions and heatstructures, mass inventory of primary and secondary sides as well as the corresponding system volumes) used for this study have been listed. Included in table 2.1 are the average "Real-Time-Multipliers" RTM0 which are the quotient of the CPU time (on a CYBER-855 machine) divided by the duration of the analyzed transient; the RTM0 should illuminate the effect of nodalization from the economical point of view.

Chapter 3

Results

Starting from thermal-hydraulic conditions very close to the ones given in table 2.1, total of ten calculations of the LOFT-experiment LP-02-6 each lasting 120 seconds have been performed using the code RELAP5/Mod2 cy36-02 with different nodalization schemes described in chapter 2.

In our understanding, with respect to reactor safety one set of "key-parameters" of a large break calculation are mainly the time behaviours of the cladding temperatures at different axial positions (peak temperature, as well as the duration of being over a certain temperature level, which may cause partial zircaloy-water reaction) and with minor importance the peak fuel temperatures. Because the reactor was scrammed after a very short time from the initiation of the experiment, the center fuel temperatures seldom exceed the values of normal operation at full power. Consequently, we shall focus on the time behaviour of the cladding temperatures. But even a satisfactory agreement between the experimental and the calculated cladding temperatures or between other significant parameters of the experiment like pressures densities or mass-flows should not automatically lead to the conclusion that the code predictions are accurate and RELAP5/Mod2 perfectly has done its job. Because one may argue that the code has given "right answer for the wrong reasons", i.e. a satis-

factory calculation of the time behaviour of the cladding temperatures could be the result of an "optimized summation" of individual errors. Therefore, one has to look carefully if the code has accurately described the main phenomena occurring during the experiment. Consequently, one has to investigate in detail the time traces of the other thermal-hydraulic parameters of importance as well.

In what follows, we would like to start with some words on the updating of the experimental data especially on the averaging process of some temperature traces and of the power (neutron flux data).

The discussion of the results of the calculations we shall start by looking at the influence of the nodalizations on computer time and mass errors.

Second, we shall discuss the capability of RELAP5/Mod2 to predict significant events of the experiment like peak cladding temperatures (value and time of their occurrence), the time when pressurizer and accumulator empties as well as the positions of the quench front during the reflood period of the experiment.

Third, we shall analyse additional thermal-hydraulic parameters of the LOFT-plant as given by RELAP5/Mod2, starting with the time behaviour of our "key parameters"

(cladding and center fuel temperatures) and we shall compare these results with the corresponding data of Experiment LP-02-6, if available.

Finally, in a separate section, we shall investigate on the question of how the code has modeled the bottom up quench occurring during experiment between five and ten seconds of the transient. This early bottom-up quench has had a very important influence on the time behaviour of the cladding temperatures because it has limited their peak values to temperatures not higher than 1000 K at the hot spot during both the blowdown and the refill phases.

3.1 Experimental Results

The experimental results have been retrieved from the LOFT-transmittal tape. For most of the experimental values only one set of data is available except for the temperature data in the core region, the neutron flux and a few other variables.

The uncertainty of most of the experimental data can be found in table VI of the "Transmittal Tape Description" (ref. [9]). We have used the values listed there for giving the respective transducer uncertainties on each individual plot, if possible.

No problems occur when averaging the four power channels to get the instantaneous power trace of the reactor. But difficulties may occur in using the surface temperature traces at the different core heights of the "hot bundle" 5, only when these values are averaged. In Figs. 3.1a and 3.1b, the temperature traces of all the available thermocouple signals at one specific level have been plotted for level 27 (27 inches from the bottom of the core) and for level 31. We have selected these two examples because at level 27 the high-

est surface temperatures have been measured during the experiment, whereas the code predicted the highest temperatures at level 31.

In Fig. 3.1a, the traces of 10 thermocouple signals at core level 27 have been plotted. Whereas six of them behave quite similar, the other four have undergone additional heat-up and quench cycles which would lead to a lower "average temperature". When computing the "reference temperature", we have omitted these four signals; the resulting reference temperature is indicated by squares. In addition to their different time behaviour, the thermocouples have indicated different peak cladding temperatures during the blowdown interval of the experiment, the temperatures ranged from about 930 to 1070 K. All thermocouples have quenched for the first time nearly at the same time due to the bottom-up reflooding, nearly 8 seconds after opening of the break valves.

In Fig. 3.1b, the time behaviour of the seven thermocouples at level 31 have been plotted. Again, at least two of these sensors have indicated cyclic heat-ups in the time interval between 10 and 50 seconds. The variation of the different peak cladding temperatures ranges only about 65 K (935 K to 1000 K). All thermocouples at this core height indicated quenching at nearly the same time during the bottom-up reflooding, namely between 7 and 8 seconds. With one exception, also the final quench occurred at nearly the same time; the average temperature out of the 5 similar thermocouple signals (the two "cyclic" ones have been omitted) has been indicated by uparrows and is used as reference temperature.

In addition to the problem of averaging, the uncertainty of the temperature measurement itself is not fully established yet. Because the thermocouples of the LOFT facility were surface mounted ones, there are still some

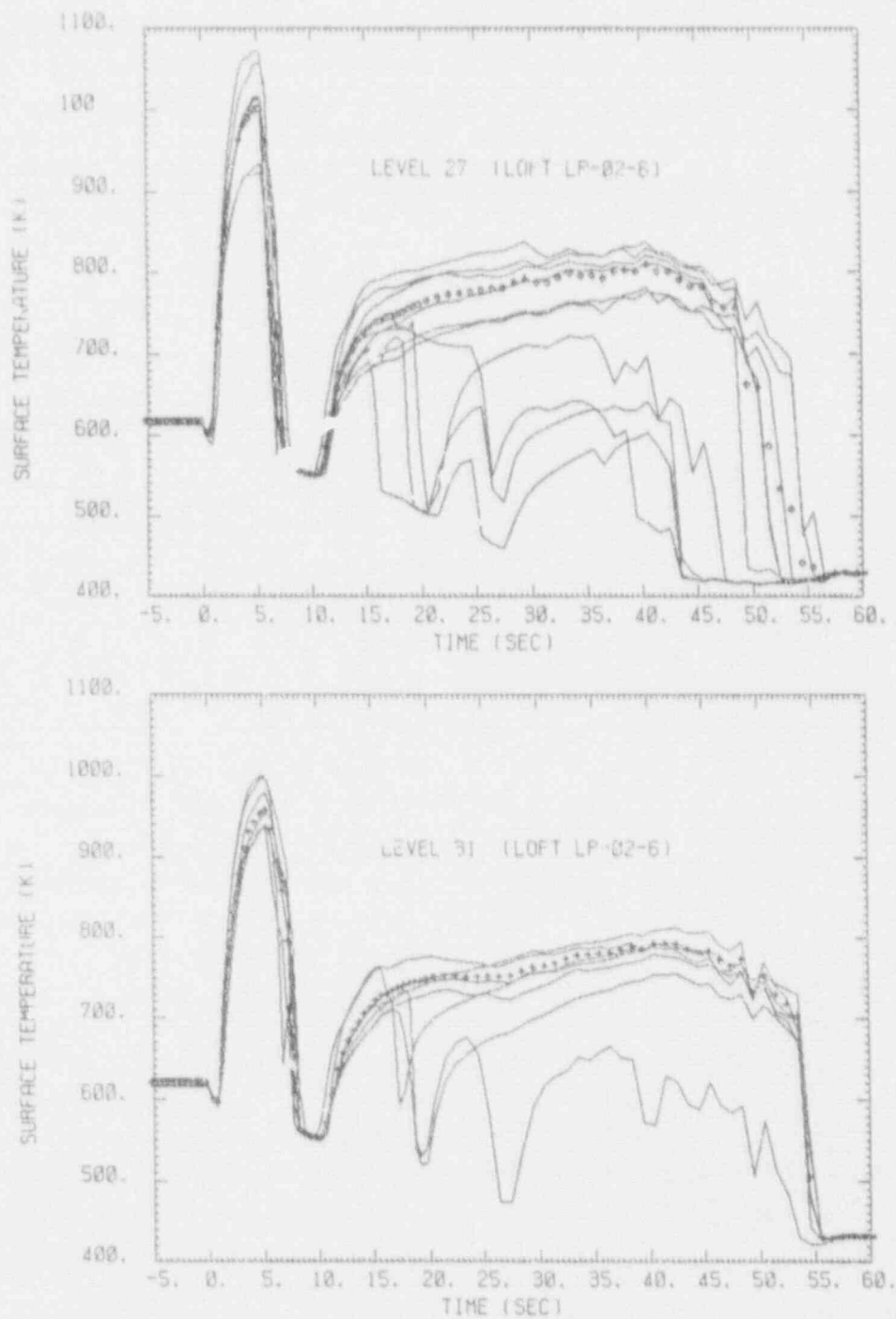


Figure 3.1: Measured cladding temperatures in center bundle 5
(averaged values (symbols) used as reference)

- a.) axial level 27
b.) axial level 31

doubts whether these thermocouples always measure the temperature of the surrounding cladding material and are not quenched in advance by impinging water (ref. [10]).

3.2 Influence of the Nodalization on Computer Time and Mass Error

Starting with the influence of the nodalization on the computer time and disregarding the accuracy of the predictions themselves for the present, a first look to the RTM0s in table 2.1 will lead to the conclusion that a severe reduction of the number of volumes and junctions will usually lead to a significant decrease of the computer time consumption, e.g. the comparison between cases 2-00C and 3-02 indicated a reduction of nearly 20%.

A more detailed analysis of the computer time needed to analyse the LOFT LP-02-6 experiment is shown in table 3.1. Here, the transient times have been subdivided into nine time intervals, the stationary part from -10 to zero seconds, the initial blowdown part (zero to 1 s) two entire blowdown parts (1 to 5 s) and (5 to 25 s), three reflood intervals (25 to 30 s), (30 to 40 s) and (40 to 60 s) with the starting sequence of the Emergency Core Cooling System (ECCS) during the first of these intervals (i.e. the feed of cold water out of the accumulator, the Low Pressure Injection System (LPIS) and the High Pressure Injection System (HPIS) into the saturated fluid of the intact loop) and finally a more stationary interval (60 to 120 s).

The reduction of the computer time due to a reduction of volumes, junctions and heat structures became mostly significant within the first and the last two time intervals, i.e. in the more or less stationary part of the tran-

sient; in addition, also the interval immediately after the opening of the break where the scram of the reactor has taken place is characterized by a rather low consumption of computer time.

The relatively low RTM-values during the more or less stationary parts of the transient have been somehow compensated during the second blowdown (5 to 25s) and the first and second reflood interval (25 to 40 s) where large number of numerical instabilities may occur due to a great degree of thermodynamic non-equilibrium in the intact cold leg and downcomer region mainly caused by the injection of cold water of the ECC system into the saturated fluid inside the intact cold leg.

A visualization of the table 3.1 has been presented in figs. 3.2a and 3.2b where the RTM-values for the different nodalizations have been plotted versus the experimental time.

In Fig. 3.2a, the RTM values are shown for the case of all the nodalizations which are not taking into account heat capacity effects (normal nodalization). One easily recognizes very strong instabilities of all the calculations in the interval 30 to 60 seconds probably due to high non-equilibrium of the two-phase flow i.e. due to cold water injection out of the accumulator into the saturated flow of the intact loop cold leg. High non-equilibrium leads to the above mentioned relatively high RTM-value in this interval of the transient. The overall benefits of the simplified versions of nodalization can well be noticed in the time regions -10 to 30 seconds and 70 to 120 seconds.

In Fig. 3.2b, the RTM-values for all the C-versions have been plotted (i.e. the versions of nodalization where the heat capacity effects of the wall material of the vessel have been taken into account). Here, compared to

Table 3.1: RTM values in different intervals of the transient

$$RTM_{interval} = [CPU(t_2) - CPU(t_1)] / [t_2 - t_1] \quad (\text{computer : CYBER-855})$$

Time interval		Nodalisation									
		2-00	2-00C	2-00Pu	2-00PUC	3-00	3-005	3-005T	3-00C	3-02	3-02C
-10	- 0	17.6	18.1	17.6	18.2	12.7	12.9	12.9	13.1	9.7	10.1
0	- 1	13.8	14.2	13.8	14.0	9.7	10.3	10.5	10.5	8.9	9.3
1	- 5	17.7	21.1	17.9	18.8	19.6	12.8	12.8	13.1	7.1	7.6
5	- 25	34.5	36.9	34.7	36.2	26.9	27.0	28.6	29.4	10.5	12.5
25	- 30	62.4	67.3	34.0	39.0	28.5	26.3	26.1	28.9	21.2	27.6
30	- 40	43.0	43.5	39.4	55.0	33.2	35.2	32.4	31.2	34.4	31.5
40	- 60	43.3	42.2	42.9	47.6	— ¹	40.2	35.9	38.4	32.5	— ²
75	- 120	12.4	13.7	13.2	15.7	—	10.2	9.6	11.5	5.2	—
-10	- 120	26.2	27.6	25.0	28.9	(32.3)	21.1	19.9	21.8	13.7	(24.5)

¹Abnormal termination of transient after 52.1 s due to water property error

²Abnormal termination of transient after 40.7 s due to water property error

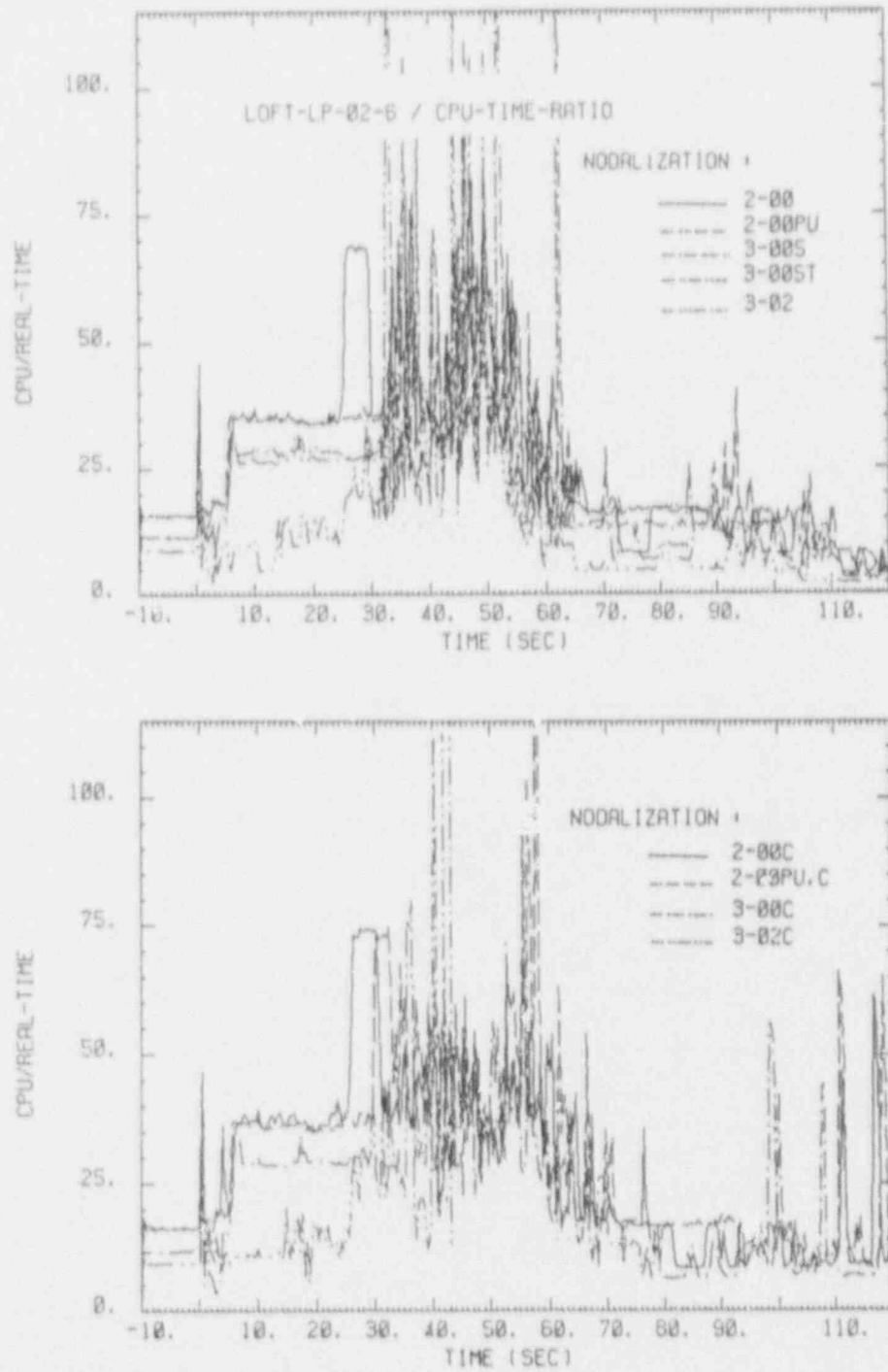


Figure 3.2: CPU-time to Real time ratio vs. time
 a) by neglecting wall heat capacity
 b) by taking into account wall heat capacity ("C")

fig. 3.2a, the large number of oscillations in the region of 30 to 60 seconds are somehow slightly dampened.

In both plots, the very narrow first peaks at nearly zero seconds are probably due to the thermodynamic non-equilibrium during the subcooled blowdown phase which only lasted some hundreds of milliseconds after the opening of the break valves.

A second basic criteria for the quality of a certain nodalization is the "mass error" which is a measure for the numerical accuracy of the code because it represents a check of the mass balance in all of the system volumes. Therefore, in Figs. 3.3a and 3.3b, the mass errors have been plotted versus the experimental time for all the calculations using different nodalizations, referred to in table 2.1. In general, quantitatively no significant differences have been found between the results with the normal and the "C" nodalizations. The absolute value of the mass error never exceeded values of 1.4 kg and for most of the transient time remained less than 0.6 kg. In any case, because the total mass inventory of the LOFT system is in the order of 7 tons, a "numerical loss" of not more than two kilograms is negligible.

3.3 Discussion of the Code-Predictions of the Main Events

Before starting the discussion of the performance of RELAP5/Mod2 in calculating the main events of the experiment, first, in Fig. 3.4 a graphic representation of the main trip setpoints has been plotted where a value of nearly one indicates that the trip is set. The scheme divides the experiment in several

characteristic sections. Shown here are the settings of the break valves, which opened at zero seconds, the power-trip at 0.13 seconds (difficult to distinguish from the break valve line) and the pump-trip at 0.63 seconds. The behaviour of the ECC-system is indicated by the —...— line. For the accumulator, its value is 0.4, for LPIS 0.35 and for HPIS 0.25. The accumulator started injection at 17.5 seconds, followed by HPIS at 21.8 seconds (trip value 0.65). Finally, the LPIS has started at 34.8 seconds (trip value equals 1). The trip curve falls back again to 0.6 when the accumulator has emptied at nearly 58 seconds (the exact time is slightly depending on the nodalization of the problem) and LPIS and HPIS remained functioning.

In Table 3.2, some main events have been listed and their occurrence during the experiment (time and value) have been compared to the equivalent code results using the different nodalizations as given in table 2.1. The setpoints of the different trips are again listed in table 3.2. First, one should notice that in contradiction to the experiment where both the reactor power and the accumulator injection have been initiated by an actual pressure-dependent setpoint, for the calculation we have used a time-dependent setpoint retrieved from the experiment thus avoiding a multiplication of errors (if the pressure is predicted wrong, this error will heavily influence the predictions of the other parameters in the following time sequences).

3.3.1 Calculation of Mass Flows in the Broken Leg

We start our comparison with the broken loop and have to look at the peak mass-flow rates as well as at the end of the subcooled break flows in the hot and cold legs.

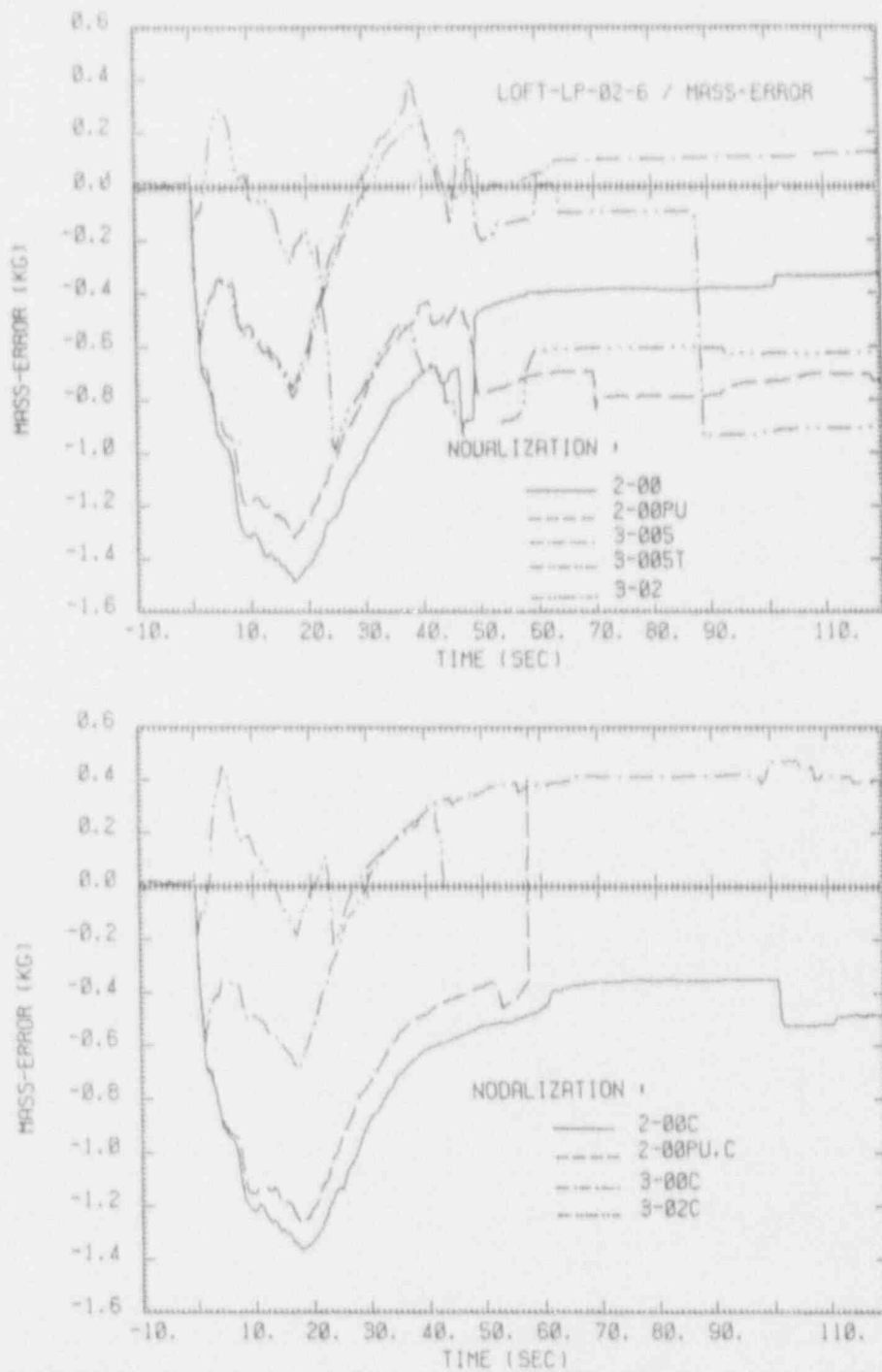


Figure 3.3: Mass error as defined by RELAP5/Mod2 vs. time
 a) by neglecting wall heat capacity
 b) by taking into account wall heat capacity ("C")

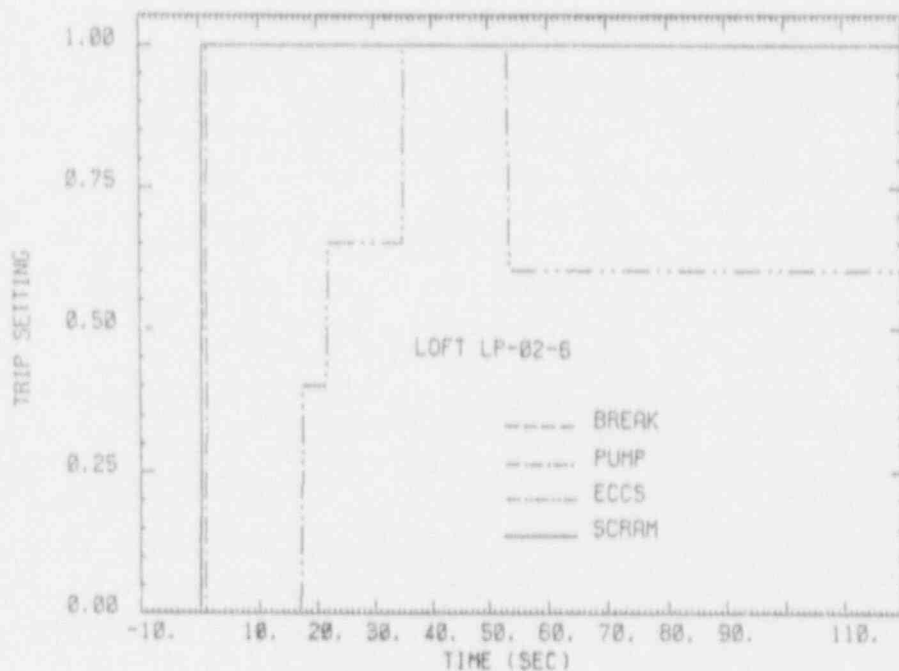


Figure 3.4: Trip setpoints for experiment LP-02-6

For all of the different runs, the end of the subcooled break flow in the hot leg lies between zero and one second. In the cold leg, the end of subcooled break flow occurs between 3.0 and 4.2 seconds, slightly depending on the selected nodalizations; the smallest values have been predicted by the 3-02 nodalizations where the cold leg is represented by only one single volume thus invalidating a correct positioning of the measurement station.

For all the nodalizations, the peak value of the mass-flow has occurred at the first printed time step after initiation of the transient (0.4 s) and has to be compared to a reference value measured at 0.25 seconds of the transient. All the nodalizations except 3-02 and 3-02C produce very similar peak values of 562 kg/s from the cold leg and 166 kg/s from the hot leg which are quite close to the measured values of 550 kg/s for the cold leg and 193 kg/s for the hot leg. It should be

noted that the most detailed versions 2-00, 2-00C, 2-00PU and 2-00PU,C indicated only 124 kg/s. Even for the nodalizations 3-02 and 3-02C with their strongly simplified piping in the intact and broken loops, the peak values for the cold leg is in quite good agreement with the experimental data (573 kg/s) whereas this value for the hot leg is about 50% higher than in all the other runs (290 kg/s).

As a general trend, it can be observed that a simplification of the piping of the broken loop tends to give higher predictions of the peak break flows, especially in the hot leg. The most complex 2-00 nodalization underpredicted the peak values about 30% whereas the most simplified 3-02 versions overpredicted it about 50%. On the other hand, one has to keep in mind that two-phase flow mass flow measurements both under stationary and transient conditions are increasingly difficult tasks because the mass

EVENT	MEAS. DATA		RELAP5/Mod2 CALCULATIONS									
	Q	unit	2-00	2-00PU	3-00	3-005	3-005T	3-02	2-00C	2-00PUC	3-00C	3-02C
Blowdown valves open	T	s					set by time trip					
Reactor scrammed ¹	T	s	0.0				set by time trip					
Stop coolant pumps	T	s	0.13				set by time trip					
Start accumul. inject. ²	T	s	0.8				set by time trip					
Start HPIS	T	s	17.5				set by time trip					
Start LPIS	T	s	21.8				set by time trip					
	T	s	34.8				set by time trip					
End of subc. break flow	T	s	3.25	4.2	4.2	4.2	4.2	4.2	4.2	4.2	4.2	4.2
cold leg	T	s	0.75	0.3	0.6	0.6	0.6	1.0	0.2	0.6	0.2	1.0
hc. leg												
Peak mass flow	T	s	0.25	0.4	0.4	0.4	0.4	0.4	0.4	0.4	0.4	0.4
broken loop _{cold leg} ³	V	kg/s	549.7	561.2	562.5	562.5	562.5	573.0	561.2	561.2	562.4	573.2
broken loop _{hot leg} ³	T	s	0.25	0.4	0.4	0.4	0.4	0.4	0.4	0.4	0.4	0.4
	V	kg/s	193.0	124.4	166.3	166.3	166.3	290.0	124.4	124.4	166.3	289.6

⁰Symbol in the Q-row stands for T=time and V =value

¹During the experiment tripped by system pressure signal

²during the experiment tripped by system pressure signal

³Differences may be due to different time steps of the measurement and the calculation

Table 3.2: Comparison of characteristic parameters inferred from experiment with equivalent RELAP5/Mod2 -results of different nodalizations

EVENT	RELAP5/Mod2 CALCULATIONS											
	2-00	2-00PU	3-00	3-005	3-005T	3-02	2-00C	2-00PUC	3-00C	3-02C		
	Q	unit	MEAS. DATA									
break mass loss (5 s) (10 s) (30 s) (70 s) (120 s)	V	ts	2.35	2.40	2.41	2.41	2.41	2.51	2.35	2.40	2.40	2.53
	V	ts	3.37	3.47	3.43	3.43	3.43	3.53	3.35	3.46	3.42	3.56
	V	ts	5.07	5.12	4.95	4.95	4.96	4.99	5.05	5.16	4.96	5.07
	V	ts	5.20	5.20	—	4.93	4.95	4.93	5.38	5.38	5.13	— ⁴
	V	ts	5.14	5.14	—	4.87	4.89	4.87	5.32	5.38	5.14	—
Peak mass loss _{total} ⁵	T	s	41.6	39.6	—	33.6	35.2	31.2	48.4	46.4	45.0	—
	V	kg	5.26	5.26	—	4.98	5.02	5.00	5.41	5.43	5.18	—
Minimum collapsed liq. lvl. reached (hot chann.) (average chann.)	T	s	7.2	4.4	4.8	4.8	5.2	4.0	6.8	4.4	4.8	4.0
	V	%	3.9	7.3	6.6	6.6	3.2	4.5	3.9	7.4	6.4	5.2
	T	s	7.2	4.4	4.8	4.8	5.2	4.0	6.8	4.4	4.8	4.0
	V	%	3.6	8.4	6.0	6.0	4.3	6.8	4.0	8.2	6.9	8.0

Table 3.2: ... cont.

⁴ Abnormal termination after 42.03 seconds of transient due to "water property error"⁵ Calculated integral Break losses reached a defined peak value because flow reversal occurred due to negative pressure difference between system pressure and suppression tank pressure⁶ no experimental value available

EVENT	MEAS. DATA		RELAP5/Mod2 CALCULATIONS											
	Q	unit		2-00	2-00PU	3-00	3-005	3-005T	3-02	2-00C	2-00PUC	3-00C	3-02C	
Pressurizer emptying ⁷ -pressure	T	s	15.5	14.4	14.4	17.6	17.6	17.6	18.4	14.4	14.4	17.6	17.6	
	V	MPa	7.4	7.85	8.29	4.01	4.01	4.01	3.46	7.9	7.9	4.1	3.7	
Accumulator emptying	T	s	56.5	55.2	54.4	52.1 ⁸	53.2	53.6	52.4	56.8	56.4	54.8	—	
Peak cladding temp. ^{9,10}	T	s	5.25	6.8	4.4	44.4	43.2	4.4	40.0	6.4	4.4	4.8	4.0	
	V	K	1074	1054	1026	1066	1066	1026	1050	1047	1026	1034	1017	
Blowdown peak cladding temperature ¹¹ in hot channel	level-02	T	s	3.3	7.2	4.4	5.2	5.2	4.4	4.0	6.8	4.4	4.8	4.0
		V	K	722	704	746	735	735	714	782	694	743	729	781
	level-11	T	s	4.8	7.6	4.4	5.2	5.2	4.8	4.0	7.2	4.4	4.8	4.0
		V	K	914	732	776	742	742	712	845	721	774	731	843
	level-21	T	s	4.8	6.8	4.4	5.2	5.2	5.2	4.0	6.4	4.4	5.2	4.0
		V	K	1037	1003	977	815	815	787	359	997	977	829	957

Table 3.2: ...cont.

⁷Empty point for the calculation is a pressurizer level less than 0.01 m

⁸Abnormal termination due to "water property error" when accumulator got nearly empty

⁹Experimental value at level-27. Indicated temperature is an average of thermocouples TE-J08-024 and TE-F08-024

¹⁰All predicted peak cladding temperatures at level-31

¹¹Reference value are averages of several temperatures inferred from thermocouple signals at the same axial level but different radial conditions

EVENT	MEAS. DATA		RELAP5/Mod2 CALCULATIONS									
	Q	unit	2-00	2-00PU	3-00	3-005	3-005T	3-02	2-00C	2-00PUC	3-00C	3-02C
level-24	T	s	4.9	4.4	5.2	5.2	5.6	6.0	6.4	4.4	5.6	5.6
	V	K	1024	994	788	788	765	872	1013	994	625	856
level-27	T	s	5.3	4.4	5.2	5.2	4.4	4.0	6.4	4.4	4.8	4.0
	V	K	1003	1018	1028	1028	1016	1006	1038	1018	1023	1004
level-31	T	s	5.3	4.4	5.2	5.2	4.4	4.0	6.4	4.4	4.8	4.0
	V	K	964	1026	1038	1038	1026	1018	1047	1026	1033	1017
level-39	T	s	5.3	4.0	5.2	5.2	4.4	4.0	6.0	4.0	4.8	4.0
	V	K	965	980	994	994	985	979	996	979	990	979
level-43.8	T	s	5.3	1.2	4.8	4.8	4.4	6.0	0.8	1.2	4.8	4.0
	V	K	861	741	929	929	923	863	787	750	926	857
level-49	T	s	5.3	1.2	0.8	0.8	0.8	4.8	0.8	0.8	0.8	0.8
	V	K	843	602	705	705	705	742	740	697	705	735
level-62	T	s	5.8	—	—	—	—	—	0.8	—	—	—
	V	K	719	—	—	—	—	—	697	—	—	—
in avg. channel level-11	T	s	4.5	4.4	5.2	5.2	4.8	4.0	6.8	4.4	4.8	4.0
	V	K	889	644	654	654	605	719	632	643	662	717

Table 3.2: ... cont.

EVENT	Q	unit	MEAS. DATA		RELAP5/Mod2 CALCULATIONS									
			2-00	2-00PU	3-00	3-005	3-005T	3-02	2-00C	2-00PUC	3-00C	3-02C		
level-21	T	s	3.8	4.4	5.2	5.2	4.0	4.0	7.2	4.4	4.8	4.0		
	V	K	728	676	691	691	650	711	658	675	668	712		
	T	s	5.3	—	5.2	5.2	—	4.0	7.2	—	4.8	4.0		
	V	K	899	—	672	672	—	701	648	—	675	709		
	T	s	5.3	—	—	—	—	4.0	—	—	—	4.0		
	V	K	849	—	—	—	—	695	—	—	—	709		
Partial bottom-up quench in hot channel	level-02	T	4.8	5.0	5.5	5.5	5.0	4.0	8.0	4.5	5.0	6.5		
	level-11	V	697	745	740	740	700	782	695	740	730	800		
	level-21	T	4.8	5.0	5.5	5.5	5.0	—	8.0	4.5	5.0	—		
	level-24	V	914	775	740	740	700	—	720	770	730	—		
	level-27	T	5.3	—	9.0	9.0	6.0	—	2.0	—	1.2	—		
	level-27	V	1035	—	782	810	785	—	620	—	780	—		
	level-27	T	5.3	—	9.0	6.0	6.0	—	—	—	1.2	—		
	level-27	V	1020	—	803	775	763	—	—	—	760	—		
	level-27	T	5.8	—	—	—	8.0	—	—	—	—	—		
	level-27	V	945	—	—	—	800	—	—	—	—	—		

Table 3.2: ... cont.

EVENT	MEAS. DATA		RELAP5/Mod2 CALCULATIONS									
	Q	unit	2-00	2-00PU	3-00	3-005	3-005T	3-02	2-00C	2-00PUC	3-00C	3-02C
level-31	T	s	6.3	—	—	—	—	—	—	—	—	—
	V	K	896	—	—	—	—	—	—	—	—	—
level-39	T	s	6.8	—	—	—	—	—	—	—	—	—
	V	K	890	—	—	—	—	—	—	—	—	—
level-43.8	T	s	6.8	1.5	—	7.0	—	1.0	—	—	—	—
	V	K	780	740	—	805	—	740	740	—	—	—
¹² level-49	T	s	15.3	1.0	—	1.0	4.8	1.0	—	1.0	7.0	—
	V	K	762	695	—	705	740	700	700	705	805	—
¹² level-62	T	s	14.3	—	—	—	—	—	—	—	3.5	—
	V	K	645	—	—	—	—	—	—	—	640	—
in avg. channel level-11	T	s	5.3	7.5	4.5	5.2	4.0	7.0	4.5	4.5	5.0	—
	V	K	867	630	635	655	720	630	645	660	620	—
level-21	T	s	5.3	7.5	4.5	5.2	4.0	7.0	4.5	4.5	5.0	—
	V	K	724	660	670	690	720	650	675	685	655	—
level-28	T	s	6.0	7.5	—	5.5	4.0	7.0	—	5.0	—	—
	V	K	855	655	—	670	703	645	—	675	—	—

¹²Top-down rewetting

Table 3.2: ... cont.

EVENT	MEAS. DATA		RELAP5/Mod2 CALCULATIONS									
	Q	unit	2-00	2-00PU	3-00	3-00S	3-00ST	3-02	2-00C	2-00PUC	3-00C	3-02C
level-39	T	s						4.6	7.0			
	V	K	760					715	645			
Quench ¹³ front during reflooding in hot channel	level-02	T	29.5		36.0	40.0	40.0					
		V	585		570	595	503					26.0
	level-11	T	40.5		45.0	43.5	40.0	44.2	29.5			
		V	670	715	640	665	589	690	620			
	level-21	T	46.0	49.0	54.0	52.0	40.0	52.0	51.5	50.0		
		V	650	753	665	720	580	770	730	745		
	level-24	T	50.0	52.2	55.0	53.5	40.0	53.0	55.0	53.5		
		V	650	753	610	665	582	745	800	785		
	level-27	T	48.0	54.5		56.0	50.0	54.5	57.5	57.2		
		V	620	760		765	760	785	760	762		
											31.5	24.0
											615	590
										41.5	¹⁴	
										590		
										52.0		
										795		
										53.0		
										685		
										53.5		
										810		

¹³Time and value of "knee temperature"

¹⁴No values due to abnormal termination of run

Table 3.2: ... cont.

Table 3.2: ... cont.

EVENT	MEAS. DATA		RELAP5/Mod2 CALCULATIONS										
	Q	unit		2-00	2-00PU	3-00	3-00S	3-00ST	3-02	2-00C	2-00PUC	3-00C	3-02C
level-31	T	s	52.0	56.5	57.0	— ¹⁵	60.0	54.5	56.0	60.0	58.5	58.5	—
	V	K	670	765	760	—	755	745	800	750	770	890	—
level-39	T	s	48.5	48.5	51.0	—	60.0	54.0	55.0	55.0	53.5	57.5	—
	V	K	610	895	875	—	735	780	790	800	780	780	—
level-43.5	T	s	53.0	33.5	—	—	54.5	—	50.5	—	—	52.5	—
	V	K	675	625	—	—	790	—	755	—	—	772	—
level-49	T	s	54.0	—	—	—	—	—	—	—	—	—	—
	V	K	605	—	—	—	—	—	—	—	—	—	—
level-62	T	s	54.0	—	—	—	—	—	—	—	—	—	—
	V	K	490	—	—	—	—	—	—	—	—	—	—
in avg. channel level-11	T	s	38.0	—	—	—	—	—	—	—	27.5	28.0	—
	V	K	540	—	—	—	—	—	—	—	550	580	—
level-21	T	s	38.0	—	—	45.0	43.5	—	—	—	27.5	28.0	—
	V	K	510	—	—	560	630	—	—	—	550	582	—
level-28	T	s	43.5	26.5	—	— ¹⁵	48.0	43.5	40.5	—	—	32.0	—
	V	K	530	635	—	—	575	555	570	—	—	525	—
level-39	T	s	39.0	—	—	—	—	44.0	43.0	—	—	—	—
	V	K	580	—	—	—	—	550	570	—	—	—	—

¹⁵No values due to abnormal termination of run

flow measurement is the result of a multiplication of two independent measurements which are assumed to produce area averaged quantities. These independent measurements are the momentum flux measurement by drag bodies (or the velocity measurement by mini-turbines) and the density measurement by a three beam X-ray densitometer. Both signals are erroneous, especially in high void flow regimes. Furthermore, it is assumed that the product of each of the individual two integrals (i.e. the area-average of the measurements) is equal to the integral of the product of the two variables, an assumption which is fulfilled rather seldom. The quantification of the error of the mass-flow measurements is quite difficult because its dependence of a variety of parameters like flow-regime, void fraction, velocities, etc.

A better picture of what is going on in the broken leg can be achieved by looking at the integral mass losses through the break at different times as listed in table 3.2 where both code predictions and experimental values have been determined by simply summing up the product values of time-step times the instantaneous mass flow at the two breaks. Here, the general trend is that the code calculated higher losses for the first 30 to 40 seconds and then stayed on a certain level (see also figs. 3.39a and b) and finally underpredicted the actual mass losses through the break. In fact, the sign of the flow even changed, indicating a small amount of backflow out of the containment into the primary system due to slightly higher containment pressures (defined as boundary condition using the experimental values) than calculated by RELAP5/Mod2 for the primary system. Because the containment has been modeled as an additional time dependent volume downstream of the break, this backflow is not "unphysical" with respect to the special

"LOFT-system" as described by our nodalization schemes. As indicated above, the pressure in this volume has been given as boundary condition according to the experimental recordings of the suppression tank pressure. To indicate the occurrence of the flow reversal, the calculated peak mass loss and the time of its occurrence have been given in table 3.2.

The code calculated similar mass losses for the different nodalizations. In fact, two groups may be distinguished, the results of the most detailed 2-00 versions which have produced slightly higher mass losses than the more simplified 3-0... versions.

3.3.2 Minimum Collapsed Liquid Level

The next value of interest is the time when the collapsed liquid level in the core region has reached its first minimum, i.e. when the core region was nearly emptied during the blowdown phase of the transient. Unfortunately, for the collapsed liquid level (or equivalent to it, the average liquid fraction in the core region), no experimental data is available. In table 3.2, the collapsed liquid level is given in percents relative to the total heated core height of 1.63 m. The comparison of the results with the different nodalizations indicated no severe discrepancies with respect to the values of the minimum collapsed liquid levels. Their ranges varied between 3.2% and 7.4% in the hot and 3.6% and 8.4% in the average channels. No significant trends have been observed with respect to the sophistication of the nodalizations. The minimum collapsed liquid level has been reached between 4.0 and 5.2 seconds after initiating the transient except for runs 2-00 and 2-00C where it took 7.2 and 6.8 seconds respectively.

3.3.3 Emptying Points of Pressurizer and Accumulator

Two of the significant events during the LOFT-experiment have been found to be the emptying of the pressurizer and the accumulator. The pressurizer emptied during the experiment at about 15.5 seconds after the opening of the break valves; at this moment, pressure in the pressurizer has reached a value of 7.4 MPa.

RELAP5/Mod2 calculated this emptying point between 14.4 seconds for the 2-00, 2-00PU, 2-00C and 2-00PU,C nodalizations and 18.4 seconds for the most simplified 3-02 but not for the equivalent 3-02C nodalization. It is not surprising that the time for emptying the pressurizer strongly depended on the chosen nodalization. Whereas the pressures in the pressurizer as predicted by the code have been found to be quite close to the experimental data for the 2-00 and 2-00PU nodalizations, for the 3-0... series of nodalizations with their crude modelling especially in the pressurizer, the RELAP5/Mod2 calculations of the pressurizer pressures are rather poor, namely around 4 MPa or even less instead of the measured 7.4 MPa (the 4 MPa is comparable to the system pressure at the time of emptying point).

The accumulator empties at about 56.5 seconds after the initiation of the experiment. In general, the code predictions seem to be sufficiently close to this experimental setpoint. This relatively good agreement of the code results with the experimental findings is not at all surprising because the emptying time has been tuned once for all for the 6-00 version of nodalization of the post test analysis of the LOFT LP-LB-1 experiment (see ref. [7]) by increasing the forward and reverse flow energy loss coefficients of the accumulator junction from 13, as given in the

original EG&G, to about 125.

3.3.4 Peak Cladding Temperatures During the Blow-down Phase

Peak cladding temperatures of 1074 K have been measured by only one of the ten thermocouples in fuel assembly 5 (center of core) on level-27, i.e. 27 inches from the bottom of the core.

The calculated peak cladding temperatures always occurred at level-31, i.e. 31 inches from the bottom of the core (by the way, for the original EG&G nodalization of the core which was used for nearly all of the pre- and post-test analyses of the LOFT experiments, core levels-27 and levels-31 fall in the same volume of the nodalization and consequently indicated the same calculated temperatures). Their values only depend on the chosen nodalization and vary between 1017 K (3-02C) up to 1054 K (2-00). The highest values have been predicted by the 2-00 versions of nodalizations because a rapid coast-down of the pumps has been allowed for this calculation resulting in a longer uncover period of the hot channel.

The next values of interest are the peak cladding temperatures reached at different core heights during the blowdown period of the experiment which occur in the first 10 seconds after opening the break valves.

With respect to the central core region (hot channel), the blowdown peak cladding temperatures have been slightly overpredicted by the code (not more than 20 K). On the other hand, the code has located the blowdown peak cladding temperatures at axial locations further downstream in the core. Whereas the cladding temperature has been measured at level-21 (1037 K, radially averaged value), the code calculated the highest cladding tem-

peratures (varying from 1017 K (3-02C) to 1054 K (2-00)) at level-31 (32), i.e. 10 inches downstream of the experimentally inferred hot spot.

With respect to the outer core (average channel) for all nodalizations, the blowdown peak cladding temperatures have been underpredicted at least between 10 K (at position 21 inches) and 200 K (at position 27 inches). The lowest underpredictions have been achieved using the most simplified nodalizations 3-02 and 3-02C.

At lower levels of the LOFT core, high flooding rate bottom-up rewetting took place during the blowdown period of the experiment. It enables the quenching of the hot rods between 4.8 and 6.8 seconds of the transient. In table 3.2, times and values of the experimental "knee cladding temperatures" have been listed at which quenching took place at a certain level of the core.

The predicting capabilities of RELAP5/Mod2 have been found to be rather poor with respect to bottom-up rewetting during the blowdown phase. Only with some of the nodalizations some kind of prediction was possible; with respect to early bottom-up quenching, the best results have been obtained with nodalization 3-005T. In chapter 3.4, we shall discuss in more detail the problem of early bottom-up rewetting. The bottom-up rewetting was also observed in the side channels of the LOFT core during the test but again the predictions of RELAP5/Mod2 have been found to be rather poor.

In addition to the early bottom up quenching, the upper parts of the core (level-49 and level-62) have been quenched due to top-down rewetting between 14.3 and 15.3 seconds. RELAP5/Mod2 was also not able to predict this phenomenon, as one can see in table 3.2 for levels-49 and levels-62 (also incor-

porated in column "partial bottom-up rewetting" of table 3.2.

3.3.5 Quench Front Positions During the Reflooding Phase

The quench front positions during the reflooding phase of the experiment have been found to be one of the most sensitive parameters of the calculations. Therefore, the last values of table 3.2 will show the comparison between the experimental results (time and value at the "knee-point" of the temperature trace of one individual thermocouple at a certain axial core level) and the equivalent code predictions at 10 different core levels where thermocouples have been installed. Because at a certain core height the core-wide radially distributed thermocouples may indicate different quench front positions, we have used an averaged value for time and temperature at one core level.

Different to our findings for the LOFT experiment LP-LB-1 (ref. [7]), where we have found enormous discrepancies between the results of the different nodalizations, for the LP-02-6 calculations the predictions of the quench front positions using the different nodalizations are quite close together. Furthermore, we have not found significant differences between the results of the nodalizations which have taken into account the heat capacity effects of the wall material and which did not; i.e. taking into account the heat capacity of the wall material has not led to negative effects on the predictions of the quench front positions like they have been found for our LP-LB-1 post-test analyses (ref. [7]). For the moment, we can give no reasonable explanations for this observations.

3.4 Time Behaviour of Significant Thermo-Hydraulic Parameters

3.4.1 Cladding Temperatures

Even it can be seen in table 3.2, that the RELAP5/Mod2 only slightly underpredicts the peak-cladding temperatures in the center channel of the core, by looking at the time history of the cladding temperatures at different axial heights of the core, it can be noted that rather significant discrepancies between the predictions and the experimental data exist. Furthermore, it can be observed more clearly that the differences between the results of the different versions of nodalizations occur.

Due to our specific nodalization of the core region which is identical for all of the investigated schemes, RELAP5/Mod2 is able to calculate the cladding temperatures in only two different representative channels, namely the "hot channel" attributed here to the center-box 5 and the "average channel" which can be attributed to one of the side boxes of the LOFT core; for the comparison with experimental data, we have used the side-box 4 (in principle, any other of the four side-boxes or an average of all of them could be used).

Let us start our discussion of the RELAP5/Mod2 calculations of the cladding temperatures in the "hot channel", i.e. box 5 of the LOFT core.

Cladding Temperatures in the Center Box

In Figs. 3.5 to 3.14, the time traces of the cladding temperatures at 10 different core heights in the center box (box 5) as calculated by RELAP5/Mod2 ("hot channel" have been compared to the average temperature (!) at

the specific core height (the averaging process has been described in chapter 3.1), using the different nodalizations as listed in table 2.1. For the sake of better readability, for each axial position two figures are given in which it is shown five comparisons of N-type (plot a; versions 2-00, 2-00PU, 3-005, 3-005T and 3-02) and four comparisons of C-type nodalizations (plot b; versions 2-00C, 2-00PU,C, 3-00C and 3-02C), i.e. where the heat capacity effects of the vessel material have been taken into account (C-type) and where these effects have been neglected (N-type).

At axial level 02, i.e. 2 inches from the bottom of the core, the experimental cladding temperatures have undergone a significant temperature increase of approximately 150 degrees mainly during the blowdown phase of the experiment, which the code has overpredicted between 20 K (for the case of rapid coastdown of the pumps, nodalization 2-00 and 2-00C) and 60 K for all the other nodalizations, where the realistic coastdown of the pumps has been imposed (figs. 3.5a and 3.5b). A first quench (bottom-up rewetting) stops this core heat-up at about 8 seconds after the initiation of the experiment. At level-002, this early quenching has been calculated by RELAP5/Mod2 for all types of nodalization.

A second heat-up of the center bundles started at approximately 13 seconds and terminated at nearly 30 seconds. This second heat-up has been "indicated" by all of the runs with quite different accuracy. In addition, for the simplified nodalizations, this core heat-up has been calculated approximately 10 seconds too long, i.e. the time of the final quenching has been overpredicted by at least 10 seconds for the 3-005 and 3-02 nodalizations.

Generally, the final quench during the reflooding phase of the experiment has been

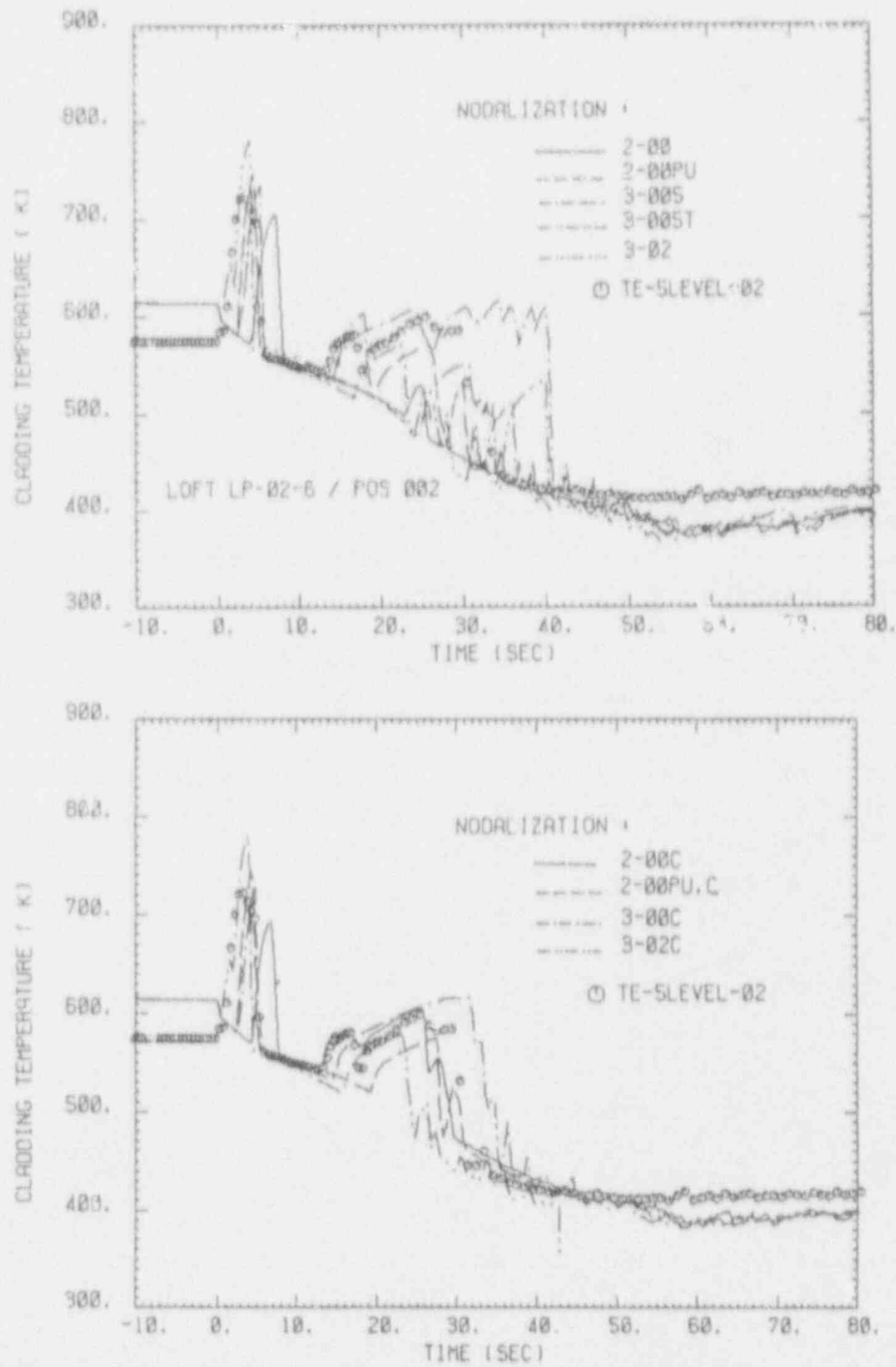


Figure 3.5: Hot-channel cladding temperatures vs. time at axial level 02 compared with the equivalent reference temperature
 a) by neglecting wall heat capacity
 b) by taking into account wall heat capacity ("C")

calculated by RELAP5/Mod2 slightly more accurate by the "C" than by the "N" versions of nodalizations; this finding is in contradiction to our earlier findings when analyzing the LOFT experiment LP-LB-1 (ref. [7]). Wherever the predictions of the different C-versions have been found to be close together, the discrepancies of the "N"-versions are significant. Here the poorest results have been achieved using the 3-005 and 3-02 nodalizations, i.e. the two most simplified ones.

At the following two axial levels (figs. 3.6 and 3.7), the peak surface temperatures generally have been underpredicted at least 50 K and for other nodalizations more than 100 K during the blowdown phase. Only for some versions, partial bottom-up quenching, one of the main phenomena of the LP-02-6 experiment, has been calculated.

For the next five axial positions, figs. 3.8 to 3.12, a general trend of overpredicting the cladding temperatures both during the blowdown (between 3 and 7 seconds of the transient) and the "refill" of the reflood phase (between 20 and 50 seconds of the transient) has been found but the first higher peak cladding temperature ("blowdown peak") has been overpredicted not more than 50 K whereas during the reflood interval the code has overpredicted the cladding temperatures not less than 150 K. Only the 3-005 and 3-005T versions tend to give certain underpredictions, especially during the reflood interval of the experiment.

For level-27, the calculations of version 3-005T has nearly perfectly reproduced the experimental data. Both the blowdown peak terminated by the bottom-up quenching and the second core heat-up during the refill interval of the experiment have been described perfectly; but we believe that this good ag-

reement is coincidental because it only happened at level-27.

It should be noted that no significant differences have been observed between the predictions of nodalizations 2-00 (rapid coastdown of the pumps) and 2-00PU (given pump speed vs. time curves) with respect to the time behaviour of the cladding temperatures. Only the temperatures at the "blow-down peak" have been always predicted slightly higher (20 to 30 K) by the 2-00 version (rapid coastdown of the pumps).

Whereas in the LOFT LP-LB-1 experiment (see ref. [7]) at the upper levels a top-down quench has been observed within the first 15 seconds (blowdown phase), there is no such strong evidence for the LP-02-6. Because the experimentally verified momentum fluxes at the exit of the core have been found to be highly positive during the first 15 seconds of the transient (see also fig. 3.13) indicating a coolant flow out of the core; on the other hand, the momentum flux meter (one drag body at a position at the inlet and one at the outlet of the core) only indicated the momentum flux at one specific position at the outlet of bundle 5, so that one cannot exclude reverse flow in some other parts of the flow area. Therefore, we have attributed the first sharp decrease of the cladding temperatures in fig. 3.12 and -less pronounced- in fig. 3.13 to bottom-up reflooding, whereas the second temperature drop (at about 15 seconds) probably is due to top-down quenching.

None of the different RELAP5/Mod2 runs has drawn a sufficiently conclusive picture of what has been going on at these two upper core levels as can be seen from Figs. 3.12 and 3.13. The initial core heat-up has been reproduced quite poorly and the second significant heat-up during the refill interval is

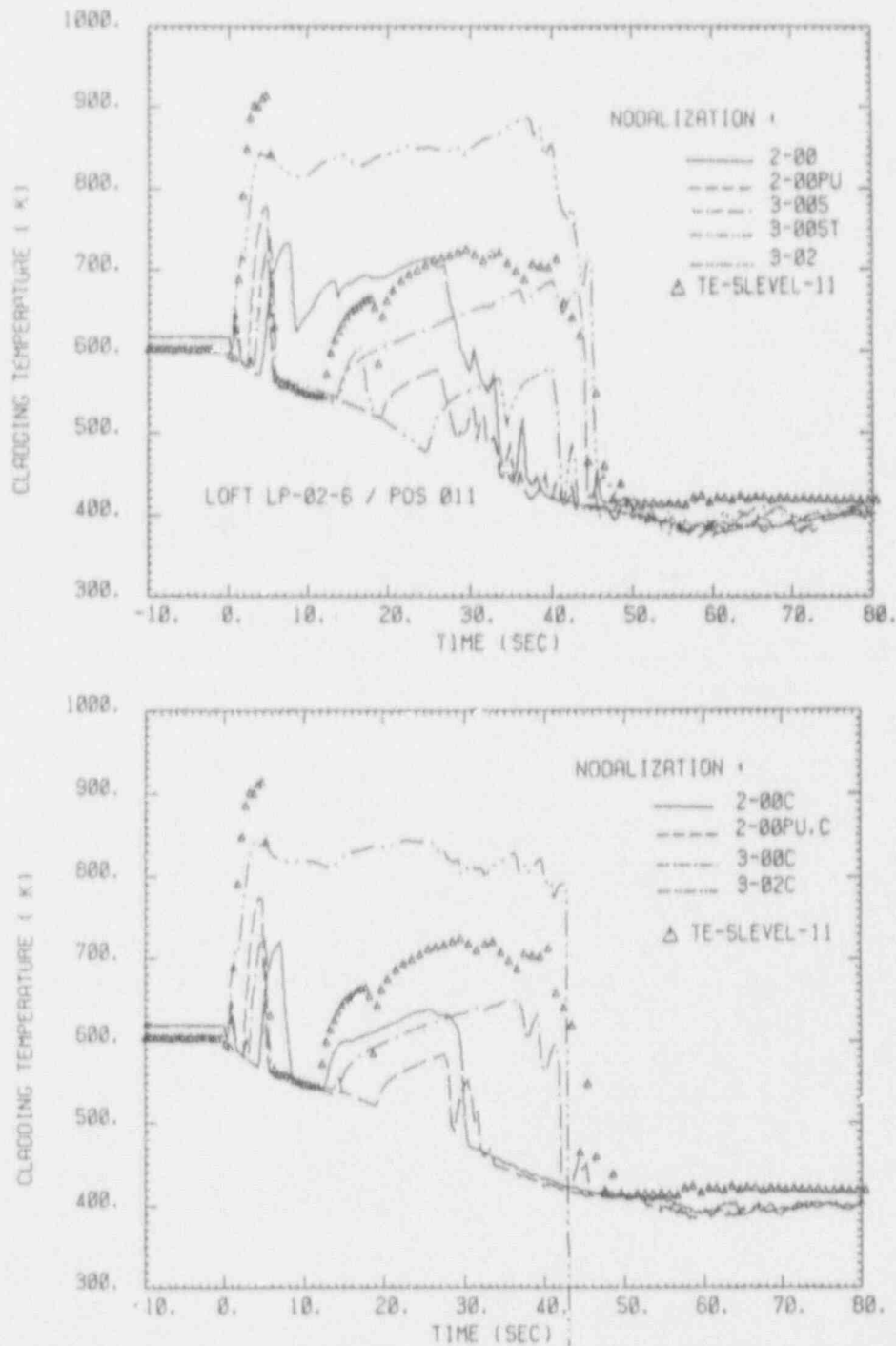


Figure 3.6: Hot-channel cladding temperatures vs. time at axial level 11 compared with the equivalent reference temperature
 a) by neglecting wall heat capacity
 b) by taking into account wall heat capacity ("C")

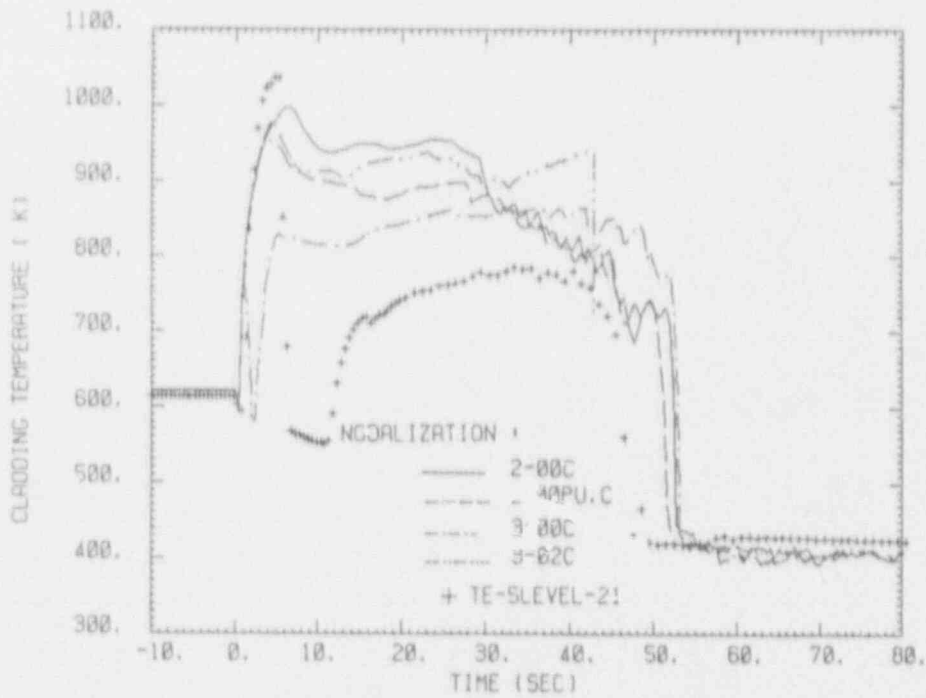
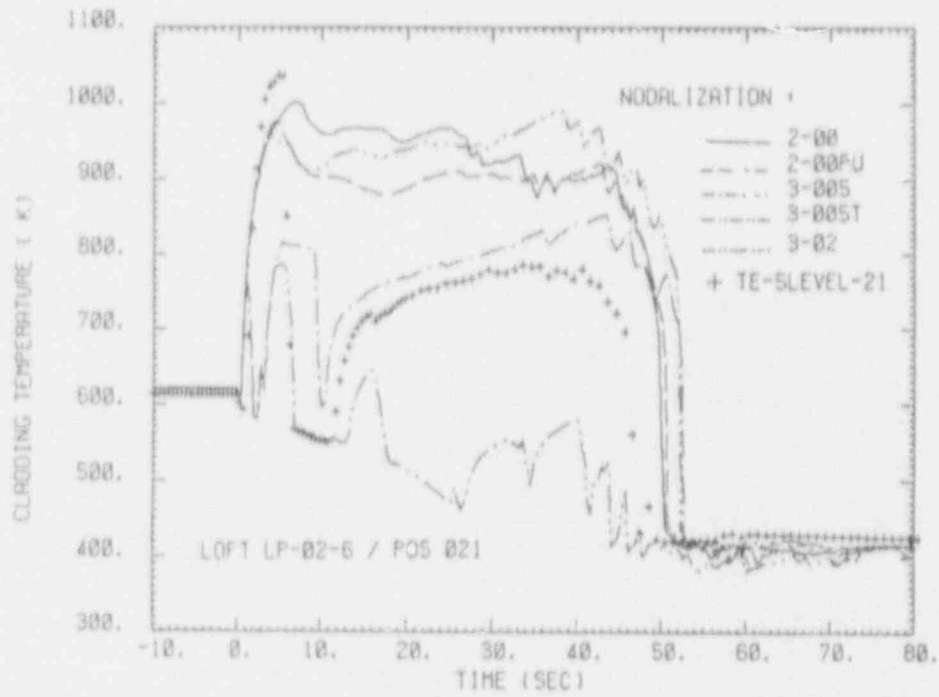


Figure 3.7: Hot-channel cladding temperatures vs. time at axial level 21 compared with the equivalent reference temperature
 a) by neglecting wall heat capacity
 b) by taking into account wall heat capacity ("C")

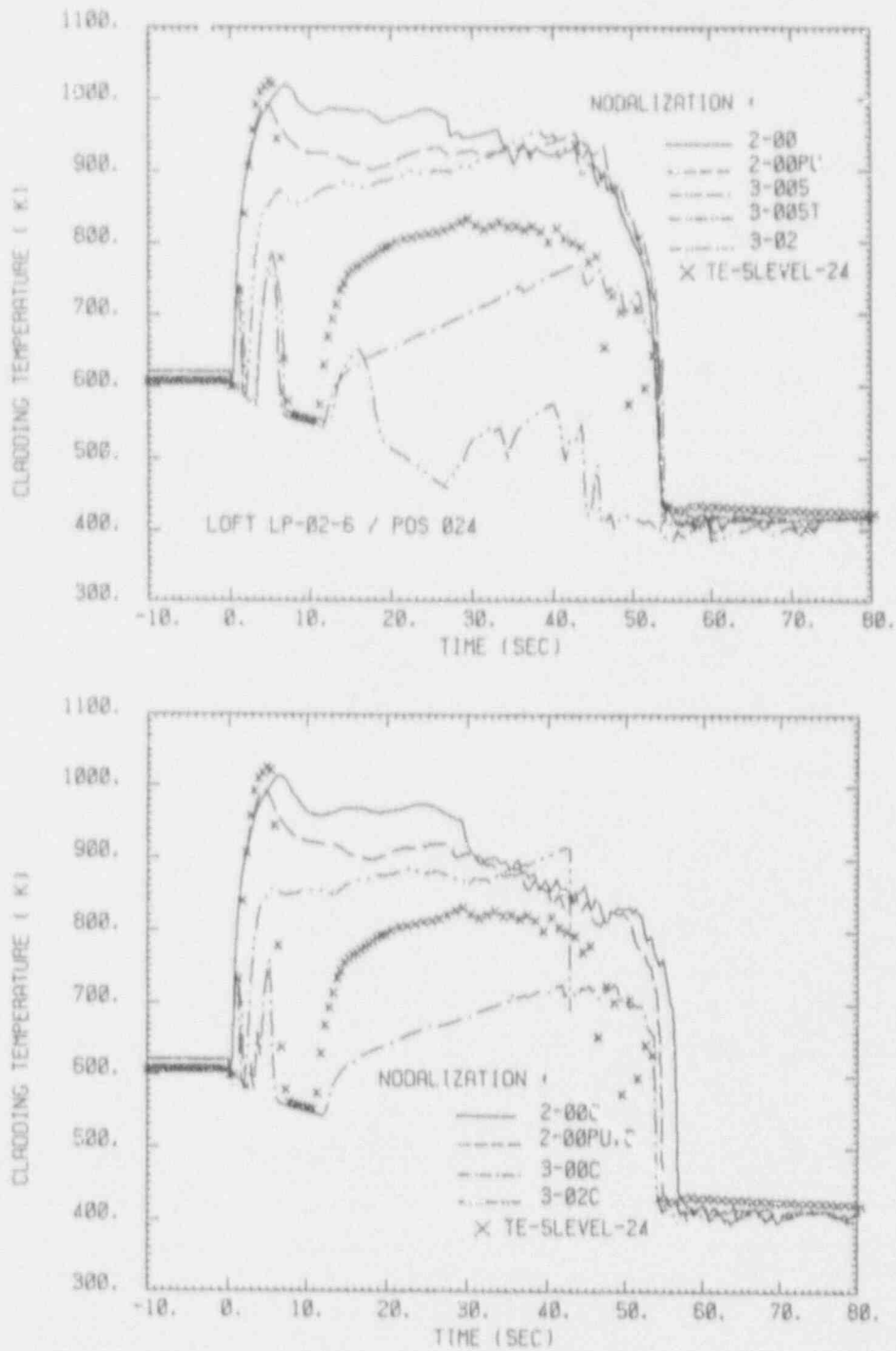


Figure 3.8: Hot-channel cladding temperatures vs. time at axial level 24 compared with the equivalent reference temperature
 a) by neglecting wall heat capacity
 b) by taking into account wall heat capacity ("C")

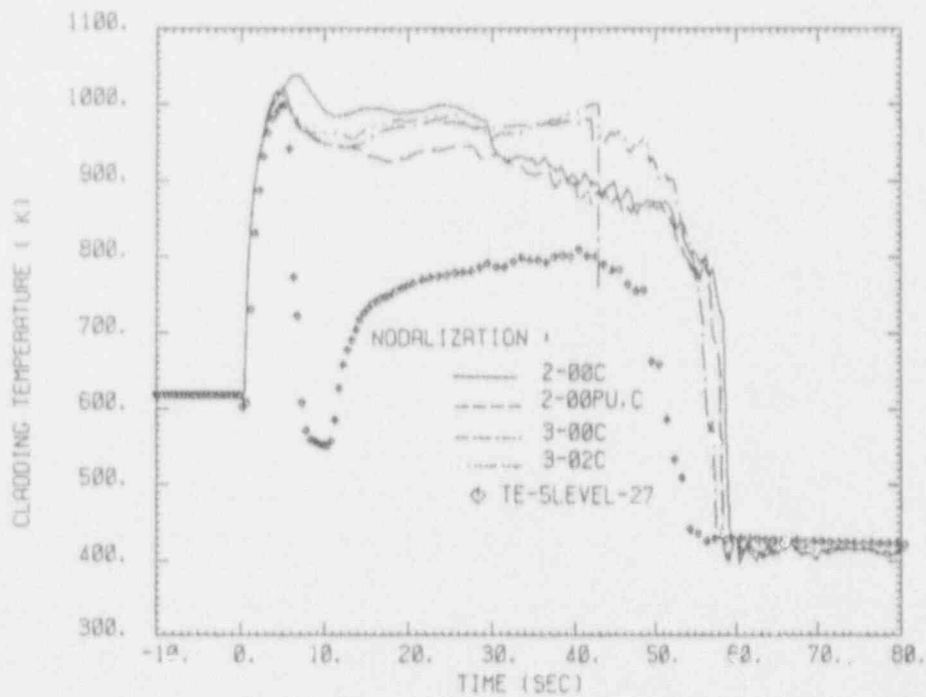
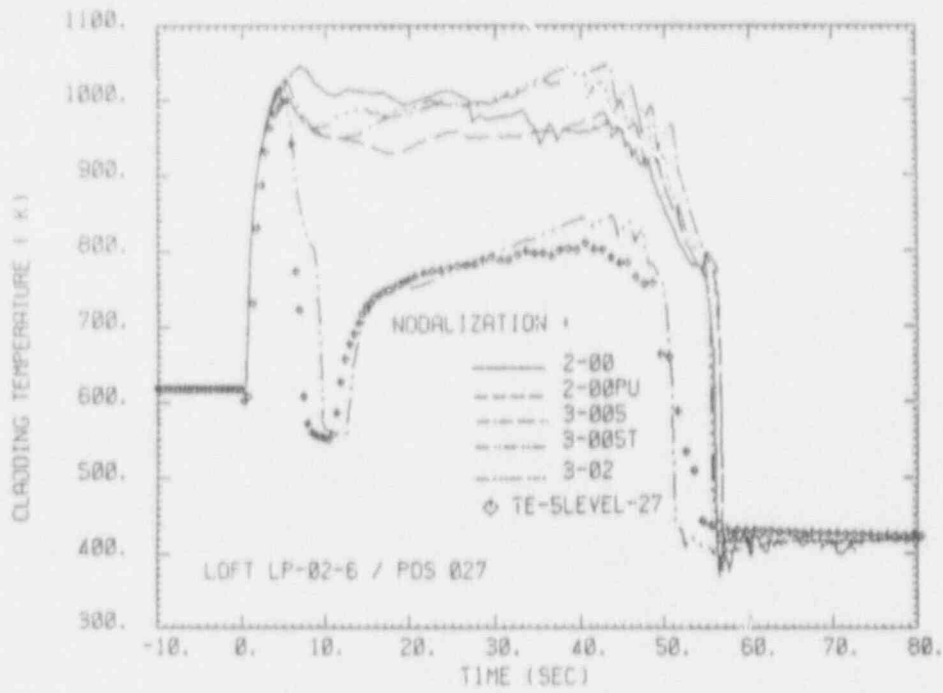


Figure 3.9: Hot-channel cladding temperatures vs. time at axial level 27 compared with the equivalent reference temperature

- by neglecting wall heat capacity
- by taking into account wall heat capacity ("C")

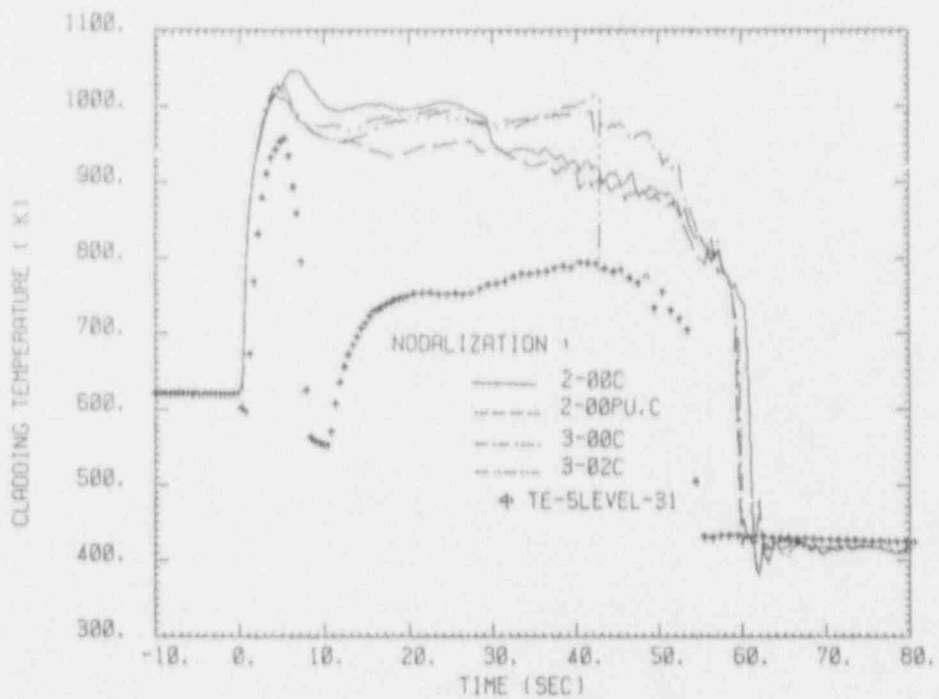
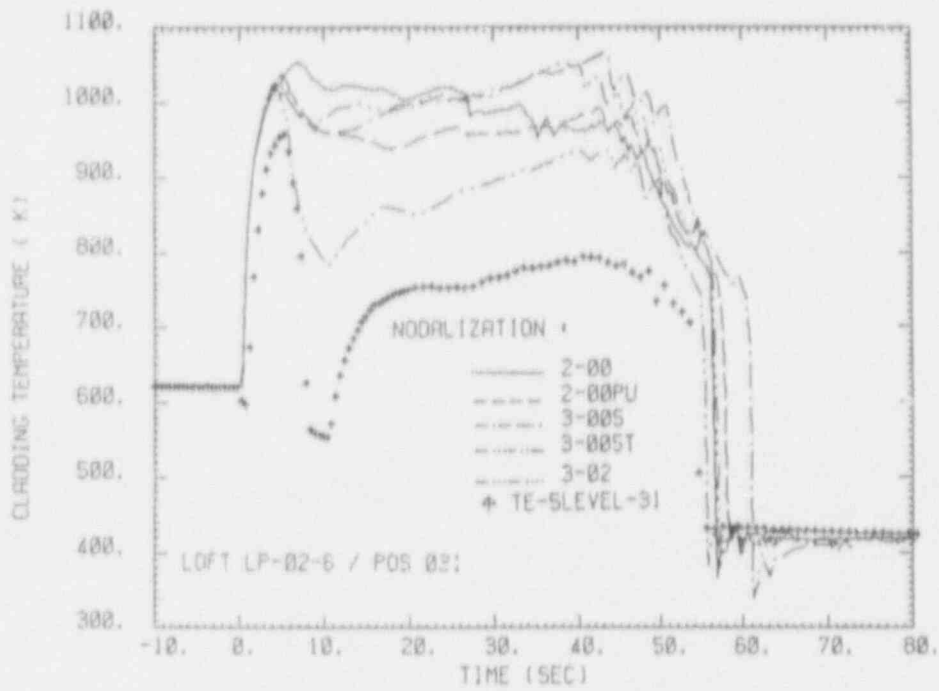


Figure 3.10: Hot-channel cladding temperatures vs. time at axial level 31 compared with the equivalent reference temperature

- a) by neglecting wall heat capacity
- b) by taking into account wall heat capacity ("C")

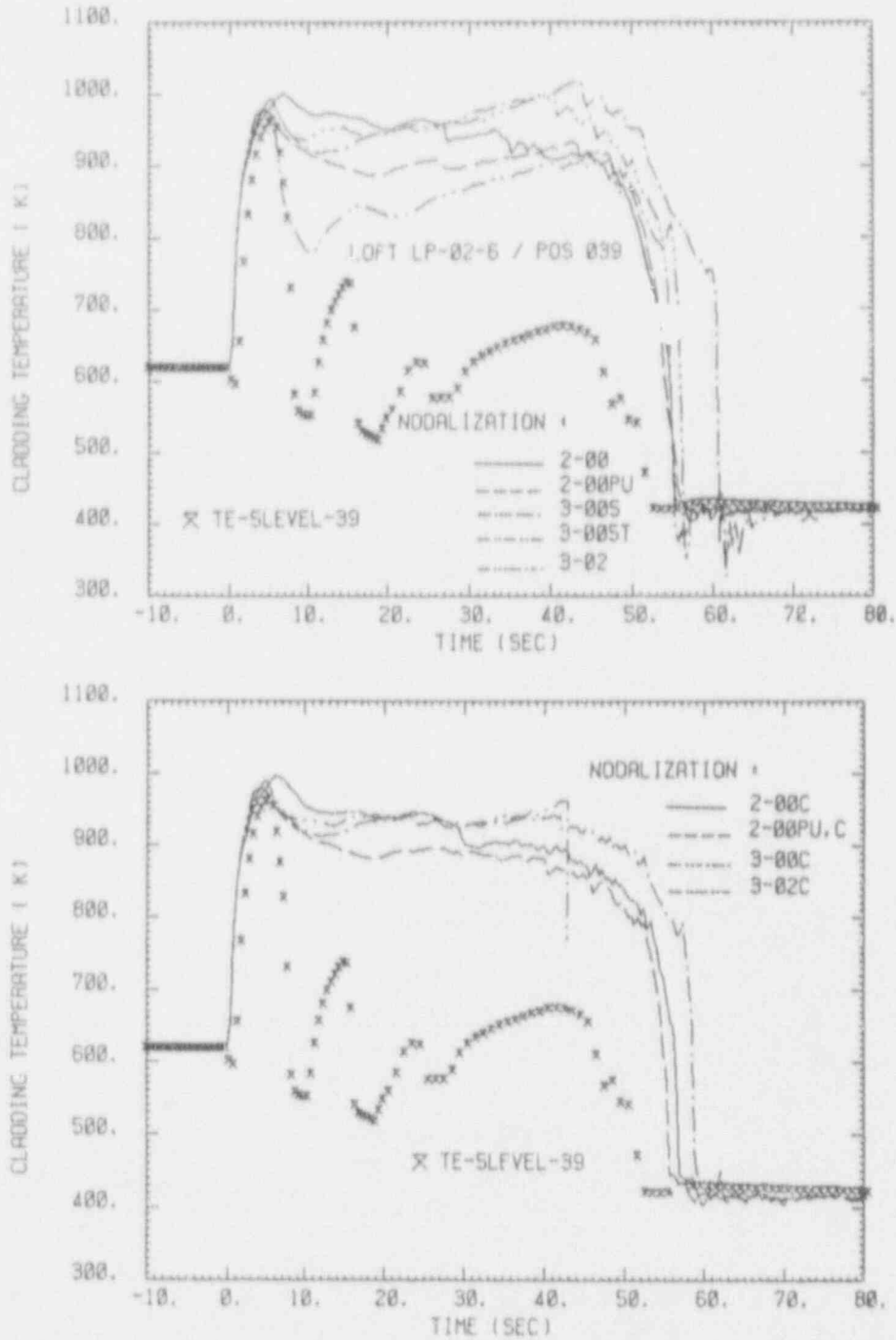


Figure 3.11: Hot-channel cladding temperatures vs. time at axial level 39 compared with the equivalent reference temperature
 a) by neglecting wall heat capacity
 b) by taking into account wall heat capacity ("C")

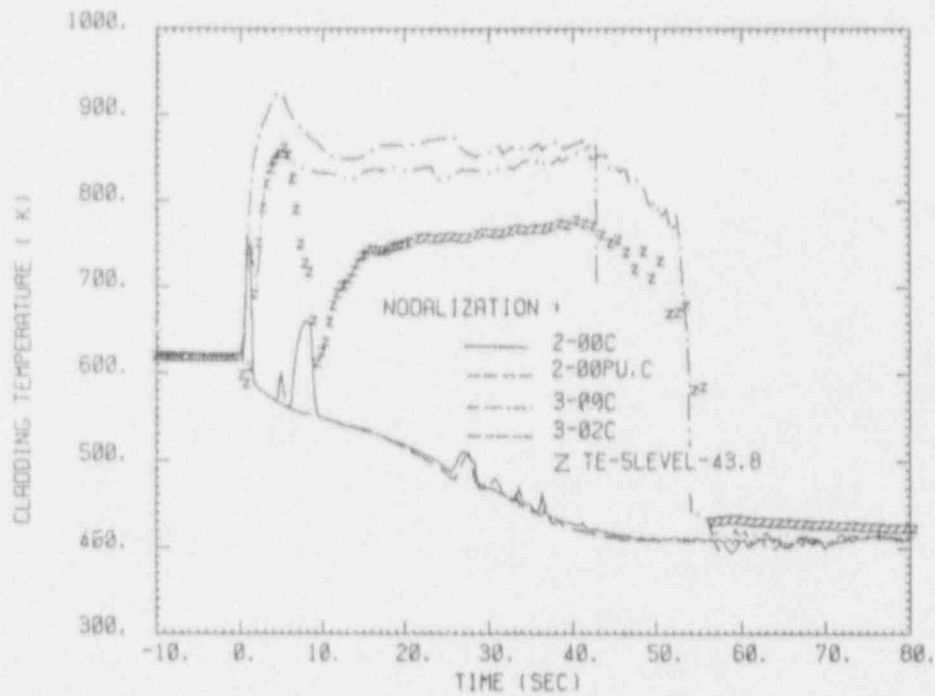
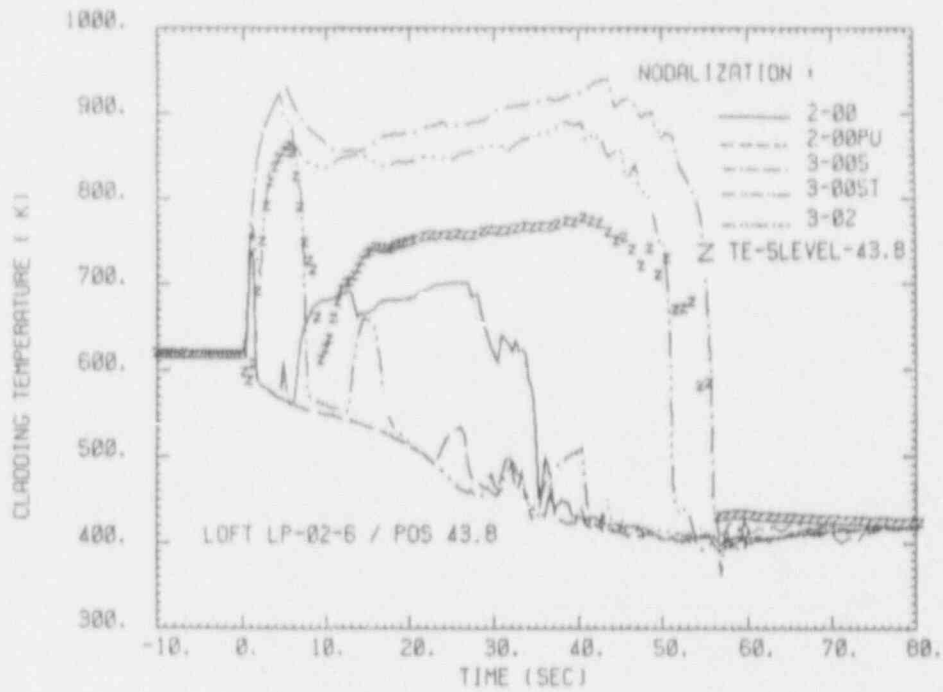


Figure 3.12: Hot-channel cladd. temperatures vs. time at axial level 43.8 compared with the equivalent reference temperature
 a) by neglecting wall heat capacity
 b) by taking into account wall heat capacity ("C")

nearly missing; some vague increase of the surface temperatures cannot be interpreted as a valuable description of the thermohydraulics in this core region.

Cladding Temperatures in Side Box 4 (Average Channel)

In figs. 3.14 to 3.17, the time traces of the cladding temperatures at four different core heights in the side box 4 as calculated by RELAP5/Mod2 for the "average channel" have been compared to an average temperature at the specific core height (if the reference is indicated by the word "level") or to one single thermocouple signal (if a specific number is given as reference, e.g. 4G14). Again, for the four axial positions, located 11, 21, 28 and 39 inches from the bottom of the core, two plots are given showing the comparison of the "N" (plot a) and the "C" type of nodalizations (plot b).

RELAP5/Mod2 was not able to predict the significant heat-up of the fuel cladding in the average channels during the blowdown phase but indicated some temperature increase during the refill phase of the experiment.

For both the blowdown phase of the experiment, surface temperatures have been underpredicted by RELAP5/Mod2 between 20 K (at axial position 21) and 200 K (positions 11 and 28). The highest surface temperatures have been calculated for the 3-02 and 3-02C nodalizations.

During the refill phase, a significant core heat-up has been calculated by RELAP5/Mod2, the magnitude of which depends on the selected nodalizations. The highest temperatures (overprediction at least 100 K) have been obtained by the 3-005 and 3-02 versions (i.e. the less elaborated ones) whereas the lowest values have been found with the 2-00 version.

Summarizing Remarks on the Cladding Temperature Calculations

Summarizing our findings with respect to RELAP5/Mod2 -calculations of the cladding temperatures in both the hot and the average channels one has to conclude that:

- generally, at most of the core levels, the peak cladding temperatures have been underpredicted not more than 100 K,
- RELAP5/Mod2 has calculated the peak cladding temperature at axial level 31, i.e. 31 inches from the bottom of the core, whereas the experimentally inferred hotspot is located at level-27,
- with respect to the cladding temperatures in the average channel, only small differences have been observed between the results of the "N" and "C" versions of nodalizations, i.e. whether the heat capacity of the wall material of the reactor vessel has been taken into account or not did not make much difference.

The reasons for the deviations are multiple. Concerning the axial shift of the hot spot (second item), one of the reasons may be an incorrect assumption of the axial power distribution in the LOFT core; as mentioned in section 2.1, we have used the one published by [5]. For investigating on this problem, the axial distributions of the cladding temperatures have been compared to the equivalent experimental data for three different time points of the transient, namely at -1.2 seconds (i.e. the stationary part of the transient), at 5.3 seconds (blowdown phase) and at 40.5 seconds, i.e. during the refill phase (Figs. 3.19a,b to 3.21a,b).

In figs. 3.18a,b, the comparison was made for the stationary phase of experiment LP-02-6. All RELAP5/Mod2 calculations

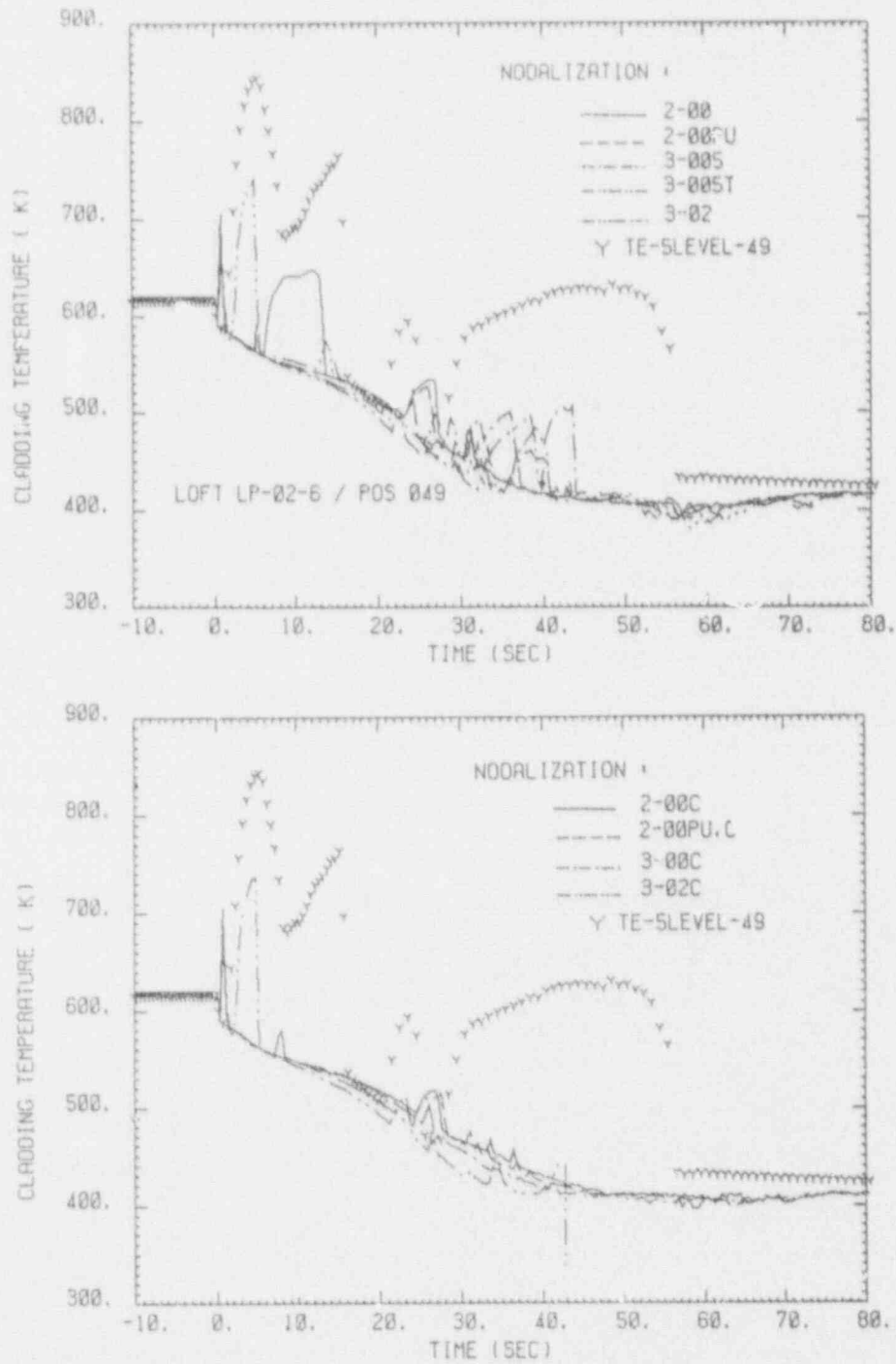


Figure 3.13: Hot-channel cladding temperatures vs. time at axial level 49 compared with the equivalent reference temperature
 a) by neglecting wall heat capacity
 b) by taking into account wall heat capacity ("C")

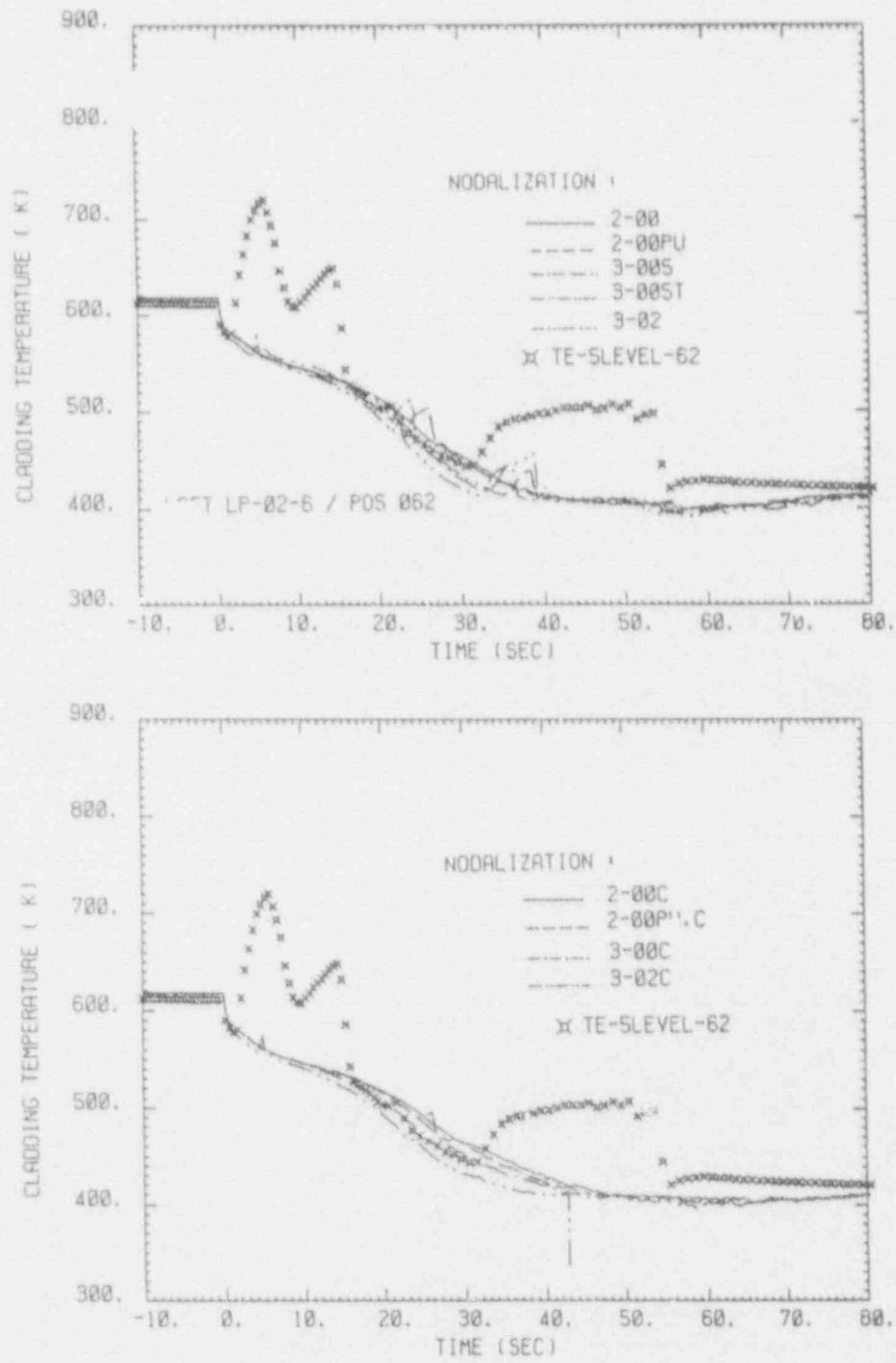


Figure 3.14: Hot-channel cladding temperatures vs. time at axial level 62 compared with the equivalent reference temperature
 a) by neglecting wall heat capacity
 b) by taking into account wall heat capacity ("C")

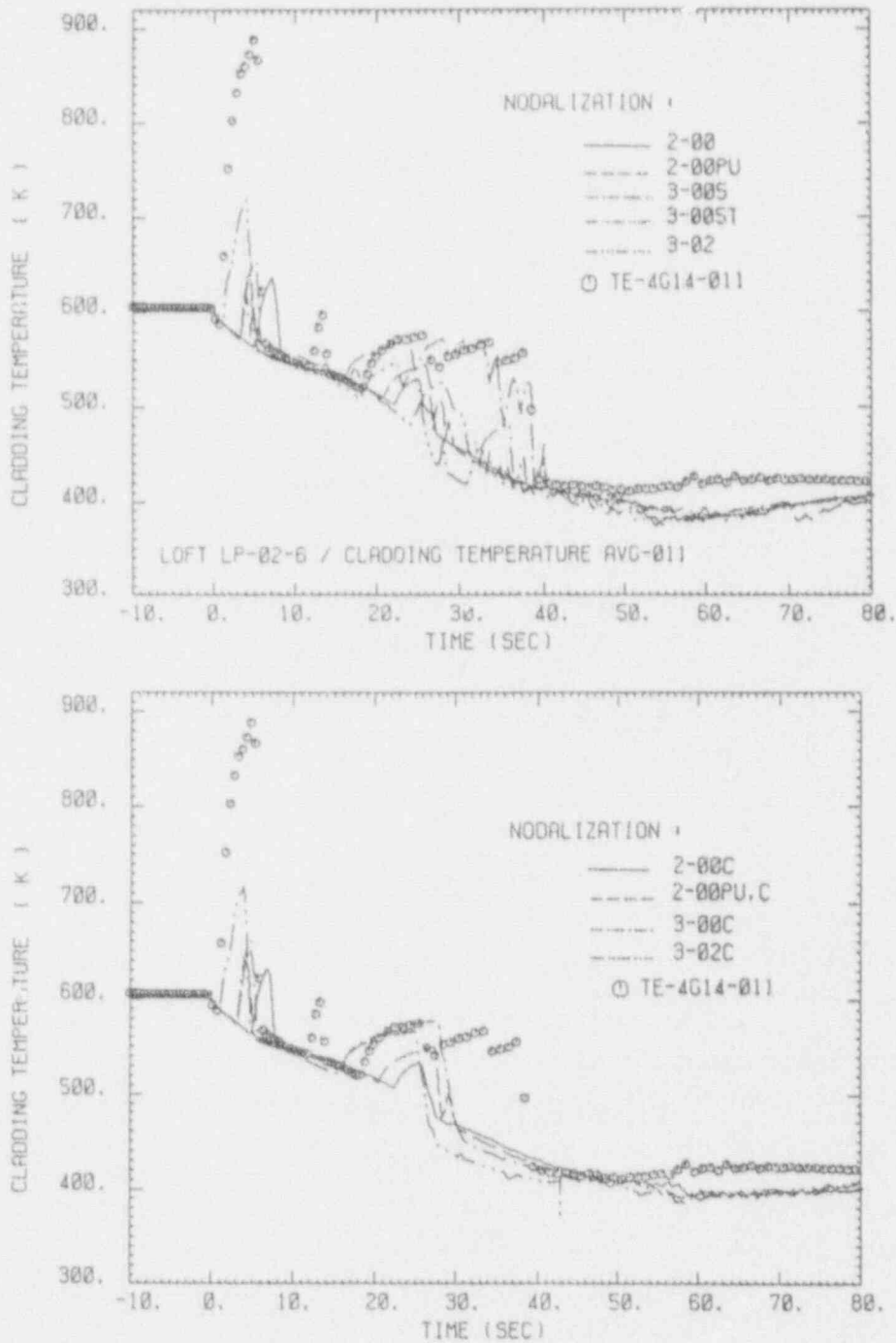


Figure 3.15: Average channel cladding temperatures vs. time at axial level 11 compared with the equivalent reference temperature
 a) by neglecting wall heat capacity
 b) by taking into account wall heat capacity ("C")

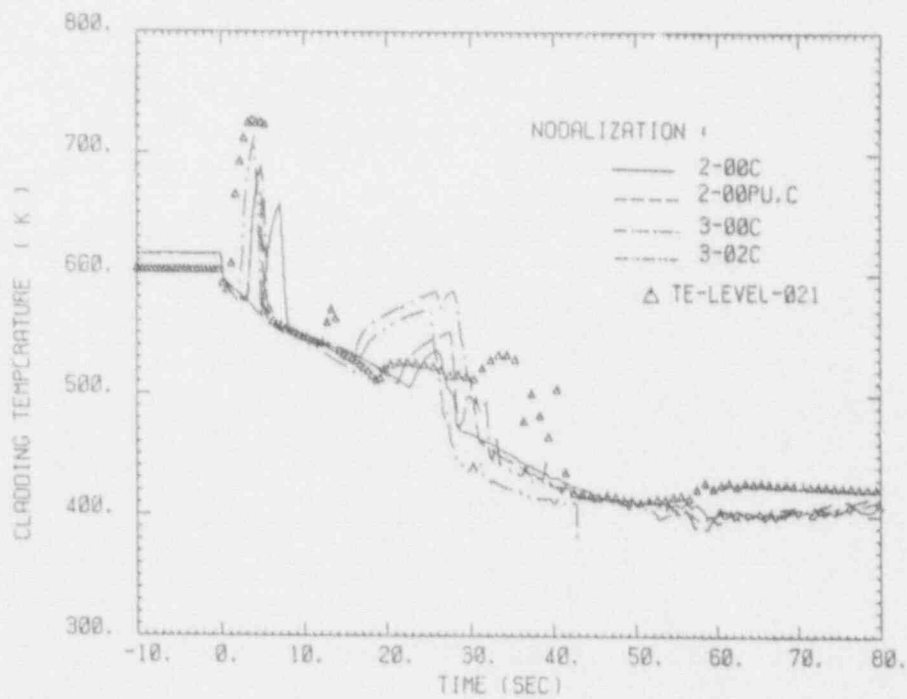
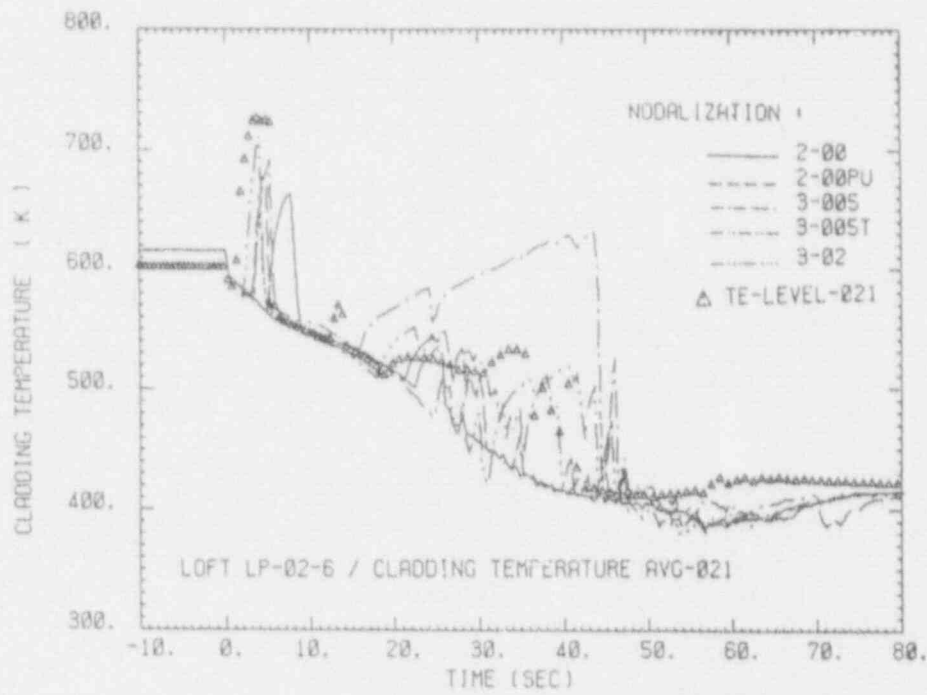


Figure 3.16: Averaged channel cladding temperatures vs. time at axial level 21 compared with the equivalent reference temperature
 a) by neglecting wall heat capacity
 b) by taking into account wall heat capacity ("C")

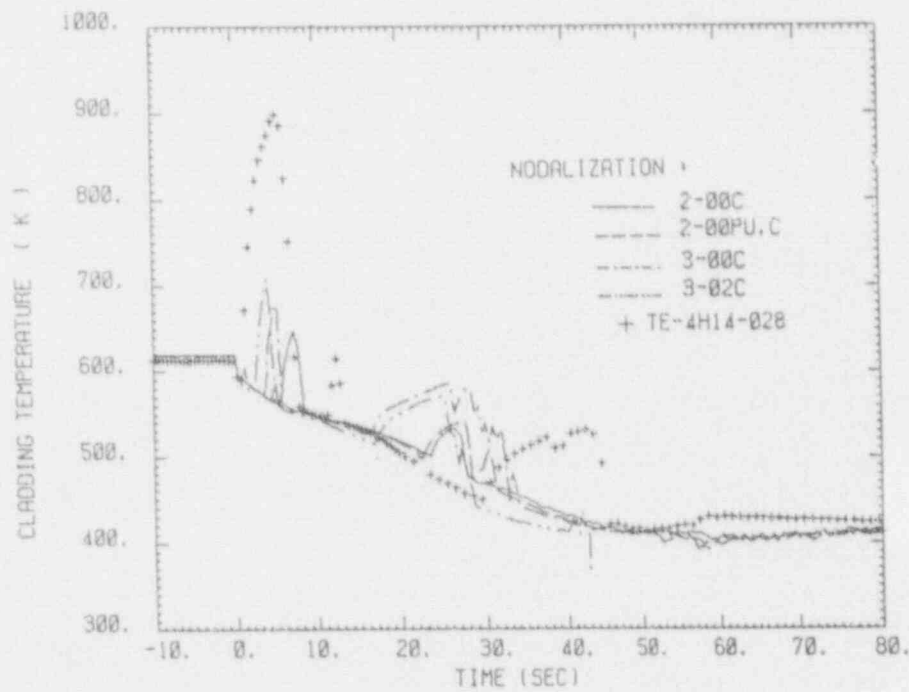
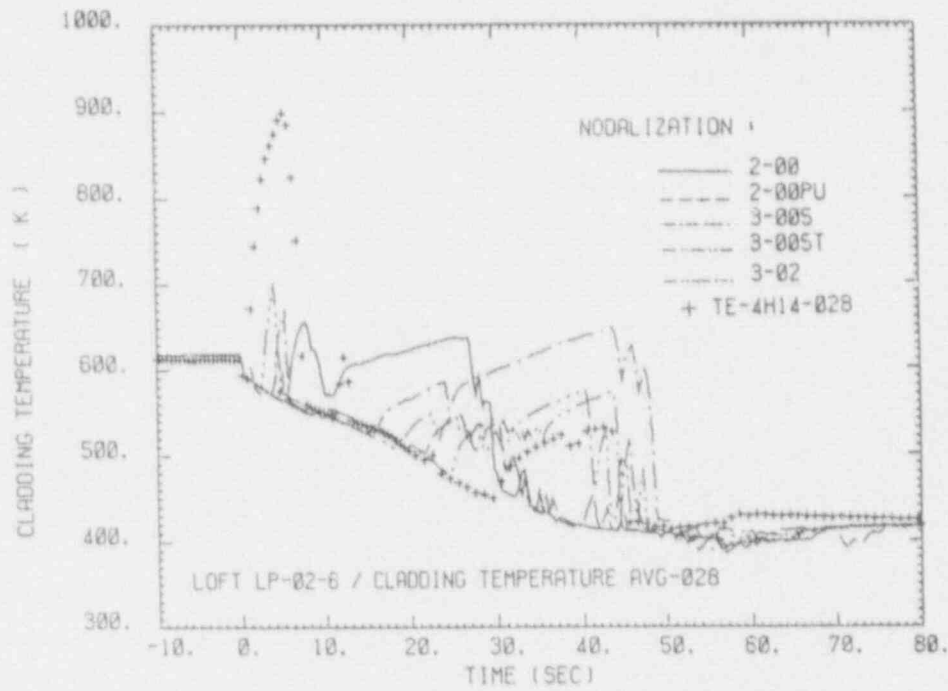


Figure 3.17: Averaged channel cladding temperatures vs. time at axial level 28 compared with the equivalent reference temperature
 a) by neglecting wall heat capacity
 b) by taking into account wall heat capacity ("C")

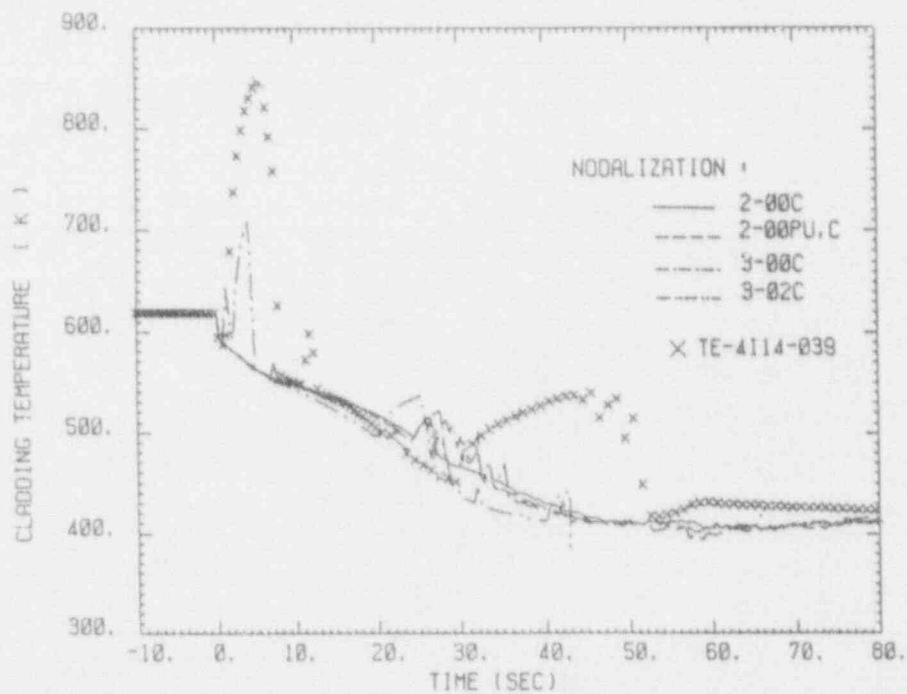
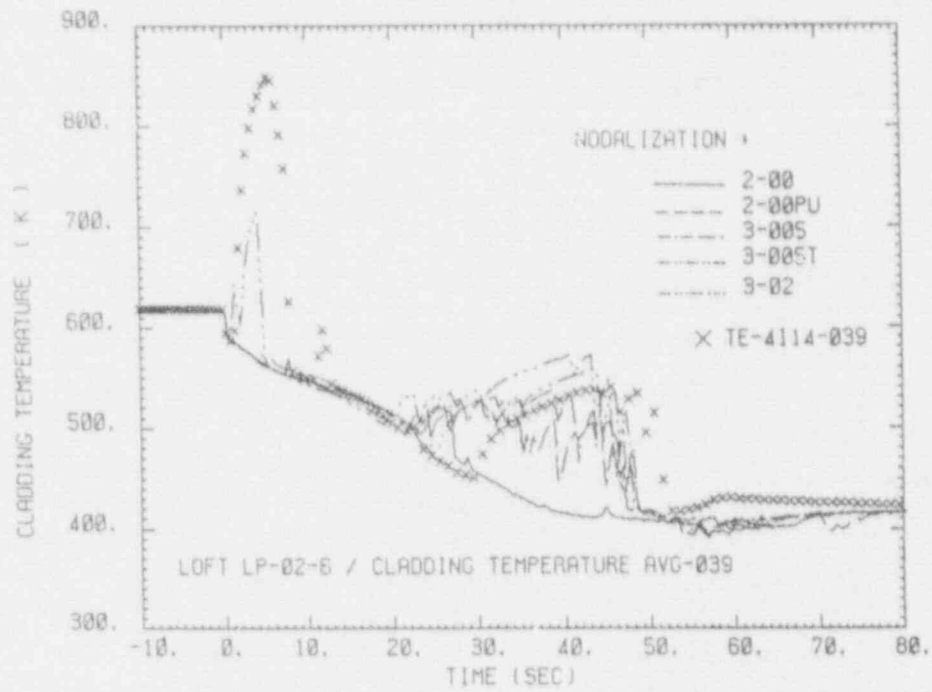


Figure 3.18: Averaged channel cladding temperatures vs. time at axial level 39 compared with the equivalent reference temperature
 a) by neglecting wall heat capacity
 b) by taking into account wall heat capacity ("C")

indicated very similar axial distributions of the cladding temperatures which only in the middle of the core (core heights .6 to 1.2) are quite close to the experimental data (circles in the plot) whereas they differ at the bottom about 40 K. In fact, the experimentally inferred axial cladding temperature distributions have been found to be much more varying than the one calculated by RELAP5/Mod2. If a change in the axial power distribution would bring any improvements is an open question and has not been tested yet.

During the blowdown interval, i.e. 5.3 seconds after the initiation of the transient, the RELAP5/Mod2 calculated axial surface temperature distributions of runs with the different nodalization schemes differ quite significantly both to each other as well as in comparison to the experimental findings (figs. 3.20a and 3.20b). The calculated peak cladding temperatures are centered around 0.75 m whereas the corresponding experimental values (triangles) have been found at approximately 0.5 m. On top of this, the RELAP5/Mod2 calculated core heat-ups were rather concentrated in the center region of the core (0.4 to 1.2m) whereas the experimental data indicated a more widened core heat up. One of the reasons may be the fact that RELAP5/Mod2 neglects the axial heat conduction in the cladding as well as in the fuel thus preventing from smoothing out steep axial temperature gradient in the cladding and the fuel (axial conduction is only considered by RELAP5/Mod2 near the quench front when the reflood model is applied).

Things do not change significantly for the remaining time point of consideration, namely 40.5 seconds after the initiation of the transient (figs. 3.21a and 3.21b). Compared to the experimental findings of a heat-up of nearly the whole core with the peak value at 0.6 m, except for nodalizations 3-02 and 3-

02C, RELAP5/Mod2 still calculated a core heat-up centered to the middle of the core with the peak value at 0.75 m. The 3-02 and 3-02C calculations have indicated a more widened core heat-up but on the other hand have overpredicted the experimental surface temperatures at least 175 K.

Void Fraction, Flow Regime and Heat Transfer Coefficients in the Core Zone

Besides the heat generation in the fuel (source), the other important quantity influencing the cladding temperature is the heat transfer from the cladding to the surrounding fluid (sink). To find some reasons for the deviations of the time traces of the cladding temperatures for different nodalizations, one has to investigate the heat transfer to the fluid at the specific nodes for these different nodalizations even no experimental reference is available.

The heat transfer, expressed by the heat transfer coefficient (HTC), is depending on the mass flow, the local void fraction and the flow-regime "assumed" by RELAP5/Mod2 which itself mainly refers to the local void fraction as well as to the mass flow and the system pressure. Consequently, erroneous mass flows and void fraction distributions will lead to wrong heat transfer coefficients and finally to questionable predictions of the cladding temperatures.

In Figs. 3.22 to 3.27 from top to bottom the local void fractions, the flow regimes as chosen by RELAP5/Mod2 and the heat transfer coefficients have been plotted versus time for axial levels 27 inches (figs. 3.22 to 3.24) and 43.8 inches from the bottom of the core. The comparison has been made for three versions of nodalizations, namely 2-00 (most detailed, plots 3.22 and 3.25), 3-005 (medium simplified, plots 3.23 and 3.26) and

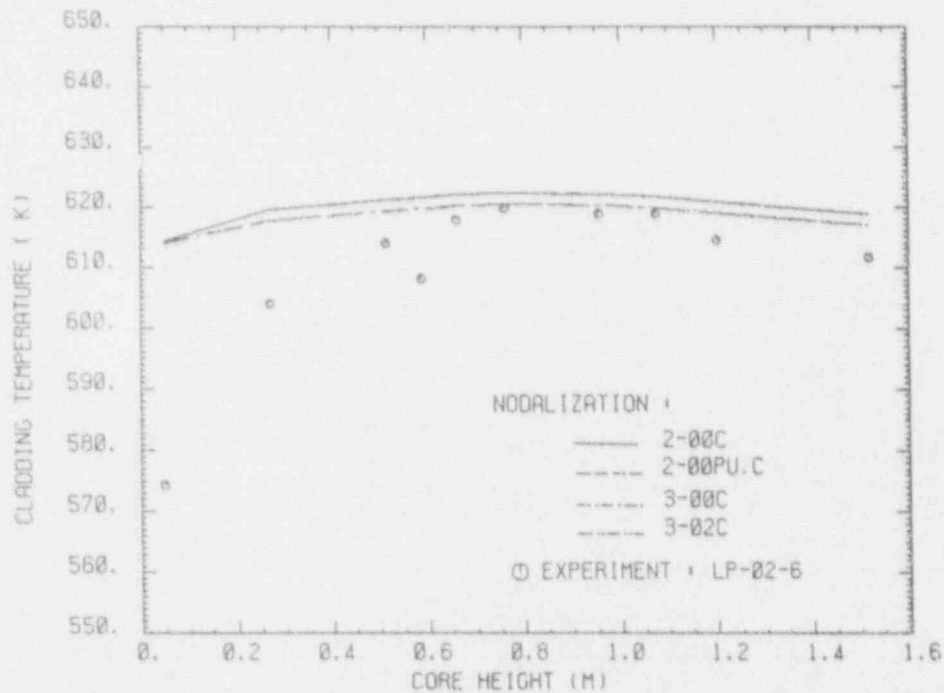
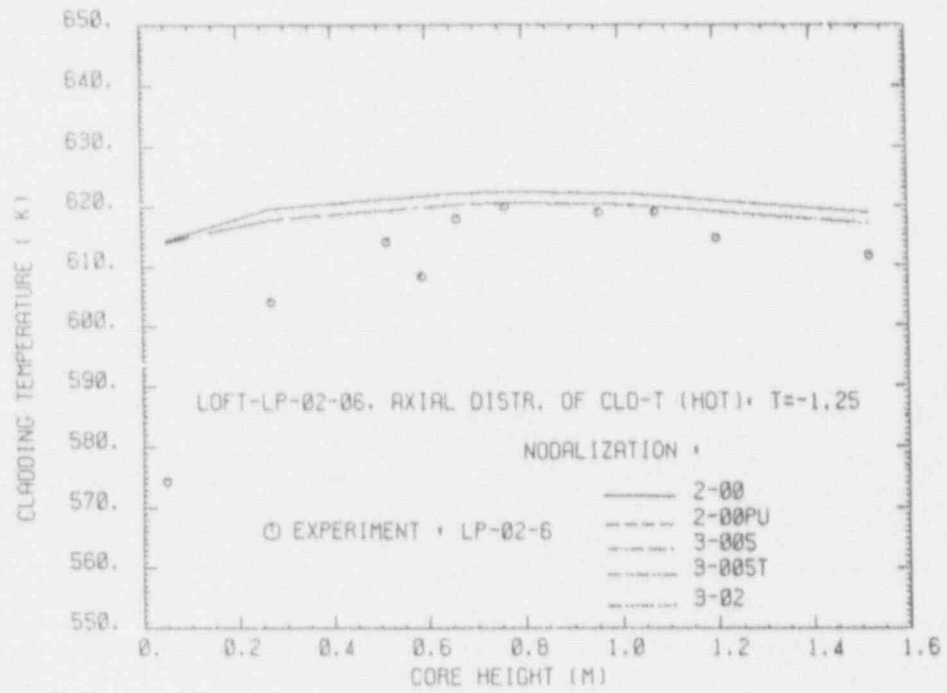


Figure 3.19: Axial cladding temperature distribution at time -1.2 s in hot channel compared with the equivalent averaged reference temperatures in box 5

- a) by neglecting wall heat capacity
- b) by taking into account wall heat capacity ("C")

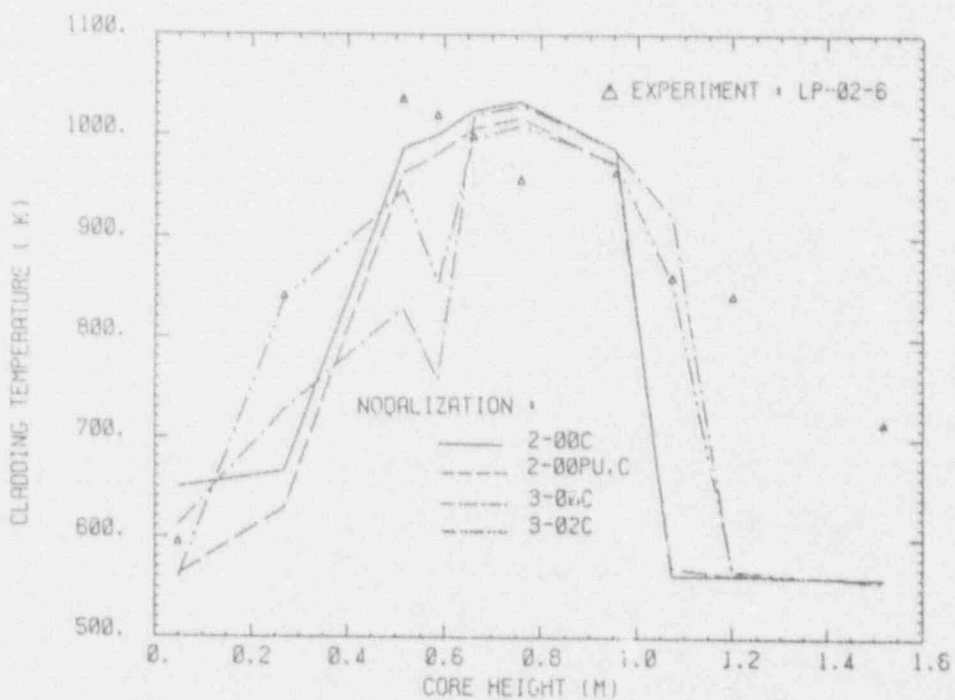
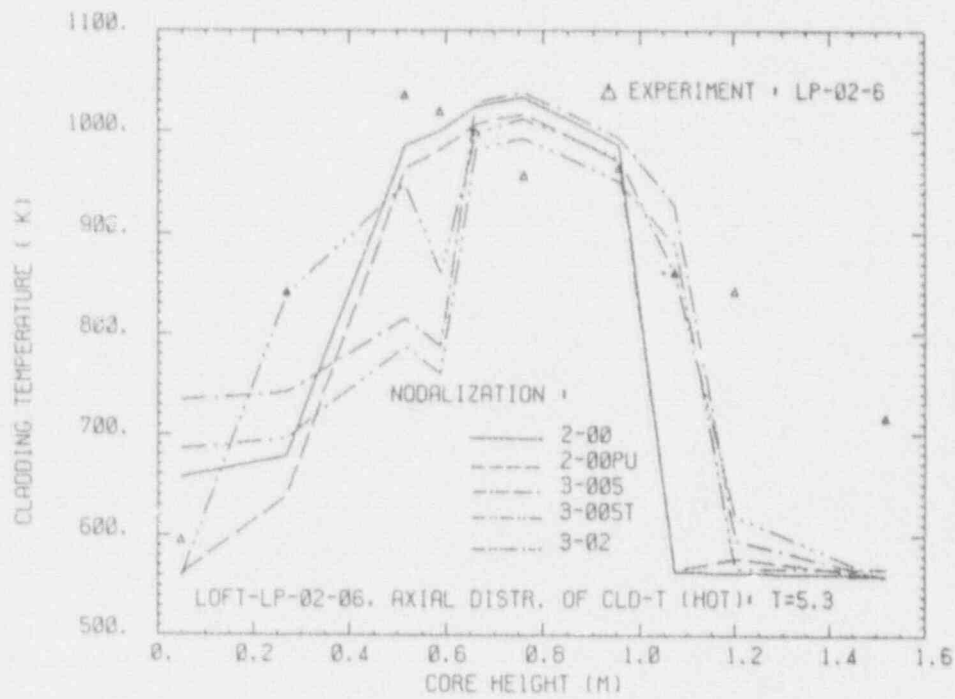


Figure 3.20: Axial cladding temperature distribution at time 5.3 s in hot channel compared with the equivalent averaged reference temperatures in box 5

- by neglecting wall heat capacity
- by taking into account wall heat capacity ("C")

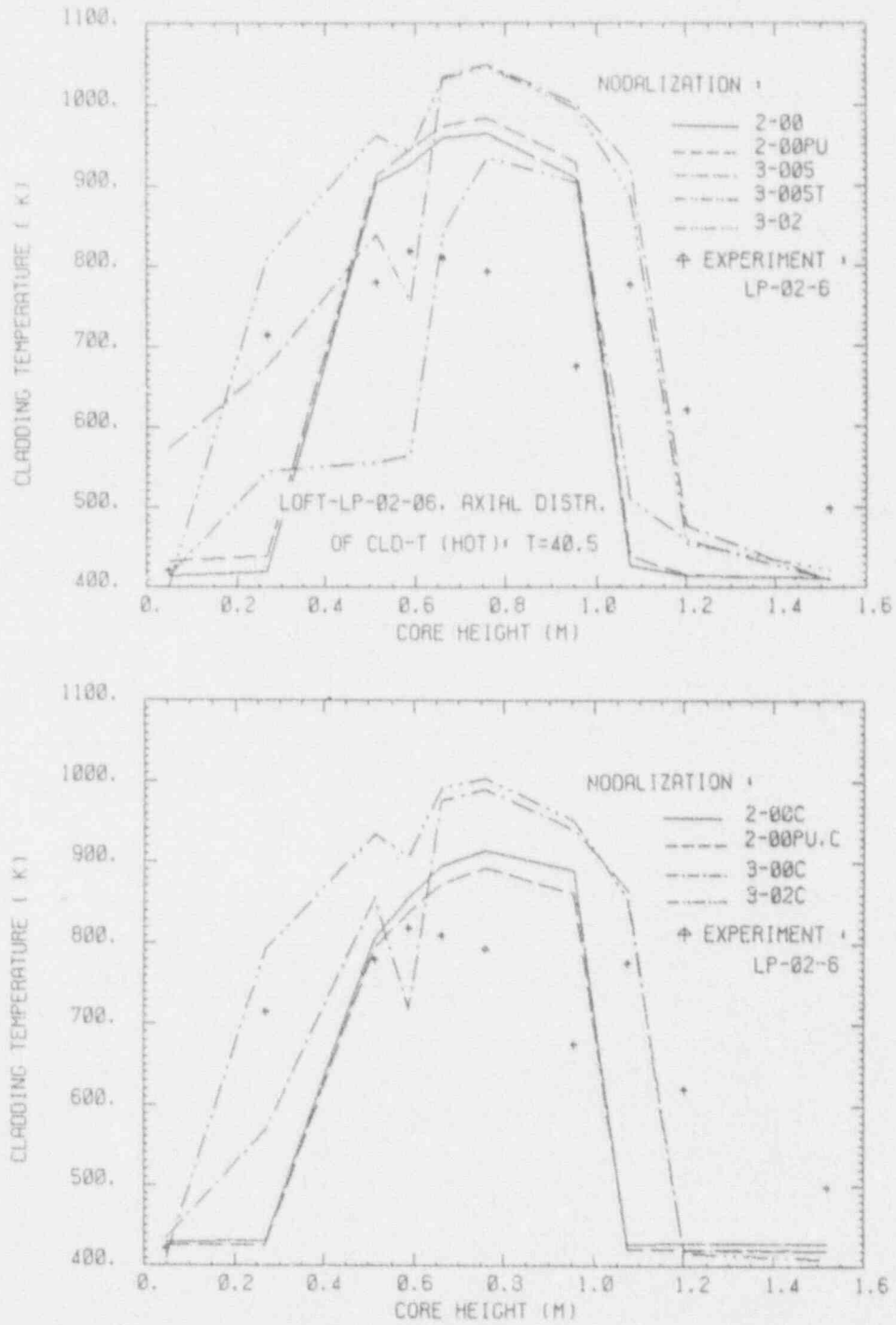


Figure 3.21: Axial cladding temperature distribution at time 40.5 s in hot channel compared with the equivalent averaged reference temperatures in box 5

- a) by neglecting wall heat capacity
- b) by taking into account wall heat capacity ("C")

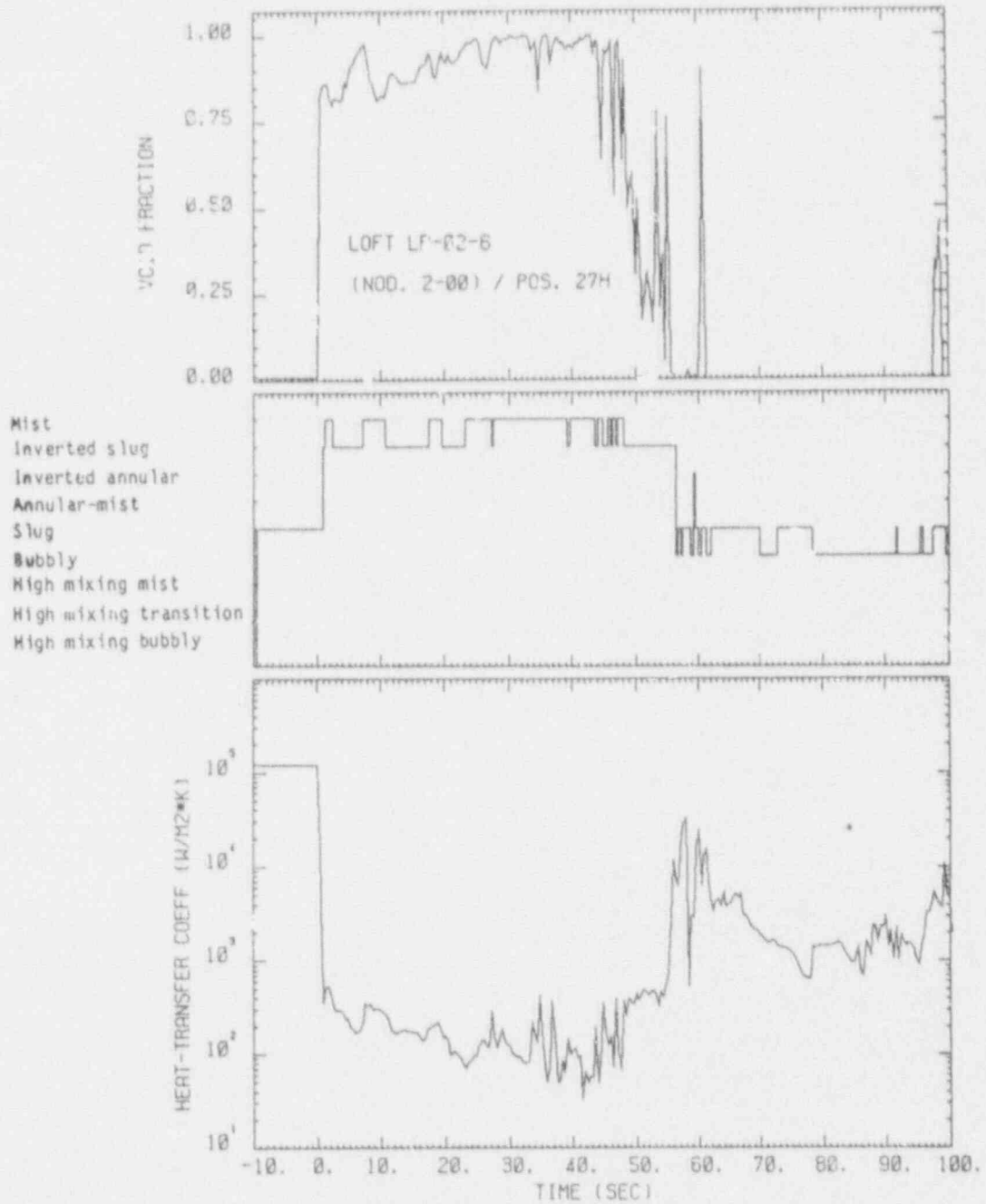


Figure 3.22: Calculated void fraction, flow regime and HTC (nodalization 2-00) for level-27 in the hot channel

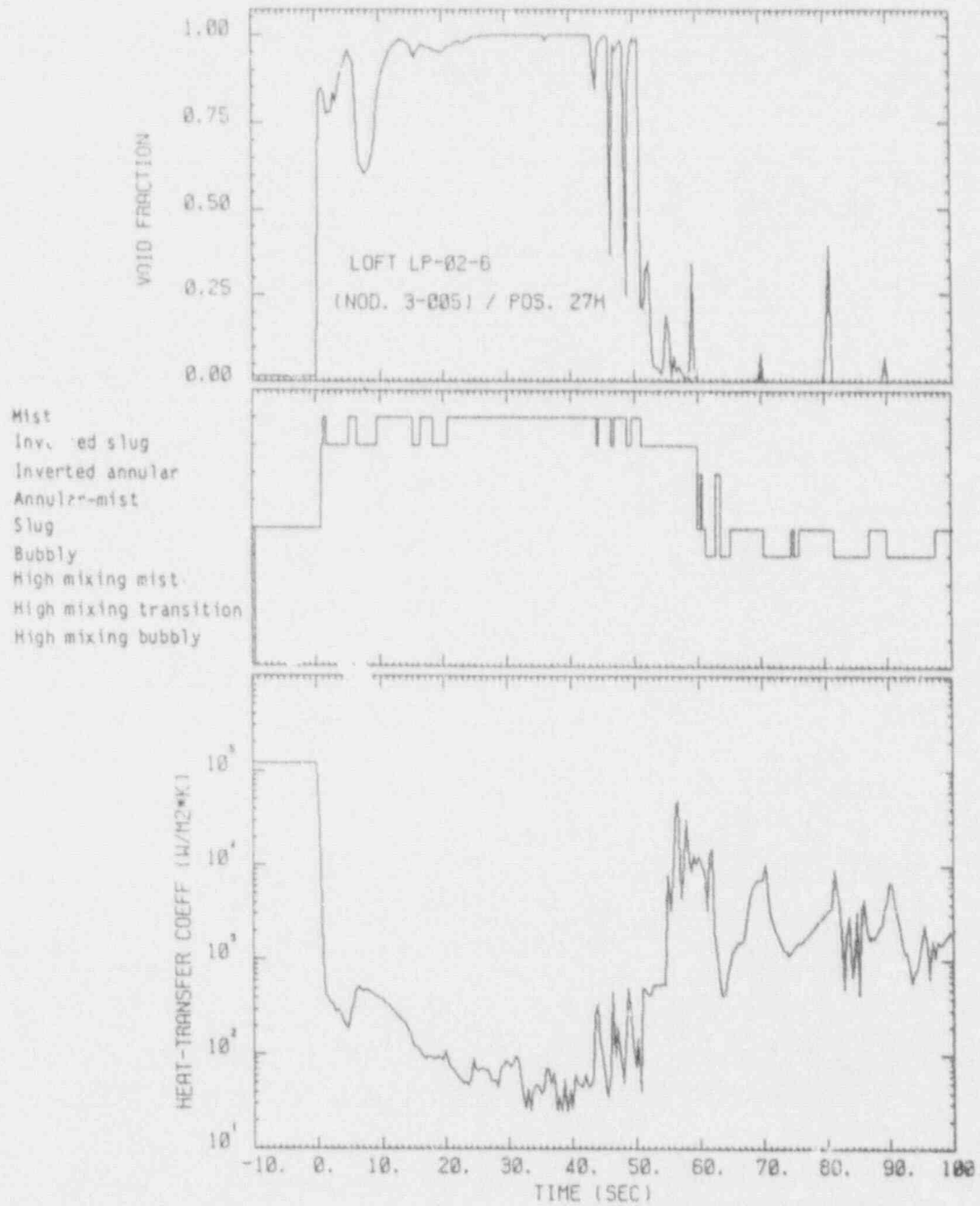


Figure 3.23: Calculated void fraction, flow regime and HTC (nodalization 3-005) for level-27 in the hot channel

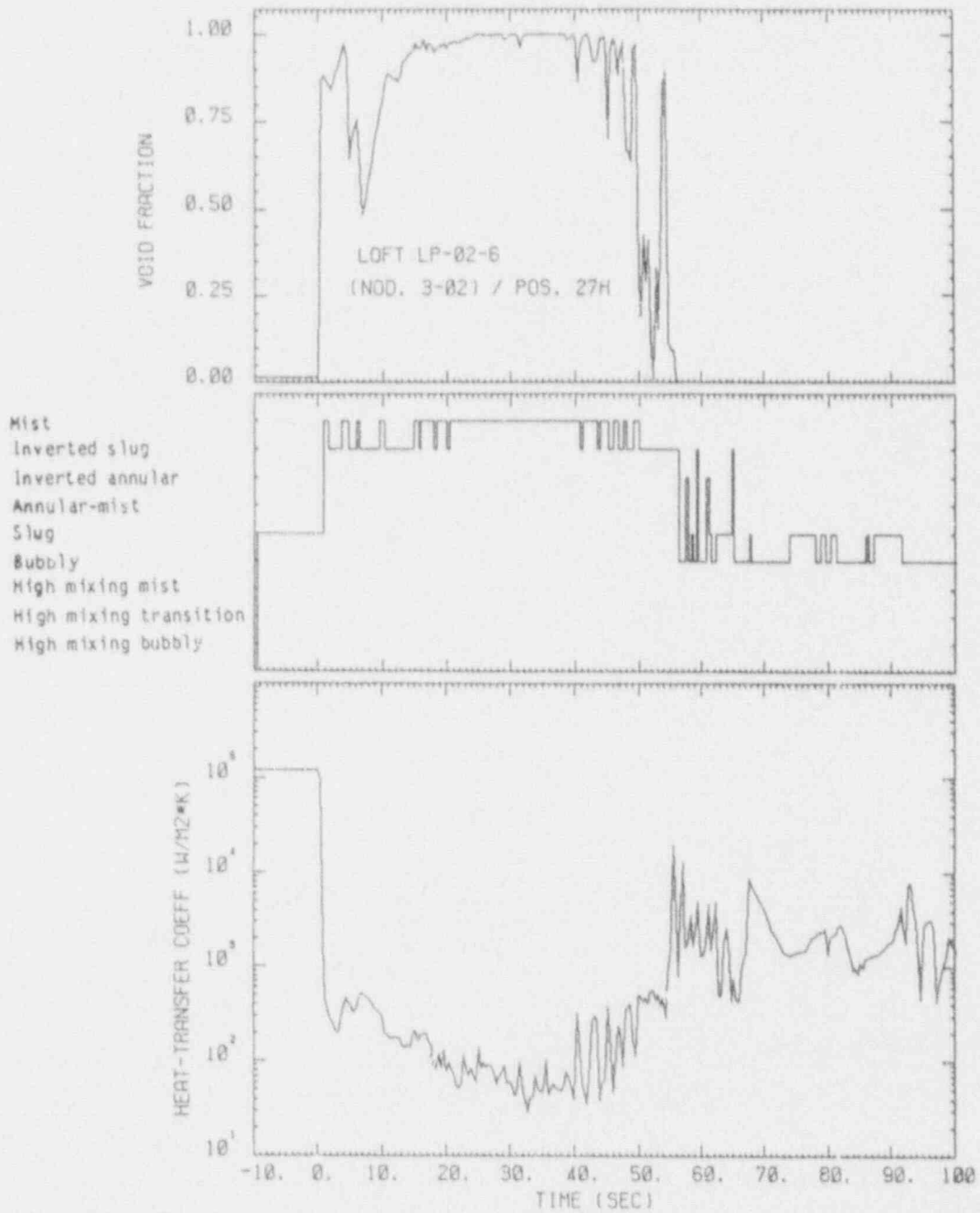


Figure 3.24: Calculated void fraction, flow regime and HTC (nodalization 3-02) for level-27 in the hot channel

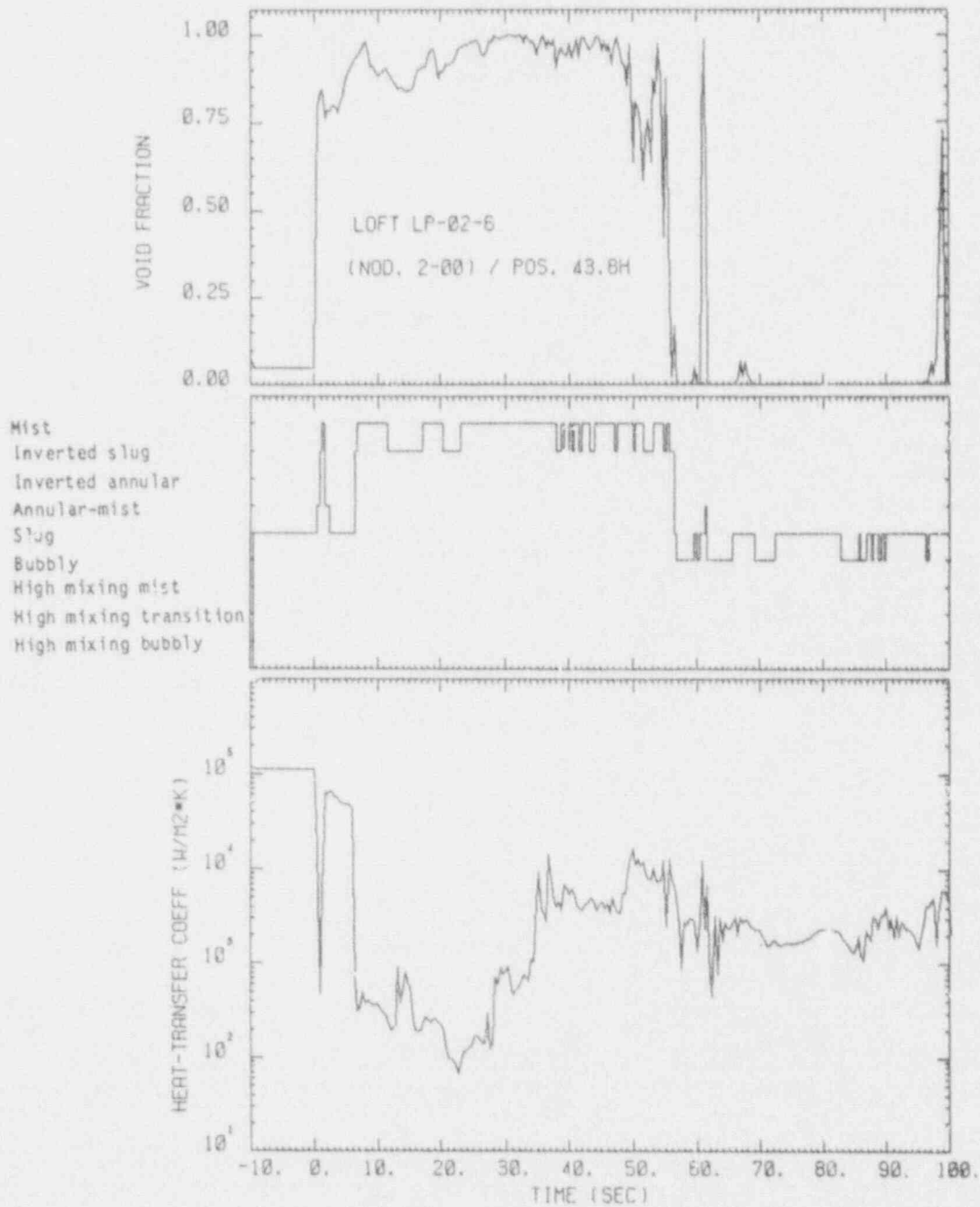


Figure 3.25: Calculated void fraction, flow regime and HTC (nodalization 2-00) for level-43.8 in the hot channel

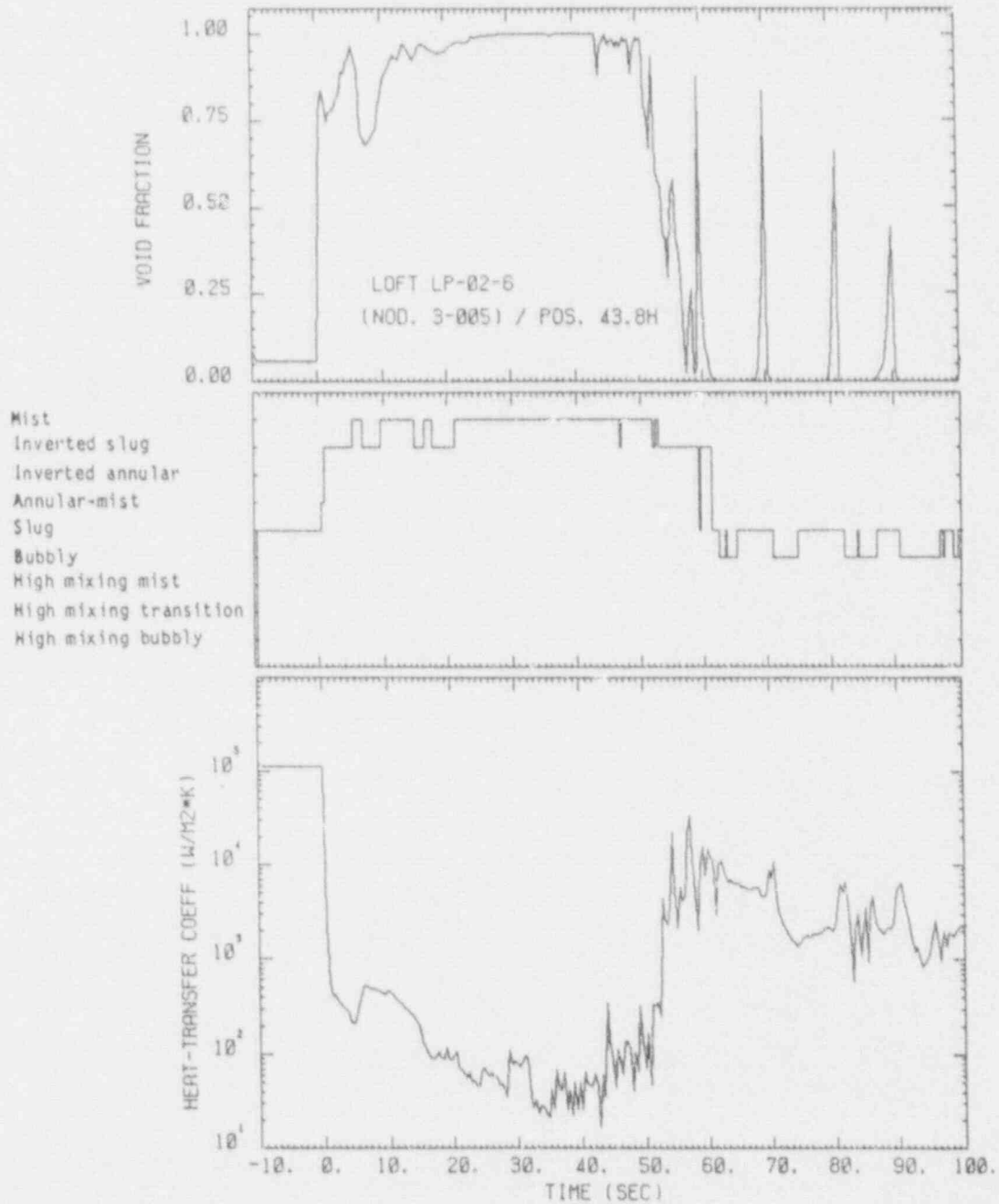


Figure 3.26: Calculated void fraction, flow regime and HTC (nodalization 3-005) for level-43.8 in the hot channel

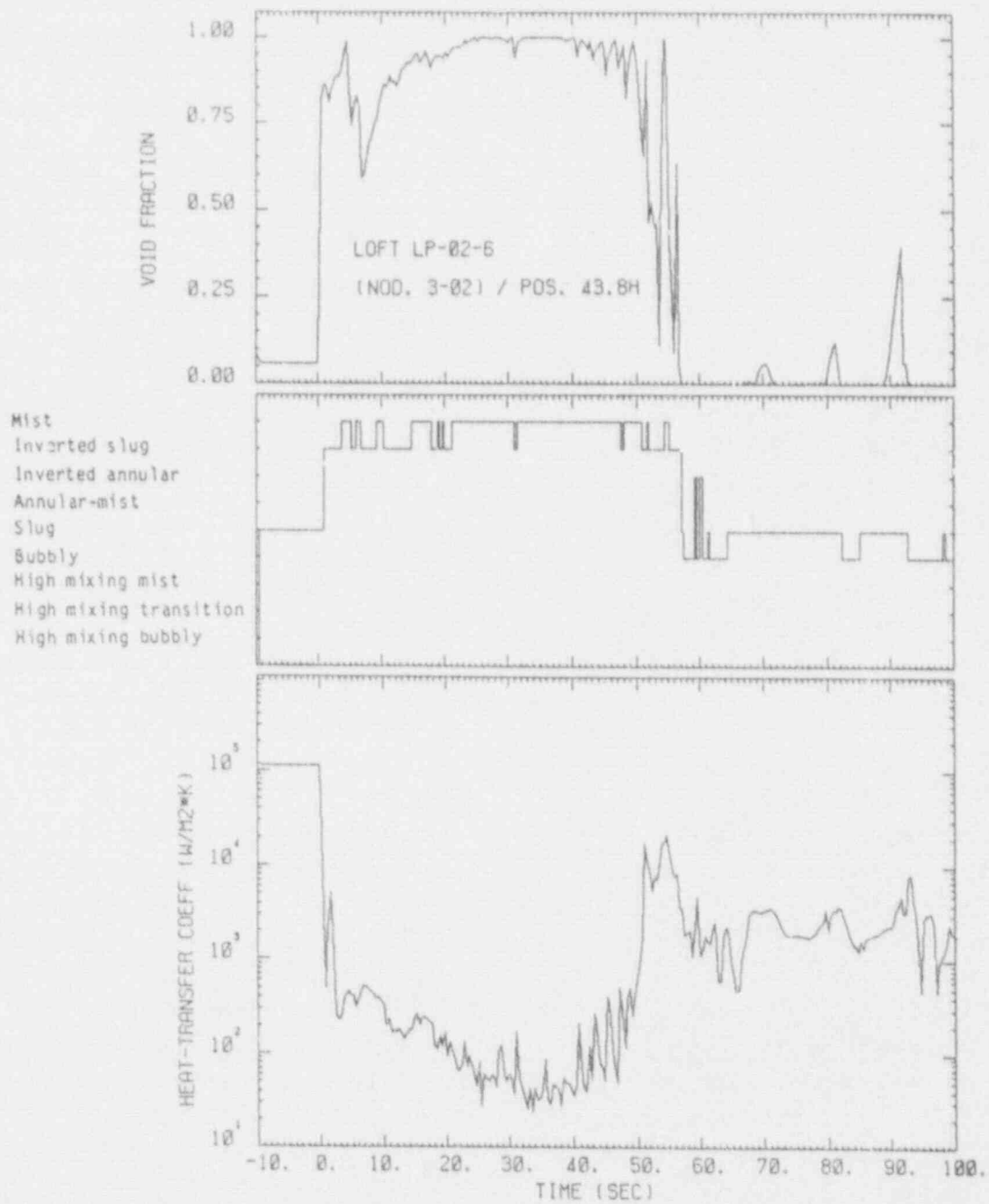


Figure 3.27: Calculated void fraction, flow regime and HTC (nodalization 3-02) for level-43.8 in the hot channel

3-02 (most simplified, plots 3.24 and 3.27).

For all three types of nodalizations, the time behaviour of the local void fraction at the equivalent axial level seem to be comparable, except that there is a "dip" in the time trace of the void fraction at 8 seconds and at the same location for the 3-005 and 3-02 nodalizations, which cannot be found in the results of the 2-00 nodalization. After the initiation of the transient, the void fraction has increased very rapidly from zero to nearly 100%, where it remained until refilling has reached level-27 at about 45 seconds and level 43.8 at 50 seconds. When the quench front has reached axial levels 27 and 43.8 respectively, the void fraction was quite unstable for about 10 to 20 seconds, the oscillations of the void fraction nearly covered half of its range.

The void fraction is one of the main parameters of RELAP5/Mod2 to determine the flow regime which itself is a key information for the evaluation of the interfacial heat transfer as well as of the interfacial shear stress coefficient which, to close the circle, again highly influences the void fraction distribution. Therefore, the graphs in the center of figs. 3.22 to 3.27 show the flow regimes, as defined by the code, as a function of time. In the stationary phase of the experiment, RELAP5/Mod2 decided for slug-flow in the hot zone of the core. After the initiation of the transient, it decided for inverted slug-flow or alternatively mist-flow until the occurrence of the quench at this specific position. Then again, slug-flow has been assumed alternatively with annular-mist-flow. Depending on the nodalization used for the calculation, a smaller or even greater number of "switches" between inverted slug and mist-flow on one side and between slug and annular-mist-flow on the other side may occur. The differences of the latter two flow regimes are minor in-

portant for the determination of the heat-transfer-coefficient (HTC) from the wall to the liquid but may result in enormous differences when evaluating the interfacial friction factors and the interfacial heat transfer coefficients. Probable oscillations in these two important quantities are then feedbacked, causing instabilities in the void fraction calculation.

The lower graphs on figs. 3.22 to 3.27 show the heat-transfer-coefficients (HTC) as a function of time. As expected, heat-transfer-coefficient drops rapidly into the inverted-slug / mist-flow regimes thus resulting in heat-up of the fuel. Occurrence of the rewetting is well indicated by the steep increase of the heat-transfer-coefficient between 40 and 60 seconds, depending on the axial location and the type of nodalization.

We would like to focus the attention of the reader on some inconsistencies between the flow regime indicator (middle plot) and the heat-transfer-coefficient (lower plot) more or less pronounced in all of the six calculated cases, namely that the time-traces of the flow regime indicator and of the heat-transfer-coefficient indicate "quench" at different times. We have reported similar inconsistencies in our LP-LB-1 post test analysis. Whereas in fig. 3.22, this discrepancy is only about two seconds (the "quench time" of the heat-transfer-coefficient is comparable to the value given by the steep negative gradient of the cladding temperature, see fig. 3.9), in fig. 3.23 this difference is raised to 24 seconds (again, the heat-transfer-coefficient "quench" is comparable to the cladding temperature "quench" on fig. 3.12). This was a calculation using the 2-00 nodalization. For the other examples, e.g. nodalizations 3-005 and 3-02, these inconsistencies are slightly smaller but still exist. Generally, they were larger at level 43.8 than at level 27. In other

words, the code calculated the heat-transfer-coefficient from the cladding to the coolant assuming completely other flow conditions than the heat-transfer-coefficient between the steam and liquid phases for longer periods.

With regard to the "stabilities" of the void fraction (upper plot), of the flow regime (middle plot) indicator as well as of the heat-transfer-coefficient (lower plot), the most simplified 3-005 and 3-02 nodalizations seem to be more stable than the more detailed version 2-00.

As we have already mentioned above, flow regime and heat transfer coefficients in the core region are strongly depending on the axial void fraction distribution as well as on the mass flows in the core region. Both of them are determined by the thermohydraulic conditions in the primary system of the LOFT reactor like the intact and broken loops, the pressurizer, the heat sink (steam generator secondary side or a more simplified version of it), the primary coolant pumps and the behaviour of the ECC-systems. The predictions of their behaviour during the transient depend on the ability of the code in describing the sequence of thermohydraulic phenomena. Therefore, a realistic description of the main phenomena has to be regarded as a "conditio sine qua non" for the predicting capability of the key parameters like the cladding temperatures.

In what follows, we shall concentrate on the description of these phenomena by considering some other important parameters. But before we start this discussion, we would like to look also at the second key parameters with respect to safety aspects, which in the case of a large break are of less importance because the reactor has been scrammed within parts of a second after the initiation of the

transient, thus drastically reducing the heat generation within the fuel.

3.4.2 Fuel Center Temperature

Only at one axial level experimentally inferred fuel center temperatures are available, namely at position 27 (i.e. 27 inches from the bottom of the core, where the "hot-spot" has been found for experiment LP-02-6). The equivalent predictions of RELAP5/Mod2 for the different nodalization schemes have been compared to the experimental data and plotted in fig. 3.28. The experimental data are average values of fuel center temperature data at 10 radially distributed positions on axial level 27 of the center box 5.

Obviously, the highest fuel temperatures have been reached at full power conditions, before the transient has been initiated. For these stationary conditions, the calculated temperatures are quite close to the experimental data, independently of the type of nodalization.

During the transient, the calculated fuel center temperatures have been found to be only in qualitative agreement with the experimentally inferred reference temperatures. Except the results of the 3-005T nodalization which is surprisingly in good agreement with the measured temperature distribution (because, as we have already mentioned, also the cladding temperatures have been calculated with excellent accuracy at this axial position; see fig. 3.9a), the fuel center temperatures have been overpredicted by RELAP5/Mod2 between 250 K and 300 K for nearly the whole time period until the rods have been quenched (10 to 55 seconds of the transient). The temperature traces as calculated by RELAP5/Mod2 using different nodalizations are similar. No significant differences have been observed between the

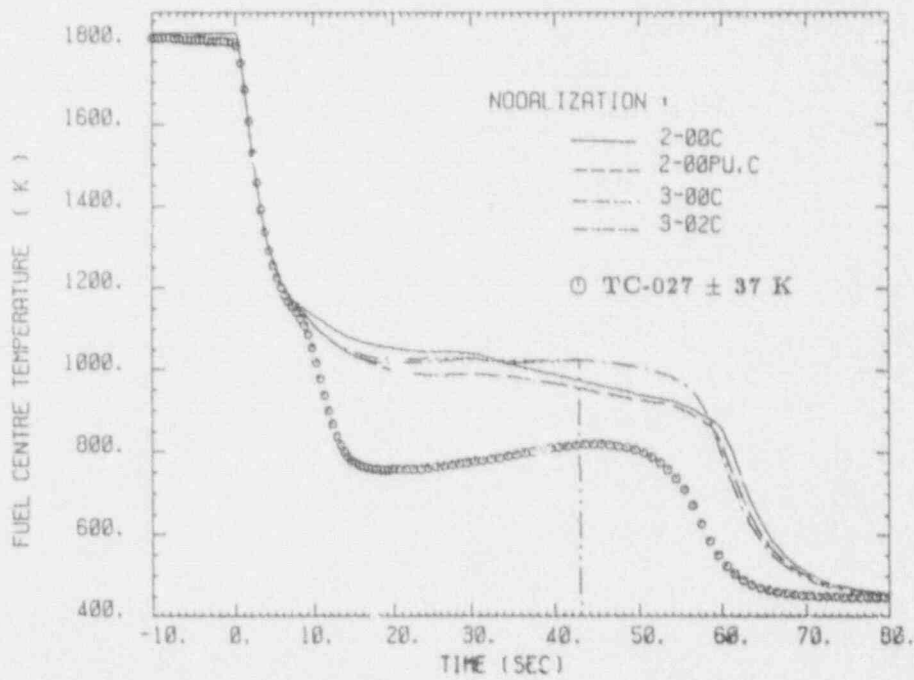
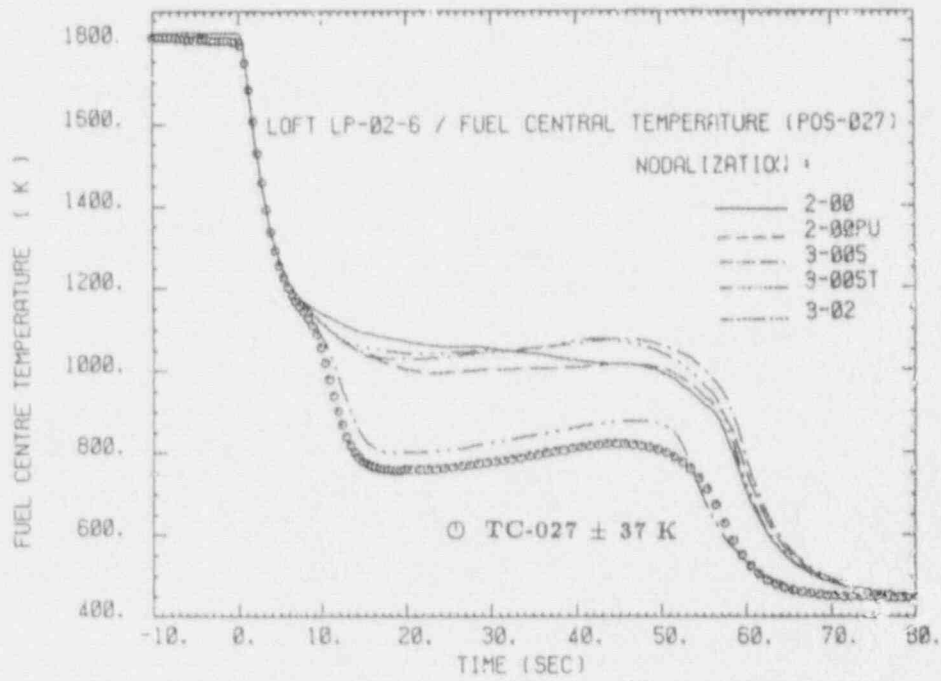


Figure 3.28: History of the fuel center temperature in the hot channel compared with averaged measured fuel temperatures at level-27

- a) by neglecting wall heat capacity
- b) by taking into account wall heat capacity ("C")

results of the most elaborated 2-00 and the most simplified 3-02 nodalization. Furthermore, the differences between the normal and the "C" versions (i.e. not taking and taking into account heat capacity effects of the vessel material) are quite small even the overprediction of the "C" versions seems to be by some degrees less.

3.4.3 System Pressures

It is a well-known fact that most of the best-estimate codes do a quite satisfactory job when predicting the system pressures. Our investigation also confirms this common knowledge.

In figs. 3.29a and b, the system pressures as calculated by RELAP5/Mod2 have been compared to the experimental data, i.e. the absolute pressures as measured by the pressure transducer mounted in the cold leg of the intact loop at station 002. As usual in this contribution, we again have separated our results into two plots, the upper showing the results of the predictions using the normal nodalizations and the lower showing the ones using the "C" versions. Obviously, for all the different nodalizations, the RELAP5/Mod2 calculations are fairly good even though smaller discrepancies occur between 5 and 30 seconds of the transient. Closest to the experimental findings seem to be the calculations of versions 3-005 and 3-00C, i.e. the results of calculations using a rather simplified type of nodalizations of the LOFT-system.

Compared to those of the system pressure the predictions of the pressure in the pressurizer have been found less accurate as one may see in figs. 3.30a and 3.30b. Here, the calculations of the runs with 3-... type of nodal-

ization, i.e. the cases with a reduced modelling of the pressurizer (instead of 11 volumes used for the pressurizer in the standard version 2-00, in the 3-... versions only 5 volumes have been used), are fairly poorer than those of the standard version 2-... which sufficiently follow the experimental data. Especially between 3 and 15 seconds, the underprediction of RELAP5/Mod2 runs using 3-... nodalizations may exceed 2 MPa. These deviations only occur in the pressurizer and are not to be found at any other location in the system; we therefore believe that these deviations are tolerable for the course of the transient because the predictions of the pressure inside the pressurizer seem to be of secondary importance.

3.4.4 Fluid-Temperature in the Downcomer

Besides the system pressure, the fluid temperatures in the downcomer may be important with respect to the void formation in the core region because these temperatures are more or less identical to those at the entrance of the core, provided a positive flow out of the downcomer into the core region occurs. Therefore, in figs. 3.31a and 3.31b, we would first like to compare the fluid temperatures as predicted by RELAP5/Mod2 using the different nodalizations with equivalent temperature traces as measured in the downcomer at position 005.

The initial values of the fluid temperatures have been predicted fairly well (-10 to zero seconds). This is also the case for the following time interval between zero and approximately 20 seconds where the temperatures follow the saturation line. Because of the rapid drop of the system pressure, the fluid temperature becomes saturated at about 8 seconds after initiation of the transient.

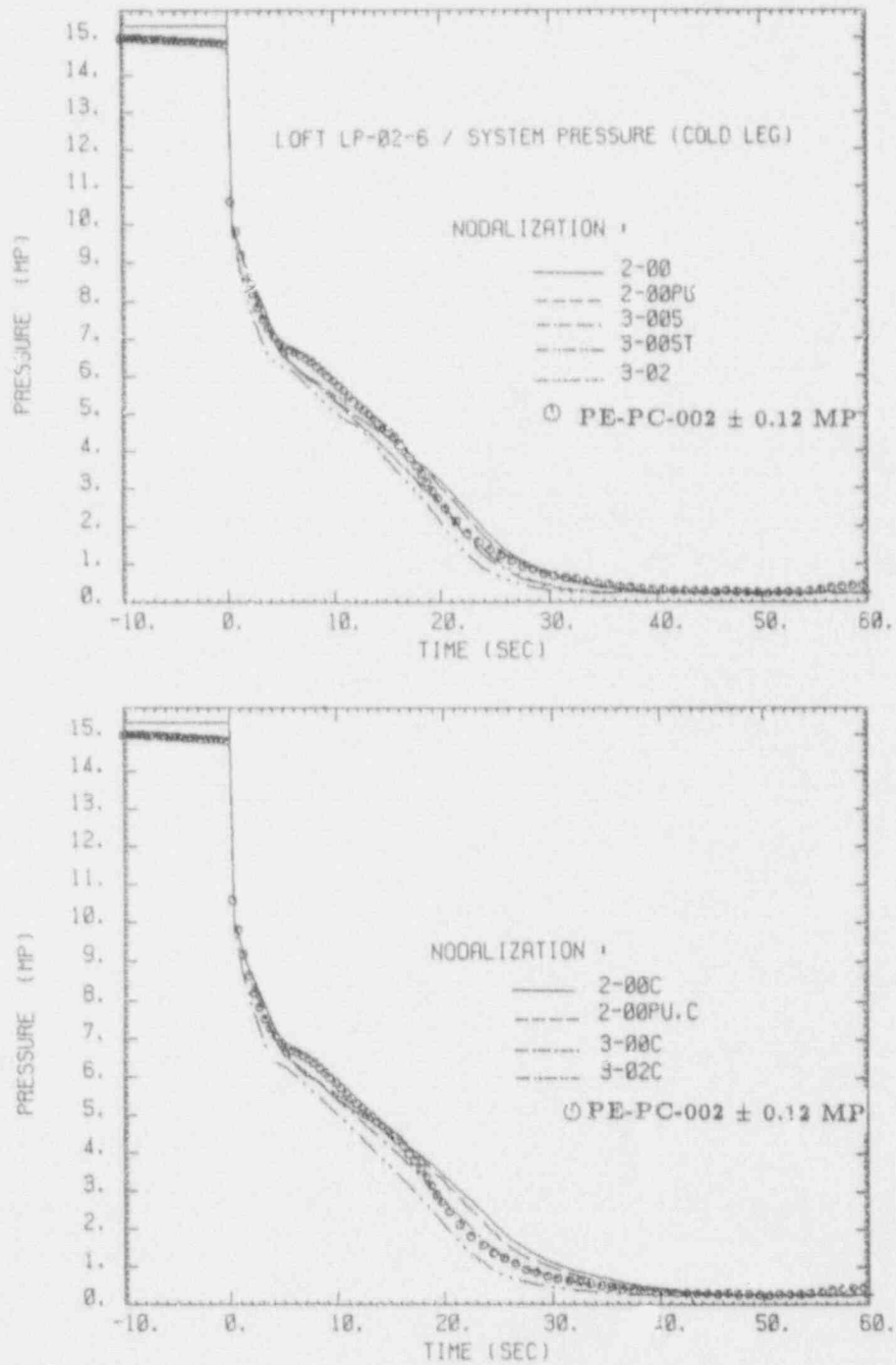


Figure 3.29: System pressures in the cold leg vs. time compared with pressure measured at station PC-002
 a) by neglecting wall heat capacity
 b) by taking into account wall heat capacity ("C")

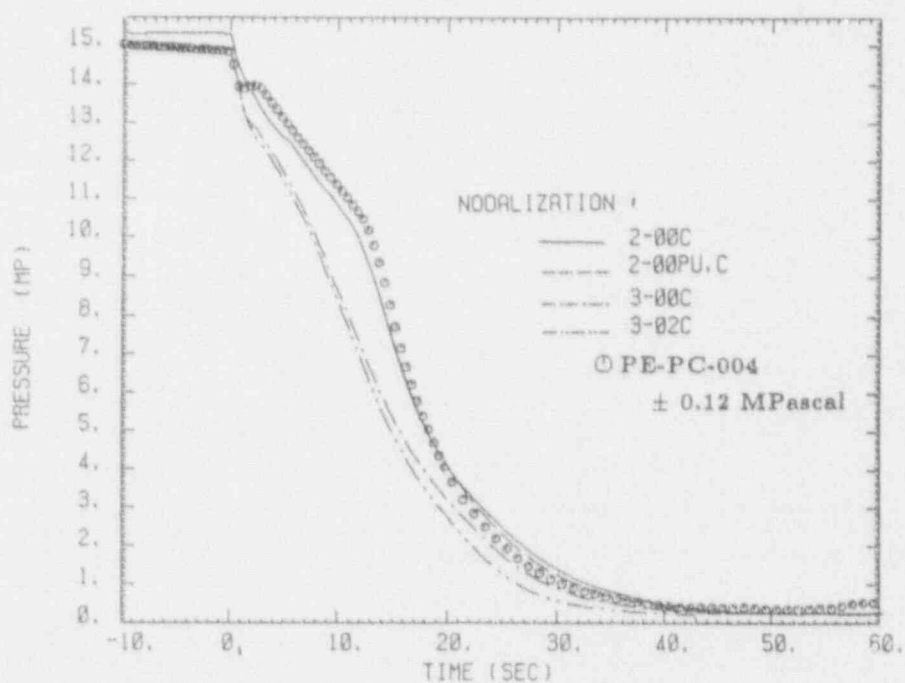
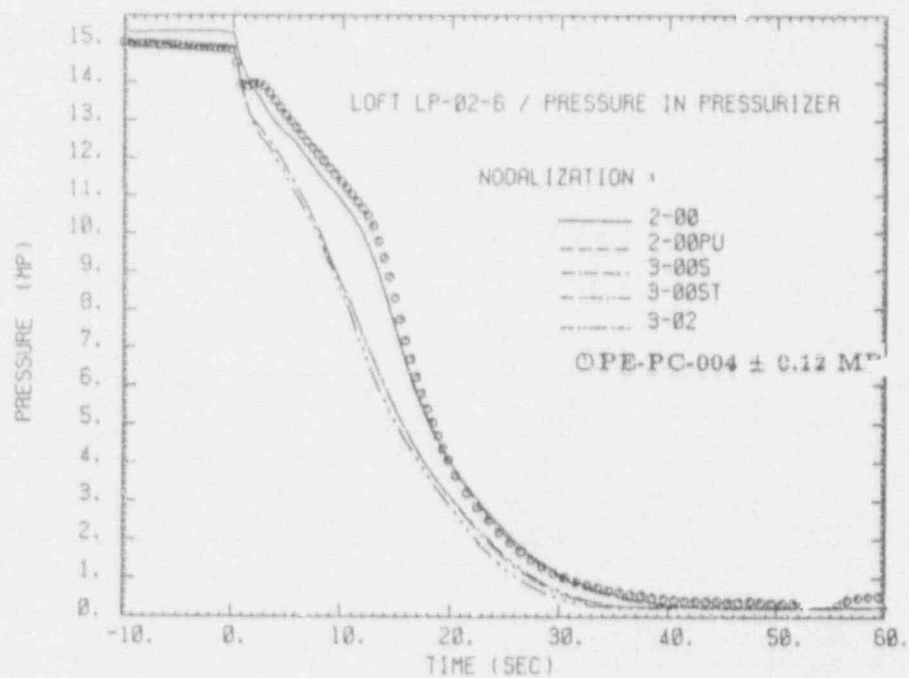


Figure 3.30: Pressures in the pressurizer vs. time compared with pressure measured at station PC-004 of the pressurizer

- a) by neglecting wall heat capacity
- b) by taking into account wall heat capacity ("C")

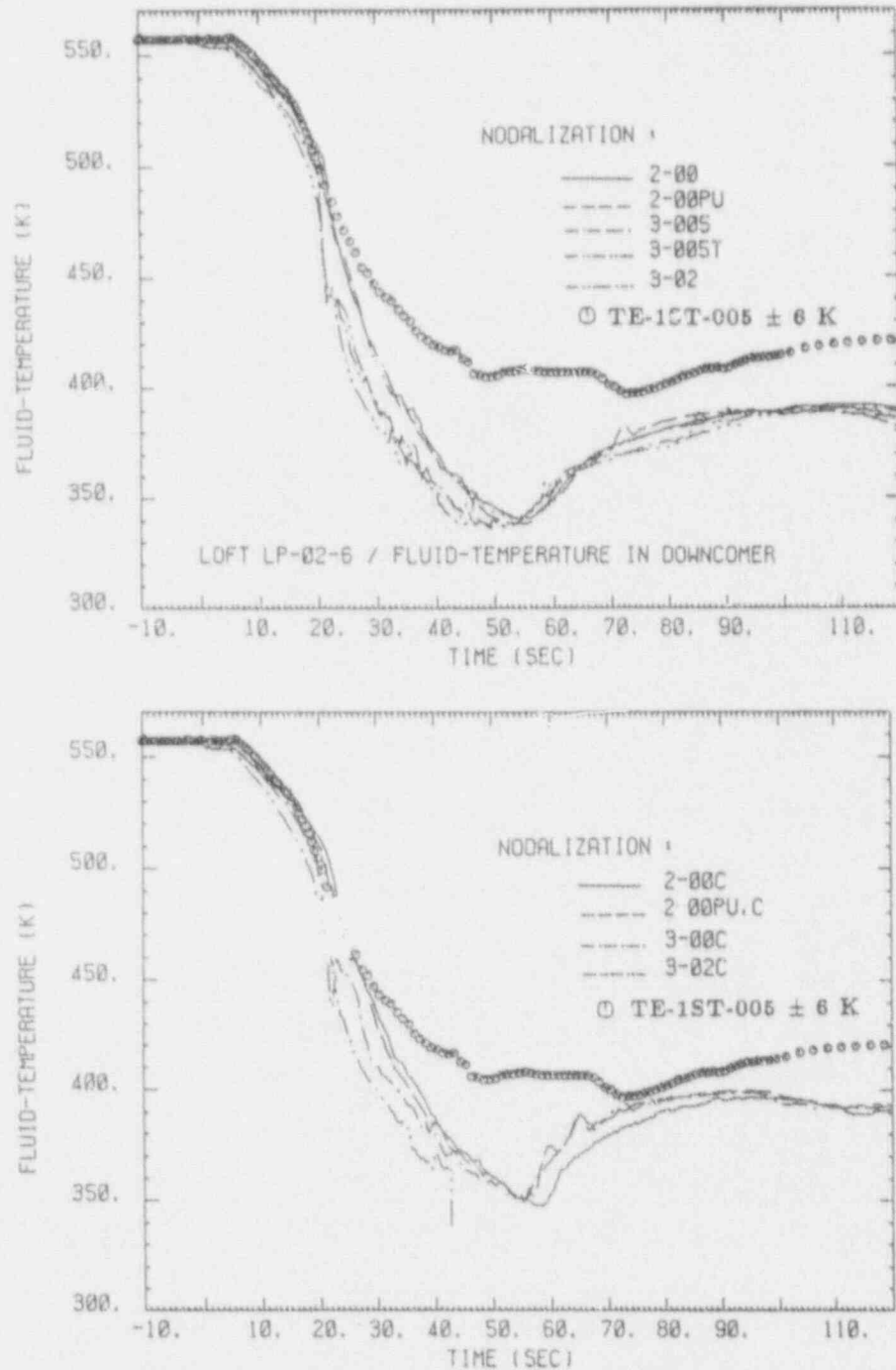


Figure 3.31: Downcomer fluid temperatures vs. time compared with fluid temperatures measured at station 1ST-005
 a) by neglecting wall heat capacity
 b) by taking into account wall heat capacity ("C")

For all the versions of nodalizations, the fluid temperatures start to deviate from saturation at approximately 25 seconds and reach the saturation temperature again at about 70 seconds. Beginning at 40 seconds, the system pressure is more or less constant (see figs. 3.29a and 3.29b). The straight line in figs. 3.31a and 3.31b for times higher than 70 seconds can be regarded as the saturation temperature at this pressure, i.e. all temperatures below this line indicate subcooled fluid. Consequently, RELAP5/Mod2 predicted a certain amount of liquid subcooling in the time interval between 20 and 70 seconds which has reached peak values of up to 70 K for all of the "N" versions of nodalization and minimum peak subcoolings of 55 degrees for most of the "C" versions. On the other hand, the thermocouple signals have indicated a significant "liquid superheat" of nearly 20 K which probably is due to a dry out of the thermocouple tip, measuring something in between saturated steam temperature and thermocouple heat-up due to radiation heat transfer.

3.4.5 Core Mass Flows

Now, we have to look at mass flows into and out of the core as calculated by RELAP5/Mod2. In figs. 3.32a and 3.32b, the mass fluxes into the core and in figs. 3.33a and 3.33b, the mass fluxes out of the hot channel have been plotted. Unfortunately, no corresponding experimental reference data are available.

In figs. 3.32a and 3.32b, the inlet mass fluxes into the hot channel as calculated by RELAP5/Mod2 using different nodalizations have been plotted. Generally, depending on the nodalization, the mass fluxes are positive for some seconds between 3.5 and 15 seconds and then remain nearly on the zero line

whereas below 3.5 seconds to 6.5 seconds i.e. during the blowdown phase, depending on the nodalization, the flow direction indicates a strong reverse flow.

Obviously, the amount of positive core mass flux during the first 15 seconds of the experiment is strongly depending on the pump behaviour because only the predictions of the 2-00 nodalization (i.e. rapid pump coast-down similar to that of experiment LP-LB-1 (see ref. [7]) have indicated a quite small amount of positive core mass flux whereas all the other runs with imposed pump behaviour, i.e. pump speed has been given as a boundary condition according to the experimental pump behaviour, indicated as significant positive inlet flux.

The mass fluxes out of the core, figs. 3.33a and 3.33b, experienced similar behaviour. Again, for the first 3.5 seconds, the fluxes are negative, i.e. the fluid streams from the upper plenum through the core into the downcomer (broken leg). Then for all the runs except the 2-00 and 2-00C nodalizations, the mass fluxes became highly positive reaching values up to $850 \text{ kg sec}^{-1} \text{ m}^{-2}$ for at least two seconds, indicating a fast liquid flow out of the core. Again, only the RELAP5/Mod2 calculations based on the 2-00 and 2-00C nodalizations (rapid coastdown of the pumps) showed rather low mass fluxes with peak values of not more than $150 \text{ kg sec}^{-1} \text{ m}^2$. The highly positive mass fluxes into and out of the core during the first seconds of the transient seem to be a consequence of the pump operation because they only occur when the pumps remained connected to their flywheels; for nodalizations 2-00 and 2-00C where the flywheels have been disconnected, the mass fluxes have been significantly lower.

Based on the RELAP5/Mod2 calculations,

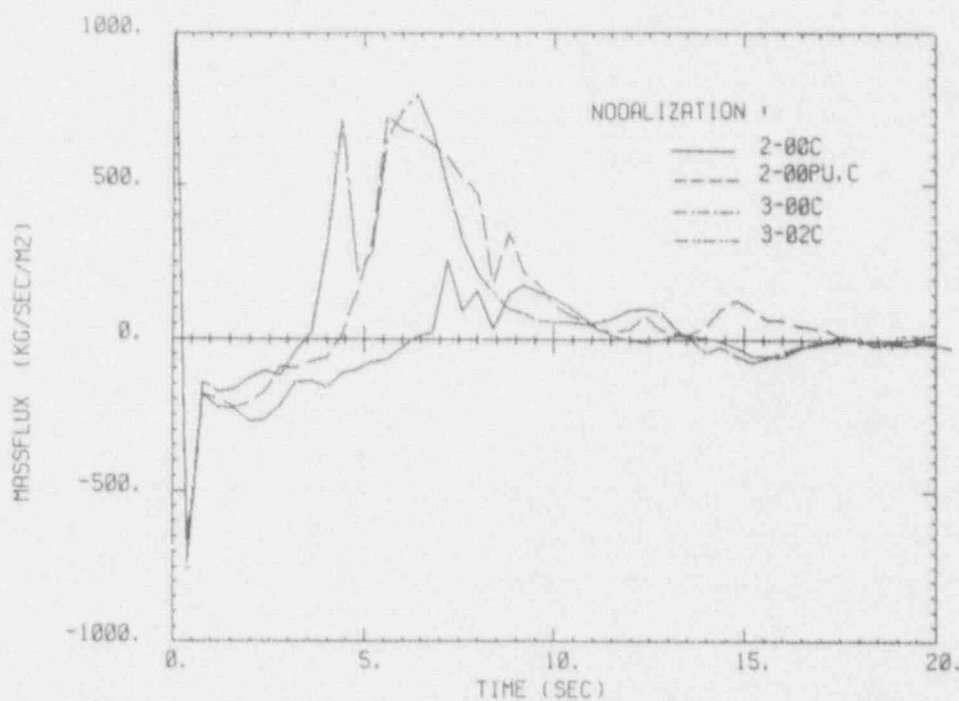
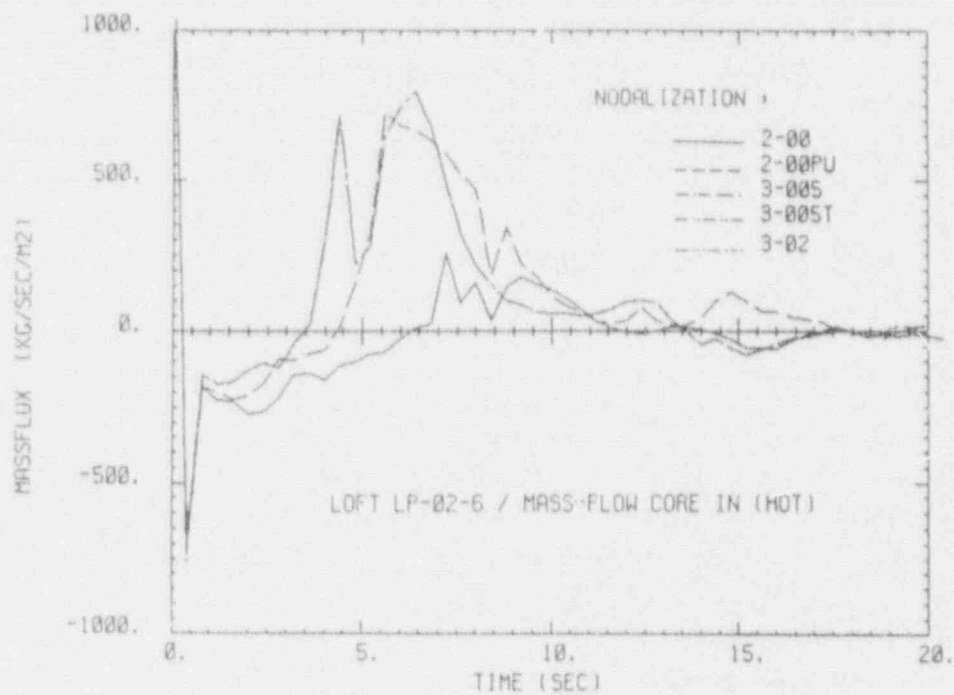


Figure 3.32: Mass fluxes into the hot channel of the core as calculated by RELAP5/Mod2

- by neglecting wall heat capacity
- by taking into account wall heat capacity ("C")

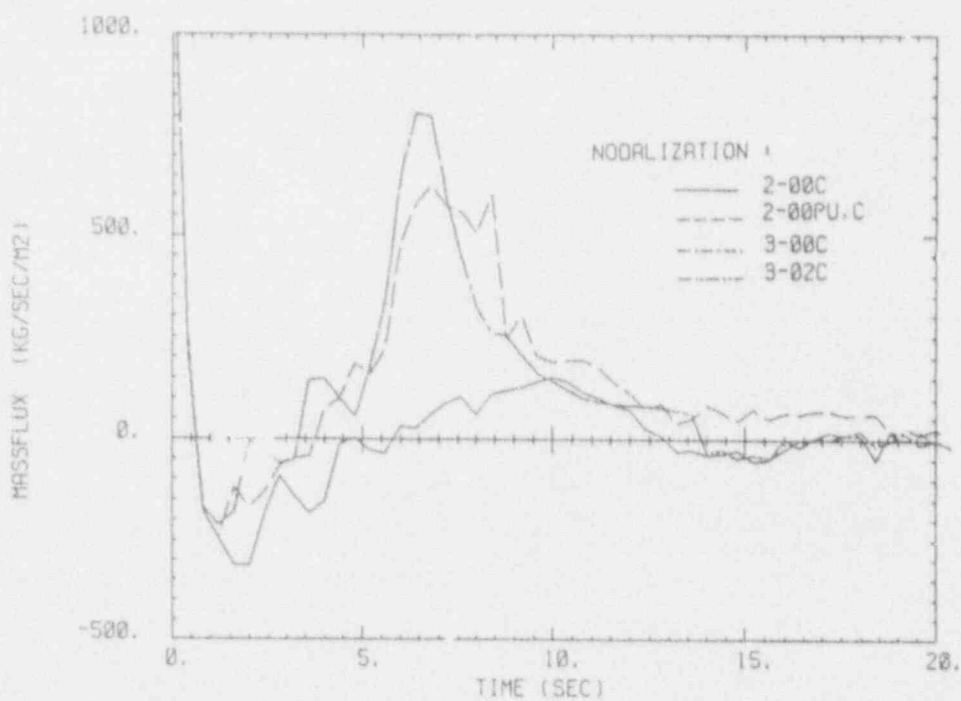
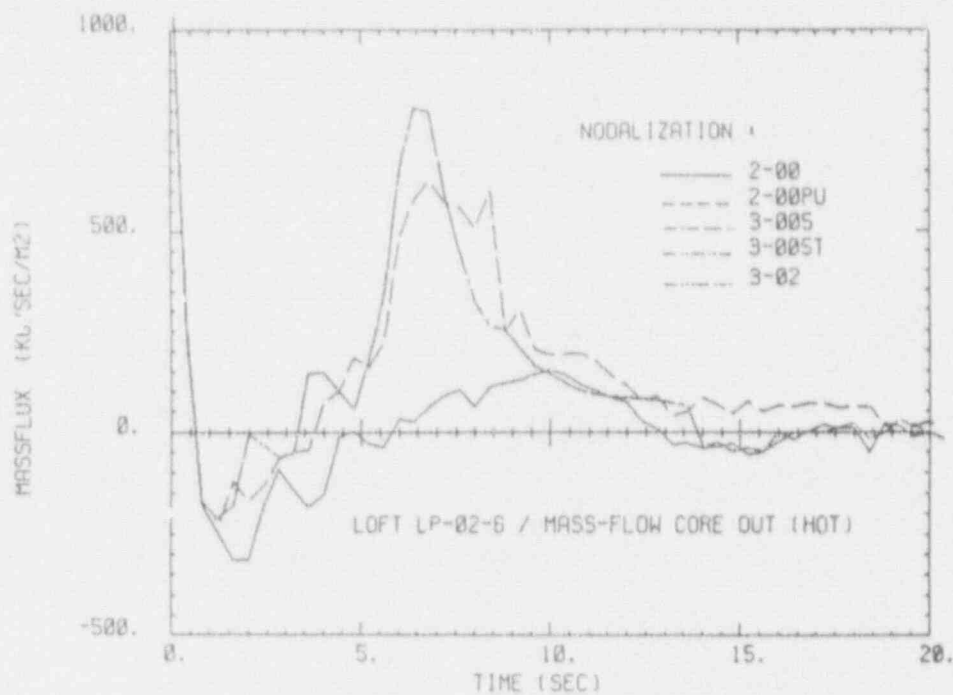


Figure 3.33: Mass fluxes out of the hot channel of the core as calculated by RELAP5/Mod2
 a) by neglecting wall heat capacity
 b) by taking into account wall heat capacity ("C")

these high positive mass fluxes into and out of the core during at least three seconds of the blowdown interval of experiment LP-02-6 are a strong indication that bottom-up reflooding could have been taken place. Consequently, if the code has failed to predict bottom-up rewetting (which on the other hand has been observed experimentally) it has to be attributed to a lack of proper modelling the rewetting phenomena within the RELAP5/Mod2 code. We shall come back to this point in chapter 3.4.

On the other hand, there is no "calculational evidence" for the assumption of a significant top-down quenching during the blowdown phase because the mass fluxes do not reach significant negative values within the first 20 seconds of the experiment. Therefore, top-down reflooding cannot be expected from these calculations.

Somehow related to the mass fluxes are the momentum fluxes. Therefore, in addition to the mass fluxes, we shall plot the in- and out-flow momentum fluxes in figs 3.34a, 3.34b, 3.35a and 3.35b, because for these parameters experimental references are available. Although these references inferred from very local measurements (small drag bodies) and as indicated in the individual plots observed high transducer uncertainties, they may allow us to see a trend of the time behaviour of the mass flows. Indeed, the time traces of the momentum fluxes and mass fluxes as calculated by RELAP5/Mod2 behave quite similar.

Both the momentum fluxes in the lower plenum (figs. 3.34a and 3.34b) and in the upper plenum (figs. 3.35a and 3.35b) deviated significantly from the measured data point. Whereas the core outlet momentum fluxes have been reproduced by RELAP5/Mod2 within the right magnitude of

$2000 \text{ kg m}^{-1}\text{s}^{-2}$, with the only difference that the measured peak is wider than the calculated one, the core inlet momentum fluxes (figs. 3.34a and 3.34b) indicated even different signs, namely a negative momentum flux of the measured and a positive one of the calculated data; in fact one single data point of the momentum flux at 5.4 seconds of the transient is positive. On the other hand, because the measured momentum fluxes give positive outflows on both sides of the core which implies an impossible fluid source inside the core, at least one of the two local momentum flux measurements is somehow dubious with respect to their applicability to global values.

3.4.6 Core Average Liquid Fractions

Very important for the behaviour of the cladding temperatures are the average liquid fractions in the core region (identical to the relative collapsed liquid levels) because low liquid fractions are essentially necessary to allow core heat-up whereas increasing liquid fractions are the consequence of a refilling process. Therefore, in figs. 3.36a and 3.36b, the average liquid fractions as calculated by RELAP5/Mod2 for different nodalizations have been plotted. Unfortunately, for this very important quantity again no experimental references have been available.

After a very sharp drop of the liquid fraction during the early blowdown phase (zero to one seconds) bottom-up reflooding is indicated by a very strong "blowdown refill peak" at approximately 8.5 seconds after initiation of the transient; this peak is less pronounced for the 2-00 and 2-00C nodalizations. Then, for all the different nodalizations, RELAP5/Mod2 predicted a minimum liquid level at approximately 30 seconds. Af-

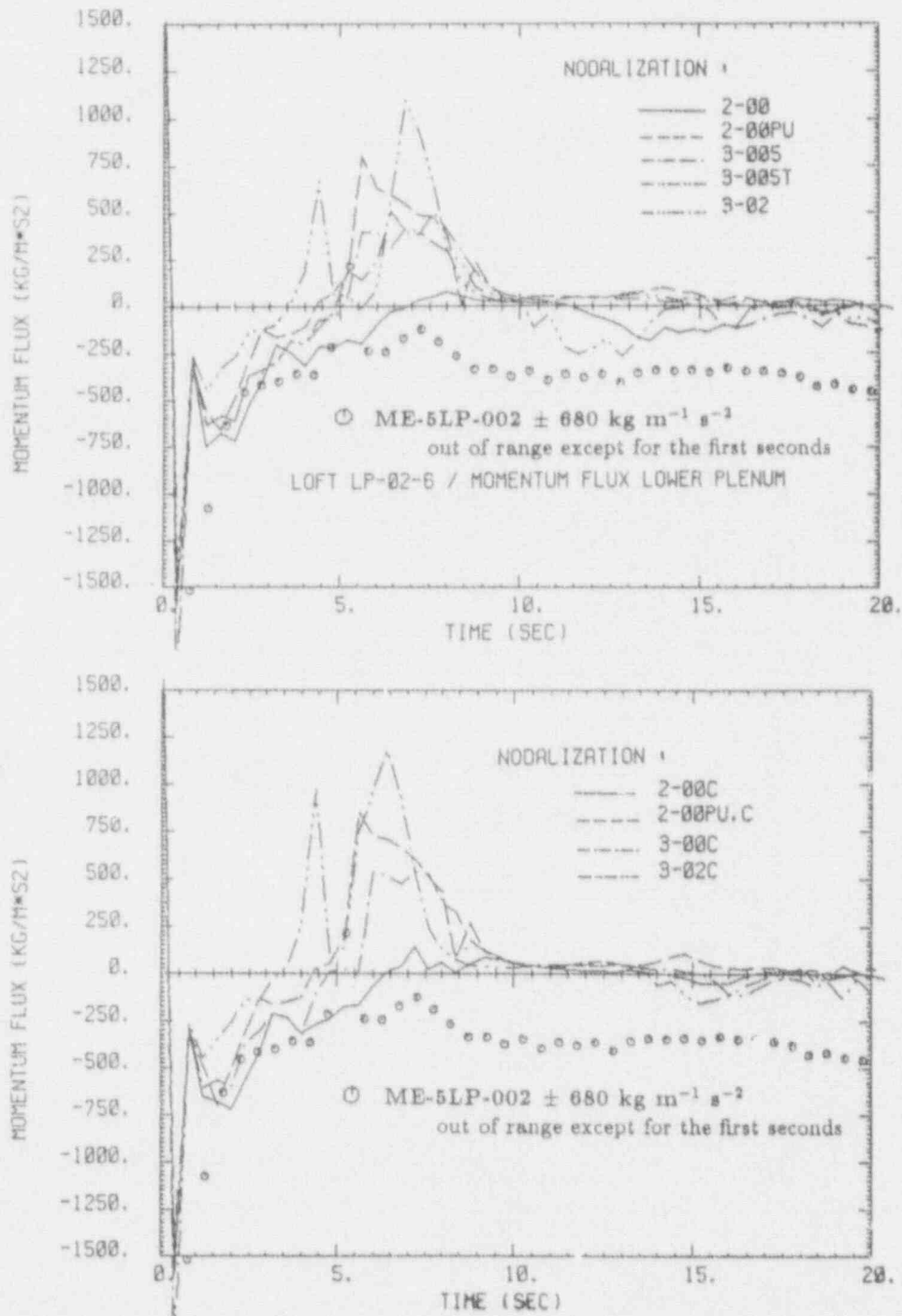


Figure 3.34: Momentum fluxes into the hot channel of the core as calculated by RELAP5/Mod2
 a) by neglecting wall heat capacity
 b) by taking into account wall heat capacity ("C")

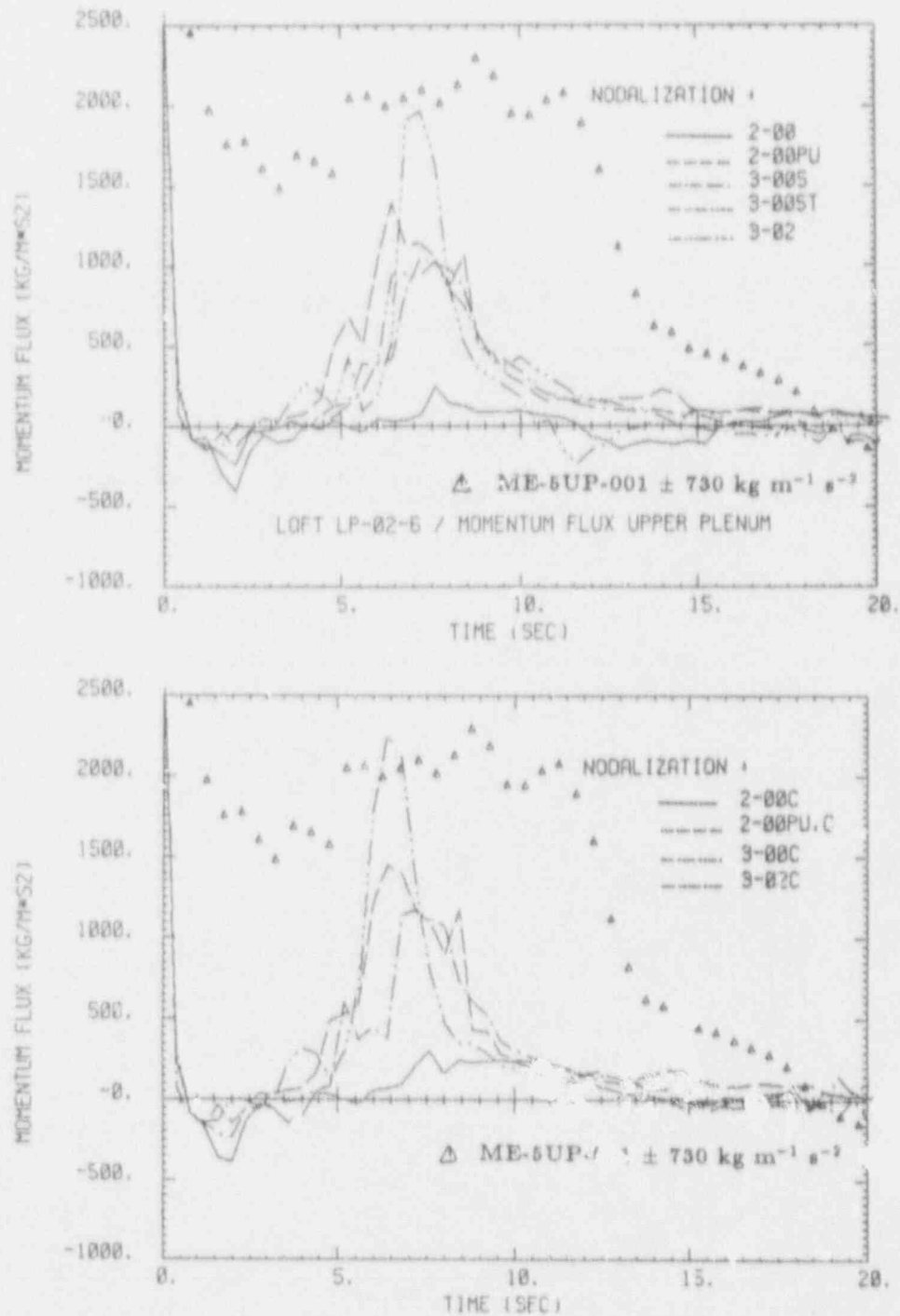


Figure 3.35: Momentum fluxes out of the hot channel of the core as calculated by RELAP5/Mod2
 a) by neglecting wall heat capacity
 b) by taking into account wall heat capacity ("C")

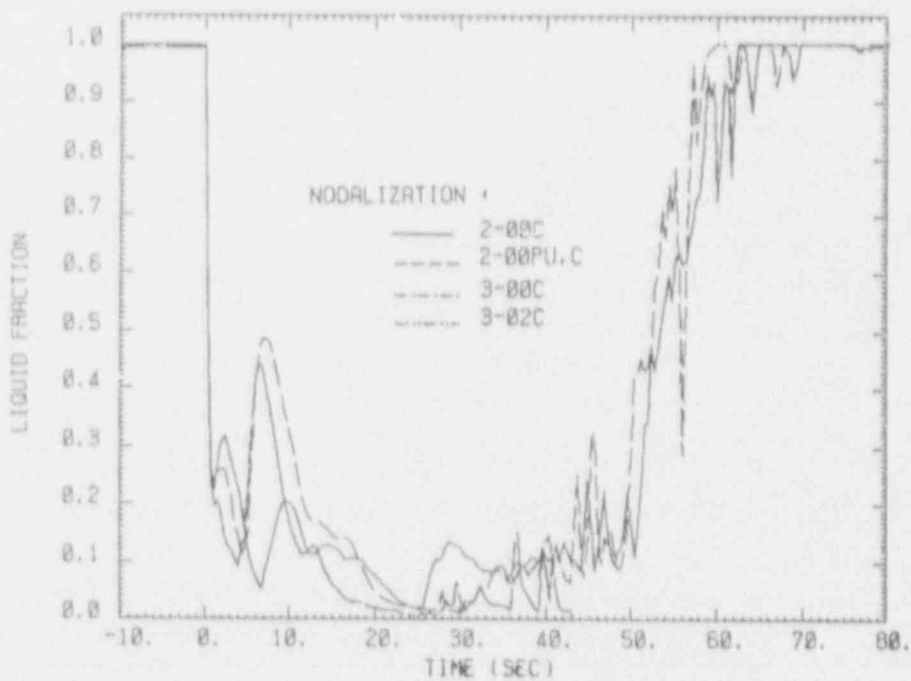
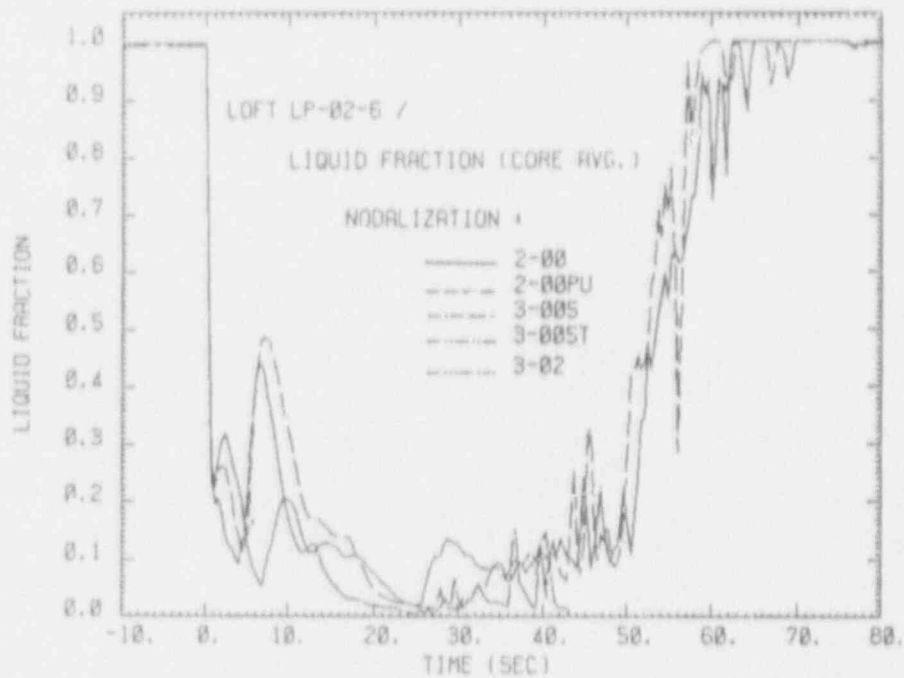


Figure 3.36: Core averaged liquid fractions vs. time
as calculated by RELAP5/Mod2
a) by neglecting wall heat capacity
b) by taking into account wall heat capacity ("C")

terwards, liquid fractions increased indicating the refill process which has been completed 60 seconds after the experiment has been initiated (liquid fraction nearly one). Although no experimental reference is available for the liquid fraction in the core region, figs. 3.36a and 3.36b can give an impression how the code treated the emptying and refilling process during the simulation of the experiment. In general, no large discrepancies have been observed between the different versions of nodalizations except the 2-00 and 2-00C nodalizations where the rapid coastdown of the pumps has dampened the "blowdown refill peak". On top of this, with respect to the time behaviour of the liquid fractions, no significant differences have been found between the "N" and the "C" type of nodalizations.

3.4.7 Mass-Flow Out of the Broken Loop

The comparison between predicted and experimental mass flows out of the break of the broken loop allows us to check the capability of RELAP5/Mod2 to describe two-phase flow under critical flow conditions. Therefore, in figs. 3.37 to 3.39, we would like to compare the RELAP5/Mod2 calculations of the mass flows in the cold and in the hot leg of the broken loop as well as the integral mass loss with the equivalent experimental data; the latter gives a clearer picture how calculations and experimental data deviate. Nevertheless, one has to keep in mind that mass flow measurements in transient two-phase flows are also a rather difficult task, because the data are the result of a multiplication of two independent measurements which are assumed to produce area averaged values.

In figs. 3.37a and 3.37b, let us start with the mass flow in the cold leg of the broken

loop. When opening the break valves, for a few hundred milliseconds the fluid is subcooled and the mass flow reaches its maximum value of 550 kg/s which value is slightly overpredicted by all the RELAP5/Mod2 calculations. The following sharp drop of the mass flow (due to fluid saturation and evaporation) has been well described by all types of nodalizations. Between 5 and 15 seconds for all of the different nodalizations, RELAP5/Mod2 has underpredicted the mass flows out of the cold leg break by about 20 to 50 kg/s. During the following time period, some instabilities have occurred for some RELAP5/Mod2 runs which probably are due to numerical instabilities. These instabilities more often have occurred in more simplified versions of nodalizations, e.g. the 3-... versions of nodalization. No severe discrepancies have been observed between the RELAP5/Mod2 results using the "N" or the "C" types of nodalization but the "C" versions seem to produce slightly more stable traces of the mass flows.

In figs. 3.38a and 3.38b, the mass flows in the hot leg of the broken loop have been plotted versus time. Except for the most simplified 3-02 and 3-02C versions of nodalization (the break line consists of only 4 volumes instead of 11 for the 2-00 and 3-00 versions), the peak values of the mass flow during the few hundred milliseconds of subcooled liquid flow conditions (measured value 193 kg/s) seemed to be slightly underpredicted whereas the two RELAP5/Mod2 runs (3-02 and 3-02C) overpredicted this peak value at least 50%.

In the interval 3 seconds up to 20 seconds, we may observe some scatter around the experimental reference which may be attributed to numerical instabilities. Again, these instabilities are slightly more pronounced for the "N" than for the "C" type of nodalizations. It is remarkable that the smoothest curves

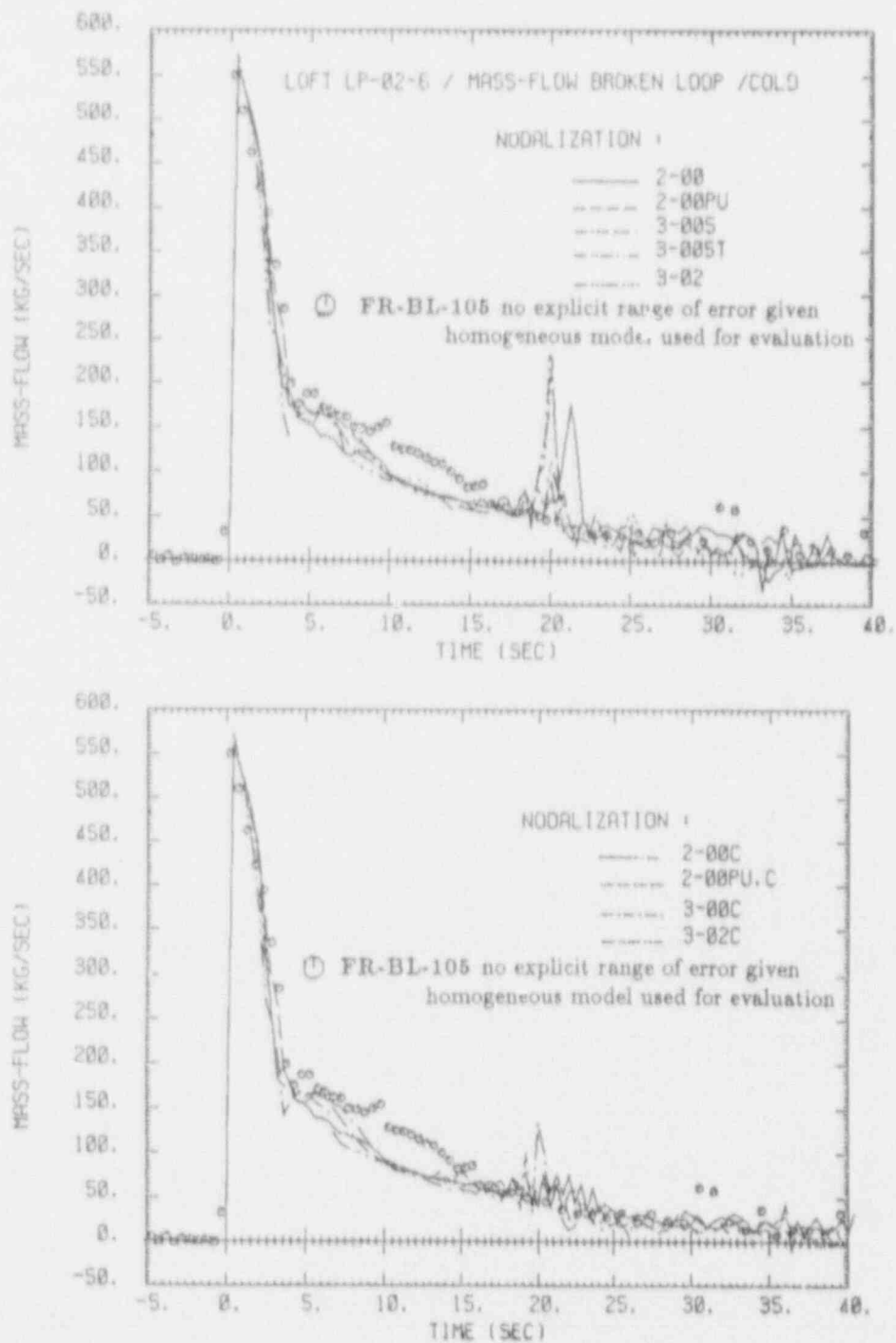


Figure 3.37: Calculated mass flows out of the broken cold leg vs. time compared to the mass flow measured at position BL-105
 a) by neglecting wall heat capacity
 b) by taking into account wall heat capacity ("C")

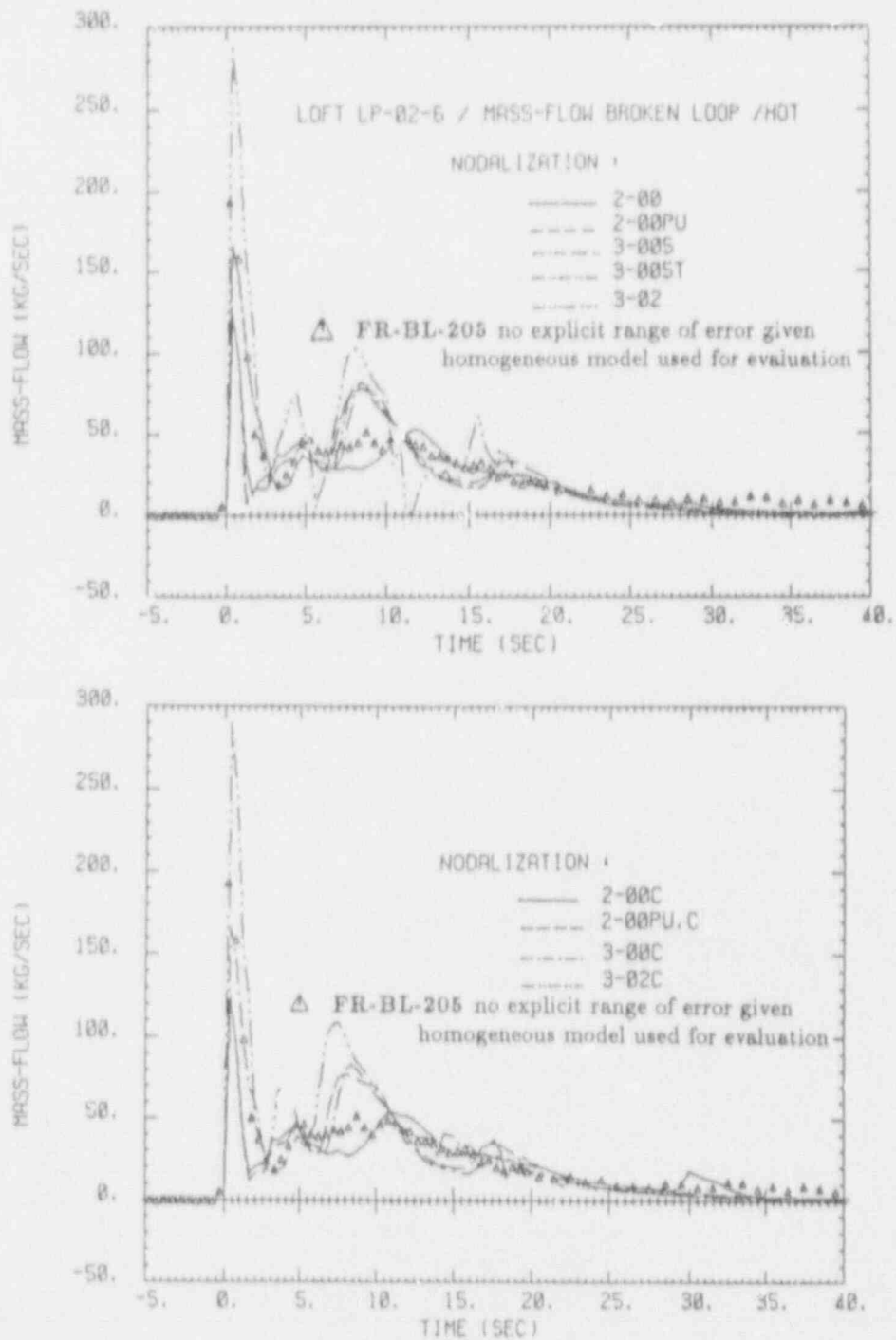


Figure 3.38: Calculated mass flows out of the broken hot leg vs. time compared to the mass flow measured at position BL-205
 a) by neglecting wall heat capacity
 b) by taking into account wall heat capacity ("C")

have been calculated by the most detailed 2-00 and 2-00C versions (straight lines) assuming additionally a rapid costdown of the pumps, whereas the equally detailed 2-00PU and 2-00PUC versions (dashed lines) using an imposed pump performance scatter similar to the other runs.

Because of the uncertainties of mass flow measuring techniques in stationary and transient two phase flows it cannot be totally excluded that deviations also are due to errors in the experimental reference values.

Because a plot of the loss of mass focusses more directly on the loss of water inventory rather than the time traces of the individual mass flows through the break, we finally shall compare the instantaneous time integrals of the two mass flows in the cold and hot legs of the broken loop (i.e. the mass losses through the break) as predicted by RELAP5/Mod2 with the equivalent values of the measurement. The integration of the mass flows for both the calculations and the experiment has been performed numerically by simply summing up the products of the two instantaneous values of the mass flows (cold and hot leg of the broken loop) times the actual time step.

In figs. 3.39a and 3.39b, these mass losses have been plotted as a function of time. Generally, for all types of nodalizations the mass losses have been overpredicted by RELAP5/Mod2 in the time interval between 3 to 60 seconds. This means that RELAP5/Mod2 calculated emptying of the vessel to be more rapidly, which should result in an earlier uncovering of the core.

After the entire blow-down phase, the calculation has been terminated because the system pressure has decreased to the pressure in the suppression tank (for the code, the sup-

pression tank pressure as a function of time is a boundary condition; the pressure history inferred from experiment LP-02-6 has been used). RELAP5/Mod2 calculated no significant increase but a slightly decrease of the mass losses (i.e. a certain amount of fluid is flowing back out of the suppression tank into the primary system; in reality an unphysical process), whereas the experimental mass loss data has still increased with a significant gradient. Again, some question marks can be raised with respect to the accuracy of the experimental reference data.

In figs. 3.39a and 3.39b, one may distinguish two different sets of curves, namely, the two 2-... type results and the other three results of the 3-... nodalizations. For the more detailed 2-... nodalizations, the loss of inventory is significantly higher than for the more simplified 3-... versions. On the other hand, no significant differences have been observed between the mass losses of the 3-005 and 3-02 runs even the simplification, especially of the broken loop, has been rather drastic; e.g. the hot leg has been reduced from 11 (3-005) to 4 (3-02) volumes and the cold leg from 4 to 1.

3.4.8 Intact Loop Mass Flow and Pump Speed

In figs. 3.40a, 3.40b, 3.41a and 3.41b, the measured mass flows in the hot and cold legs of the intact loop have been compared with the equivalent quantities as calculated by RELAP5/Mod2 using our different nodalizations. In both cases, the stationary values (-10 to zero seconds) differ significantly from the measured values. Surprisingly, the measured mass flows in this stationary phase (even if all possible leaks are closed) differ from 265 kg/s in the cold leg to 300 kg/s in the hot leg (for the initialization of the

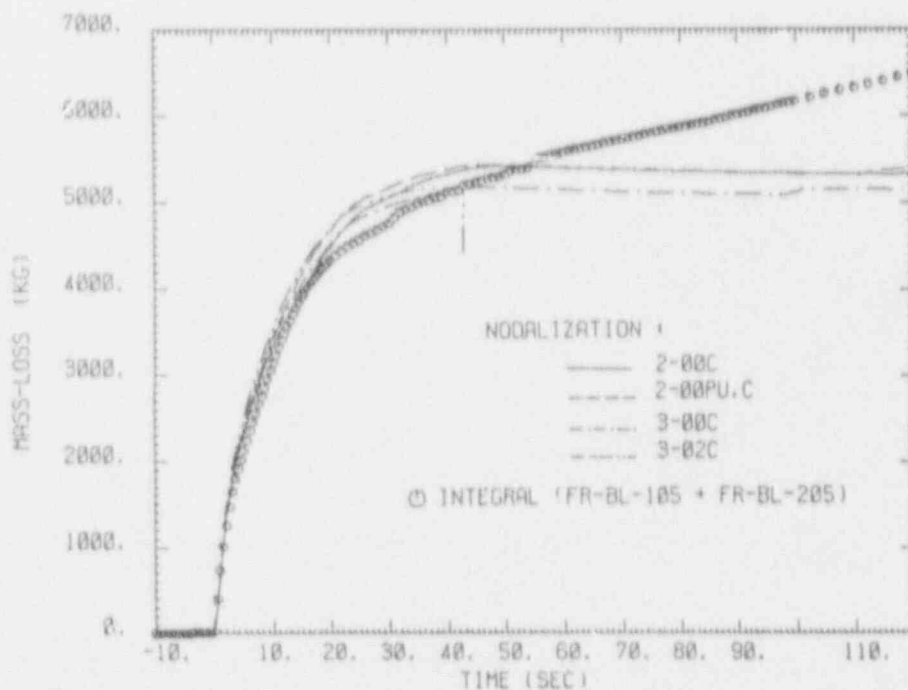
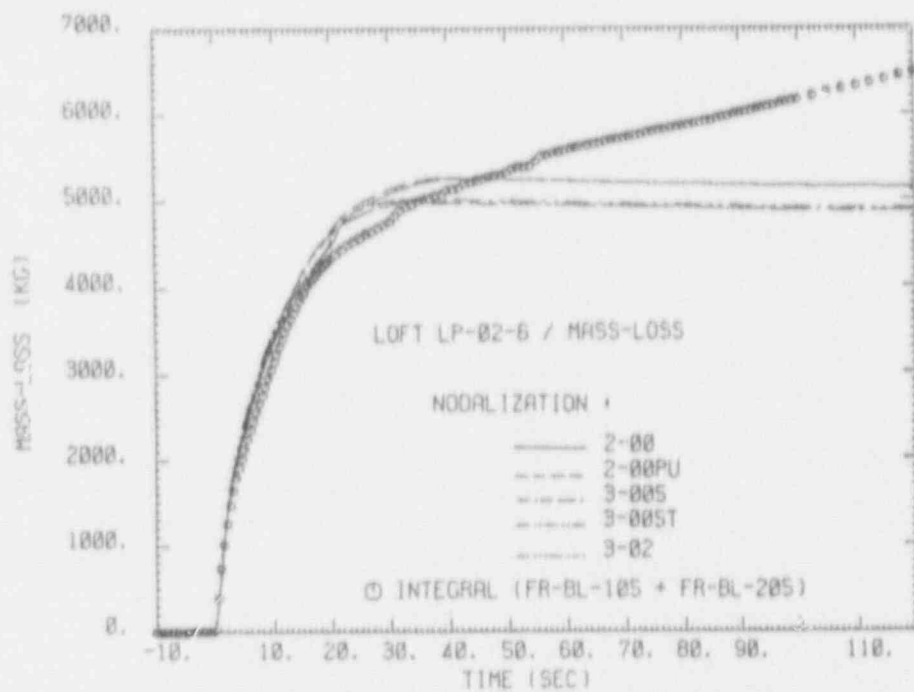


Figure 3.39: Calculated mass losses out of the double ended break vs. time compared to the integrated mass flows measured at position BL-105 and BL-205

- by neglecting wall heat capacity
- by taking into account wall heat capacity ("C")

problem, we have used the values given in the quick-look report). With respect to the accuracy of the measurements, the uncertainties of mass flow measurements in two-phase flows as mentioned above, again, have to be taken into account.

In fig. 3.40a and 3.40b, the hot leg mass flows inferred from LOFT experiment LP-02-6 have been compared to the RELAP5/Mod2 calculations. For the first second (highly transient part of the experiment) and after 30 seconds, the discrepancies between the measurement and all of the calculational cases with different nodalizations are remarkably small. Between one and four seconds, all RELAP5/Mod2 cases have predicted a significant "overshoot" of the mass flow which also is observable to a lesser degree in the measured data. Later, between six and 22 seconds of the transient, RELAP5/Mod2 has underpredicted the mass flows; in fact, a flow reversal has been indicated by the calculations which is not significant in the measurement. The calculations of this flow reversal seem to be slightly higher for the "N" than for the "C" versions of nodalization. For the time period after 30 seconds, the calculated mass flows are nearly zero, whereas the measurement still indicated some positive amount of flow. But because the measured flowrate is relatively low, it may be due to uncertainties of the measuring technique.

In figs. 3.41a and 3.41b, the mass flow in the cold leg of the intact loop has been compared to the equivalent RELAP5/Mod2 calculations. Generally, the predictions seem to be more unstable than both the experimental data and the hot leg results. Only the curves of very low mass flow at times greater than 60 seconds seem to be somehow smoother.

The stepwise increase of the experimentally inferred mass flow during the first 5 seconds of the experiment (260 to 330 kg/s) could not be calculated by any of the RELAP5/Mod2 runs but some smaller hints have been given that such a mass flow increase may exist.

Except the results with nodalizations 2-00 and 2-00C (rapid pump coastdown) the decaying part of the mass flow between 6 and 10 seconds has been reproduced quite satisfactorily by RELAP5/Mod2; the abnormal behaviours of the 2-00 and 2-00C predictions are probably due to the "wrong" description of the pump performance.

During the time period between 10 and 20 seconds, RELAP5/Mod2 has slightly overpredicted the mass flows in the cold leg.

Relatively high instabilities occur in the time period between 20 and 55 seconds. Here, the experimental data also exhibits significant oscillations, indicating some strong flow instabilities. Because between 20 and 40 seconds, the accumulator has fed approximately 35 kg/s of highly subcooled ECC water and in addition to this, the instabilities only occur in the cold leg of the intact loop where the ECCs is connected to the loop, we tend to attribute these instabilities to the functioning ECC system.

Because for all the other nodalizations the pump speed has been a boundary condition and consequently matches perfectly with the measured data, only the results of the 2-00 and 2-00C nodalizations are of some interest. Therefore, in figs. 3.42a and 3.42b, we may concentrate on these two relative pump speeds as calculated by RELAP5/Mod2 which have been compared to the equivalent average experimental data. Here, the relative pump speed is defined as

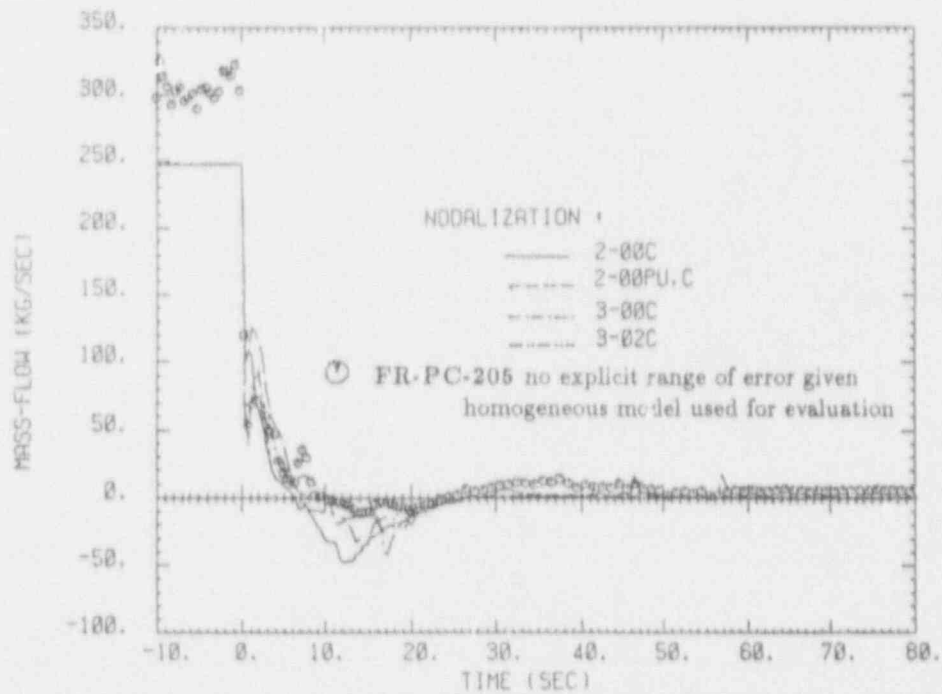
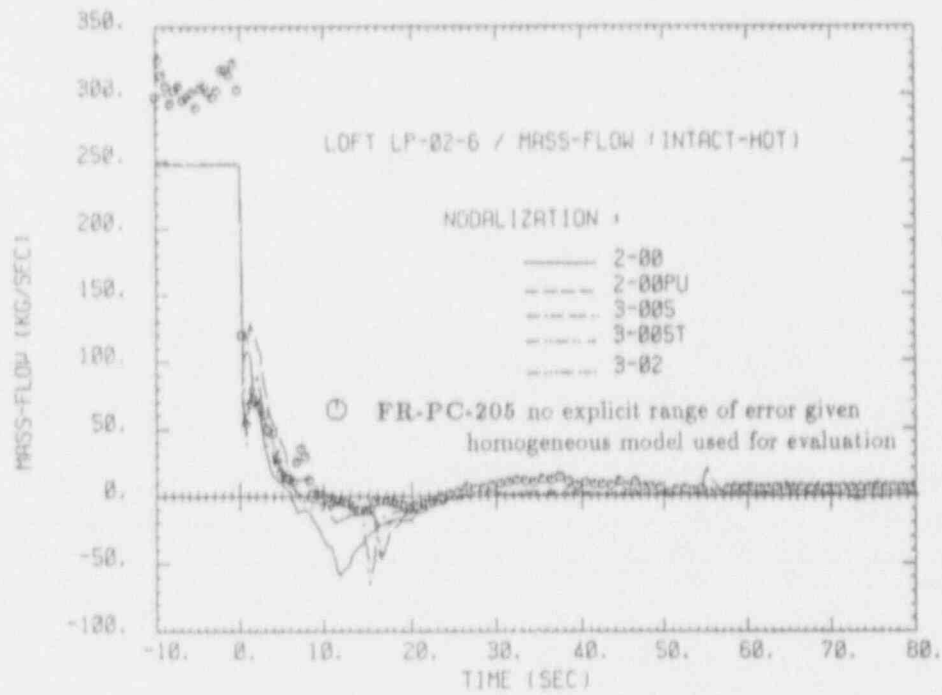


Figure 3.40: Calculated mass flows in the intact hot leg vs. time compared to the mass flow measured at position PC-205

- a) by neglecting wall heat capacity
- b) by taking into account wall heat capacity ("C")

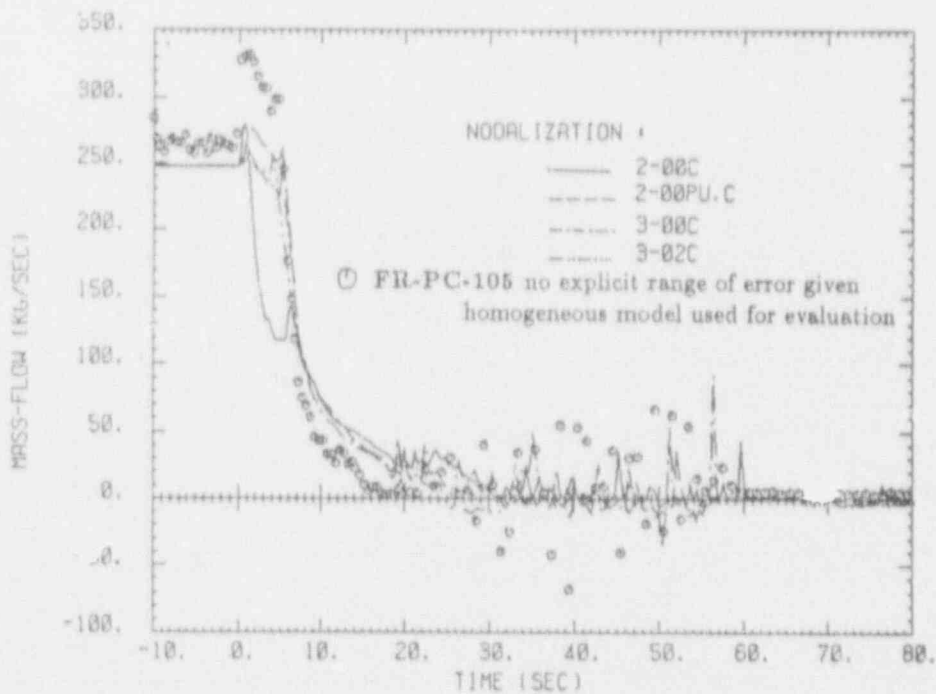
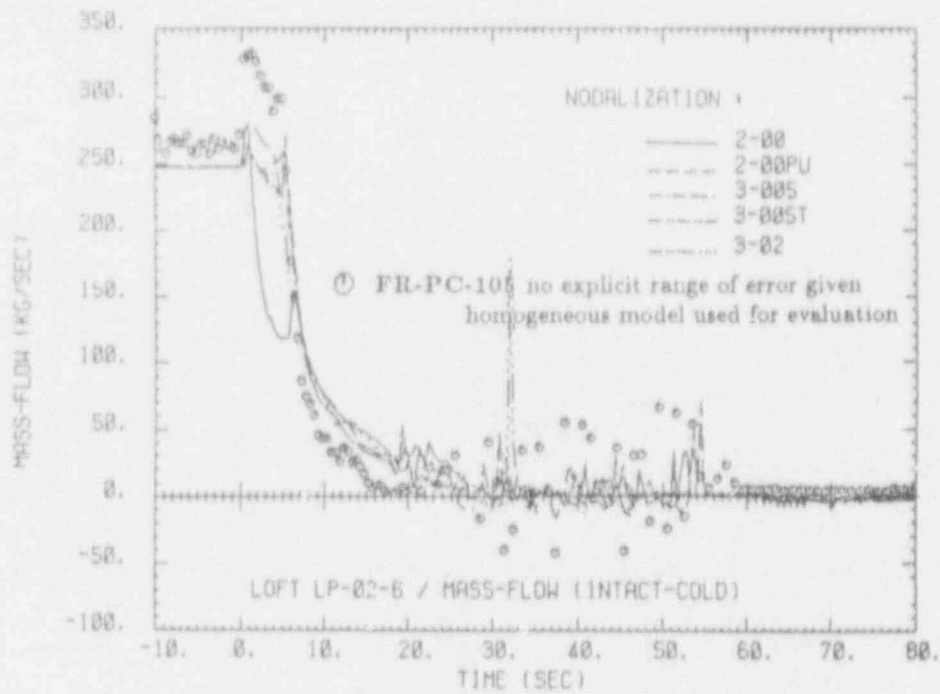


Figure 3.41: Calculated mass flows in the intact cold leg vs. time compared to the mass flow measured at position PC-105
 a) by neglecting wall heat capacity
 b) by taking into account wall heat capacity ("C")

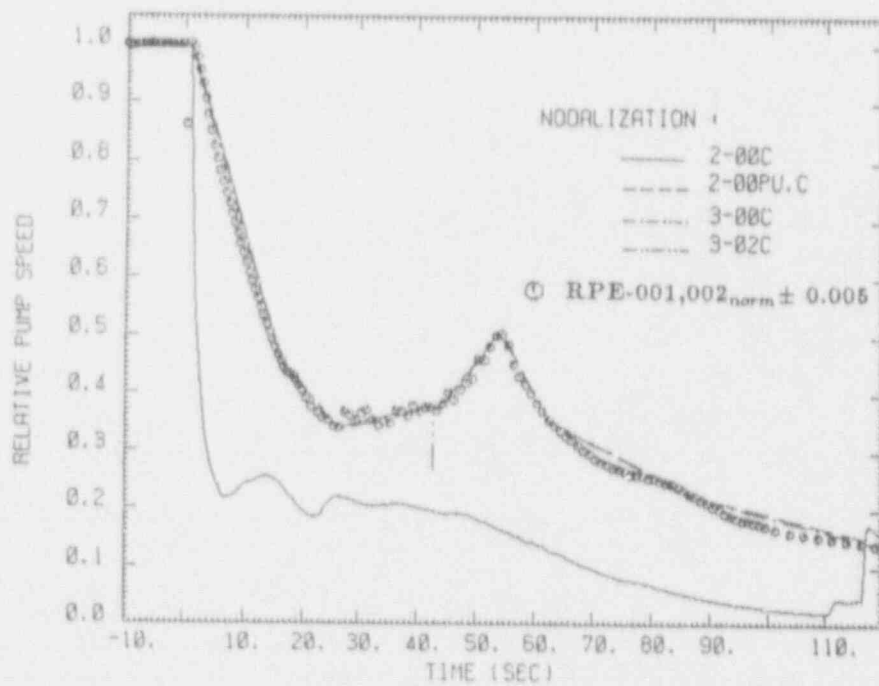
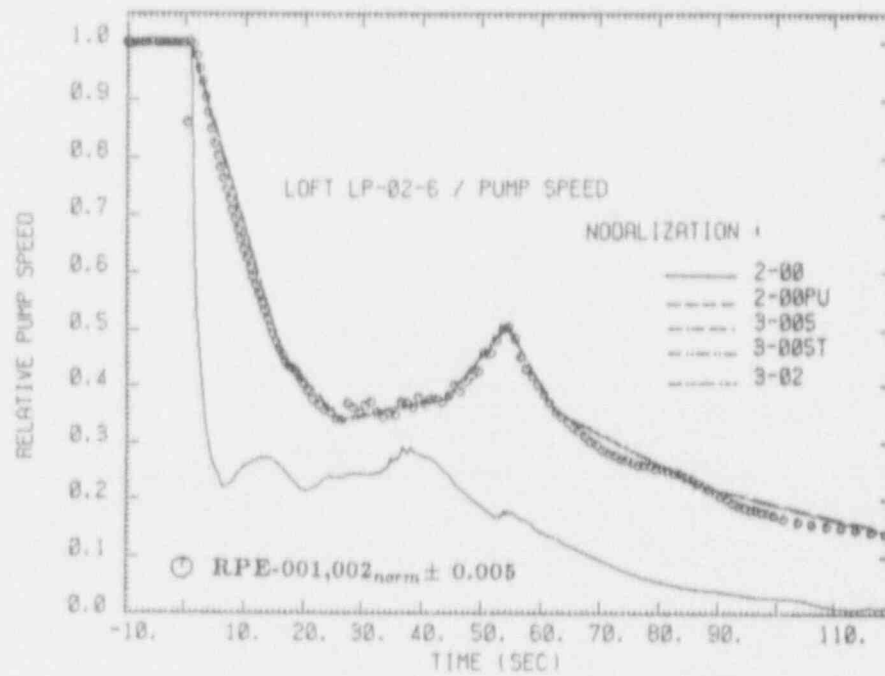


Figure 3.42: Calculated relative pump speed vs. time compared with the measured ones (averaged value of two pumps)

- a) by neglecting wall heat capacity
- b) by taking into account wall heat capacity ("C")

the actual value divided by the initial speed under stationary conditions; because the absolute value of the pump speeds has been adjusted so that the intact loop mass flow is equivalent to the experimental one given on table 1.1, only relative values can be compared. Indeed, the coast down of the pumps is much more rapid than for the other cases plotted for reference in the two graphs which may have induced different thermohydraulic conditions inside the whole LOFT system.

3.4.9 ECC System

In figs. 3.43 to 3.46, experimentally inferred accumulator liquid level, accumulator pressure, accumulator flowrate as well as the flowrates of the low pressure injection systems (LPIS) have been compared to the equivalent RELAP5/Mod2 calculations. Because the HPIS system has supplied water with a constant flowrate and its value has been a boundary condition, no discrepancies between experimental and RELAP5/Mod2 calculated results are expected; therefore, plots of the HPIS flowrates have been omitted.

The time point of starting the accumulator injection has been defined by a time-trip (boundary condition) instead of a code calculated pressure trip which would model the LOFT system in a more realistic way, but on the other hand would multiply deviations in the RELAP5/Mod2 calculation of the system pressure to other parameters of interest of the whole LOFT system (e.g. a later start of the ECCS would probably influence significantly the shapes of the cladding temperature traces). Furthermore, the empty-point of the accumulator, i.e. the time when the accumulator level approaches zero, has been adjusted once for all for the 6-00 nodalization of the LOFT LP-LB-1 experiment (see ref. [7])

by multiplying the forward and backward energy loss coefficients of the accumulator volume by nearly 3; for all the other types of nodalizations, the same coefficients have been used. In addition, it was necessary to close the valve 610 (see figs. 2.1, 2.3 and 2.4) after the accumulator was emptied to avoid an execution error of RELAP5/Mod2 (message: arithmetic overflow). This error is probably due to an improper modelling of incondensibles (nitrogen) by RELAP5/Mod2; nitrogen is released by the accumulator into the system after emptying.

First, in figs. 3.43a and 3.43b, the liquid levels in the accumulator as calculated by RELAP5/Mod2 have been plotted in the time interval the accumulator is activated and compared to the experimental data. The curves are satisfactory close to the experimental points. The longest accumulator times have been achieved by using the most detailed 2... types of nodalizations whereas the results closest to the measurements are those inferred from the most simplified 3-02 runs, even the discrepancies between the different results are quite low, namely less than 5 second.

In figs. 3.44a and 3.44b, the pressure in the accumulator vessel inferred from the measurement has been compared to the equivalent pressures as calculated by RELAP5/Mod2. Generally, the code tended to slightly overpredict the real pressures but the difference is less than 0.3 MPa. Because in contrary to the experiment, as already mentioned above, for the RELAP5/Mod2 predictions a valve has to be closed for numerical reasons, the predicted pressure remained constant after this valve has been closed.

Closest to the measurements we have found the results of the 3-02 nodalizations, i.e. of the most simplified versions of the LOFT system. The poorest results on the other hand

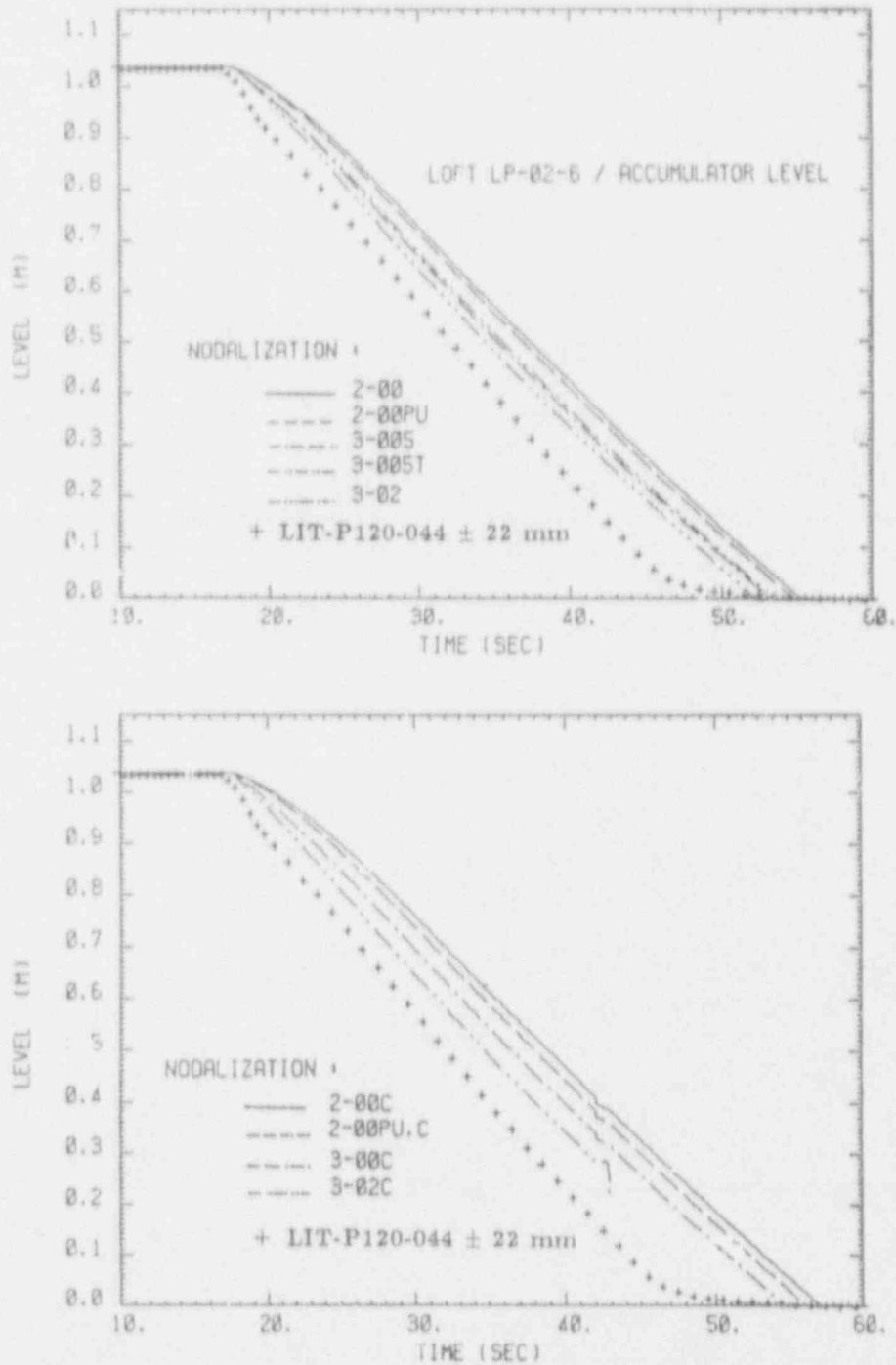


Figure 3.43: Calculated accumulator fluid levels vs. time compared with the measured level
 a) by neglecting wall heat capacity
 b) by taking into account wall heat capacity ("C")

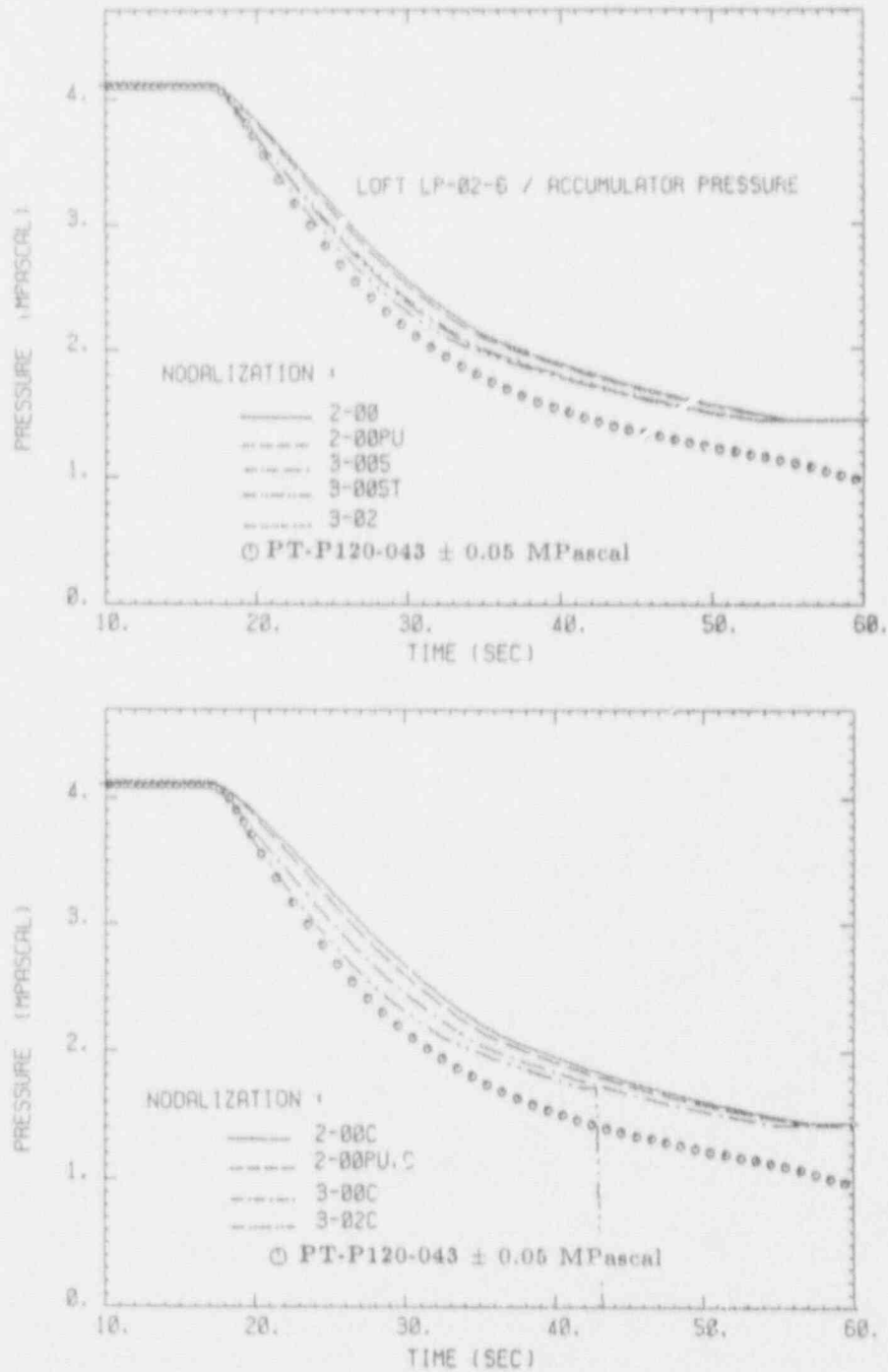


Figure 3.44: Calculated accumulator pressure vs. time compared with the measured pressure

- a) by neglecting wall heat capacity
- b) by taking into account wall heat capacity ("C")

have been found to be the 2-00 and 2-00C calculations.

In figs. 3.45a and 3.45b, the flowrates out of the accumulator as calculated by RELAP5/Mod2 using our different nodalizations have been plotted but unfortunately, no experimental data has been available. The highest flowrates have been calculated using the most simplified 3-02 and 3-02C types of nodalization whereas the lowest values have been calculated with the 2-00 and 2-00C cases.

Finally, in figs. 3.46a and 3.46b, the flowrates of the Low Pressure Injection System (LPIS) have been compared to the equivalent RELAP5/Mod2 results. For all the different nodalizations, the calculated results have been found to be rather poor although with respect to the qualitative aspect of the total mass injected, the predictions are acceptable.

At the beginning of the LPIS action, a sudden decrease from 6 to 1.5 kg/s followed by an increase from 4.5 to 7 kg/s can be observed in the experimental data which has not at all been calculated by RELAP5/Mod2. This strange behaviour of the LPIS mass flow is believed to be due to a short high pressure nitrogen release out of the accumulator into the system at the moment when it has been emptied completely. This nitrogen release for some seconds caused a small increase of the system pressure (which can be observed in the system pressure data of figs. 3.29a and 3.29b at around 60 s) and even a larger increase directly in the ECCS-piping thus reducing the LPIS flow-rate which is governed by the pressure difference between ECCS-piping pressure and the constant LPIS pressure. After some seconds, this increase in the ECCS-piping pressure diminishes and the LPIS flowrate recovered. Because the "nitrogen injection" has not been taken into

account by the RELAP5/Mod2 calculations, the code has calculated a more or less smooth curve which is close to the experimental data after the experimentally observed flow instability has been dampened and which more or less represents the time-average of the experimentally inferred LPIS mass flow between 40 and 65 seconds.

3.5 Investigation on the Prediction of Early Bottom-Up Rewetting

The occurrence of a high flowrate, early bottom up quench front has been regarded as one of the "key events" of LOFT large break experiments and also of experiment LP-02-6. This early bottom-up quench rewetted the whole core between approximately 4.5 and 8 seconds after the initiation of the transient thus reducing drastically the general core heat-up during this experiment. As we have already mentioned, RELAP5/Mod2 was not able to predict this early bottom-up quench.

One of the features of RELAP5/Mod2 code is the fact that it uses different sets of heat-transfer correlations under non-reflood and reflood conditions (e.g. correlations for nucleate boiling, transition boiling and film boiling). On top of this, the calculation of the temperature distribution of the fuel rod is enhanced by subdividing the axial length (corresponding to the length of the connected hydrodynamic volume) into several "fine meshes" to better model the occurrence of steep temperature gradients inside the cladding during reflooding. The "switching" from normal operation to reflooding can be achieved by three different methods:

1. external trip (to be set by user defined

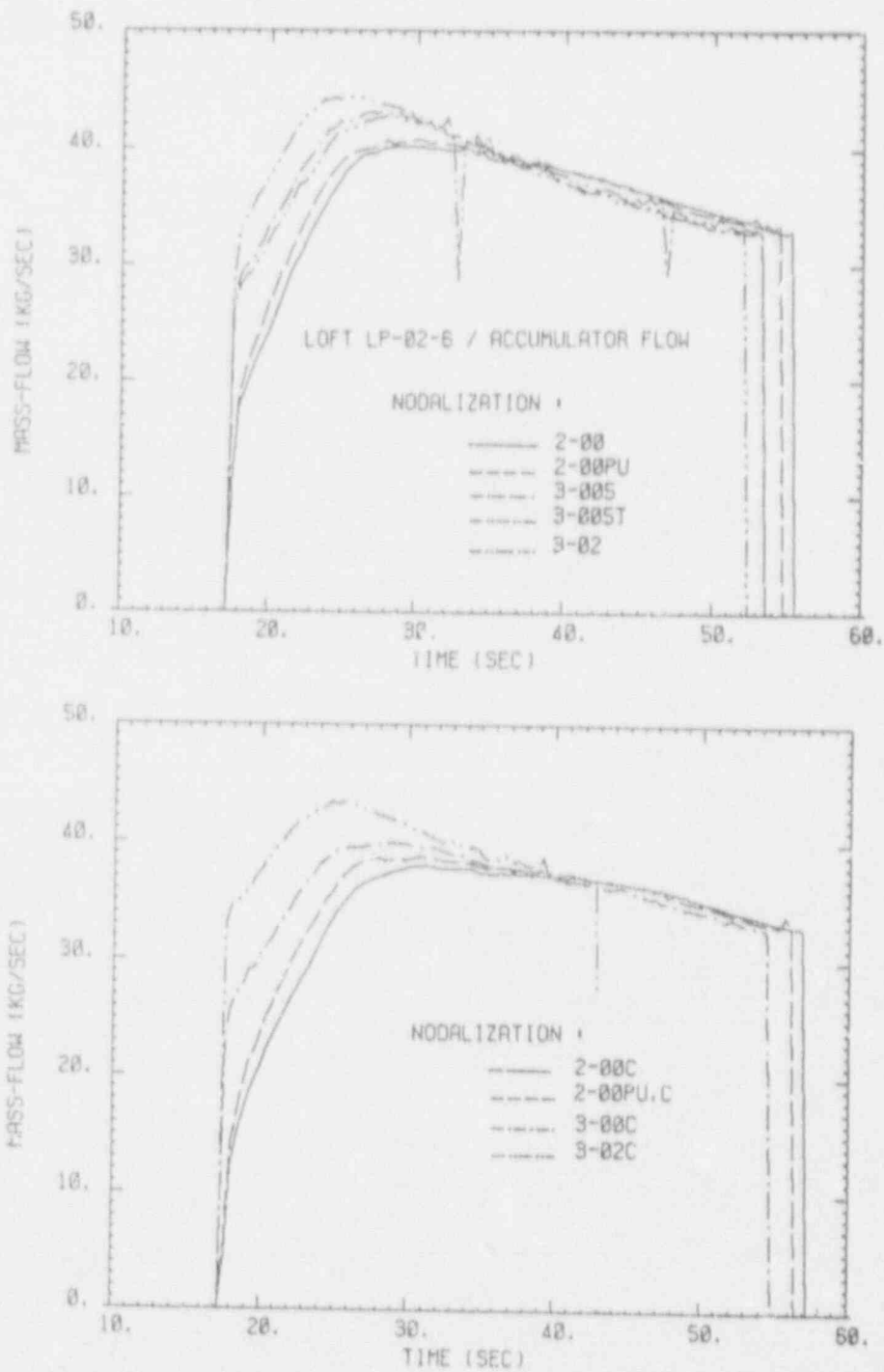


Figure 3.45: Calculated accumulator mass flows vs. time
 a) by neglecting wall heat capacity
 b) by taking into account wall heat capacity ("C")

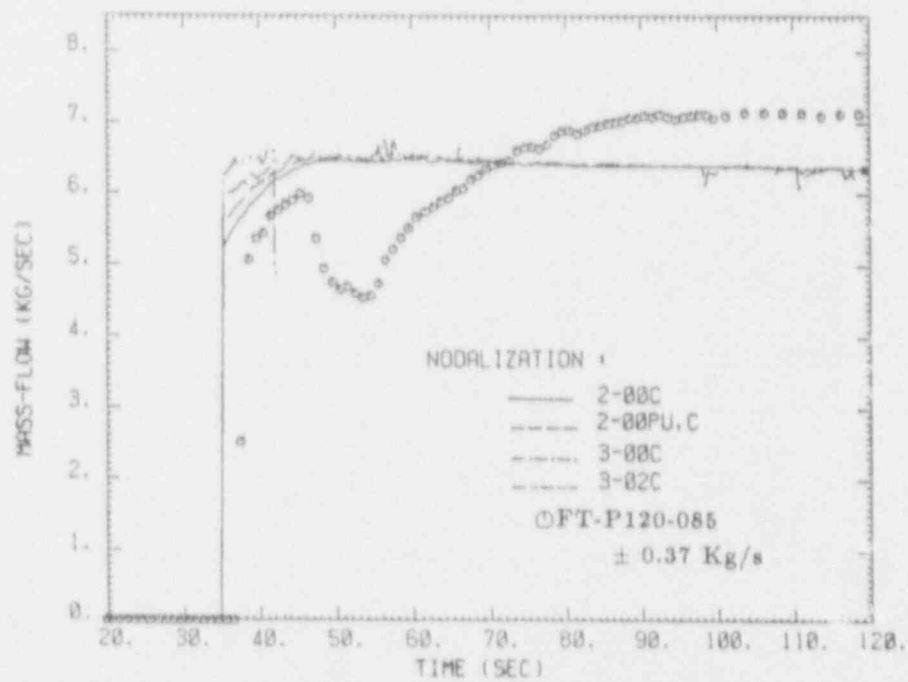
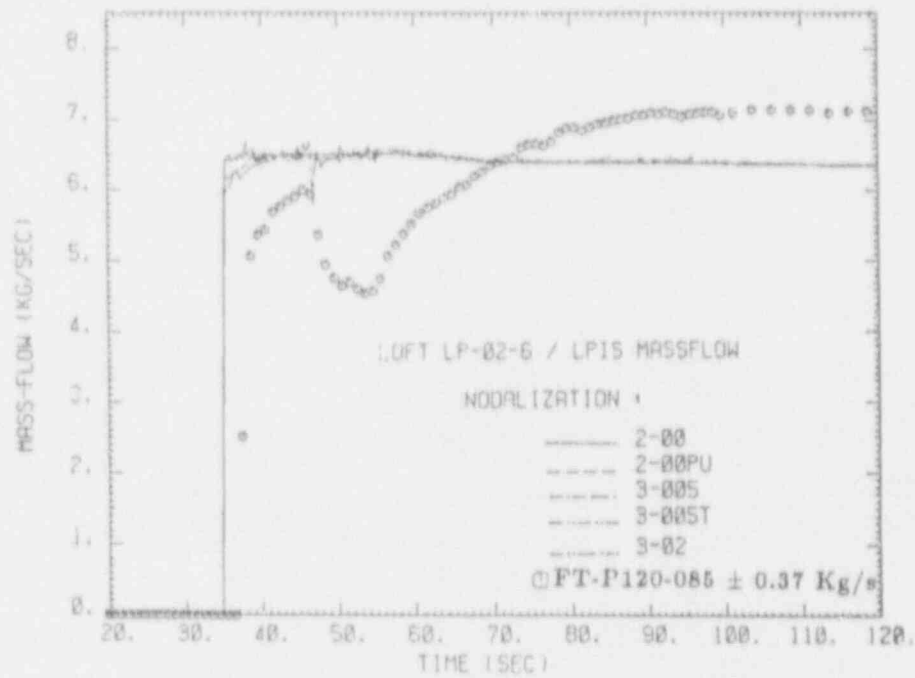


Figure 3.46: Calculated LPIS discharges vs. time compared with the measurement
 a) by neglecting wall heat capacity
 b) by taking into account wall heat capacity ("C")

options)

2. internally set by the code when the connected hydrodynamic volumes are nearly empty
3. internally set by the code when dryout begins in the connected hydrodynamic volumes

In addition, the last two cases are limited to system pressures less than 10 bars. Once the reflood calculation has been initiated, it remains activated until the end of the calculation.

Obviously, the choice of a slightly different heat transfer correlations combined with as a better tracing of the axial cladding temperature distribution by "fine meshing" will have an important influence on the prediction of cladding temperatures. Consequently, the time of the reflood initiation, i.e. the "switch" between both the different sets of correlations and the numerical solution schemes may have a very important result. Therefore, one may argue that the calculation of the early bottom-up quench by RELAP5/Mod2 in experiment LP-02-6 only failed because the reflood option has not been initiated early enough.

For investigation of this problem, we have performed two different RELAP5/Mod2 calculation, using first nodalization 3-005 with reflood initiation option one (3-005T). Because we have observed earlier (see ref. [7]) that the last two options produce equivalent results, we have not calculated the problem using option number two. For version 3-005, the reflood option usually has been initiated automatically by the code between 30 and 40 seconds after opening of the break valves when the system pressure has fallen below 10

bars and the collapsed liquid level in the core has reached its minimum (see figs. 3.29 and 3.36). For version 3-005T, the reflood option initiation trip has been set externally when the average collapsed liquid level in the core-region reached a value of less than 10%. According to fig. 3.36, this happened for the first time approximately 4 seconds after the initiation of the experiment; this external initiation of the reflood option is independent of the system pressure.

In figs. 3.47 a to k, the cladding temperatures measured at 10 axial positions in the center box 5 (hot channel) have been compared to the equivalent two RELAP5/Mod2 calculations; figs. 3.47 have to be regarded as an extract out of the figs. 3.5 to 3.14, which have been discussed above. From a general point of view, for all the ten levels, the deviations between the two predictions are quite considerable. On the other hand, with respect to early bottom-up rewetting during the first 10 seconds of the experiment, no significant differences have been observed for the first four levels, namely levels-02, -11, -21 and -24 (figs. 3.47 a to d).

Significant deviations start at level-27 (fig. 3.47e). Here, the 3-005T calculation (i.e. the run with external triggering of the reflood option) has done a nearly perfect job in predicting the time trace of the cladding temperature both during early bottom-up rewetting as well as the during final refill, whereas the 3-005 calculation failed totally in predicting bottom-up rewetting. This optimistic picture has already been changed at the next position, level-31 and again at level-39, even the 3-005T calculations still have been closer to the experimentally inferred reference data (figs 3.47f and g). At level-43.8 (fig. 3.47h), for the 3-005T calculation RELAP5/Mod2 did an acceptable job concerning the prediction of early bottom-up rewet-

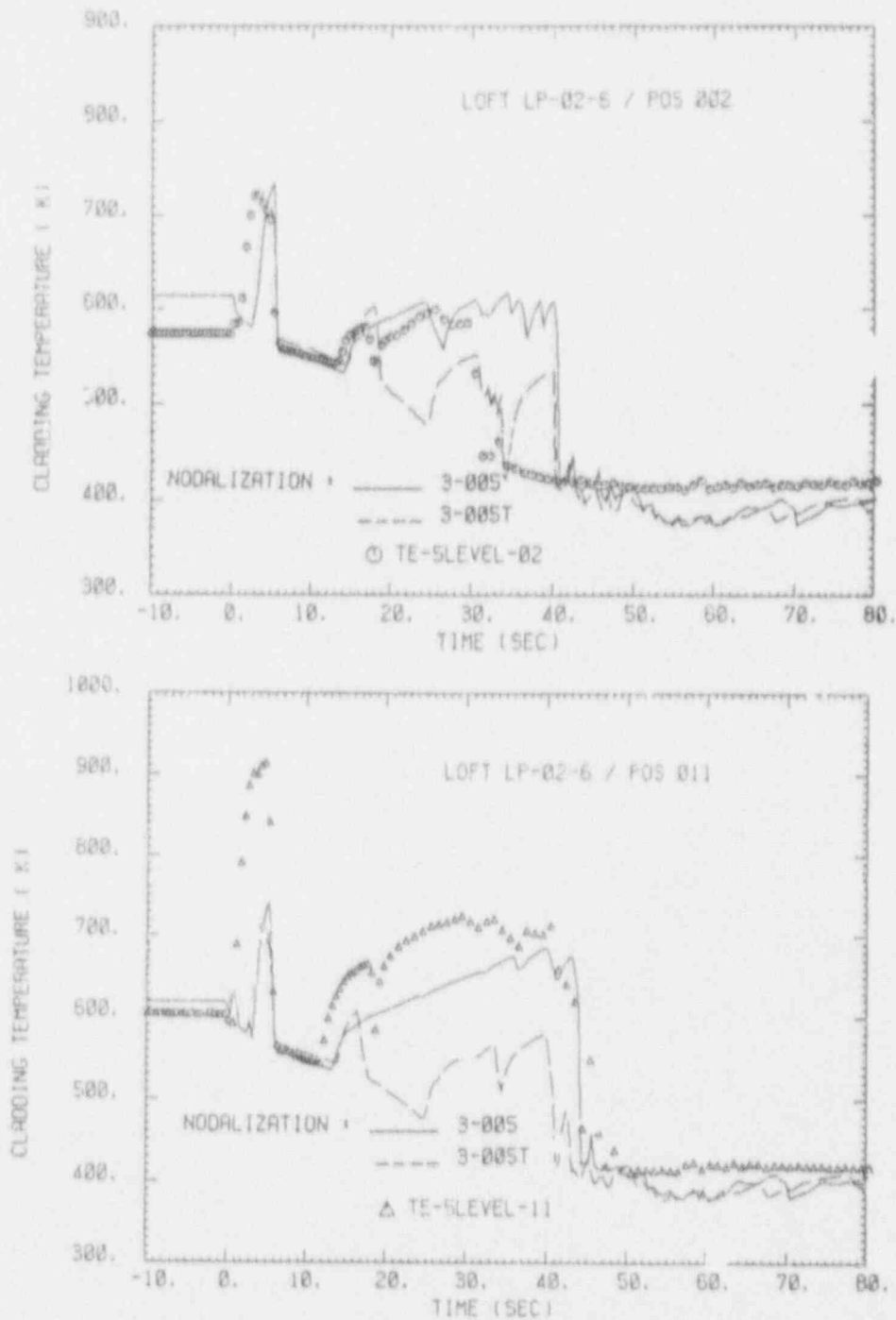


Figure 3.47: Comparison of cladding temperatures calculated by RELAP5/Mod2 without (3-005) and with (3-005T) external triggering of the reflood option

- a) at level-02
- b) at level-11

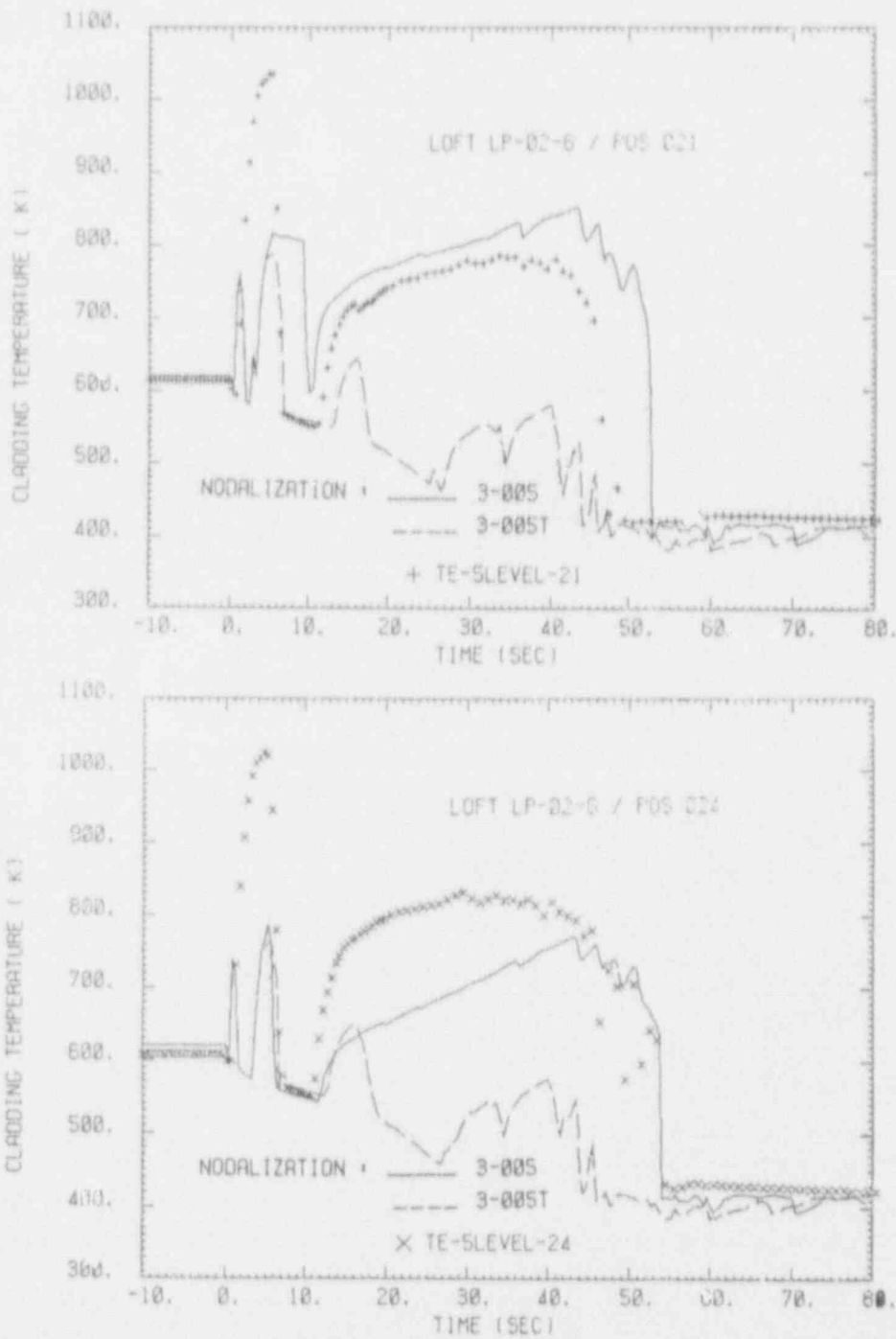


Figure 3.47: Comparison of cladding temperatures calculated by RELAP5/Mod2 without (3-005) and with (3-005T) external triggering of the reflood option
 c) at level-21
 d) at level-24

ting but failed in calculating the second core heat-up during the refill phase of the experiment whereas the calculation 3-005 totally has missed the early bottom-up rewetting.

For the last two levels -49 and -62 (figs. 3.47 i and k), again no dramatic differences between the RELAP5/Mod2 results of the two nodalizations have been observed; in fact, both calculations have missed what was really happened during the experimental transient at these core levels.

In figs. 3.48a to d, the comparison has been made for the predictions of the average channel at the four available core levels of side box 4. Here, for both of the RELAP5/Mod2 calculations, the results are rather poor. With respect to the prediction of early bottom-up rewetting, none of them was able even to describe the core heat-up from which the cladding can be cooled down by bottom-up rewetting. Some exceptions to this statement we may identify at level-21 (fig. 3.48b) where the standard nodalization 3-005 indicated some short temperature rise between 4 and 6 seconds which is still 40 K lower than the temperatures inferred from the experiment.

On the other hand, the core heat-up during the refill phase has been calculated by the two RELAP5/Mod2 -runs but it is hard to decide which one of the two versions made a better calculation because at some levels, the 3-005 results are more "on the line" (e.g. figs 3.48a and 3.48d) whereas at the two other levels the 3-005T calculations seemed to be slightly better (figs. 3.48b and 3.48c).

Finally, in fig. 3.49, we would like to look again at the time behaviour of the center fuel temperature where reference temperatures are available only for level-27. In this graph, the prediction of the 3-005T RE-

LAP5/Mod2 calculation seems to be nearly perfect. This is not at all surprising because we have already found the cladding temperature trace at this core level to be in excellent agreement with the measurement. On the other hand, we have seen this good agreement with the reference cladding temperatures only at level 27 which may lead us to the conclusion that the center fuel temperatures also might deviate at the other core levels where no reference data is available.

Summarizing our observations with respect to early bottom-up rewetting, one has to conclude that RELAP5/Mod2 generally has not been able to predict this phenomenon. A change in the logic of initiating the reflood option (which forces RELAP5/Mod2 both to use a slightly modified heat transfer package and to subdivide the axial meshing of the cladding as predetermined by the length of the adjacent hydrodynamic volume in order to keep better track of the axial temperature distribution in the vicinity of the quench front) resulted only partially in better predictions without explaining the physical phenomena but on the other hand created worse results in other phases of the transient. E.g. compared to the ones of the standard 3-005-RELAP5/Mod2 calculation, the results of the 3-005T RELAP5/Mod2 prediction have been found to be always lower.

In a recent work, Analytis and Lübbsmeyer (ref. [8]) investigated the failure of RELAP5/Mod2 in describing the early bottom-up phenomenon by looking at the differences in the heat transfer packages under rewetting and non-rewetting conditions. It has been found, that these differences are negligible small. There is only one statement which prevents RELAP5/Mod2 from describing the early bottom up phenomena and this state-

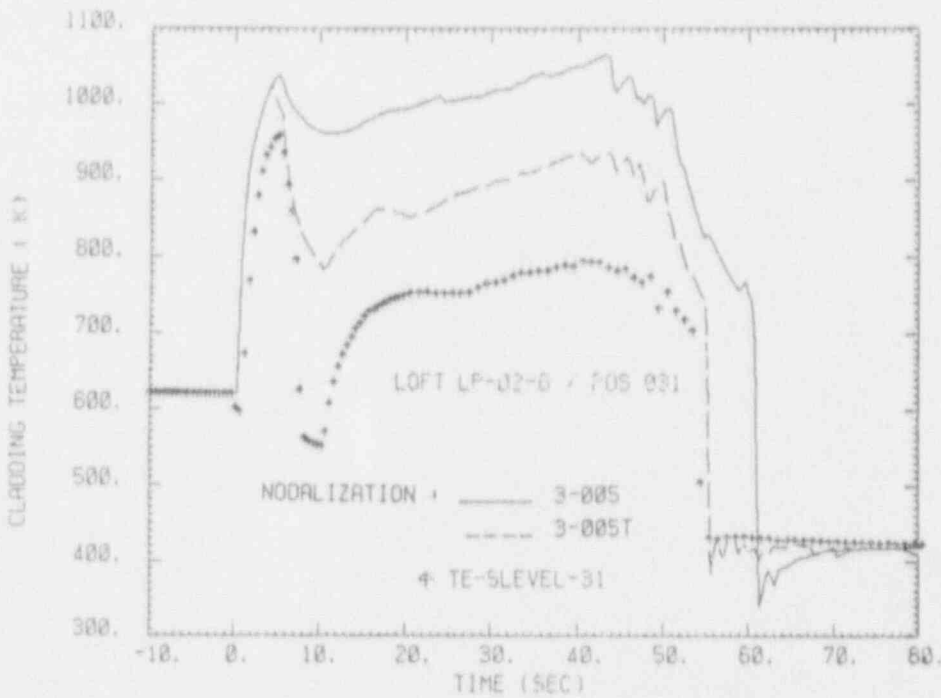
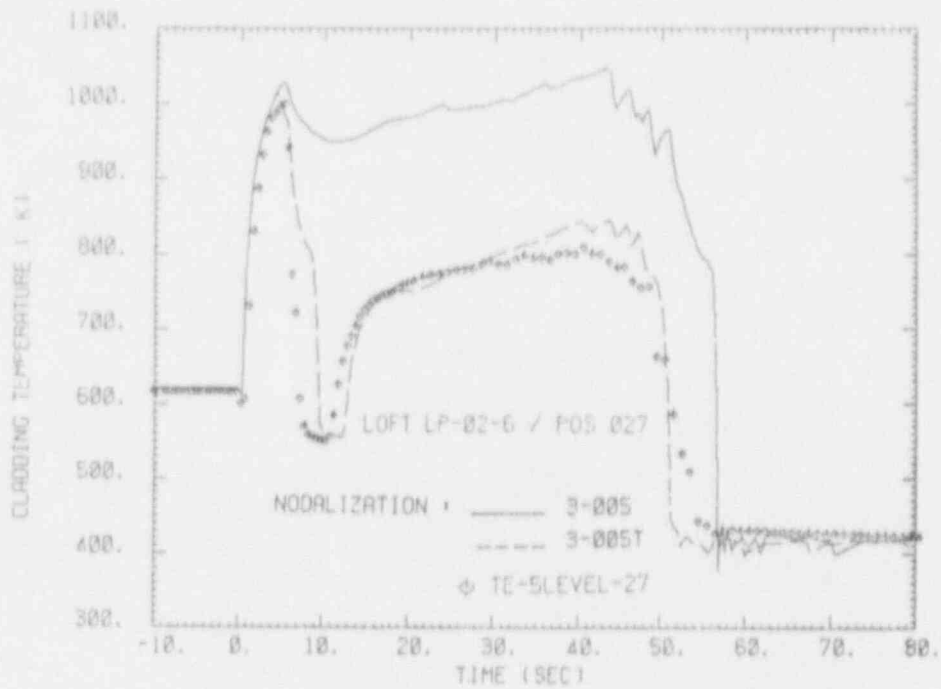


Figure 3.47: Comparison of cladding temperatures calculated by RELAP5/Mod2 without (3-005) and with (3-005T) external triggering of the reflood option

e) at level-27

f) at level-32

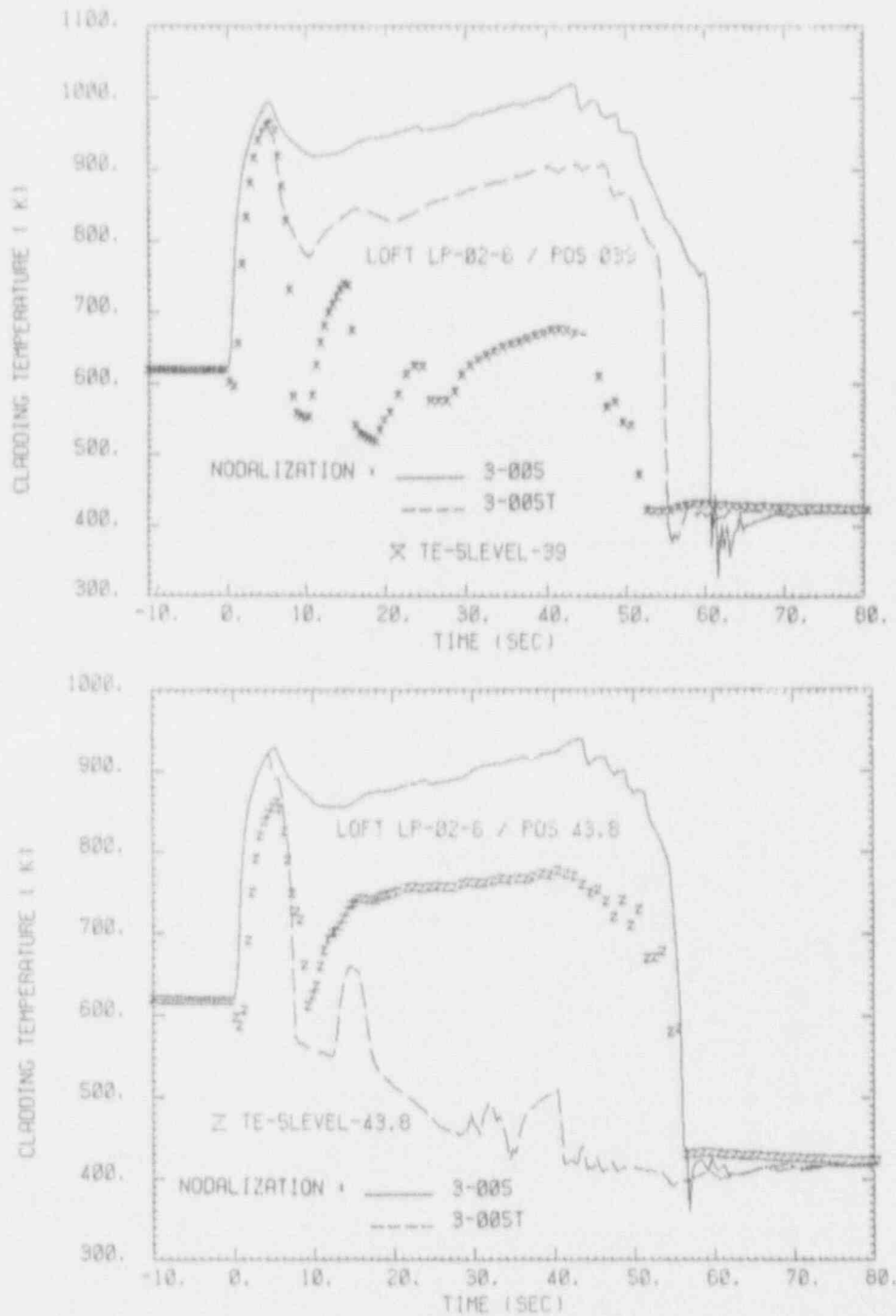


Figure 3.47: Comparison of cladding temperatures calculated by RELAP5/Mod2 without (3-005) and with (3-005T) external triggering of the reflow option

g) at level-39

h) at level-43.8

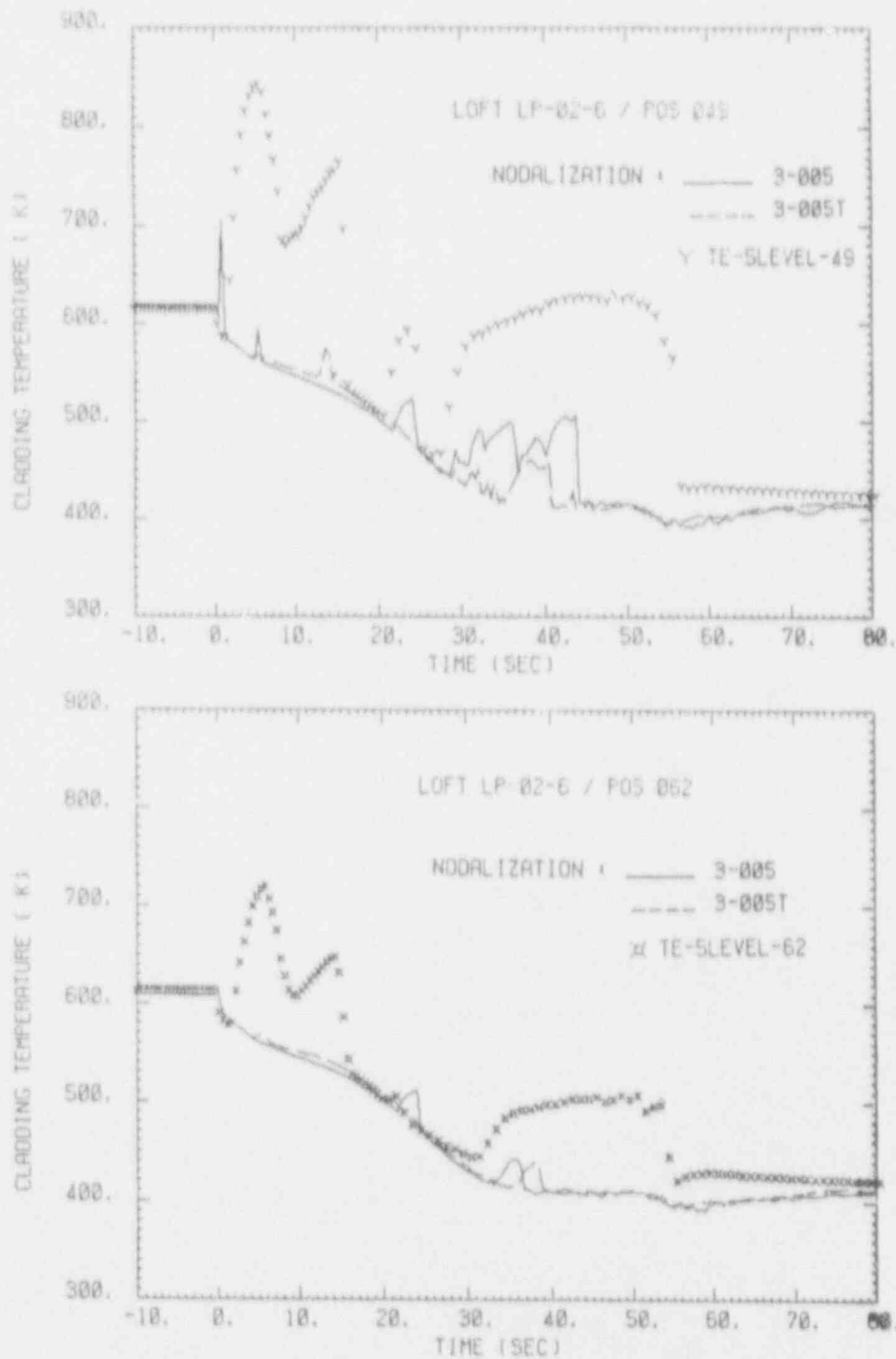


Figure 3.47: Comparison of cladding temperatures calculated by RELAP5/Mod2 without (3-005) and with (3-005T) external triggering of the re^{rod} option

- i) at level-49
- k) at level-62

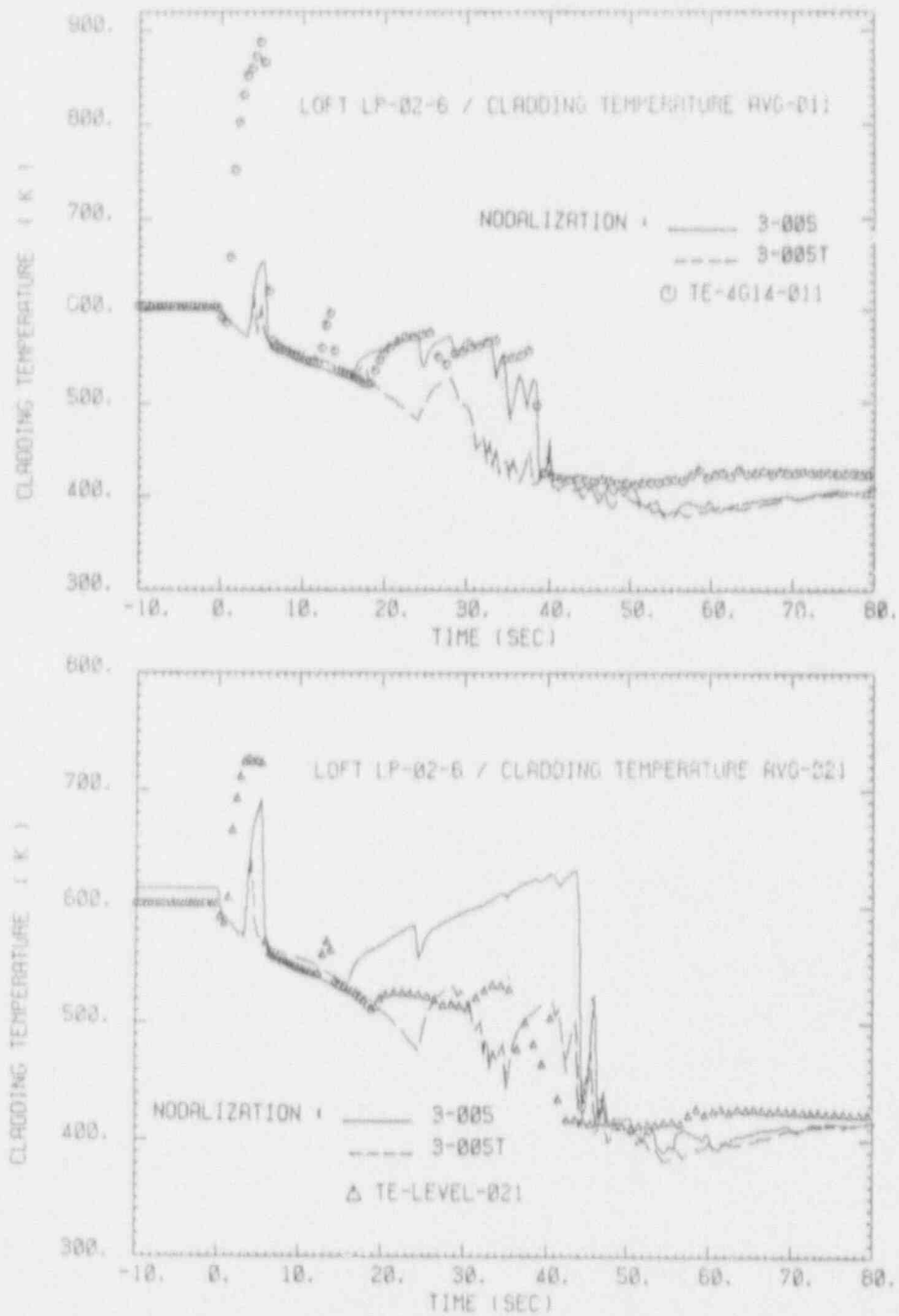


Figure 3.48: Comparison of cladding temperatures calculated by RELAP5/Mod2 without (3-005) and with (3-005T) external triggering of the reflood option

a) at level-11 (average channel)
 b) at level-21 (average channel)

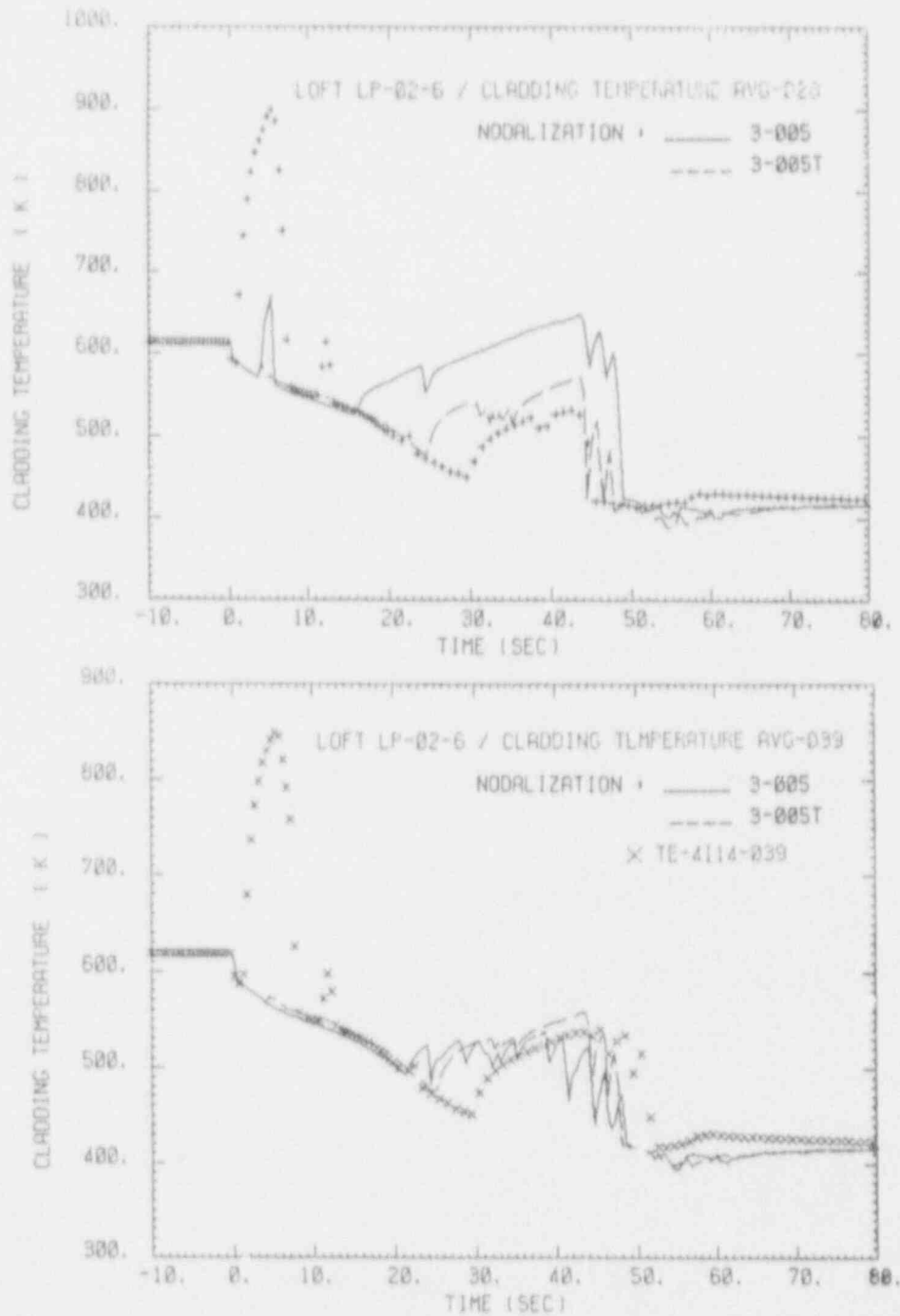


Figure 3.48: Comparison of cladding temperatures calculated by RELAP5/Mod2 without (3-005) and with (3-005T) external triggering of the reflood option
 c) at level-28 (average channel)
 d) at level-39 (average channel)

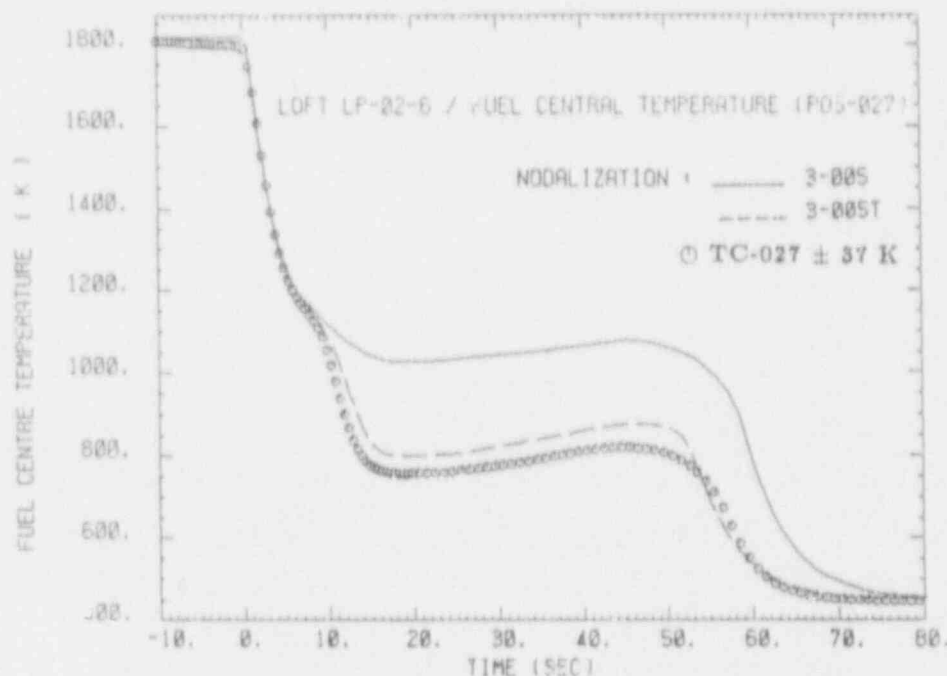


Figure 3.49: Comparison of the fuel center temperatures calculated by RELAP5/Mod2 without (3-005) and with (3-005T) external triggering of the reflow option at level 27

ment is independent of the status of the re-flooding option of the RELAP5/Mod2 code. In the frozen version of RELAP5, the heat transfer logic forces the code to stay in film boiling and does not allow it for any reason to return to transition boiling if the cladding temperature is higher than $1350 \text{ K} - T_{\text{saturation}}$. The same restriction is valid in the Post and Pre-dryout flow regimes where the code is prevented from returning to nucleate boiling, if the above temperature criterion is valid. By removing these two restrictions, one was able to calculate the early bottom up rewetting using the 3-005 nodalization (e.g. without "artificial initialization of the reflow option) much more accurate at nearly all core level than the results shown in this report.

Chapter 4

Conclusions

Experiment LP-02-6 was conducted in the Loss-Of-Fluid Test (LOFT) facility at the Idaho National Engineering Laboratory. It was the first large break loss-of-coolant accident simulation and the fourth experiment overall conducted on the LOFT test facility under the auspices of the OECD.

During this experiment, the cladding temperatures remained at temperatures lower than 1060 K which mainly was due to fact that high mass flow, early bottom-up rewetting took place during the blowdown phase of the experiment, approximately 4.5 to 8 seconds after opening of the break valves. In addition, in the upper part of the core, heat-up might have been delayed due to partial top-down quenching between 15 and 18 seconds of the experiment.

For the plant to be analysed, the "adequate nodalization" is usually unknown and only some very rough criteria can be given to the code user. Consequently, the accuracy of a prediction may be strongly related to the "experience" of the code user, a quite unsatisfactory conclusion. Therefore, we have analysed the LP-02-6 experiment by using the best estimate code RELAP5/Mod2 cy36-02 with different nodalizations of the loft system. Starting with a nodalization similar to the one used by the code developers at INEL (specially developed for small break LOCAs), we have reduced the numbers

of volumes, junctions and heat structures in the primary Loop of the LOFT system to nearly half whereas the entire vessel stayed unchanged to meet the requirements of the given experimental axial positions, especially for the cladding temperature measurements. We further have investigated on the influence of fine meshing in the core zone during reflooding on quench time and temperature and on the influence of the time of initialization of the reflood option with respect to RELAP5/Mod2's predicting capabilities of the quench phenomena.

- RELAP5/Mod2 , cy36-02 has calculated the general thermo-hydraulic behaviour of experiment LP-02-6 satisfactorily although it failed in describing the early bottom-up rewetting which happened between 4 and 8 seconds of the transient (blowdown phase) quenching the whole core. Independently of the chosen nodalization, most of the investigated parameters like pressures, mass flows in the broken and intact loops, pump speed and ECC systems have error bounds less than $\pm 20\%$. The cladding temperatures have been both over- and underpredicted (depending on the investigated core level) but not more than 150 K. For all nodalizations, the hot spot has been calculated at a position more downstream

of the core; instead at the experimentally inferred position 27 inches from the bottom of the core, RELAP5/Mod2 always calculated the hot spot at axial level 31. We believe that the, generally spoken, relatively good agreement of most of the RELAP5/Mod2 results with the measured LOFT data is not really surprising because codes like RELAP5/Mod2 have been extensively used for analysing LOFT experiments and LOFT results have been extensively used to eliminate insufficiencies both in the codes themselves as well as in the more plant specific nodalization of the problem. Therefore, even if these "adjustments" have been mainly made for small break LOCAs, one has to be aware of the fact that both the code and the LOFT specific nodalization (also used here as the basic nodalization scheme), are somehow "LOFT tuned" which resulted in these quite acceptable results.

- With respect to the computation time, the degree of specification of the nodalization, i.e. the numbers of volumes and junctions, is of course an important parameter. But not always a lower number of junctions and volumes automatically has led to a faster calculation. Sometimes, with respect to computing time, the profit of a much reduced nodalization is rather small.
- For large break LOCAs, the nodalization seems to be important only for the cladding temperatures, where significant differences can be observed for the different nodalizations under investigation. But, opposite to our findings when analysing the DT-LB-1 experiment (see ref. [7]), the differences in the times of final quenching are usually rather small

and within a band of less than ten seconds. Also for the other parameters, the deviations between the results of the calculation with the different nodalizations under investigation remain relatively small.

- The time point of initiating the re-flood option determines the "quench behaviour" of the code because it starts the fine-meshing in the core-zone thus enabling a more correct tracing of the axial cladding temperature distribution and consequently a better re-flood modeling. Therefore, the comparison of two of three possible methods of initiating the re-flood option have manifested a strong dependence of the results on this settings. An external trip based on the fluid level in the core alone has led to much lower values of the cladding temperatures at nearly all axial levels of the LOFT core but still was not able to correctly calculate the early bottom-up rewetting which has quenched the whole core within the first 4.5 to 8 seconds of the experiment and therefore has had a very important influence on the behaviour of the whole system. Early bottom-up rewetting probably is a consequence of the coast-down behaviour of the primary pumps. RELAP5/Mod2 has been able to give an indication for this dependence. Looking at the different mass fluxes as calculated by the code using different assumptions about the pump coast-down behaviour, one easily will observe the strong relationship between coast-down behaviour and mass flux; e.g. rapid pump coast-down lead to much lower core in and out mass fluxes than normal coast-down (see figs. 3.32 and 3.33).

- Finally, a remarkable inconsistency has been observed concerning the heat transfer and flow regime logics of RELAP5/Mod2. During the refill phase of the calculation, at the same time RELAP5/Mod2 assumed different flow regimes on one side for its calculation of the interfacial shear stresses and interfacial heat transfers and on the other side for the determination of the heat transfer from the wall to the fluid (liquid). This unphysical modeling of the thermo-hydraulic conditions in the core region of the LOFT reactor may invalidate even results which have been proved as to be satisfactory by a pure comparison with the experimental data, e.g. at the same axial position and at the same time, RELAP5/Mod2 assumed both wet and dry surface by defining mist flow and slug flow for the same volume.

Chapter 5

Appendices

5.1 References

- [1] Reeder, D.G. : LOFT System and Test Description
NUREG/CR-0247 Tree-1208 (1978, update 9/80)
- [2] Ybaronndo, et.al. : Examination of LOFT Scaling
74-WA-HT-53, ANS proceedings, New York (1974)
- [3] Adams, J.P.; Keith, G.C and Doyle, L.B. : Quick Look Report
on OECD LOFT-Experiment LP-02-6
OECD LOFT-T-3404, EG&G Idaho Inc. (1983)
- [4] Andreani, M and Grütter, H.P : Post-Test Analysis of
OECD LOFT-Experiment LP-SB-3 by RELAP5/Mod2
EIR internal report TM-32-85-18 (1985)
- [5] Lorenzini, E; Orlandelli, C.M. and Spada, A : LOFT LP-LB-1
Post-Test Analysis using RELAP5/Mod1 computer
code
ENEA Safety Research Program (1984)
- [6] Ransom, V.H., et.al. : RELAP5/Mod2 Code Manual
NUREG/CR-4312 (1985)
- [7] Lübbsmeyer, D. : Post-Test-Analysis of OECD LOFT Experiment LP-LB-1
with RELAP5/Mod2 -cy36-02
NUREC/JA-00073 (1991)

- [8] Analytis, G.Th. and Lübbesmeyer, D. : Analysis of LOFT Experiment LP-02-6 by Standard and Modified RELAP5/Mod2
Trans. Am. Nucl. Soc. 56, 394 (1988)
- [9] Anonymous : OECD LOFT Experiment LP-02-6 : Tape Descriptions and Supplementary Information
- [10] Brittain, I. and Aksan, S.N. : OECD-LOFT Large Break LOCA Experiments : Phenomenology and Computer Code Analyses
PSI-report 72 (or AEEW-TRS-1003), August 1990

*-----1-----1-----1-----1-----1-----1-----1-----		LP2-	38	
* transient plot requests		LP2-	39	
*-----1-----1-----1-----1-----1-----1-----1-----		LP2-	40	
00000301	cputime	0	*LP2-	41
00000302	emass	0	*LP2-	42
00000303	p	340010000	*LP2-	43
00000304	rho	340010000	*LP2-	44
00000305	mflowj	340010000	*LP2-	45
00000306	cntrlvar	404	*LP2-	46
00000307	tempf	340010000	*LP2-	47
00000308	tempg	340010000	*LP2-	48
00000309	p	342010000	*LP2-	49
00000310	p	344010000	*LP2-	50
*			LP2-	51
00000311	p	305010000	*LP2-	52
00000312	rho	305010000	*LP2-	53
00000313	mflowj	305010000	*LP2-	54
00000314	cntrlvar	414	*LP2-	55
00000315	tempf	305010000	*LP2-	56
00000316	tempg	305010000	*LP2-	57
00000317	p	315070000	*LP2-	58
*			LP2-	59
00000318	rho	180010000	*LP2-	60
00000319	mflowj	185020000	*LP2-	61
00000320	cntrlvar	424	*LP2-	62
00000321	velf	180010000	*LP2-	63
00000322	tempf	180010000	*LP2-	64
00000323	tempg	180010000	*LP2-	65
00000324	cntrlvar	80	*LP2-	66
*			LP2-	67
00000325	rho	100010000	*LP2-	68
00000326	mflowj	100020000	*LP2-	69
00000327	cntrlvar	434	*LP2-	70
00000328	tempf	100010000	*LP2-	71
00000329	tempg	100010000	*LP2-	72
00000330	p	100010000	*LP2-	73
00000331	p	420010000	*LP2-	74
*			LP2-	75
00000332	cntrlvar	460	*LP2-	76
00000333	cntrlvar	461	*LP2-	77
00000334	cntrlvar	462	*LP2-	78
00000335	cntrlvar	463	*LP2-	79
00000336	cntrlvar	464	*LP2-	80

*			LP2-	81
00000337	mflowj	610000000	*LP2-	82
00000338	cntrlvar	4	*LP2-	83
00000339	p	620010000	*LP2-	84
00000340	mflowj	630000000	*LP2-	85
00000341	mflowj	640000000	*LP2-	86
*			LP2-	87
00000342	p	240010000	*LP2-	88
00000343	voidf	240010000	*LP2-	89
00000344	cntrlvar	240	*LP2-	90
00000345	voidf	225010000	*LP2-	91
00000346	voidf	210020000	*LP2-	92
00000347	velfj	225020000	*LP2-	93
00000348	cntrlvar	444	*LP2-	94
00000349	cntrlvar	454	*LP2-	95
00000350	cntrlvar	90	*LP2-	96
00000351	cntrlvar	91	*LP2-	97
00000352	cntrlvar	93	*LP2-	98
00000353	cntrlvar	98	*LP2-	99
00000354	voidg	231010000	*LP2-	100
00000355	voidg	231020000	*LP2-	101
00000356	voidg	231040000	*LP2-	102
00000357	voidg	231050000	*LP2-	103
00000358	voidg	231060000	*LP2-	104
00000359	voidg	231070000	*LP2-	105
00000360	voidg	231090000	*LP2-	106
00000361	voidg	231100000	*LP2-	107
00000362	voidg	231110000	*LP2-	108
00000363	voidg	231130000	*LP2-	109
00000364	cntrlvar	470	*LP2-	110
*			LP2-	111
00000365	tempf	202010000	*LP2-	112
00000366	tempf	210020000	*LP2-	113
00000367	tempf	210030000	*LP2-	114
00000368	tempf	210040000	*LP2-	115
00000369	tempf	220010000	*LP2-	116
00000370	httemp	231000110	*LP2-	117
00000371	httemp	231000210	*LP2-	118
00000372	httemp	231000410	*LP2-	119
00000373	httemp	231000510	*LP2-	120
00000374	httemp	231000610	*LP2-	121
00000375	httemp	231000710	*LP2-	122
00000376	httemp	231000910	*LP2-	123


```

00000510  time      0          ge  null      0          10.0      1  *LP2- 167
*
*
*   scram
00000511  time      0          ge  timeof   510        0.13     1  *LP2- 171
*   pcp trip
00000512  time      0          ge  timeof   510        0.8      1  *LP2- 173
*   lpis on
00000513  time      0          ge  timeof   510       34.8     1  *LP2- 175
*   hpis on
00000514  time      0          ge  timeof   510       21.8     1  *LP2- 177
*   accumulator valve
00000515  time      0          ge  timeof   510       17.5     1  *LP2- 179
*   broken leg bypass
00000516  time      0          ge  null      0          1.0+9    1  *LP2- 181
*-----1-----1-----1-----1-----1-----1-----1-----
*
*   different related trips
*-----1-----1-----1-----1-----1-----1-----1-----
* lt 681 ecc check valve          card 6000301
*-----1-----1-----1-----1-----1-----1-----1-----
00000577  mflowj    600000000 ge  null      0          0.0      n  *LP2- 188
00000578  p         605010000 gt  p         185010000 0.        n  *LP2- 189
00000681  577      and      578      n
*-----1-----1-----1-----1-----1-----1-----1-----
* lt 682 accumulator valve      card 6100301
*-----1-----1-----1-----1-----1-----1-----1-----
00000582  cntrlvar  4          lt  null      0          1.0-4    1  *LP2- 194
00000682  -582     and      515      n
*-----1-----1-----1-----1-----1-----1-----1-----
* lt 685-686 steam valve        card 5400301
*-----1-----1-----1-----1-----1-----1-----1-----
* open trip
00000589  p         530010000 gt  null      0          5.55+6  n  *LP2- 200
00000590  p         530010000 lt  null      0          5.50+6  n  *LP2- 201
00000670  685      or       589      n
00000671  -590     and     -686     n
00000685  671     and      670     n
* close trip
00000591  p         530010000 gt  null      0          5.10+6  n  *LP2- 206
00000592  p         530010000 lt  null      0          5.05+6  n  *LP2- 207
00000672  686     or       592     n
00000673  -591     and      672     n

```


1051201	5.7985497	5.8006973	0.							* (M = 247.55 kg/s)	LP2- 253
*-----	-----1-----	-----1-----	-----1-----	-----1-----	-----1-----	-----1-----	-----1-----	-----1-----	-----1-----		LP2- 254
* pressurizer connection tee											LP2- 255
*-----	-----1-----	-----1-----	-----1-----	-----1-----	-----1-----	-----1-----	-----1-----	-----1-----	-----1-----		LP2- 256
1070000	"pzs t "			branch							*LP2- 257
1070001	1	0									*LP2- 258
1070101	0.0620253	0.2810215	0.0		0.0	0.0	0.0	0.0			*LP2- 259
1070102	4.0e-5	0.0	00								*LP2- 260
1070200	0	1.52852+7	1410746.		2453006.	0.					*LP2- 261
1071101	107010000	110000000	0.0		0.135	0.135	0000				*LP2- 262
1071201	5.9346313	5.9351082	0.							* (M = 247.57 kg/s)	LP2- 263
*-----	-----1-----	-----1-----	-----1-----	-----1-----	-----1-----	-----1-----	-----1-----	-----1-----	-----1-----		LP2- 264
* pressurizer connection tee steam generator side											LP2- 265
*-----	-----1-----	-----1-----	-----1-----	-----1-----	-----1-----	-----1-----	-----1-----	-----1-----	-----1-----		LP2- 266
1100000	"pzs t sg"			branch							*LP2- 267
1100001	1	0									*LP2- 268
1100101	0.0606063	0.9207292	0.0		0.0	0.0	0.0	0.0			*LP2- 269
1100102	4.0e-5	0.0	00								*LP2- 270
1100200	0	1.52827+7	1410749.		2453066.	0.					*LP2- 271
1101101	110010000	112000000	0.0		0.15	0.15	0000				*LP2- 272
1101201	6.2683144	6.2684364	0.							* (M = 247.57 kg/s)	LP2- 273
*-----	-----1-----	-----1-----	-----1-----	-----1-----	-----1-----	-----1-----	-----1-----	-----1-----	-----1-----		LP2- 274
* hot leg piping											LP2- 275
*-----	-----1-----	-----1-----	-----1-----	-----1-----	-----1-----	-----1-----	-----1-----	-----1-----	-----1-----		LP2- 276
1120000	"hot leg "			pipe							*LP2- 277
1120001	2										*LP2- 278
1120101	0.0	2									*LP2- 279
1120201	0.0	1									*LP2- 280
1120301	1.38893	1									*LP2- 281
1120302	0.707687	2									*LP2- 282
1120401	0.0796973	1									*LP2- 283
1120402	0.0579614	2									*LP2- 284
1120501	0.0	2									*LP2- 285
1120601	0.0	1									*LP2- 286
1120602	90.0	2									*LP2- 287
1120701	0.0	1									*LP2- 288
1120702	0.246447	2									*LP2- 289
1120801	4.0e-5	0.0	2								*LP2- 290
1120901	0.20	0.20	1								*LP2- 291
1121001	00	2									*LP2- 292
1121101	0000	1									*LP2- 293
1121201	0	1.52785+7	1410752.		2453166.	0.	0.	1			*LP2- 294
1121202	0	1.52814+7	1410754.		2453098.	0.	0.	2			*LP2- 295

1121300	0							*LP2- 296
1121301	6.2683678	6.2683411	0.	1	*	(M = 247.57 kg/s)		LP2- 297
*-----1-----1-----1-----1-----1-----1-----1-----								LP2- 298
* sg inlet plenum								LP2- 299
*-----1-----1-----1-----1-----1-----1-----1-----								LP2- 300
1140000	"sg in pl"		branch					*LP2- 301
1140001	2	0						*LP2- 302
1140101	0.0	0.629795	0.33532	0.0	90.0	0.512756		*LP2- 303
1140102	4.e-5	0.0102	00					*LP2- 304
1140200	0	1.52E60+7	1410762.	2453710.	0.			*LP2- 305
1141101	112010000	114000000	0.0512	0.0	0.0	0100		*LP2- 306
1142101	114010000	115000000	0.0	0.0	0.0	0100		*LP2- 307
1141201	4.391552	4.3915901	0.		*	(M = 247.57 kg/s)		LP2- 308
1142201	2.3794098	2.3794098	0.		*	(M = 247.56 kg/s)		LP2- 309
*-----1-----1-----1-----1-----1-----1-----1-----								LP2- 310
* sg u-tubes								LP2- 311
*-----1-----1-----1-----1-----1-----1-----1-----								LP2- 312
1150000	"sg tubes"		pipe					*LP2- 313
1150001	8							*LP2- 314
1150101	0.0	8						*LP2- 315
1150201	0.151171	7						*LP2- 316
1150301	0.902	1						*LP2- 317
1150302	0.6096	3						*LP2- 318
1150303	0.462908	5						*LP2- 319
1150304	0.6096	7						*LP2- 320
1150305	0.902	8						*LP2- 321
1150401	0.136356	1						*LP2- 322
1150402	0.0921538	3						*LP2- 323
1150403	0.0699783	5						*LP2- 324
1150404	0.0921538	7						*LP2- 325
1150405	0.136356	8						*LP2- 326
1150501	0.0	8						*LP2- 327
1150601	90.0	4						*LP2- 328
1150602	-90.0	8						*LP2- 329
1150701	0.902	1						*LP2- 330
1150702	0.6096	3						*LP2- 331
1150703	0.299572	4						*LP2- 332
1150704	-0.299572	5						*LP2- 333
1150705	-0.6096	7						*LP2- 334
1150706	-0.902	8						*LP2- 335
1150801	1.27-7	0.01022	8					*LP2- 336
1150901	0.0	0.0	7					*LP2- 337
1151001	00	8						*LP2- 338

1151101	0000	7							*LP2- 339
1151201	0	1.52468+7	1367802.	2453930.	0.	0.	1		*LP2- 340
1151202	0	1.52390+7	1333644.	2454120.	0.	0.	2		*LP2- 341
1151203	0	1.52326+7	1306228.	2454274.	0.	0.	3		*LP2- 342
1151204	0	1.52275+7	1288303.	2454396.	0.	0.	4		*LP2- 343
1151205	0	1.52260+7	1272624.	2454434.	0.	0.	5		*LP2- 344
1151206	0	1.52275+7	1255106.	2454396.	0.	0.	6		*LP2- 345
1151207	0	1.52300+7	1239987.	2454336.	0.	0.	7		*LP2- 346
1151208	0	1.52331+7	1226804.	2454260.	0.	0.	8		*LP2- 347
1151300	0								*LP2- 348
1151301	2.3187809	2.3187809	0.				1	* (M = 247.56 kg/s)	LP2- 349
1151302	2.274889	2.274889	0.				2	* (M = 247.56 kg/s)	LP2- 350
1151303	2.242157	2.242157	0.				3	* (M = 247.56 kg/s)	LP2- 351
1151304	2.2215405	2.2215405	0.				4	* (M = 247.56 kg/s)	LP2- 352
1151305	2.2040806	2.2040806	0.				5	* (M = 247.56 kg/s)	LP2- 353
1151306	2.1854172	2.1854172	0.				6	* (M = 247.56 kg/s)	LP2- 354
1151307	2.1697006	2.1697006	0.				7	* (M = 247.56 kg/s)	LP2- 355
*----	----	----	----	----	----	----	----	----	LP2- 356
* sg outlet plenum									LP2- 357
*----	----	----	----	----	----	----	----	----	LP2- 358
1160000	"sg out p"		branch						*LP2- 359
1160001	2	0							*LP2- 360
1160101	0.0	0.629795	0.33532	0.0	-90.0	-0.512756			*P2- 361
1160102	4.e-5	0.0102	00						*LP2- 362
1160200	0	1.52375+7	1226810.	2454156.	0.				*LP2- 363
1161101	115010000	116000000	0.0	0.0	0.0	0100			*LP2- 364
1162101	116010000	118000000	0.0512	0.0	0.0	0100			*LP2- 365
1161201	2.1562672	2.1562672	0.					* (M = 247.56 kg/s)	LP2- 366
1162201	3.9985161	3.9985161	0.					* (M = 247.56 kg/s)	LP2- 367
*----	----	----	----	----	----	----	----	----	LP2- 368
* pump suction piping									LP2- 369
*----	----	----	----	----	----	----	----	----	LP2- 370
1180000	"pmp suc "		pipe						*LP2- 371
1180001	3								*LP2- 372
1180101	0.0	3							*LP2- 373
1180201	0.0	2							*LP2- 374
1180301	0.546638	1							*LP2- 375
1180302	0.688596	2							*LP2- 376
1180303	0.558577	3							*LP2- 377
1180401	0.0445625	1							*LP2- 378
1180402	0.0445137	2							*LP2- 379
1180403	0.0354278	3							*LP2- 380
1180501	0.0	3							*LP2- 381

1300101	0.0	0.457201	0.0177444	0.0	90.0	0.457201	*LP2- 425
1300102	4.0e-5	0.0	00				*LP2- 426
1300200	0	1.52183+7	1226821.	2454620.	0.		*LP2- 427
*-----1-----1-----1-----1-----1-----1-----1-----							LP2- 428
* primary coolant pump 1							LP2- 429
*-----1-----1-----1-----1-----1-----1-----1-----							LP2- 430
1350000	"pcpump1"		pump				*LP2- 431
1350101	.0366	0.0	0.0991	0.0	90.	0.317900	*LP2- 432
1350102	0						*LP2- 433
1350108	130010000	0.0	0.017	0.017	0000		*LP2- 434
1350109	140000000	0.0	0.05	0.05	0000		*LP2- 435
1350200	0	1.52814+7	1226902.	2453096.	0.		*LP2- 436
1350201	0	4.1930466	4.1930466	0.		* (M = 116.55 kg/s)	LP2- 437
1350202	0	4.1928749	4.1928749	0.		* (M = 116.55 kg/s)	LP2- 438
1350301	0 0	0	-1	-1	512	0	*LP2- 439
1350302	369.	0.448699	.3155	96.	500.6	1.431	*LP2- 440
*						(pump speed = 165.56995 rev/s)	LP2- 441
1350303	613.6	0.	207.433	.0444	19.5987	0.	*LP2- 442
1350310	0.0	0.0	0.0				*LP2- 443
*-----1-----1-----1-----1-----1-----1-----1-----							LP2- 444
* pump 1 outlet pump side							LP2- 445
*-----1-----1-----1-----1-----1-----1-----1-----							LP2- 446
1400000	"pmp1 out"		snglvol				*LP2- 447
1400101	0.0	0.502185	0.0183849	0.0	0.0	0.0	*LP2- 448
1400102	4.0e-5	0.0	00				*LP2- 449
1400200	0	1.53468+7	1226905.	2451526.	0.		*LP2- 450
*-----1-----1-----1-----1-----1-----1-----1-----							LP2- 451
* pmp1 outlet pipe tee side							LP2- 452
*-----1-----1-----1-----1-----1-----1-----1-----							LP2- 453
1450000	"pmp1 out"		branch				*LP2- 454
1450001	2	0					*LP2- 455
1450101	0.0	1.40843	0.0633861	0.0	0.0	0.0	*LP2- 456
1450102	4.0e-5	0.0	00				*LP2- 457
1450200	0	1.53488+7	1226911.	2451478.	0.		*LP2- 458
1451101	140010000	145000000	0.0	0.0	0.0	0000	*LP2- 459
1452101	145010000	150000000	0.0	0.57456	0.050347	0000	*LP2- 460
1451201	4.191433	4.191433	0.			* (M = 116.55 kg/s)	LP2- 461
1452201	3.4095764	3.4095764	0.			* (M = 116.55 kg/s)	LP2- 462
*-----1-----1-----1-----1-----1-----1-----1-----							LP2- 463
* pump outlet tee							LP2- 464
*-----1-----1-----1-----1-----1-----1-----1-----							LP2- 465
1500000	"pmp out"		branch				*LP2- 466
1500001	1	0					*LP2- 467

1500101	0.0	0.496511	0.0316011	0.0	0.0	0.0	*LP2- 468
1500102	4.0e-5	0.0	00				*LP2- 469
1500200	0	1.53404+7	1226911.	2451678.	0.		*LP2- 470
1501101	150010000	175000000	0.063427	0.0	0.0	0000	*LP2- 471
1501201	5.1387558	5.1387558	0.	* (M = 247.56 kg/s)			LP2- 472
*-----1-----1-----1-----1-----1-----1-----1-----							LP2- 473
* pump 2 suction tee outlet							LP2- 474
*-----1-----1-----1-----1-----1-----1-----1-----							LP2- 475
1550000	"pmp2 sct"		branch				*LP2- 476
1550001	1	0					*LP2- 477
1550101	0.0	1.00308	0.0640548	0.0	90.	0.520704	*LP2- 478
1550102	4.0e-5	0.0	00				*LP2- 479
1550200	0	1.52253+7	1226819.	2454448.	0.		*LP2- 480
1551101	155010000	160000000	0.0	0.13	0.13	0000	*LP2- 481
1551201	4.4447289	4.4447289	0.	* (M = 131.01 kg/s)			LP2- 482
*-----1-----1-----1-----1-----1-----1-----1-----							LP2- 483
* pump 2 inlet pipe							LP2- 484
*-----1-----1-----1-----1-----1-----1-----1-----							LP2- 485
1600000	"pmp2 in1"		snglvol				*LP2- 486
1600101	0.0	0.457201	0.0177444	0.0	90.	0.457201	*LP2- 487
1600102	4.0e-5	0.0	00				*LP2- 488
1600200	0	1.52158+7	1226820.	2454678.	0.		*LP2- 489
*-----1-----1-----1-----1-----1-----1-----1-----							LP2- 490
* primary coolant pump 2							LP2- 491
*-----1-----1-----1-----1-----1-----1-----1-----							LP2- 492
1650000	"pcpump2"		pump				*LP2- 493
1650101	.0366	0.0	0.0991	0.0	90.	0.317900	*LP2- 494
1650102	0						*LP2- 495
1650108	160010000	0.0	0.017	0.017	0000		*LP2- 496
1650109	170000000	0.0	0.1	0.1	0000		*LP2- 497
1650200	0	1.52797+7	1226905.	2453138.	0.		*LP2- 498
1650201	0	4.7132797	4.7132797	0.	* (M = 131.01 kg/s)		LP2- 499
1650202	0	4.7130966	4.7130966	0.	* (M = 131.01 kg/s)		LP2- 500
1650301	135 135	135	-1	-1	512	0	*LP2- 501
1650302	369.	0.4724932	.3155	96.	500.6	1.431	*LP2- 502
* (pump speed = 174.34998 rev/s)							LP2- 503
1650303	613.6	0.	207.433	.0444	19.5987	0.	*LP2- 504
1650310	0.0	0.0	0.0				*LP2- 505
*-----1-----1-----1-----1-----1-----1-----1-----							LP2- 506
* pump 2 outlet							LP2- 507
*-----1-----1-----1-----1-----1-----1-----1-----							LP2- 508
1700000	"pmp2 out"		branch				*LP2- 509
1700001	1	0					*LP2- 510

1700101	0.0	0.514071	0.0192958	0.0	0.0	0.0		*LP2- 511
1700102	4.0e-5	0.0	00					*LP2- 512
1700200	0	1.53458+7	1226908.	2451548.	0.			*LP2- 513
1701101	170010000	150000000	0.036611	0.3847	0.6316	0000		*LP2- 514
1701201	4.7113152	4.7113152	0.				* (M = 131.01 kg/s)	LP2- 515
*-----1-----1-----1-----1-----1-----1-----1-----								LP2- 516
* intact loop cold leg pipe								LP2- 517
*-----1-----1-----1-----1-----1-----1-----1-----								LP2- 518
1750000	"ilcl pip"		pipe					*LP2- 519
1750001	2							*LP2- 520
1750101	0.0	2						*LP2- 521
1750201	0.0	1						*LP2- 522
1750301	0.558577	1						*LP2- 523
1750302	0.613244	2						*LP2- 524
1750401	0.035428	1						*LP2- 525
1750402	0.038895	2						*LP2- 526
1750501	0.0	2						*LP2- 527
1750601	0.0	2						*LP2- 528
1750701	0.0	2						*LP2- 529
1750801	4.0e-5	0.0	2					*LP2- 530
1750901	0.0	0.0	1					*LP2- 531
1751001	00	2						*LP2- 532
1751101	0000	1						*LP2- 533
1751201	0	1.53401+7	1226913.	2451686.	0.	0.	1	*LP2- 534
1751202	0	1.53399+7	1226914.	2451692.	0.	0.	2	*LP2- 535
1751300	0							*LP2- 536
1751301	5.1389198	5.1389198	0.				1 * (M = 247.56 kg/s)	LP2- 537
*-----1-----1-----1-----1-----1-----1-----1-----								LP2- 538
* ecc connection tee								LP2- 539
*-----1-----1-----1-----1-----1-----1-----1-----								LP2- 540
1800000	"ecc t "		branch					*LP2- 541
1800001	1	0						*LP2- 542
1800101	0.0	1.15189	0.0730598	0.0	0.0	0.0		*LP2- 543
1800102	4.0e-5	0.0	00					*LP2- 544
1800200	0	1.53395+7	1226918.	2451702.	0.			*LP2- 545
1801101	175010000	180000000	0.0	0.0	0.0	0000		*LP2- 546
1801201	5.1389236	5.1389236	0.				* (M = 247.56 kg/s)	LP2- 547
*-----1-----1-----1-----1-----1-----1-----1-----								LP2- 548
* reactor vessel nozzle - intact loop cold leg								LP2- 549
*-----1-----1-----1-----1-----1-----1-----1-----								LP2- 550
1850000	"rvn ilcl"		branch					*LP2- 551
1850001	2	0						*LP2- 552
1850101	0.0	1.00965	0.0644920	0.0	0.0	0.0		*LP2- 553

2020601	-90.0	1								*LP2- 597
2020801	3.81-6	0.172	1							*LP2- 598
2021001	00	1								*LP2- 599
2021201	0	1.53206+7	1226923.	2452154.	0.	0.	1			*LP2- 600
*-----	-----1-----	-----1-----	-----1-----	-----1-----	-----1-----	-----1-----	-----1-----			LP2- 601
* junction - middle to lower inlet annulus intact side										LP2- 602
*-----	-----1-----	-----1-----	-----1-----	-----1-----	-----1-----	-----1-----	-----1-----			LP2- 603
2050000	"inanmlit"		sngljun							*LP2- 604
2050101	202010000	210000000	0.0709408	0.0	0.0	0100				*LP2- 605
2050201	0	1.7637691	1.7637691	0.					* (M = 175.29 kg/s)	LP2- 606
*-----	-----1-----	-----1-----	-----1-----	-----1-----	-----1-----	-----1-----	-----1-----			LP2- 607
* inlet annulus lower volume intact side										LP2- 608
*-----	-----1-----	-----1-----	-----1-----	-----1-----	-----1-----	-----1-----	-----1-----			L ← 609
2100000	"int dowc"		annulus							+ 610
2100001	4									*LP 611
2100101	0.1464354	1								*LP2- 612
2100102	0.0	4								*LP2- 613
2100201	0.0709408	3								*LP2- 614
2100301	0.2525361	1								*LP2- 615
2100302	1.5200561	2								*LP2- 616
2100303	1.2616333	3								*LP2- 617
2100304	1.0792591	4								*LP2- 618
2100401	0.0	1								*LP2- 619
2100402	0.1581866	2								*LP2- 620
2100403	0.1217000	3								*LP2- 621
2100404	0.0986806	4								*LP2- 622
2100501	0.0	4								*LP2- 623
2100601	-90.	4								*LP2- 624
2100801	3.81-6	0.172	4							*LP2- 625
2100901	0.0	0.0	3							*LP2- 626
2101001	00	04								*LP2- 627
2101101	00000	03								*LP2- 628
2101201	0	1.53177+7	1226925.	2452224.	0.	0.	1			*LP2- 629
2101202	0	1.53233+7	1226937.	2452090.	0.	0.	2			*LP2- 630
2101203	0	1.53331+7	1226945.	2451854.	0.	0.	3			*LP2- 631
2101204	0	1.53414+7	1226952.	2451654.	0.	0.	4			*LP2- 632
2101300	0									*LP2- 633
2101301	3.2533512	3.2533512	0.		1				* (M = 175.29 kg/s)	LP2- 634
2101302	3.253336	3.253336	0.		2				* (M = 175.29 kg/s)	LP2- 635
2101303	3.2533035	3.2533035	0.		3				* (M = 175.29 kg/s)	LP2- 636
*-----	-----1-----	-----1-----	-----1-----	-----1-----	-----1-----	-----1-----	-----1-----			LP2- 637
* junction - lower downcomer to lower plenum intact side										LP2- 638
*-----	-----1-----	-----1-----	-----1-----	-----1-----	-----1-----	-----1-----	-----1-----			LP2- 639

2150000	"inanmuit"		sngljun					*LP2- 640
2150101	210010000	222000000	0.0709408	0.0000	0.0000	0100		*LP2- 641
2150201	0	2.5241261	2.5241261	0.			* (M = 175.29 kg/s)	LP2- 642
*----	-----1-----	-----1-----	-----1-----	-----1-----	-----1-----	-----1-----		LP2- 643
* lower plenum bottom volume								LP2- 644
*----	-----1-----	-----1-----	-----1-----	-----1-----	-----1-----	-----1-----		LP2- 645
2200000	"lwr pl b"		snglvol					*LP2- 646
2200101	0.0	0.3741720	0.29656	0.0	90.	0.3741720		*LP2- 647
2200102	4.0e-5	0.0	00					*LP2- 648
2200200	0	1.53399+7	1227769.	2451692.	0.			*LP2- 649
*----	-----1-----	-----1-----	-----1-----	-----1-----	-----1-----	-----1-----		LP2- 650
* lower plenum top volume								LP2- 651
*----	-----1-----	-----1-----	-----1-----	-----1-----	-----1-----	-----1-----		LP2- 652
2220000	"lwr pl t"		branch					*LP2- 653
2220001	2	0						*LP2- 654
2220101	0.0	0.3533183	0.2592277	0.0	90.	0.3533183		*LP2- 655
2220102	3.81-6	0.0	00					*LP2- 656
2220200	0	1.53426+7	1226974.	2451628.	0.			*LP2- 657
2221101	222010000	220000000	0.0	0.005	0.005	0000		*LP2- 658
2222101	222000000	225000000	0.1499	1.5	1.5	0000		*LP2- 659
2221201	0.	0.	0.				* (M = -1.556-4 kg/s)	LP2- 660
2222201	2.1743755	2.1743755	0.				* (M = 247.56 kg/s)	LP2- 661
*----	-----1-----	-----1-----	-----1-----	-----1-----	-----1-----	-----1-----		LP2- 662
* lower core support structure								LP2- 663
*----	-----1-----	-----1-----	-----1-----	-----1-----	-----1-----	-----1-----		LP2- 664
2250000	"l core s"		branch					*LP2- 665
2250001	3	0						*LP2- 666
2250101	0.2832456	0.5709989	0.0	0.0	90.0	0.5709989		*LP2- 667
2250102	3.81-6	0.095	00					*LP2- 668
2250200	0	1.53385+7	1226979.	2451724.	0.			*LP2- 669
2251101	225010000	230000000	0.0	1.5	1.5	00100		*LP2- 670
2252101	225010000	231000000	0.0	1.5	1.5	00100		*LP2- 671
2253101	225010000	235000000	0.0	12.	12.	00100		*LP2- 672
2251201	1.7612839	1.7612839	0.				* (M = 197.33 kg/s)	LP2- 673
2252201	1.661684	1.661684	0.				* (M = 38.994 kg/s)	LP2- 674
2253201	0.706759	0.706759	0.				* (M = 11.235 kg/s)	LP2- 675
*----	-----1-----	-----1-----	-----1-----	-----1-----	-----1-----	-----1-----		LP2- 676
* active core : average channels (75!)								LP2- 677
*----	-----1-----	-----1-----	-----1-----	-----1-----	-----1-----	-----1-----		LP2- 678
2300000	"core avg"		pipe					*LP2- 679
2300001	5							*LP2- 680
2300101	0.147510	1						*LP2- 681
2300102	0.137871	2						*LP2- 682

*-----1-----1-----1-----1-----1-----1-----1-----									LP2- 769
* core bypass volume (7!)									LP2- 770
*-----1-----1-----1-----1-----1-----1-----1-----									LP2- 771
2350000	"core byp"		pipe						*LP2- 772
2350001	3								*LP2- 773
2350101	2.0930-2	3							*LP2- 774
2350201	0.0	2							*LP2- 775
2350301	0.5588068	3							*LP2- 776
2350401	0.0	3							*LP2- 777
2350501	0.0	3							*LP2- 778
2350601	90.0	3							*LP2- 779
2350801	3.81-6	0.003	3						*LP2- 780
2350901	0.0	0.0	2						*LP2- 781
2351001	00	3							*LP2- 782
2351101	0000	2							*LP2- 783
2351201	0	1.53317+7	1226988.	2451888.	0.	0.	1		*LP2- 784
2351202	0	1.53263+7	1226996.	2452016.	0.	0.	2		*LP2- 785
2351203	0	1.53210+7	1227005.	2452146.	0.	0.	3		*LP2- 786
2351300	0								*LP2- 787
2351301	0.7067657	0.7067657	0.	1	*	(M = 11.235 kg/s)			LP2- 788
2351302	0.7067709	0.7067709	0.	2	*	(M = 11.235 kg/s)			LP2- 789
*-----1-----1-----1-----1-----1-----1-----1-----									LP2- 790
* upper end boxes and support structure									LP2- 791
*-----1-----1-----1-----1-----1-----1-----1-----									LP2- 792
2400000	"upr end"		branch						*LP2- 793
2400001	3	0							*LP2- 794
2400101	0.2423341	0.5867979	0.0	0.0	90.0	0.5867979			*LP2- 795
2400102	3.81-6	0.145	00						*LP2- 796
2400200	0	1.53134+7	1410433.	2452314.	0.0016037				*LP2- 797
2401101	230010000	240000000	0.0	1.5	1.5	00100			*LP2- 798
2402101	231010000	240000000	0.0	1.5	1.5	00100			*LP2- 799
2403101	235010000	240000000	0.0	2.	12.	00100			*LP2- 800
2401201	2.0379944	2.1104431	0.				*	(M = 197.33 kg/s)	LP2- 801
2402201	2.0633316	2.7305183	0.				*	(M = 38.994 kg/s)	LP2- 802
2403201	0.7067766	0.7620459	0.				*	(M = 11.235 kg/s)	LP2- 803
*-----1-----1-----1-----1-----1-----1-----1-----									LP2- 804
* upper core support structure - cross flow region									LP2- 805
*-----1-----1-----1-----1-----1-----1-----1-----									LP2- 806
2450000	"upr cr s"		branch						*LP2- 807
2450001	2	0							*LP2- 808
2450101	0.0	0.4933248	0.1280806	0.0	90.0	0.4933248			*LP2- 809
2450102	3.81-6	0.145	00						*LP2- 810
2450200	0	1.53098+7	1410683.	2452392.	0.				*LP2- 811

2451101	240010000	245000000	0.0	0.0	0.0	0000	*LP2- 812	
2452101	245010000	251000000	0.0	0.0	0.0	0000	*LP2- 813	
2451201	1.4857721	1.6411304	0.	* (M = 247.55 kg/s)			LP2- 814	
2452201	0.	0.0901192	0.	* (M = -3.466-4 kg/s)			LP2- 815	
*-----1-----1-----1-----1-----1-----1-----1-----1-----							LP2- 816	
* upper flow skirt region							LP2- 817	
*-----1-----1-----1-----1-----1-----1-----1-----1-----							LP2- 818	
2500000	"u flw sk"	branch					*LP2- 819	
2500001	1	0						*LP2- 820
2500101	0.1547532	0.7850547	0.0	0.0	90.	0.7850547	*LP2- 821	
2500102	3.81-6	0.131	00					*LP2- 822
2500200	0	1.53042+7	1410729.	2452526.	0.		*LP2- 823	
2501101	245010000	250000000	0.0	0.0	0.0	0000	*LP2- 824	
2501201	2.3244343	2.4370956	0.	* (M = 247.55 kg/s)			LP2- 825	
*-----1-----1-----1-----1-----1-----1-----1-----1-----							LP2- 826	
* dead end of fuel modules							LP2- 827	
*-----1-----1-----1-----1-----1-----1-----1-----1-----							LP2- 828	
2510000	"de fl m"	snglvol					*LP2- 829	
2510101	0.0	0.7844123	0.1154214	0.0	90.0	0.7844123	*LP2- 830	
2510102	3.81-6	0.214	00					*LP2- 831
2510200	0	1.53062+7	1391389.	2452502.	0.		*LP2- 832	
*-----1-----1-----1-----1-----1-----1-----1-----1-----							LP2- 833	
* upper head							LP2- 834	
*-----1-----1-----1-----1-----1-----1-----1-----1-----							LP2- 835	
2520000	"upr head"	branch					*LP2- 836	
2520001	1	0						*LP2- 837
2520101	0.2622585	0.2869580	0.0	0.0	90.0	0.2869580	*LP2- 838	
2520102	3.81-6	0.0	00					*LP2- 839
2520200	0	1.53017+7	1410736.	2452600.	0.		*LP2- 840	
2521101	250010000	252000000	0.0	0.006	0.006	0000	*LP2- 841	
2521201	2.3240528	2.3864136	0.	* (M = 247.55 kg/s)			LP2- 842	
*-----1-----1-----1-----1-----1-----1-----1-----1-----							LP2- 843	
* upper plenum bottom volume							LP2- 844	
*-----1-----1-----1-----1-----1-----1-----1-----1-----							LP2- 845	
2550000	"upr pl b"	branch					*LP2- 846	
2550001	2	0						*LP2- 847
2550101	0.2622585	0.6312304	0.0	0.0	90.0	0.6312304	*LP2- 848	
2550102	3.81-6	0.0	00					*LP2- 849
2550200	0	1.53013+7	1387737.	2452618.	0.		*LP2- 850	
2551101	250010000	255000000	0.0	0.006	0.006	0000	*LP2- 851	
2552101	255010000	260000000	0.0	0.03	0.03	0000	*LP2- 852	
2551201	0.	0.0596712	0.	* (M = -2.917-4 kg/s)			LP2- 853	
2552201	0.	0.0020278	0.	* (M = -1.428-4 kg/s)			LP2- 854	

2750101	272010000	280000000	0.0709408	0.0	0.0	0100	*LP2-	898
2750201	0	0.7271585	0.7271585	0.		* (M = 72.267 kg/s)	LP2-	899
*----	-----1-----	-----1-----	-----1-----	-----1-----	-----1-----	-----1-----	LP2-	900
* inlet annulus lower volume broken side							LP2-	901
*----	-----1-----	-----1-----	-----1-----	-----1-----	-----1-----	-----1-----	LP2-	902
2800000	"brok dow"	annulus					*LP2-	903
2800001	4						*LP2-	904
2800101	0.1464354	1					*LP2-	905
2800102	0.0						*LP2-	906
2800201	0.0709408	3					*LP2-	907
2800301	0.2525361	1					*LP2-	908
2800302	1.5200561	2					*LP2-	909
2800303	1.2616333	3					*LP2-	910
2800304	1.0792591	4					*LP2-	911
2800401	0.0	1					*LP2-	912
2800402	0.1581866	2					*LP2-	913
2800403	0.1217000	3					*LP2-	914
2800404	0.0986806	4					*LP2-	915
2800501	0.0	4					*LP2-	916
2800601	-90.	4					*LP2-	917
2800801	3.81-6	0.172	4				*LP2-	918
2800901	0.0	0.0	3				*LP2-	919
2801001	00	04					*LP2-	920
2801101	0000	03					*LP2-	921
2801201	0	1.53144+7	1226943.	2452304.	0.	0.	1	*LP2-
2801202	0	1.53208+7	1226966.	2452150.	0.	0.	2	*LP2-
2801203	0	1.53311+7	1226985.	2451904.	0.	0.	3	*LP2-
2801204	0	1.53397+7	1226999.	2451696.	0.	0.	4	*LP2-
2801300	0							*LP2-
2801301	1.3412704	1.3412704	0.	1	* (M = 72.267 kg/s)		LP2-	927
2801302	1.3412666	1.3412666	0.	2	* (M = 72.267 kg/s)		LP2-	928
2801303	1.3412552	1.3412552	0.	3	* (M = 72.267 kg/s)		LP2-	929
*----	-----1-----	-----1-----	-----1-----	-----1-----	-----1-----	-----1-----	LP2-	930
2850000	"lrdc2lpb"	sngljun					*LP2-	931
2850101	280010000	222000000	0.0709408	0.0000	0.0000	0100	*LP2-	932
2850201	0	1.0406351	1.040635	0.		* (M = 72.266 kg/s)	LP2-	933
*----	-----1-----	-----1-----	-----1-----	-----1-----	-----1-----	-----1-----	LP2-	934
2900000	"lwrinan"	sngljun					*LP2-	935
2900101	200000000	270000000	0.0296780	1.8341	1.8341	0003	*LP2-	936
2900201	0	3.2060738	3.2060738	0.		* (M = 72.268 kg/s)	LP2-	937
*----	-----1-----	-----1-----	-----1-----	-----1-----	-----1-----	-----1-----	LP2-	938
*							LP2-	939
*							LP2-	940

3150000	"sg+pmp s"		pipe	*LP2- 984
3150001	8			*LP2- 985
3150101	0.0	8		*LP2- 986
3150201	8.36	-3	1	*LP2- 987
3150202	1.12	-2	2	*LP2- 988
3150203	0.105626		3	*LP2- 989
3150204	1.12	-2	4	*LP2- 990
3150205	8.3647	-3	7	*LP2- 991
3150301	0.919969		1	*LP2- 992
3150302	1.987956		2	*LP2- 993
3150303	0.849744		4	*LP2- 994
3150304	1.987956		5	*LP2- 995
3150305	1.371350		6	*LP2- 996
3150306	1.365029		7	*LP2- 997
3150307	1.674812		8	*LP2- 998
3150401	7.75291	-3	1	*LP2- 999
3150402	0.1721108		2	*LP2-1000
3150403	8.97552	-2	4	*LP2-1001
3150404	0.1721108		5	*LP2-1002
3150405	1.82303	-2	6	*LP2-1003
3150406	5.46687	-2	7	*LP2-1004
3150407	1.82489	-2	8	*LP2-1005
3150601	90.0		3	*LP2-1006
3150602	-90.0		7	*LP2-1007
3150603	90.0		8	*LP2-1008
3150701	0.679201		1	*LP2-1009
3150702	1.987956		2	*LP2-1010
3150703	0.457202		3	*LP2-1011
3150704	-0.457202		4	*LP2-1012
3150705	-1.987956		5	*LP2-1013
3150707	-1.371350		6	*LP2-1014
3150708	-0.520701		7	*LP2-1015
3150709	1.212851		8	*LP2-1016
3150801	4.0e-5	0.0	8	*LP2- 017
3150901	0.93596	0.93596	1	*LP2-1018
3150902	2.0	2.0	2	*LP2-1019
3150903	0.5	0.5	3	*LP2-1020
3150904	2.0	2.0	4	*LP2-1021
3150905	0.23025	0.23025	5	*LP2-1022
3150906	2.534	2.534	6	*LP2-1023
3150907	5.069	5.069	7	*LP2-1024
3151001	00		8	*LP2-1025
3151101	0000		7	*LP2-1026

3151201	0	1.52904+7	1365077.	2452664.	0.	0.	1	*LP2-1027
3151202	0	1.52900+7	1333628.	2452890.	0.	0.	2	*LP2-1028
3151203	0	1.52814+7	1306323.	2453098.	0.	0.	3	*L'
3151204	0	1.52814+7	1288477.	2453098.	0.	0.	4	*Lr
3151205	0	1.52903+7	1272854.	2452884.	0.	0.	5	*LP2 31
3151206	0	1.53026+7	1255389.	2452588.	0.	0.	6	*LP2-1032
3151207	0	1.53095+7	1240304.	2452420.	0.	0.	7	*LP2-1033
3151208	0	1.53069+7	1227222.	2452482.	0.	0.	8	*LP2-1034
3151300	0							*LP2-1035
3151301	0.	0.	0.	7	*	(M = -3.560-4 kg/s)		LP2-1036
*-----1-----1-----1-----1-----1-----1-----1-----1-----1-----								LP2-1037
* hot leg break valve								LP2-1038
*-----1-----1-----1-----1-----1-----1-----1-----1-----1-----								LP2-1039
3170000	"hl break"		valve					*LP2-1040
3170101	315010000	700000000	8.3647-3	1.'0813	1.06560	0100		*LP2-1041
3170102	0.93	0.84						*LP2-1042
3170201	0	0.	0.	0.	*	(M = 0.0000 kg/s)		LP2-1043
3170300	trpvlv							*LP2-1044
3170301	310							*LP2-1045
*-----1-----1-----1-----1-----1-----1-----1-----1-----1-----								LP2-1046
* reactor vessel nozzle - broken loop cold leg								LP2-1047
*-----1-----1-----1-----1-----1-----1-----1-----1-----1-----								LP2-1048
3350000	"rvn blcl"		branch					*LP2-1049
3350001	2	0						*LP2-1050
3350101	0.0	0.749305	0.047979	0.0	0.0	0.0		*LP2-1051
3350102	4.0e-5	0.0	00					*LP2-1052
3350200	0	1.53130+7	1227348.	2452330.	0.			*LP2-1053
3351101	272000000	335000000	0.064130	1.455594	0.812933	0002		*LP2-1054
3352101	335010000	340000000	0.063426	0.1005	0.1005	0000		*LP2-1055
3351201	0.	0.	0.	*	(M = -1.935-4 kg/s)			LP2-1056
3352201	0.	0.	0.	*	(M = -1.687-4 kg/s)			LP2-1057
*-----1-----1-----1-----1-----1-----1-----1-----1-----1-----								LP2-1058
* cold leg pipe to reflood assist bypass tee								LP2-1059
*-----1-----1-----1-----1-----1-----1-----1-----1-----1-----								LP2-1060
3400000	"clp-rabs"		branch					*LP2-1061
3400001	1	0						*LP2-1062
3400101	0.0	0.698336	0.0443927	0.0	0.0	0.0		*LP2-1063
3400102	4.0e-5	0.0	00					*LP2-1064
3400200	0	1.53130+7	1227348.	2452336.	0.			*LP2-1065
3401101	340010000	342000000	0.063426	0.1005	0.1005	0000		*LP2-1066
3401201	0.	0.	0.	*	(M = -1.457-4 kg/s)			LP2-1067
*-----1-----1-----1-----1-----1-----1-----1-----1-----1-----								LP2-1068
* broken loop cold leg rab. to dtt								LP2-1069

3700801	4.0-5	0.0	3							*LP2-1113
3700901	0.28	0.28	1							*LP2-1114
3700902	0.84	0.84	2							*LP2-1115
3701001	00	3								*LP2-1116
3701101	0000	2								*LP2-1117
3701201	0	1.53106+7	1227348.	2452394.	0.	0.	1			*LP2-1118
3701202	0	1.53082+7	1227348.	2452452.	0.	0.	2			*LP2-1119
3701203	0	1.53082+7	1227348.	2452452.	0.	0.	3			*LP2-1120
3701300	0									*LP2-1121
3701301	0.	0.	0.	2						* (M = -9.649-5 kg/s) LP2-1122
*-----1-----1-----1-----1-----1-----1-----1-----										
* reflood assist bypass valves LP2-1123										
*-----1-----1-----1-----1-----1-----1-----1-----										
* LP2-1125										
3750000	"rabs val"		valve							*LP2-1126
3750101	370010000	380000000	0.0	0.90+4	0.90+4	0000				*LP2-1127
3750201	0	0.	0.	0.						* (M = 0.0000 kg/s) LP2-1128
3750300	trpvlv									*LP2-1129
3750301	516									*LP2-1130
*-----1-----1-----1-----1-----1-----1-----1-----										
* reflood assist bypass piping - hot leg side LP2-1132										
*-----1-----1-----1-----1-----1-----1-----1-----										
* LP2-1133										
3800000	"rabs h 1"		pipe							*LP2-1134
3800001	3									*LP2-1135
3800101	0.0776	1								*LP2-1136
3800102	0.0388	3								*LP2-1137
3800201	0.0388	2								*LP2-1138
3800301	0.0	3								*LP2-1139
3800401	0.0915	1								*LP2-1140
3800402	0.048	2								*LP2-1141
3800403	0.0489	3								*LP2-1142
3800601	0.0	1								*LP2-1143
3800602	-90.0	2								*LP2-1144
3800603	0.0	3								*LP2-1145
3800701	0.0	1								*LP2-1146
3800702	-0.64	2								*LP2-1147
3800703	0.0	3								*LP2-1148
3800801	4.0-5	0.0	3							*LP2-1149
3800901	0.84	0.84	1							*LP2-1150
3800902	0.28	0.28	2							*LP2-1151
3801001	00	3								*LP2-1152
3801101	0000	2								*LP2-1153
3801201	0	1.52974+7	1410329.	2452712.	0.	0.	1			*LP2-1154
3801202	0	1.52996+7	1410329.	2452660.	0.	0.	2			*LP2-1155


```

3801203  0          1.53017+7 1410329. 2452608.  0.      0.      3 *LP2-1156
3801300  0                                     *LP2-1157
3801301  0.          0.          0.          2 * (M = 7.006-5 kg/s) LP2-1158
*-----1-----1-----1-----1-----1-----1-----1----- LP2-1159
*                                                                 LP2-1160
*                                                                 LP2-1161
*$$$$$$$$$$$$$$$$$$$$$$$$$$$$$$$$$$$$$$$$$$$$$$$$$$$$$$$$$$$$$$$$ LP2-1162
*                                                                 LP2-1163
*   pressurizer [ 400 ] LP2-1164
*                                                                 LP2-1165
*$$$$$$$$$$$$$$$$$$$$$$$$$$$$$$$$$$$$$$$$$$$$$$$$$$$$$$$$$$$$$$$$ LP2-1166
*                                                                 LP2-1167
*-----1-----1-----1-----1-----1-----1-----1----- LP2-1168
* surge line pcs side LP2-1169
*-----1-----1-----1-----1-----1-----1-----1----- LP2-1170
4000000  "srg ln p"          branch *LP2-1171
4000001  2          0                                     *LP2-1172
4000101  1.44561-3 2.30          0.0          0.0          90.0          0.54 *LP2-1173
4000102  2.3622-5  0.0          00                                     *LP2-1174
4000200  0          1.52834+7 1454066. 2453048.  0.      *LP2-1175
4001101  107000000 400000000 1.44561-3 3.9          3.9          0002 *LP2-1176
4002101  400010000 405000000 1.44561-3 2.85          2.85          1000 *LP2-1177
4001201  -0.012242 -0.012187 0.          * (M =-0.0118 kg/s) LP2-1178
4002201  -0.012243 -0.012243 0.          * (M =-0.0117 kg/s) LP2-1179
*-----1-----1-----1-----1-----1-----1-----1----- LP2-1180
* pressurizer surge line LP2-1181
*-----1-----1-----1-----1-----1-----1-----1----- LP2-1182
4050000  "srg ln p"          pipe *LP2-1183
4050001  2                                     *LP2-1184
4050101  1.44561-3 2 *LP2-1185
4050201  1.44561-3 1 *LP2-1186
4050301  2.30          2 *LP2-1187
4050401  0.0          2 *LP2-1188
4050601  90.0          2 *LP2-1189
4050701  0.30          2 *LP2-1190
4050801  2.3622-5  0.0          2 *LP2-1191
4050901  2.85          2.85          1 *LP2-1192
4051001  00          2 *LP2-1193
4051101  1000          1 *LP2-1194
4051201  0          1.52807+7 1470594. 2453114.  0.      0.      1 *LP2-1195
4051202  0          1.52787+7 1476693. 2453100.  0.      0.      2 *LP2-1196
4051300  0                                     *LP2-1197
4051301  -0.01224  -0.01224  0.          1 * (M =-0.0117 kg/s) LP2-1198

```


5003201	2.6684513	3.3779411	0.						* (M = 119.69 kg/s)	LP2-1285
*-----1-----1-----1-----1-----1-----1-----1-----1-----1-----										LP2-1286
* separator bypass										LP2-1287
*-----1-----1-----1-----1-----1-----1-----1-----1-----1-----										LP2-1288
5030000	"sepbypas"			branch						*LP2-1289
5030001	2	0								*LP2-1290
5030101	0.0	0.4445	0.4384	0.0	90.0	0.4445				*LP2-1291
5030102	4.e-5	0.3678	00							*LP2-1292
5030200	0	5401448.	1170419.	2594416.	0.7823005					*LP2-1293
5031101	505000000	503000000	0.98627	C.0	0.0	0100				*LP2-1294
5032101	503010000	520000000	0.98627	0.8	0.0	0100				*LP2-1295
5031201	0.	0.362268	0.						* (M = 1.3335 kg/s)	LP2-1296
5032201	-3.233191	0.0685197	0.						* (M = 1.4555 kg/s)	LP2-1297
*-----1-----1-----1-----1-----1-----1-----1-----1-----1-----										LP2-1298
* separator outlet region										LP2-1299
*-----1-----1-----1-----1-----1-----1-----1-----1-----1-----										LP2-1300
5050000	"lwr sepr"			branch						*LP2-1301
5050001	1	0								*LP2-1302
5050101	0.0	1.2131	1.4850	0.0	-90.0	-1.2131				*LP2-1303
5050102	4.e-5	1.9048	00							*LP2-1304
5050200	0	5405752.	1172323.	2594434.	0.1483094					*LP2-1305
5051101	505010000	508000000	0.0	0.0	0.0	0100				*LP2-1306
5051201	0.4016728	0.0678293	0.						* (M = 95.591 kg/s)	LP2-1307
*-----1-----1-----1-----1-----1-----1-----1-----1-----1-----										LP2-1308
* feed inlet volume										LP2-1309
*-----1-----1-----1-----1-----1-----1-----1-----1-----1-----										LP2-1310
5080000	"upr dwnc"			branch						*LP2-1311
5080001	1	0								*LP2-1312
5080101	0.0	0.6096	0.22107	0.0	-90.0	-0.6096				*LP2-1313
5080102	4.e-5	0.163697	00							*LP2-1314
5080200	0	5411968.	1113044.	2594394.	0.001081					*LP2-1315
5081101	508010000	510000000	0.0	0.0	0.0	0100				*LP2-1316
5081201	0.6533933	0.4960883	0.						* (M = 119.60 kg/s)	LP2-1317
*-----1-----1-----1-----1-----1-----1-----1-----1-----1-----										LP2-1318
* steam generator downcomer										LP2-1319
*-----1-----1-----1-----1-----1-----1-----1-----1-----1-----										LP2-1320
5100000	"dwncmr "			annulus						*LP2-1321
5100001	3									*LP2-1322
5100101	0.232	3								*LP2-1323
5100201	0.0	2								*LP2-1324
5100301	0.6096	3								*LP2-1325
5100401	0.0	3								*LP2-1326
5100601	-90.0	3								*LP2-1327

5151301	0.9967246	1.3567104	0.	1	*	(M = 119.61 kg/s)	LP2-1371
5151302	1.5849476	2.2897224	0.	2	*	(M = 119.64 kg/s)	LP2-1372
5151303	2.1229439	3.1752205	0.	3	*	(M = 119.66 kg/s)	LP2-1373
5151304	2.5998421	3.8117561	0.	4	*	(M = 119.68 kg/s)	LP2-1374
*----	----	----	----	----	----	----	LP2-1375
* lower portion of steam dome							LP2-1376
*----	----	----	----	----	----	----	LP2-1377
5200000	"lwr stm "		branch				*LP2-1378
5200001	1	0					*LP2-1379
5200101	0.0	0.46956	0.705312	0.0	90.0	0.46956	*LP2-1380
5200102	4.e-5	1.383	00				*LP2-1381
5200200	0	5401000.	1172058.	2594344.	0.9999995		*LP2-1382
5201101	520010000	525000000	0.0	0.0	0.0	0000	*LP2-1383
5201201	0.4609571	0.5822439	0.			* (M = 24.079 kg/s)	LP2-1384
*----	----	----	----	----	----	----	LP2-1385
* upper portion of steam dome							LP2-1386
*----	----	----	----	----	----	----	LP2-1387
5250000	"upr stm "		branch				*LP2-1388
5250001	1	0					*LP2-1389
5250101	0.0	0.46956	0.705312	0.0	90.0	0.46956	*LP2-1390
5250102	4.e-5	1.383	00				*LP2-1391
5250200	0	5400872.	1172051.	2594390.	0.9999971		*LP2-1392
5251101	525010000	530000000	0.0	0.8	0.8	0100	*LP2-1393
5251201	11.321671	18.869934	0.			* (M = 24.080 kg/s)	LP2-1394
*----	----	----	----	----	----	----	LP2-1395
* steam pipe from generator to control valve							LP2-1396
*----	----	----	----	----	----	----	LP2-1397
5300000	"steam pi"		snglvol				*LP2-1398
5300101	0.04635	25.074	0.0	0.0	0.0	0.0	*LP2-1399
5300102	4.e-5	0.0	00				*LP2-1400
5300200	0	5386864.	1171229.	2594480.	0.9999856		*LP2-1401
*----	----	----	----	----	----	----	LP2-1402
* steam flow control valve							LP2-1403
*----	----	----	----	----	----	----	LP2-1404
5400000	"cv-p4-10"		valve				*LP2-1405
5400101	530010000	541000000	0.0047772	0.0	0.0	1100	*LP2-1406
5400201	0	15.548279	18.917633	0.		* (M = 24.080 kg/s)	LP2-1407
5400300	mtrvly						*LP2-1408
5400301	687	688	0.20	0.58774	540		*LP2-1409
20254000	normarea						*LP2-1410
20254001	0.0	0.0					*LP2-1411
20254002	9.25-4	9.25-4					*LP2-1412
20254003	1.0	1.0					*LP2-1413

6200102	4.0-5	0.0	00					*LP2-1500
6200200	4.11+6	302.00	0.0					*LP2-1501
6201101	615000000	8.2132-3	125.	125.	00000			*LP2-1502
6202200	0.0	1.03795	3.3266	0.8	0.04445	1		*LP2-1503
+	0.0	0.0						*LP2-1504
*----	1----	1----	1----	1----	1----	1----	1----	LP2-1505
* bwst lpis								LP2-1506
*----	1----	1----	1----	1----	1----	1----	1----	LP2-1507
6250000	"bwst lps"		tmdpvol					*LP2-1508
6250101	20.44	5.0	0.0	0.0	90.0	5.0		*LP2-1509
6250102	4.0e-5	0.0	00					*LP2-1510
6250200	3							*LP2-1511
6250201	0.0	1.0+5	300.0					*LP2-1512
*----	1----	1----	1----	1----	1----	1----	1----	LP2-1513
* low pressure injection system								LP2-1514
*----	1----	1----	1----	1----	1----	1----	1----	LP2-1515
6300000	"lpis"		tmdpjun					*LP2-1516
6300101	625000000	605000000	5.9896-3					*LP2-1517
6300200	1	513	p	605010000				*LP2-1518
6300201	-1.0	0.0	0.0	0.0				*LP2-1519
6300202	0.0	0.0	0.0	0.0				*LP2-1520
6300203	8.483+4	7.045	0.0	0.0				*LP2-1521
6300204	4.297+5	6.091	0.0	0.0				*LP2-1522
6300205	7.745+5	5.045	0.0	0.0				*LP2-1523
6300206	9.448+5	4.313	0.0	0.0				*LP2-1524
6300207	1.119+6	3.454	0.0	0.0				*LP2-1525
6300208	1.186+6	3.173	0.0	0.0				*LP2-1526
6300209	1.257+6	2.673	0.0	0.0				*LP2-1527
6300210	1.326+6	2.159	0.0	0.0				*LP2-1528
6300211	1.395+6	1.536	0.0	0.0				*LP2-1529
6300212	1.464+6	0.7182	0.0	0.0				*LP2-1530
6300213	1.517+6	0.0	0.0	0.0				*LP2-1531
*----	1----	1----	1----	1----	1----	1----	1----	LP2-1532
* bwst hpis								LP2-1533
*----	1----	1----	1----	1----	1----	1----	1----	LP2-1534
6350000	"bwst hps"		tmdpvol					*LP2-1535
6350101	20.44	5.0	0.0	0.0	90.0	5.0		*LP2-1536
6350102	4.0-5	0.0	00					*LP2-1537
6350200	3							*LP2-1538
6350201	0.0	1.0+5	305.0					*LP2-1539
*----	1----	1----	1----	1----	1----	1----	1----	LP2-1540
* high pressure injection system								LP2-1541
*----	1----	1----	1----	1----	1----	1----	1----	LP2-1542

7050202	0.0	106681.	1.0							*LP2-1586
7050203	0.25	118070.	1.0							*LP2-1587
7050204	0.75	197780.	1.0							*LP2-1588
7050205	2.25	188490.	1.0							*LP2-1589
7050206	5.25	205010.	1.0							*LP2-1590
7050207	20.	309910.	1.0							*LP2-1591
7050208	45.	259190.	1.0							*LP2-1592
7050209	70.	307540.	1.0							*LP2-1593
7050210	120.	314600.	1.0							*LP2-1594
7050211	1.+5	100000.	1.0							*LP2-1595
*-----1-----1-----1-----1-----1-----1-----1-----										LP2-1596
*										LP2-1597
*										LP2-1598
.....										LP2-1599
.....										LP2-1600
*										LP2-1601
* ---- heat structures -----										LP2-1602
*										LP2-1603
.....										LP2-1604
.....										LP2-1605
*										LP2-1606
*-----1-----1-----1-----1-----1-----1-----1-----										LP2-1607
* steam generator heat structures										LP2-1608
*-----1-----1-----1-----1-----1-----1-----1-----										LP2-1609
11150000	8	8	2	0	0.0051054					*LP2-1610
11150100	0	1								*LP2-1611
11150101	7	0.006348984								*LP2-1612
11150201	6	7								*LP2-1613
11150301	0.0	7								*LP2-1614
11150400	-1									*LP2-1615
11150401	567.10	564.39	561.68	558.98	556.27	553.56	550.85	548.15		*LP2-1616
11150402	563.90	561.75	559.60	557.44	555.29	553.14	550.98	548.83		*LP2-1617
11150403	561.20	559.47	557.74	556.01	554.28	552.55	550.83	549.10		*LP2-1618
11150404	559.10	557.60	556.10	554.60	553.10	551.61	550.11	548.61		*LP2-1619
11150405	557.16	555.85	554.54	553.22	551.91	550.60	549.28	547.97		*LP2-1620
11150406	554.98	553.87	552.77	551.66	550.55	549.44	548.33	547.22		*LP2-1621
11150407	552.91	551.95	550.99	550.03	549.07	548.11	547.15	546.20		*LP2-1622
11150408	551.00	550.16	549.33	548.49	547.65	546.82	545.98	545.14		*LP2-1623
11150501	115010000	10000	1	1	1124.71	3				*LP2-1624
11150502	115040000	10000	1	1	849.063	5				*LP2-1625
11150503	115060000	10000	1	1	1124.71	8				*LP2-1626
11150601	515010000	10000	1	1	1124.71	3				*LP2-1627
11150602	515040000	0	1	1	849.063	4				*LP2-1628

11150603	515040000	0	1	1	849.063	5					*LP2-1629
11150604	515030000	-10000	1	1	1124.71	8					*LP2-1630
11150701	0	0	0	0	8						*LP2-1631
11150801	0	0	0	0	8						*LP2-1632
11150901	0	0	0	0	8						*LP2-1633
*											LP2-1634
*----	----	----	----	----	----	----	----	----	----	----	LP2-1635
* active core											LP2-1636
*											LP2-1637
* peripheral fuel modules											LP2-1638
*----	----	----	----	----							LP2-1639
12300000	5	10	2	0	0.0	2	1	32			*LP2-1640
12300001	7.869e+6	230050000									*LP2-1641
12300011	1.0e-6	2.0e-6	0.0	0.0	5						*LP2-1642
12300100	0	1									*LP2-1643
12300101	5	4.647-3									*LP2-1644
12300102	1	4.742-3									*LP2-1645
12300103	3	5.359-3									*LP2-1646
12300201	1	5									*LP2-1647
12300202	-2	6									*LP2-1648
12300203	-3	9									*LP2-1649
12300301	1.00	5									*LP2-1650
12300302	0.0	9									*LP2-1651
12300400	-1										*LP2-1652
12300401	1147.01	1124.64	1059.17	957.45	830.77	693.34	626.88	619.18			*LP2-1653
+	611.69	604.48									*LP2-1654
12300402	1310.59	1281.81	1198.11	1067.83	905.60	729.61	644.50	634.63			*LP2-1655
+	625.05	615.81									*LP2-1656
12300403	1394.25	1362.15	1268.77	1123.46	942.49	746.17	651.23	640.23			*LP2-1657
+	629.53	619.22									*LP2-1658
12300404	1185.14	1161.65	1093.33	987.00	854.59	710.94	641.47	633.42			*LP2-1659
+	625.60	618.05									*LP2-1660
12300405	781.08	773.68	752.13	718.60	676.84	631.55	609.64	607.10			*LP2-1661
+	604.63	602.25									*LP2-1662
12300501	0	0	0	1	466.992	1					*LP2-1663
12300502	0	0	0	1	210.795	3					*LP2-1664
12300503	0	0	0	1	356.730	4					*LP2-1665
12300504	0	0	0	1	1064.091	5					*LP2-1666
12300601	230010000	0	1	1	466.991	1					*LP2-1667
12300602	230020000	10000	1	1	210.795	3					*LP2-1668
12300603	230040000	0	1	1	356.730	4					*LP2-1669
12300604	230050000	0	1	1	1064.091	5					*LP2-1670
12300701	900	.20308197	0.0	0.0	1						*LP2-1671

12310412	1096.11	1075.41	1014.25	918.68	801.88	682.31	637.74	631.64	*LP2-1715
+	625.64	619.93							*LP2-1716
12310413	911.85	899.10	861.45	802.61	730.69	657.07	629.63	625.88	*LP2-1717
+	622.19	618.67							*LP2-1718
12310501	0	0	0	1	30.5947	1			*LP2-1719
12310502	0	0	0	1	58.035052	2			*LP2-1720
12310503	0	0	0	1	19.344287	8			*LP2-1721
12310504	0	0	0	1	29.017526	12			*LP2-1722
12310505	0	0	0	1	46.370817	13			*LP2-1723
12310601	231010000	0	1	1	30.5947	1			*LP2-1724
12310602	231020000	0	1	1	58.035052	2			*LP2-1725
12310603	231030000	10000	1	1	19.344287	8			*LP2-1726
12310604	231090000	10000	1	1	29.017526	12			*LP2-1727
12310605	231130000	0	1	1	46.370817	13			*LP2-1728
12310701	900	1.74501-2	0.0	0.0	1				*LP2-1729
12310702	900	3.7340-2	0.0	0.0	2				*LP2-1730
12310703	900	1.4071-2	0.0	0.0	3				*LP2-1731
12310704	900	1.4937-2	0.0	0.0	4				*LP2-1732
12310705	900	1.5587-2	0.0	0.0	5				*LP2-1733
12310706	900	1.6235-2	0.0	0.0	6				*LP2-1734
12310707	900	1.6452-2	0.0	0.0	7				*LP2-1735
12310708	900	1.6127-2	0.0	0.0	8				*LP2-1736
12310709	900	2.2017-2	0.0	0.0	9				*LP2-1737
12310710	900	1.8672-2	0.0	0.0	10				*LP2-1738
12310711	900	1.4612-2	0.0	0.0	11				*LP2-1739
12310712	900	1.1203-2	0.0	0.0	12				*LP2-1740
12310713	900	1.1675-2	0.0	0.0	13				*LP2-1741
12310901	0	0.013633	0.0	0.0	13				*LP2-1742
*----	1	1	1	1	1	1	1		LP2-1743
*									LP2-1744
* wall heat structures (core)									LP2-1745
*									LP2-1746
* volume 200									LP2-1747
*----	1	1	1	1	1	1	1		LP2-1748
12000000	1	5	2	0	0.508				*LP2-1749
12000100	0	1							*LP2-1750
12000101	4	0.7264							*LP2-1751
12000201	4	4							*LP2-1752
12000301	0.0	4							*LP2-1753
12000400	-1								*LP2-1754
12000401	555.98	555.99	556.01	556.03	556.05				*LP2-1755
12000501	200010000	0	1	1	.093810	1			*LP2-1756
12000601	0	0	0	1	.09381	1			*LP2-1757

12000701	0	0.0	0.0	0.0	1			*LP2-1758
12000801	0	0.1524	0.0	0.0	1			*LP2-1759
*-----	1	-----	1	-----	1	-----	1	LP2-1760
* volume 202								LP2-1761
*-----	1	-----	1	-----	1	-----	1	LP2-1762
12020000	1	5	2	0	0.508			*LP2-1763
12020100	0	1						*LP2-1764
12020101	4	0.7264						*LP2-1765
12020201	4	4						*LP2-1766
12020301	0.0	4						*LP2-1767
12020400	-1							*LP2-1768
12020401	556.02	556.02	556.03	556.04	556.05			*LP2-1769
12020501	202010000	0	1	1	.1426	1		*LP2-1770
12020601	0	0	0	1	.1426	1		*LP2-1771
12020701	0	0.0	0.0	0.0	1			*LP2-1772
12020801	0	0.1524	0.0	0.0	1			*LP2-1773
*-----	1	-----	1	-----	1	-----	1	LP2-1774
* volume 210								LP2-1775
*-----	1	-----	1	-----	1	-----	1	LP2-1776
12100000	4	5	2	0	0.47			*LP2-1777
12100100	0	1						*LP2-1778
12100101	4	0.7264						*LP2-1779
12100201	1	4						*LP2-1780
12100301	0.0	4						*LP2-1781
12100400	-1							*LP2-1782
12100401	555.94	555.97	555.99	556.02	556.05			*LP2-1783
12100402	555.94	555.97	555.99	556.02	556.05			*LP2-1784
12100403	555.94	555.97	556.00	556.02	556.05			*LP2-1785
12100404	555.95	555.97	556.00	556.03	556.05			*LP2-1786
12100501	210010000	0	1	1	0.1267	1		*LP2-1787
12100502	210020000	0	1	1	0.7603	2		*LP2-1788
12100503	210030000	0	1	1	0.6308	3		*LP2-1789
12100504	210040000	0	1	1	0.5396	4		*LP2-1790
12100601	0	0	0	1	0.1267	1		*LP2-1791
12100602	0	0	0	1	0.7603	2		*LP2-1792
12100603	0	0	0	1	0.6308	3		*LP2-1793
12100604	0	0	0	1	0.5396	4		*LP2-1794
12100701	0	0.0	0.0	0.0	4			*LP2-1795
12100801	0	0.1016	0.0	0.0	4			*LP2-1796
*-----	1	-----	1	-----	1	-----	1	LP2-1797
* volume 220								LP2-1798
*-----	1	-----	1	-----	1	-----	1	LP2-1799
12200000	1	5	2	0	0.47			*LP2-1800

12700101	4	0.7264						*LP2-1844
12700201	4	4						*LP2-1845
12700301	0.0	4						*LP2-1846
12700400	-1							*LP2-1847
12700401	555.97	555.99	556.01	556.03	556.04			*LP2-1848
12700501	270010000	0	1	1	0.09381	1		*LP2-1849
12700601	0	0	0	1	0.09381	1		*LP2-1850
12700701	0	0.0	0.0	0.0	1			*LP2-1851
12700801	0	0.1524	0.0	0.0	1			*LP2-1852
*-----1-----1-----1-----1-----1-----1-----1-----								LP2-1853
* volume 272								LP2-1854
*-----1-----1-----1-----1-----1-----1-----1-----								LP2-1855
12720000	1	5	2	0	0.508			*LP2-1856
12720100	0	1						*LP2-1857
12720101	4	0.7264						*LP2-1858
12720201	4	4						*LP2-1859
12720301	0.0	4						*LP2-1860
12720400	-1							*LP2-1861
12720401	555.97	555.99	556.01	556.03	556.04			*LP2-1862
12720501	272010000	0	1	1	0.1426	1		*LP2-1863
12720601	0	0	0	1	0.1426	1		*LP2-1864
12720701	0	0.0	0.0	0.0	1			*LP2-1865
12720801	0	0.1524	0.0	0.0	1			*LP2-1866
*-----1-----1-----1-----1-----1-----1-----1-----								LP2-1867
* volume 280								LP2-1868
*-----1-----1-----1-----1-----1-----1-----1-----								LP2-1869
12800000	4	5	2	0	0.47			*LP2-1870
12800100	0	1						*LP2-1871
12800101	4	0.7264						*LP2-1872
12800201	1	4						*LP2-1873
12800301	0.0	4						*LP2-1874
12800400	-1							*LP2-1875
12800401	555.97	555.99	556.00	556.02	556.04			*LP2-1876
12800402	555.96	555.98	556.00	556.02	556.04			*LP2-1877
12800403	555.97	555.99	556.01	556.03	556.05			*LP2-1878
12800404	555.97	555.99	556.01	556.03	556.05			*LP2-1879
12800501	280010000	0	1	1	0.1267	1		*LP2-1880
12800502	280020000	0	1	1	0.7603	2		*LP2-1881
12800503	280030000	0	1	1	0.6308	3		*LP2-1882
12800504	280040000	0	1	1	0.5396	4		*LP2-1883
12800601	0	0	0	1	0.1267	1		*LP2-1884
12800602	0	0	0	1	0.7603	2		*LP2-1885
12800603	0	0	0	1	0.6308	3		*LP2-1886

20100200	tbl/fctn	3	1	* gap	LP2-1930				
20100300	tbl/fctn	1	1	* zr	LP2-1931				
20100400	tbl/fctn	1	1	* s-steel	LP2-1932				
20100500	c-steel				*LP2-1933				
20100600	tbl/fctn	1	1	* inconel 600	LP2-1934				
*----	----	1----	----	1----	----	1----	----	1----	LP2-1935
* uo2 - thermal conductivity					LP2-1936				
*----	----	1----	----	1----	----	1----	----	1----	LP2-1937
20100101	2.7315e2	8.44			*LP2-1938				
20100102	4.1667e2	6.46			*LP2-1939				
20100103	5.3315e2	5.782385			*LP2-1940				
20100104	6.99817e2	4.633177			*LP2-1941				
20100105	8.66483e2	3.880307			*LP2-1942				
20100106	1.03315e3	3.357625			*LP2-1943				
20100107	1.08871e3	3.155129			*LP2-1944				
20100108	1.19982e3	2.983787			*LP2-1945				
20100109	1.28315e3	2.836674			*LP2-1946				
20100110	1.36648e3	2.713792			*LP2-1947				
20100111	1.53315e3	2.521680			*LP2-1948				
20100112	1.61648e3	2.448990			*LP2-1949				
20100113	1.69982e3	2.391875			*LP2-1950				
20100114	1.97759e3	2.289762			*LP2-1951				
20100115	2.25537e3	2.307069			*LP2-1952				
20100116	2.53315e3	2.433413			*LP2-1953				
20100117	2.81093e3	2.661870			*LP2-1954				
20100118	3.08871e3	2.994171			*LP2-1955				
*----	----	1----	----	1----	----	1----	----	1----	LP2-1956
* uo2 - volumetric heat capacity					LP2-1957				
*----	----	1----	----	1----	----	1----	----	1----	LP2-1958
20100151	2.73150e2	2.310427e6			*LP2-1959				
20100152	3.23150e2	2.571985e6			*LP2-1960				
20100153	3.73150e2	2.746357e6			*LP2-1961				
20100154	6.7315e2	3.138694e6			*LP2-1962				
20100155	1.37315e3	3.443844e6			*LP2-1963				
20100156	1.77315e3	3.531030e6			*LP2-1964				
20100157	1.97315e3	3.792588e6			*LP2-1965				
20100158	2.17315e3	4.228518e6			*LP2-1966				
20100159	2.37315e3	4.882412e6			*LP2-1967				
20100160	2.67315e3	6.015829e6			*LP2-1968				
20100161	2.77315e3	6.320980e6			*LP2-1969				
20100162	2.87315e3	6.582538e6			*LP2-1970				
20100163	2.97315e3	6.713317e6			*LP2-1971				
20100164	3.11315e3	6.800503e6			*LP2-1972				

20100165	4.69982e3	6.800503e6		*LP2-1973
*----	----	----	----	LP2-1974
* helium(gap) - thermal conductivity				LP2-1975
*----	----	----	----	LP2-1976
20100201	helium	1.00		*LP2-1977
*----	----	----	----	LP2-1978
* helium(gap) - volumetric heat capacity				LP2-1979
*----	----	----	----	LP2-1980
20100251	273.15	5.4		*LP2-1981
20100252	5000.0	5.4		*LP2-1982
*----	----	----	----	LP2-1983
* zircaloy-4 - thermal conductivity			from matpro	LP2-1984
*----	----	----	----	LP2-1985
20100301	380.4	13.6		*LP2-1986
20100302	469.3	14.6		*LP2-1987
20100303	577.6	15.8		*LP2-1988
20100304	685.9	17.3		*LP2-1989
20100305	774.8	18.4		*LP2-1990
20100306	872.0	19.8		*LP2-1991
20100307	973.2	21.8		*LP2-1992
20100308	1073.2	23.2		*LP2-1993
20100309	1123.2	25.4		*LP2-1994
20100310	1152.3	24.2		*LP2-1995
20100311	1232.2	25.5		*LP2-1996
20100312	1331.2	26.6		*LP2-1997
20100313	1404.2	28.2		*LP2-1998
20100314	1576.2	33.0		*LP2-1999
20100315	1625.2	36.7		*LP2-2000
20100316	1755.2	41.2		*LP2-2001
20100317	2273.2	55.0		*LP2-2002
*----	----	----	----	LP2-2003
* zircaloy-4 - volumetric heat capacity			from matpro	LP2-2004
*----	----	----	----	LP2-2005
20100351	300.0	1.841e6		*LP2-2006
20100352	400.0	1.978e6		*LP2-2007
20100353	640.0	2.168e6		*LP2-2008
20100354	1090.0	2.456e6		*LP2-2009
20100355	1093.0	3.288e6		*LP2-2010
20100356	1113.0	3.865e6		*LP2-2011
20100357	1133.0	4.028e6		*LP2-2012
20100358	1153.0	4.709e6		*LP2-2013
20100359	1173.0	5.345e6		*LP2-2014
20100360	1193.0	5.044e6		*LP2-2015

20100361	1213.0	4.054e6	*LP2-2016
20100362	1233.0	3.072e6	*LP2-2017
20100363	1243.0	2.332e6	*LP2-2018
20100364	1477.0	2.332e6	*LP2-2019
*-----1-----1-----1-----1-----1-----1-----1-----			LP2-2020
* s-steel - thermal conductivity			LP2-2021
*-----1-----1-----1-----1-----1-----1-----1-----			LP2-2022
20100401	273.15	12.98	*LP2-2023
20100402	1199.82	25.1	*LP2-2024
*-----1-----1-----1-----1-----1-----1-----1-----			LP2-2025
* s-steel - volumetric heat capacity			LP2-2026
*-----1-----1-----1-----1-----1-----1-----1-----			LP2-2027
20100451	273.15	3.83e6	*LP2-2028
20100452	366.5	3.83e6	*LP2-2029
20100453	477.59	4.190e6	*LP2-2030
20100454	588.59	4.336e6	*LP2-2031
20100455	699.82	4.504e6	*LP2-2032
20100456	810.93	4.639e6	*LP2-2033
20100457	922.04	4.773e6	*LP2-2034
20100458	1144.26	5.076e6	*LP2-2035
20100459	1366.5	5.376e6	*LP2-2036
20100460	1477.59	5.546e6	*LP2-2037
*-----1-----1-----1-----1-----1-----1-----1-----			LP2-2038
* inconel-600 - thermal conductivity			LP2-2039
*-----1-----1-----1-----1-----1-----1-----1-----			LP2-2040
20100601	366.5	13.85	*LP2-2041
20100602	477.6	15.92	*LP2-2042
20100603	588.7	18.17	*LP2-2043
20100604	700.0	20.42	*LP2-2044
20100605	810.9	22.50	*LP2-2045
20100606	922.0	24.92	*LP2-2046
20100607	1033.2	26.83	*LP2-2047
20100608	1144.3	29.42	*LP2-2048
20100609	1477.6	36.06	*LP2-2049
*-----1-----1-----1-----1-----1-----1-----1-----			LP2-2050
* inconel-600 volumetric heat capacity			LP2-2051
*-----1-----1-----1-----1-----1-----1-----1-----			LP2-2052
20100651	366.5	3.908+6	*LP2-2053
20100652	477.6	4.084+6	*LP2-2054
20100653	588.7	4.260+6	*LP2-2055
20100654	700.0	4.436+6	*LP2-2056
20100656	810.9	4.665+6	*LP2-2057
20100657	922.0	4.929+6	*LP2-2058

*-----1-----1-----1-----1-----1-----1-----1-----						LP2-2102
* 007 reactor vessel downcomer level intact side						LP2-2103
*-----1-----1-----1-----1-----1-----1-----1-----						LP2-2104
20500700	rvdclvn		sum	1.	5.3137665 0	*LP2-2105
20500701	0.0	0.1876129	voidf	200010		*LP2-2106
20500702		0.2851823	voidf	202010000		*LP2-2107
20500703		0.2525361	voidf	210010000		*LP2-2108
20500704		1.5200561	voidf	210020000		*LP2-2109
20500705		1.2616333	voidf	210030000		*LP2-2110
20500706		1.0792591	voidf	210040000		*LP2-2111
20500707		0.3533183	voidf	222010000		*LP2-2112
20500708		0.3741720	voidf	220010000		*LP2-2113
*-----1-----1-----1-----1-----1-----1-----1-----						LP2-2114
* 008 reactor vessel downcomer level broken side						LP2-2115
*-----1-----1-----1-----1-----1-----1-----1-----						LP2-2116
20500800	rvdclbk		sum	1.	5.3137665 0	*LP2-2117
20500801	0.0	0.1876129	voidf	270010000		*LP2-2118
20500802		0.2851823	voidf	272010000		*LP2-2119
20500803		0.2525361	voidf	280010000		*LP2-2120
20500804		1.5200561	voidf	280020000		*LP2-2121
20500805		1.2616333	voidf	280030000		*LP2-2122
20500806		1.0792591	voidf	280040000		*LP2-2123
20500807		0.3533183	voidf	222010000		*LP2-2124
20500808		0.3741720	voidf	220010000		*LP2-2125
*-----1-----1-----1-----1-----1-----1-----1-----						LP2-2126
* 230 level average channel						LP2-2127
*-----1-----1-----1-----1-----1-----1-----1-----						LP2-2128
20523000	"lvl avg"		sum	1.	1.6842699 0	*LP2-2129
20523001	0.0	.432	voidf	230010000		*LP2-2130
20523002		.195	voidf	230020000		*LP2-2131
20523003		.195	voidf	230030000		*LP2-2132
20523004		.28833	voidf	230040000		*LP2-2133
20523005		.5744204	voidf	230050000		*LP2-2134
*-----1-----1-----1-----1-----1-----1-----1-----						LP2-2135
* 231 level hot channel						LP2-2136
*-----1-----1-----1-----1-----1-----1-----1-----						LP2-2137
20523100	"lvl hot"		sum	1.	1.6332083 0	*LP2-2138
20523101	0.0	.1397017	voidf	231010000		*LP2-2139
20523102		.265	voidf	231020000		*LP2-2140
20523103		.08833	voidf	231030000		*LP2-2141
20523104		.08833	voidf	231040000		*LP2-2142
20523105		.08833	voidf	231050000		*LP2-2143
20523106		.08833	voidf	231060000		*LP2-2144

20523107	.08833	voidf	231070000	*LP2-2145
20523108	.08833	voidf	231080000	*LP2-2146
20523109	.1325	voidf	231090000	*LP2-2147
20523110	.1325	voidf	231100000	*LP2-2148
20523111	.1325	voidf	231110000	*LP2-2149
20523112	.1325	voidf	231120000	*LP2-2150
20523113	.2117387	voidf	231130000	*LP2-2151
*-----1-----1-----1-----1-----1-----1-----1-----				LP2-2152
* 235 level bypass channel				LP2-2153
*-----1-----1-----1-----1-----1-----1-----1-----				LP2-2154
20523500	"lvl byps"	sum	0.5588068 1.6764202 0	*LP2-2155
20523501	0.0	1.0	voidf 235010000	*LP2-2156
20523502	1.0	voidf	235020000	*LP2-2157
20523503	1.0	voidf	235030000	*LP2-2158
*-----1-----1-----1-----1-----1-----1-----1-----				LP2-2159
* 240 average voidfraction coreliquid void fraction				LP2-2160
*-----1-----1-----1-----1-----1-----1-----1-----				LP2-2161
20524000	"void avg"	sum	2.9926155 0.9995193 0	*LP2-2162
20524001	0.0	.14751	cntrlvar 230	*LP2-2163
20524002	3.0897-2	cntrlvar	231	*LP2-2164
20524003	2.093-2	cntrlvar	235	*LP2-2165
*-----1-----1-----1-----1-----1-----1-----1-----				LP2-2166
* 250 reactor vessel level				LP2-2167
*-----1-----1-----1-----1-----1-----1-----1-----				LP2-2168
20525000	rvlvl	sum	1. 6.5309792 0	*LP2-2169
20525001	0.0	0.7747094	voidf 260010000	*LP2-2170
20525002	0.6312304	voidf	255010000	*LP2-2171
20525003	0.286958	voidf	252010000	*LP2-2172
20525004	0.7850547	voidf	250010000	*LP2-2173
20525005	0.4933248	voidf	245010000	*LP2-2174
20525006	0.5867979	voidf	240010000	*LP2-2175
20525007	0.74	cntrlvar	230	*LP2-2176
20525008	0.155	cntrlvar	231	*LP2-2177
20525009	0.105	cntrlvar	235	*LP2-2178
20525010	0.5709989	voidf	225010000	*LP2-2179
20525011	0.3533183	voidf	222010000	*LP2-2180
20525012	0.3741720	voidf	220010000	*LP2-2181
*-----1-----1-----1-----1-----1-----1-----1-----				LP2-2182
* 075-076 mass loss calculator				LP2-2184
*-----1-----1-----1-----1-----1-----1-----1-----				LP2-2185
20507500	losssum	sum	1. 0. 0	*LP2-2186
20507501	0.0	1.0	mflowj 317000000	*LP2-2187

20507502	1.0	mflowj	347000000		*LP2-2188	
*-----1-----1-----1-----1-----1-----1-----1-----					LP2-2189	
20507600	lossmas	integral	1.	0.	0	*LP2-2190
20507601	cntrlvar	75				*LP2-2191
*-----1-----1-----1-----1-----1-----1-----1-----						LP2-2192
*						LP2-2193
*						LP2-2194
*-----1-----1-----1-----1-----1-----1-----1-----						LP2-2195
* 080-081	average values of pumps					LP2-2196
*						LP2-2197
* 080	average pump speed					LP2-2198
*-----1-----1-----1-----1-----1-----1-----1-----						LP2-2199
20508000	avgpmps	sum	1.	169.95996	0	*LP2-2200
20508001	0.0	0.5	pmpvel	135		*LP2-2201
20508002		0.5	pmpvel	165		*LP2-2202
*-----1-----1-----1-----1-----1-----1-----1-----						LP2-2203
* 081	average pump head					LP2-2204
*-----1-----1-----1-----1-----1-----1-----1-----						LP2-2205
20508100	avgpmpH	sum	1.	134888.12	0	*LP2-2206
20508101	0.0	0.5	pmphead	135		*LP2-2207
20508102		0.5	pmphead	165		*LP2-2208
*-----1-----1-----1-----1-----1-----1-----1-----						LP2-2209
*						LP2-2210
* 090-098	power to fluid calculation					LP2-2211
*						LP2-2212
* 090	power average channel					LP2-2213
*-----1-----1-----1-----1-----1-----1-----1-----						LP2-2214
20509000	"power a"	sum	1.	3.55872+7	0	*LP2-2215
20509001	0.0	1.0	q	230010000		*LP2-2216
20509002		1.0	q	230020000		*LP2-2217
20509003		1.0	q	230030000		*LP2-2218
20509004		1.0	q	230040000		*LP2-2219
20509005		1.0	q	230050000		*LP2-2220
*-----1-----1-----1-----1-----1-----1-----1-----						LP2-2221
* 091	power hot channel					LP2-2222
*-----1-----1-----1-----1-----1-----1-----1-----						LP2-2223
20509100	"power h"	sum	1.	1.04137+7	0	*LP2-2224
20509101	0.0	1.0	q	231010000		*LP2-2225
20509102		1.0	q	231020000		*LP2-2226
20509103		1.0	q	231030000		*LP2-2227
20509104		1.0	q	231040000		*LP2-2228
20509105		1.0	q	231050000		*LP2-2229
20509106		1.0	q	231060000		*LP2-2230

20509107	1.0	q	231070000	*LP2-2231
20509108	1.0	q	231080000	*LP2-2232
20509109	1.0	q	231090000	*LP2-2233
20509110	1.0	q	231100000	*LP2-2234
20509111	1.0	q	231110000	*LP2-2235
20509112	1.0	q	231120000	*LP2-2236
20509113	1.0	q	231130000	*LP2-2237
*-----1-----1-----1-----1-----1-----1-----1-----				LP2-2233
* 092 total power				LP2-2239
*-----1-----1-----1-----1-----1-----1-----1-----				LP2-2240
20509200	power	sum	1. 4.60009+7 0	*LP2-2241
20509201	0.0	1.0	cntrlvar 90	*LP2-2242
20509202		1.0	cntrlvar 91	*LP2-2243
*-----1-----1-----1-----1-----1-----1-----1-----				LP2-2244
* 093 heat sink (steam generator)				LP2-2245
*-----1-----1-----1-----1-----1-----1-----1-----				LP2-2246
20509300	"heat sk"	sum	-1. 4.60636+7 0	*LP2-2247
20509301	0.0	1.0	q 115010000	*LP2-2248
20509302		1.0	q 115020000	*LP2-2249
20509303		1.0	q 115030000	*LP2-2250
20509304		1.0	q 115040000	*LP2-2251
20509305		1.0	q 115050000	*LP2-2252
20509306		1.0	q 115060000	*LP2-2253
20509307		1.0	q 115070000	*LP2-2254
20509308		1.0	q 115080000	*LP2-2255
*-----1-----1-----1-----1-----1-----1-----1-----				LP2-2256
* LP2-2257				LP2-2257
* 095 - 098 power of structure heat capacity				LP2-2258
* LP2-2259				LP2-2259
* 095 structures downcomer intact loop				LP2-2260
*-----1-----1-----1-----1-----1-----1-----1-----				LP2-2261
20509500	"hc intl"	sum	1. 1511.0059 0	*LP2-2262
20509501	0.0	1.0	q 200010000	*LP2-2263
20509502		1.0	q 202010000	*LP2-2264
20509503		1.0	q 210010000	*LP2-2265
20509504		1.0	q 210020000	*LP2-2266
20509505		1.0	q 210030000	*LP2-2267
20509506		1.0	q 210040000	*LP2-2268
*-----1-----1-----1-----1-----1-----1-----1-----				LP2-2269
* 096 structures downcomer broken loop				LP2-2270
*-----1-----1-----1-----1-----1-----1-----1-----				LP2-2271
20509600	"hc brkl"	sum	1. 1591.3711 0	*LP2-2272
20509601	0.0	1.0	q 270010000	*LP2-2273

20509602	1.0	q	272010000			*LP2-2274
20509603	1.0	q	280010000			*LP2-2275
20509604	1.0	q	280020000			*LP2-2276
20509605	1.0	q	280030000			*LP2-2277
20509606	1.0	q	280040000			*LP2-2278
*-----1-----1-----1-----1-----1-----1-----1-----						LP2-2279
* 097 structures core barrel						LP2-2280
*-----1-----1-----1-----1-----1-----1-----1-----						LP2-2281
20509700 "hc core"		sum	1.	150.18909	0	*LP2-2282
20509701 0.0	1.0	q	220010000			*LP2-2283
20509702	1.0	q	220000000			*LP2-2284
20509703	1.0	q	225010000			*LP2-2285
*-----1-----1-----1-----1-----1-----1-----1-----						LP2-2286
* 098 structures total						LP2-2287
*-----1-----1-----1-----1-----1-----1-----1-----						LP2-2288
20509800 heatcap		sum	1.	3252.5664	0	*LP2-2289
20509801 0.0	1.0	cntrlvar	95			*LP2-2290
20509802	1.0	cntrlvar	96			*LP2-2291
20509803	1.0	cntrlvar	97			*LP2-2292
*-----1-----1-----1-----1-----1-----1-----1-----						LP2-2293
*						LP2-2294
* 510 - 520 trip-sets						LP2-2295
*						LP2-2296
* 510 blow-down valves						LP2-2297
*-----1-----1-----1-----1-----1-----1-----1-----						LP2-2298
20551000 blowdown		tripunit	1.	0.	0	*LP2-2299
20551001 510						*LP2-2300
*-----1-----1-----1-----1-----1-----1-----1-----						LP2-2301
* 511 power scram						LP2-2302
*-----1-----1-----1-----1-----1-----1-----1-----						LP2-2303
20551100 powerscr		tripunit	1.	0.	0	*LP2-2304
20551101 511						*LP2-2305
*-----1-----1-----1-----1-----1-----1-----1-----						LP2-2306
* 512 pump trip						LP2-2307
*-----1-----1-----1-----1-----1-----1-----1-----						LP2-2308
20551200 pumptrip		tripunit	1.	0.	0	*LP2-2309
20551201 512						*LP2-2310
*-----1-----1-----1-----1-----1-----1-----1-----						LP2-2311
* 523 lpis trip						LP2-2312
*-----1-----1-----1-----1-----1-----1-----1-----						LP2-2313
20552300 lpistrip		tripunit	1.	0.	0	*LP2-2314
20552301 513						*LP2-2315
*-----1-----1-----1-----1-----1-----1-----1-----						LP2-2316

* 524 hpis trip							LP2-2317
*-----1-----1-----1-----1-----1-----1-----1-----							LP2-2318
20552400 hpistrip		tripunit	1.	0.	0		*LP2-2319
20552401 514							*LP2-2320
*-----1-----1-----1-----1-----1-----1-----1-----							LP2-2321
* 525 accumulator valve							LP2-2322
*-----1-----1-----1-----1-----1-----1-----1-----							LP2-2323
20552500 accumulv		tripunit	1.	0.	0		*LP2-2324
20552501 682							*LP2-2325
*-----1-----1-----1-----1-----1-----1-----1-----							LP2-2326
* 514 eccs							LP2-2327
*-----1-----1-----1-----1-----1-----1-----1-----							LP2-2328
20551400 eccs		sum	1.	0.	0		*LP2-2329
20551401 0.0	.35	cntrlvar	523				*LP2-2330
20551402	.25	cntrlvar	524				*LP2-2331
20551403		cntrlvar	525				*LP2-2332
*-----1-----1-----1-----1-----1-----1-----1-----							LP2-2333
* 516 steam valve							LP2-2334
*-----1-----1-----1-----1-----1-----1-----1-----							LP2-2335
20552600 steamvop		tripunit	1.	0.	0		*LP2-2336
20552601 685							*LP2-2337
20552700 steamvcl		tripunit	-1.	0.	0		*LP2-2338
20552701 686							*LP2-2339
20551600 steamvlv		sum	1.	0.	(*LP2-2340
20551601 0.0	1.0	cntrlvar	526				*LP2-2341
20551602	1.0	cntrlvar	527				*LP2-2342
*-----1-----1-----1-----1-----1-----1-----1-----							LP2-2343
*							LP2-2344
* 400-454 calculation of fluid-momentum flux							LP2-2345
*							LP2-2346
* 404 momentum flux of junction 34001							LP2-2347
*-----1-----1-----1-----1-----1-----1-----1-----							LP2-2348
20540000 "abs vf"		stdfnctn	1.	3.02597-6	0		*LP2-2349
20540001	abs	velfj	340010000				*LP2-2350
20540100 "abs vg"		stdfnctn	1.	3.02597-6	0		*LP2-2351
20540101	abs	velgj	340010000				*LP2-2352
*							LP2-2353
20540200 "momflux1"		mult	1.	-6.9531-9	0		*LP2-2354
20540201 voidfj	340010000	rhofj	340010000				*LP2-2355
20540202 velfj	340010000	cntrlvar	400				*LP2-2356
20540300 "momflux2"		mult	1.	0.	0		*LP2-2357
20540301 voidgj	340010000	rhogj	340010000				*LP2-2358
20540302 velgj	340010000	cntrlvar	401				*LP2-2359


```

*
* 434 momentum flux of junction 10002
*-----1-----1-----1-----1-----1-----1-----1-----
20543000 "abs vf"          stdfnctn 1.          5.5588271 0
20543001          abs          velfj      100020000
20543100 "abs vg"          stdfnctn 1.          5.6727905 0
20543101          abs          velgj      100020000
*
20543200 "momflux1"        mult       1.          22119.25 0
20543201 voidfj      100020000 rhofj      100020000
20543202 velfj      100020000 cntrlvar  430
20543300 "momflux2"        mult       1.          0.0038276 0
20543301 voidgj      100020000 rhogj      100020000
20543302 velgj      100020000 cntrlvar  431
*
20543400 "mf3401"          sum         1.          22119.266 0
20543401          0.0          1.0          cntrlvar  432
20543402          1.0          1.0          cntrlvar  433
*-----1-----1-----1-----1-----1-----1-----
*
* 444 momentum flux of junction 22502
*-----1-----1-----1-----1-----1-----1-----1-----
20544000 "abs vf"          stdfnctn 1.          1.661684 0
20544001          abs          velfj      225020000
20544100 "abs vg"          stdfnctn 1.          1.661684 0
20544101          abs          velgj      225020000
*
20544200 "momflux1"        mult       1.          2097.1621 0
20544201 voidfj      225020000 rhofj      225020000
20544202 velfj      225020000 cntrlvar  440
20544300 "momflux2"        mult       1.          0.          0
20544301 voidgj      225020000 rhogj      225020000
20544302 velgj      225020000 cntrlvar  441
*
20544400 "mf3401"          sum         1.          2097.1621 0
20544401          0.0          1.0          cntrlvar  442
20544402          1.0          1.0          cntrlvar  443
*-----1-----1-----1-----1-----1-----1-----
*
* 454 momentum flux of junction 24002
*-----1-----1-----1-----1-----1-----1-----1-----
20545000 "abs vf"          stdfnctn 1.          2.0633316 0
20545001          abs          velfj      240020000

```


20545100	"abs vg"		stdfnctn	1.	2.7305183 0	*LP2-2446
20545101		abs	velgj	240020000		*LP2-2447
*						LP2-2448
20545200	"momflux1"		mult	1.	2665.6641 0	*LP2-2449
20545201	voidfj	240020000	rhofj	240020000		*LP2-2450
20545202	velfj	240020000	cntrlvar	450		*LP2-2451
20545300	"momflux2"		mult	1.	35.657471 0	*LP2-2452
20545301	voidgj	240020000	rhogj	240020000		*LP2-2453
20545302	velgj	240020000	cntrlvar	451		*LP2-2454
*						LP2-2455
20545400	"mf3401"		sum	1.	2701.3223 0	*LP2-2456
20545401		0.0	1.0	cntrlvar	452	*LP2-2457
20545402			1.0	cntrlvar	453	*LP2-2458
*-----1-----1-----1-----1-----1-----1-----1-----						LP2-2459
*						LP2-2460
* 460 - 464	pressure differences					LP2-2461
*						LP2-2462
*-----1-----1-----1-----1-----1-----1-----1-----						LP2-2463
*						LP2-2464
20546000	"pde001"		sum	1.	116991.5 0	*LP2-2465
20546001		0.0	-1.0	p	120010000	*LP2-2466
20546002			1.0	p	150010000	*LP2-2467
*						LP2-2468
20546100	"pde002"		sum	1.	-57892.87 0	*LP2-2469
20546101		0.0	-1.0	p	112020000	*LP2-2470
20546102			1.0	p	120010000	*LP2-2471
*						LP2-2472
20546200	"pde003"		sum	1.	-8259.594 0	*LP2-2473
20546201		0.0	-1.0	p	100010000	*LP2-2474
20546202			1.0	p	112020000	*LP2-2475
*						LP2-2476
20546300	"pde005"		sum	1.	-972.8379 0	*LP2-2477
20546301		0.0	-1.0	p	150010000	*LP2-2478
20546302			1.0	p	180010000	*LP2-2479
*						LP2-2480
20546400	"pde006"		sum	1.	-49866.19 0	*LP2-2481
20546401		0.0	-1.0	p	180010000	*LP2-2482
20546402			1.0	p	100010000	*LP2-2483
*-----1-----1-----1-----1-----1-----1-----1-----						LP2-2484
*						LP2-2485
* 470	reactor-power					LP2-2486
*-----1-----1-----1-----1-----1-----1-----1-----						LP2-2487
20547000	"reac.pow"		function	1.	4.50000+7 0	*LP2-2488

1351304	-4.068300e-01	1.624000e+00	*LP2-2532
1351305	-2.001710e-01	1.470500e+00	*LP2-2533
1351306	0.000000e+00	1.403600e+00	*LP2-2534
*-----1-----1-----1-----1-----1-----1-----1-----1-----			LP2-2535
* head curve no. 4			LP2-2536
*-----1-----1-----1-----1-----1-----1-----1-----1-----			LP2-2537
1351400	1	4	*LP2-2538
1351401	-1.000000e+00	2.472200e+00	*LP2-2539
1351402	-8.229700e-01	1.996800e+00	*LP2-2540
1351403	-6.333200e-01	1.589700e+00	*LP2-2541
1351404	-4.553400e-01	1.327900e+00	*LP2-2542
1351405	-2.710900e-01	1.194900e+00	*LP2-2543
1351406	-1.771600e-01	1.060500e+00	*LP2-2544
1351407	-9.073000e-02	1.015600e+00	*LP2-2545
1351408	0.000000e+00	9.342790e-01	*LP2-2546
*-----1-----1-----1-----1-----1-----1-----1-----1-----			LP2-2547
* head curve no. 5			LP2-2548
*-----1-----1-----1-----1-----1-----1-----1-----1-----			LP2-2549
1351500	1	5	*LP2-2550
1351501	0.000000e+00	2.500000e-01	*LP2-2551
1351502	2.000000e-01	2.800000e-01	*LP2-2552
1351503	4.000000e-01	3.400000e-01	*LP2-2553
1351504	4.118000e-01	2.768000e-01	*LP2-2554
1351505	5.976300e-01	4.584000e-01	*LP2-2555
1351506	7.934670e-01	6.992000e-01	*LP2-2556
1351507	1.000000e+00	1.000000e+00	*LP2-2557
*-----1-----1-----1-----1-----1-----1-----1-----1-----			LP2-2558
* head curve no. 6			LP2-2559
*-----1-----1-----1-----1-----1-----1-----1-----1-----			LP2-2560
1351600	1	6	*LP2-2561
1351601	0.000000e+00	9.342790e-01	*LP2-2562
1351602	9.109900e-02	9.229000e-01	*LP2-2563
1351603	1.865090e-01	8.963000e-01	*LP2-2564
1351604	2.717620e-01	8.750000e-01	*LP2-2565
1351605	4.558720e-01	8.433000e-01	*LP2-2566
1351606	5.744060e-01	8.355000e-01	*LP2-2567
1351607	7.405760e-01	8.466000e-01	*LP2-2568
1351608	7.666190e-01	8.489000e-01	*LP2-2569
1351609	8.714710e-01	8.838000e-01	*LP2-2570
1351610	1.000000e+00	1.000000e+00	*LP2-2571
*-----1-----1-----1-----1-----1-----1-----1-----1-----			LP2-2572
* head curve no. 7			LP2-2573
*-----1-----1-----1-----1-----1-----1-----1-----1-----			LP2-2574

1351700	1	7	*LP2-2575
1351701	-1.000000e+00	-1.000000e+00	*LP2-2576
1351702	-8.000000e-01	-6.300000e-01	*LP2-2577
1351703	-6.000000e-01	-3.000000e-01	*LP2-2578
1351704	-4.000000e-01	-5.000000e-02	*LP2-2579
1351705	-2.000000e-01	1.500000e-01	*LP2-2580
1351706	0.000000e+00	2.500000e-01	*LP2-2581
*----	----1----	----1----	----1----
* head curve no. 8			LP2-2582
*----	----1----	----1----	----1----
			LP2-2583
*----	----1----	----1----	----1----
			LP2-2584
1351800	1	8	*LP2-2585
1351801	-1.000000e+00	-1.000000e+00	*LP2-2586
1351802	-8.000000e-01	-9.700000e-01	*LP2-2587
1351803	-6.000000e-01	-9.500000e-01	*LP2-2588
1351804	-4.000000e-01	-8.800000e-01	*LP2-2589
1351805	-2.000000e-01	-8.000000e-01	*LP2-2590
1351806	0.000000e+00	-6.700000e-01	*LP2-2591
*----	----1----	----1----	----1----
* single phase torque data			LP2-2592
*----	----1----	----1----	----1----
			LP2-2593
* torque curve no. 1			LP2-2594
*----	----1----	----1----	----1----
			LP2-2595
*----	----1----	----1----	----1----
			LP2-2596
1351900	2	1	*LP2-2597
1351901	0.000000e+00	6.032000e-01	*LP2-2598
1351902	1.930000e-01	6.325000e-01	*LP2-2599
1351903	3.930000e-01	7.369000e-01	*LP2-2600
1351904	5.955200e-01	8.331000e-01	*LP2-2601
1351905	7.978200e-01	9.229000e-01	*LP2-2602
1351906	1.000000e+00	1.000000e+00	*LP2-2603
*----	----1----	----1----	----1----
* torque curve no. 2			LP2-2604
*----	----1----	----1----	----1----
			LP2-2605
*----	----1----	----1----	----1----
			LP2-2606
1352000	2	2	*LP2-2607
1352001	0.000000e+00	-6.700000e-01	*LP2-2608
1352002	4.000000e-01	-2.500000e-01	*LP2-2609
1352003	5.000000e-01	1.500000e-01	*LP2-2610
1352004	7.372550e-01	5.265860e-01	*LP2-2611
1352005	7.680490e-01	6.065940e-01	*LP2-2612
1352006	8.672300e-01	7.436600e-01	*LP2-2613
1352007	1.000000e+00	1.000000e+00	*LP2-2614
*----	----1----	----1----	----1----
* torque curve no. 3			LP2-2615
*----	----1----	----1----	----1----
			LP2-2616
*----	----1----	----1----	----1----
			LP2-2617

1352100	2	3	*LP2-2618
1352101	-1.000000e+00	1.984300e+00	*LP2-2619
1352102	-8.009600e-01	1.394000e+00	*LP2-2620
1352103	-6.063800e-01	1.097500e+00	*LP2-2621
1352104	-4.068600e-01	8.220000e-01	*LP2-2622
1352105	-1.992800e-01	6.648000e-01	*LP2-2623
1352106	0.000000e+00	6.032000e-01	*LP2-2624
*-----1-----1-----1-----1-----1-----1-----1-----			LP2-2625
* torque curve no. 4			LP2-2626
*-----1-----1-----1-----1-----1-----1-----1-----			LP2-2627
1352200	2	4	*LP2-2628
1352201	-1.000000e+00	1.984300e+00	*LP2-2629
1352202	-8.223400e-01	1.830800e+00	*LP2-2630
1352203	-6.337100e-01	1.682400e+00	*LP2-2631
1352204	-4.585300e-01	1.557000e+00	*LP2-2632
1352205	-2.670230e-01	1.436200e+00	*LP2-2633
1352206	-1.761070e-01	1.387900e+00	*LP2-2634
1352207	-8.931000e-02	1.348100e+00	*LP2-2635
1352208	0.000000e+00	1.233610e+00	*LP2-2636
*-----1-----1-----1-----1-----1-----1-----1-----			LP2-2637
* torque curve no. 5			LP2-2638
*-----1-----1-----1-----1-----1-----1-----1-----			LP2-2639
1352300	2	5	*LP2-2640
1352301	0.000000e+00	-4.500000e-01	*LP2-2641
1352302	4.000000e-01	-2.500000e-01	*LP2-2642
1352303	5.000000e-01	0.000000e+00	*LP2-2643
1352304	1.000000e+00	3.569000e-01	*LP2-2644
*-----1-----1-----1-----1-----1-----1-----1-----			LP2-2645
* torque curve no. 6			LP2-2646
*-----1-----1-----1-----1-----1-----1-----1-----			LP2-2647
1352400	2	6	*LP2-2648
1352401	0.000000e+00	1.233610e+00	*LP2-2649
1352402	9.064300e-02	1.196500e+00	*LP2-2650
1352403	1.885690e-01	1.109600e+00	*LP2-2651
1352404	2.734700e-01	1.041600e+00	*LP2-2652
1352405	4.586690e-01	8.958000e-01	*LP2-2653
1352406	5.744800e-01	7.807000e-01	*LP2-2654
1352407	7.381600e-01	6.134000e-01	*LP2-2655
1352408	7.685200e-01	5.849000e-01	*LP2-2656
1352409	8.700570e-01	4.877000e-01	*LP2-2657
1352410	1.000000e+00	3.569000e-01	*LP2-2658
*-----1-----1-----1-----1-----1-----1-----1-----			LP2-2659
* torque curve no. 7			LP2-2660

```

*---- -1- -1- -1- -1- -1- -1- -1- LP2-2661
1352500 2 7 *LP2-2662
1352501 -1.000000e+00 -1.000000e+00 *LP2-2663
1352502 -3.000000e-01 -9.000000e-01 *LP2-2664
1352503 -1.000000e-01 -5.000000e-01 *LP2-2665
1352504 0.000000e+00 -4.500000e-01 *LP2-2666
*---- -1- -1- -1- -1- -1- -1- LP2-2667
* torque curve no. 8 LP2-2668
*---- -1- -1- -1- -1- -1- -1- LP2-2669
1352600 2 8 *LP2-2670
1352601 -1.000000e+00 -1.000000e+00 *LP2-2671
1352602 -2.500000e-01 -9.000000e-01 *LP2-2672
1352603 -8.000000e-02 -8.000000e-01 *LP2-2673
1352604 0.000000e+00 -6.700000e-01 *LP2-2674
*---- -1- -1- -1- -1- -1- -1- LP2-2675
* two - phase multiplier data from 13-6 test data LP2-2676
*---- -1- -1- -1- -1- -1- -1- LP2-2677
* head curve LP2-2678
*---- -1- -1- -1- -1- -1- -1- LP2-2679
1353000 0 *LP2-2680
1353001 0.000000e+00 0.000000e+00 *LP2-2681
1353002 1.000000e-01 0.000000e+00 *LP2-2682
1353003 2.000000e-01 1.000000e-01 *LP2-2683
1353004 3.000000e-01 2.000000e-01 *LP2-2684
1353005 3.500000e-01 3.000000e-01 *LP2-2685
1353006 4.000000e-01 6.000000e-01 *LP2-2686
1353007 5.000000e-01 6.000000e-01 *LP2-2687
1353008 6.000000e-01 6.000000e-01 *LP2-2688
1353009 7.000000e-01 6.000000e-01 *LP2-2689
1353010 8.000000e-01 5.000000e-01 *LP2-2690
1353011 9.000000e-01 3.000000e-01 *LP2-2691
1353012 1.000000e+00 0.000000e+00 *LP2-2692
*---- -1- -1- -1- -1- -1- -1- LP2-2693
* torque curve LP2-2694
*---- -1- -1- -1- -1- -1- -1- LP2-2695
1353100 0 *LP2-2696
1353101 0.000000e+00 0.000000e+00 *LP2-2697
1353102 1.000000e-01 0.000000e+00 *LP2-2698
1353103 2.000000e-01 1.000000e-01 *LP2-2699
1353104 3.000000e-01 3.000000e-01 *LP2-2700
1353105 3.500000e-01 5.000000e-01 *LP2-2701
1353106 4.000000e-01 7.500000e-01 *LP2-2702
1353107 5.000000e-01 7.500000e-01 *LP2-2703

```


1353108	6.000000e-01	7.500000e-01	*LP2-2704	
1353109	7.000000e-01	7.500000e-01	*LP2-2705	
1353110	8.000000e-01	7.500000e-01	*LP2-2706	
1353111	9.000000e-01	5.000000e-01	*LP2-2707	
1353112	1.000000e+00	0.000000e+00	*LP2-2708	
*----	----1----	----1----	----1----	LP2-2709
* pump 2-phase difference data			LP2-2710	
*----	----1----	----1----	----1----	LP2-2711
* head curve no. 1			LP2-2712	
*----	----1----	----1----	----1----	LP2-2713
1354100	1	1	*LP2-2714	
1354101	0.000000e+00	1.000000e+00	*LP2-2715	
1354102	1.000000e+00	1.000000e+00	*LP2-2716	
*----	----1----	----1----	----1----	LP2-2717
* head curve no. 2			LP2-2718	
*----	----1----	----1----	----1----	LP2-2719
1354200	1	2	*LP2-2720	
1354201	0.000000e+00	1.000000e+00	*LP2-2721	
1354202	1.000000e+00	1.000000e+00	*LP2-2722	
*----	----1----	----1----	----1----	LP2-2723
* head curve no. 3			LP2-2724	
*----	----1----	----1----	----1----	LP2-2725
1354300	1	3	*LP2-2726	
1354301	-1.000000e+00	-1.160000e+00	*LP2-2727	
1354302	-9.000000e-01	-1.240000e+00	*LP2-2728	
1354303	-8.000000e-01	-1.770000e+00	*LP2-2729	
1354304	-7.000000e-01	-2.360000e+00	*LP2-2730	
1354305	-6.000000e-01	-2.790000e+00	*LP2-2731	
1354306	-5.000000e-01	-2.910000e+00	*LP2-2732	
1354307	-4.000000e-01	-2.670000e+00	*LP2-2733	
1354308	-2.500000e-01	-1.690000e+00	*LP2-2734	
1354309	-1.000000e-01	-5.000000e-01	*LP2-2735	
1354310	0.000000e+00	0.000000e+00	*LP2-2736	
*----	----1----	----1----	----1----	LP2-2737
* head curve no. 4			LP2-2738	
*----	----1----	----1----	----1----	LP2-2739
1354400	1	4	*LP2-2740	
1354401	-1.000000e+00	-1.160000e+00	*LP2-2741	
1354402	-9.000000e-01	-7.800000e-01	*LP2-2742	
1354403	-8.000000e-01	-5.000000e-01	*LP2-2743	
1354404	-7.000000e-01	-3.100000e-01	*LP2-2744	
1354405	-6.000000e-01	-1.700000e-01	*LP2-2745	
1354406	-5.000000e-01	-8.000000e-02	*LP2-2746	

1354407	-3.500000e-01	0.000000e+00	*LP2-2747
1354408	-2.000000e-01	5.000000e-02	*LP2-2748
1354409	-1.000000e-01	8.000000e-02	*LP2-2749
1354410	0.000000e+00	1.100000e-01	*LP2-2750
*----	----1----	----1----	LP2-2751
* head curve no. 5			LP2-2752
*----	----1----	----1----	LP2-2753
1354500	1	5	*LP2-2754
1354501	0.000000e+00	0.000000e+00	*LP2-2755
1354502	2.000000e-01	-3.400000e-01	*LP2-2756
1354503	4.000000e-01	-6.500000e-01	*LP2-2757
1354504	6.000000e-01	-9.300000e-01	*LP2-2758
1354505	8.000000e-01	-1.190000e+00	*LP2-2759
1354506	1.000000e+00	-1.470000e+00	*LP2-2760
*----	----1----	----1----	LP2-2761
* head curve no. 6			LP2-2762
*----	----1----	----1----	LP2-2763
1354600	1	6	*LP2-2764
1354601	0.000000e+00	1.100000e-01	*LP2-2765
1354602	1.000000e-01	1.300000e-01	*LP2-2766
1354603	2.500000e-01	1.500000e-01	*LP2-2767
1354604	4.000000e-01	1.300000e-01	*LP2-2768
1354605	5.000000e-01	7.000000e-02	*LP2-2769
1354606	6.000000e-01	-4.000000e-02	*LP2-2770
1354607	7.000000e-01	-2.300000e-01	*LP2-2771
1354608	8.000000e-01	-5.100000e-01	*LP2-2772
1354609	9.000000e-01	-9.100000e-01	*LP2-2773
1354610	1.000000e+00	-1.470000e+00	*LP2-2774
*----	----1----	----1----	LP2-2775
* head curve no. 7			LP2-2776
*----	----1----	----1----	LP2-2777
1354700	1	7	*LP2-2778
1354701	-1.000000e+00	0.000000e+00	*LP2-2779
1354702	0.000000e+00	0.000000e+00	*LP2-2780
*----	----1----	----1----	LP2-2781
* head curve no. 8			LP2-2782
*----	----1----	----1----	LP2-2783
1354800	1	8	*LP2-2784
1354801	-1.000000e+00	0.000000e+00	*LP2-2785
1354802	0.000000e+00	0.000000e+00	*LP2-2786
*----	----1----	----1----	LP2-2787
* torque curve no. 1			LP2-2788
*----	----1----	----1----	LP2-2789

1354900	2	1	*LP2-2790
1354901	0.000000e+00	1.000000e+00	*LP2-2791
1354906	1.000000e+00	1.000000e+00	*LP2-2792
*-----1-----1-----1-----1-----1-----1-----1-----			LP2-2793
* torque curve no. 2			LP2-2794
*-----1-----1-----1-----1-----1-----1-----1-----			LP2-2795
1355000	2	2	*LP2-2796
1355001	0.000000e+00	1.000000e+00	*LP2-2797
1355007	1.000000e+00	1.000000e+00	*LP2-2798
*-----1-----1-----1-----1-----1-----1-----1-----			LP2-2799
* torque curve no. 3			LP2-2800
*-----1-----1-----1-----1-----1-----1-----1-----			LP2-2801
1355100	2	3	*LP2-2802
1355101	-1.000000e+00	1.984300e+00	*LP2-2803
1355102	-8.009600e-01	1.394000e+00	*LP2-2804
1355103	-6.063800e-01	1.097500e+00	*LP2-2805
1355104	-4.068600e-01	8.220000e-01	*LP2-2806
1355105	-1.992800e-01	6.648000e-01	*LP2-2807
1355106	0.000000e+00	6.032000e-01	*LP2-2808
*-----1-----1-----1-----1-----1-----1-----1-----			LP2-2809
* torque curve no. 4			LP2-2810
*-----1-----1-----1-----1-----1-----1-----1-----			LP2-2811
1355200	2	4	*LP2-2812
1355201	-1.000000e+00	1.984300e+00	*LP2-2813
1355202	-8.223400e-01	1.830800e+00	*LP2-2814
1355203	-6.337100e-01	1.682400e+00	*LP2-2815
1355204	-4.585300e-01	1.557000e+00	*LP2-2816
1355205	-2.670230e-01	1.436200e+00	*LP2-2817
1355206	-1.761070e-01	1.387900e+00	*LP2-2818
1355207	-8.931000e-02	1.348100e+00	*LP2-2819
1355208	0.000000e+00	1.233610e+00	*LP2-2820
*-----1-----1-----1-----1-----1-----1-----1-----			LP2-2821
* torque curve no. 5			LP2-2822
*-----1-----1-----1-----1-----1-----1-----1-----			LP2-2823
1355300	2	5	*LP2-2824
1355301	0.000000e+00	-4.500000e-01	*LP2-2825
1355302	4.000000e-01	-2.500000e-01	*LP2-2826
1355303	5.000000e-01	0.000000e+00	*LP2-2827
1355304	1.000000e+00	3.569000e-01	*LP2-2828
*-----1-----1-----1-----1-----1-----1-----1-----			LP2-2829
* torque curve no. 6			LP2-2830
*-----1-----1-----1-----1-----1-----1-----1-----			LP2-2831
1355400	2	6	*LP2-2832

1355401	0.000000e+00	1.233610e+00	*LP2-2833
1355402	9.064300e-02	1.196500e+00	*LP2-2834
1355403	1.885690e-01	1.109600e+00	*LP2-2835
1355404	2.734700e-01	1.041600e+00	*LP2-2836
1355405	4.586690e-01	8.958000e-01	*LP2-2837
1355406	5.744800e-01	7.807000e-01	*LP2-2838
1355407	7.381600e-01	6.134000e-01	*LP2-2839
1355408	7.685200e-01	5.849000e-01	*LP2-2840
1355409	8.700570e-01	4.877000e-01	*LP2-2841
1355410	1.000000e+00	3.569000e-01	*LP2-2842
*----	----1----	----1----	----1----
* torque curve no. 7			LP2-2843
*----	----1----	----1----	----1----
			LP2-2844
* torque curve no. 7			LP2-2845
*----	----1----	----1----	----1----
1355500	2	7	*LP2-2846
1355501	-1.000000e+00	-1.000000e+00	*LP2-2847
1355502	-3.000000e-01	-9.000000e-01	*LP2-2848
1355503	-1.000000e-01	-5.000000e-01	*LP2-2849
1355504	0.000000e+00	-4.500000e-01	*LP2-2850
*----	----1----	----1----	----1----
* torque curve no. 8			LP2-2851
*----	----1----	----1----	----1----
			LP2-2852
* torque curve no. 8			LP2-2853
*----	----1----	----1----	----1----
1355600	2	8	*LP2-2854
1355601	-1.000000e+00	-1.000000e+00	*LP2-2855
1355602	-2.500000e-01	-9.000000e-01	*LP2-2856
1355603	-8.000000e-02	-8.000000e-01	*LP2-2857
1355604	0.000000e+00	-6.700000e-01	*LP2-2858
*----	----1----	----1----	----1----
*			LP2-2859
			LP2-2860
.....	RELAP5/MOD2	(LP-02-6 / Mk.2-00C)	*LP2-2861

BIBLIOGRAPHIC DATA SHEET

(See instructions on the reverse.)

1. REPORT NUMBER
(Assigned by NRC. Add Vol., Subd., Rev.,
and Addendum Numbers, if any.)

NUREG/IA-0088
PSI-Bericht Nr. 92

2. TITLE AND SUBTITLE

Post-Test-Analysis and Nodalization Studies of OECD LOFT Experiment LP-02-6
with RELAP5/MOD2 CY36-02

3. DATE REPORT PUBLISHED

MONTH | YEAR
August | 1992

4. FIN OR GRANT NUMBER

A4682

5. AUTHOR(S)

D. Lubbesmeyer

6. TYPE OF REPORT

Technical

7. PERIOD COVERED (Give Dates)

8. PERFORMING ORGANIZATION - NAME AND ADDRESS (If NRC, provide Division, Office or Region, U.S. Nuclear Regulatory Commission, and mailing address; if contractor, provide name and mailing address.)

Paul Scherrer Institute (PSI)
Wurenlingen and Villigen
H-5232 Villigen PSI
Switzerland

9. SPONSORING ORGANIZATION - NAME AND ADDRESS (If NRC, type "Same as above"; if contractor, provide NRC Division, Office or Region, U.S. Nuclear Regulatory Commission, and mailing address.)

Office of Nuclear Regulatory Research
U.S. Nuclear Regulatory Commission
Washington, D.C. 20555

10. SUPPLEMENTARY NOTES

11. ABSTRACT (200 words or less)

This report presents the results and analysis of nine post-test calculations of the Experiment LP-02-6 by using RELAP5/MOD2 CY36-02 computer code with different nodalizations. Starting with a "standard nodalization" we have reduced the number of volumes and junctions as well as the number of radial zones in the fuel rods, for different nodalization studies. Except for the cladding temperatures, only small discrepancies have been observed for the other main parameters of the results of runs using different nodalizations but reduced number of volumes and junctions usually have lead to a decreased running time for the problem. The time behaviors of the cladding temperatures have been significantly affected by the chosen nodalizations. The most comparable results with the experimental data have been achieved by using medium number of nodes. With respect to high mass-flux, early bottom-up rewetting, one of the key-events of Experiment LP-02-6 as well as of most of the other LOFT large break experiments, RELAP5/MOD2 was not able to predict this phenomenon except with a certain manipulation by initiating the reflood option.

12. KEY WORDS/DESCRIPTORS (List words or phrases that will assist researchers in locating the report.)

RELAP5/MOD2, LP-02-6, LOFT

13. AVAILABILITY STATEMENT

Unlimited

14. SECURITY CLASSIFICATION

(This Page)

Unclassified

(The Report)

Unclassified

15. NUMBER OF PAGES

16. PRICE

THIS DOCUMENT WAS PRINTED USING RECYCLED PAPER

UNITED STATES
NUCLEAR REGULATORY COMMISSION
WASHINGTON, D.C. 20555-0001

SPECIAL FOURTH-CLASS RATE
POSTAGE AND FEES PAID
USNRC
PERMIT NO. G-67

OFFICIAL BUSINESS
PENALTY FOR PRIVATE USE, \$300

120555139531 1 1AN1C1
US NRC-OADM
DIV FOIA & PUBLICATIONS SVCS
TPS-PDR-NUREG
P-211
WASHINGTON DC 20555